ANNUAL REPORT 2003

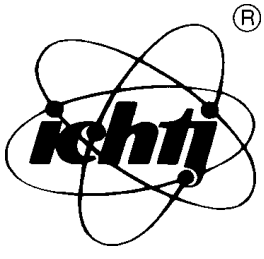

INSTITUTE
OF NUCLEAR CHEMISTRY
AND TECHNOLOGY

EDITORS

Wiktor Smułek, Ph.D.
Ewa Godlewska-Para, M.Sc.

PRINTING

Sylwester Wojtas

CONTENTS

GENERAL INFORMATION

The Institute of Nuclear Chemistry and Technology (INCT) is one of the successors of the Institute of Nuclear Research (INR) which was established in 1955. The latter Institute, once the biggest Institute in Poland, has exerted a great influence on the scientific and intelectual life in this country. The INCT came into being as one of the independent units established after the dissolution of the INR in 1983.

At present, the Institute research activity is focused on:

- radiation chemistry and technology,
- radiochemistry and coordination chemistry,
- radiobiology,
- application of nuclear methods in material and process engineering,
- design of instruments based on nuclear techniques,
- trace analysis and radioanalytical techniques,
- environmental research.

In the above fields we offer research programmes for Ph.D. students.

At this moment, with its nine electron accelerators in operation and with the staff experienced in the field of electron beam (EB) applications, the Institute is one of the most advanced centres of radiation research and EB processing. The accelerators are installed in the following Institute units:

- pilot plant for radiation sterilization of medical devices and transplants,
- pilot plant for radiation modification of polymers,
- experimental pilot plant for food irradiation,
- pilot plant for removal of SO_2 and NO_x from flue gases,
- pulse radiolysis laboratory, in which the nanosecond set-up was put into operation in 2001. A new 10 MeV accelerator was constructed in the INCT for this purpose.

Based on the technology elaborated in our Institute an industrial installation for electron beam flue gas treatment has been implemented at the EPS "Pomorzany" (Dolna Odra PS Group). This is the second full scale industrial EB installation for SO_2 and NO_x removal all over the world.

***

In 2003 the INCT scientists published 77 papers in scientific journals registered in the Philadelphia list, among them 31 papers in journals with an impact factor (IF) higher than 1.0. Seven chapters of scientific books published in 2003 were written by the INCT workers.

14 research projects and 1 implementation project have been granted by the Polish State Committee for Scientific Research to the INCT research teams in 2003. Additionally, the International Atomic Energy Agency accepted 1 research contract and 2 technical contracts proposed by the INCT scientists and started supporting them financially. European Commission of Scientific and Technical Research approved the participation of prof. **Zbigniew Zagórski** in COST D27 project "Prebiotic chemistry and early evolution".

Annual rewards of the INCT Director-General for the best publications in the period 2001-2002 were granted to the following research teams:

- First award to dr. **Maria Wojewódzka**, **Iwona Buraczewska**, dr. **Iwona Grądzka** and assoc. prof. **Marcin Kruszewski** for two experimental papers on the development of the comet method for the determination of DNA double strand breaks.
- Second award to dr. **Andrzej Deptuła**, **Wiesława Łada**, **Tadeusz Olczak**, prof. **Andrzej G. Chmielewski** and **Bożena Sartowska** for a series of papers on the synthesis and the structural studies of modern materials obtained with the sol-gel process.
- Third award to prof. **Rajmund Dybczyński** for a series of three review papers concerning the actual problems of ensuring the quality in inorganic trace analysis, especially taking into account neutron activation analysis (NAA).

Four scientific meetings have been organized by the INCT in 2003:

- Jubilee Conference "Tissue Grafts in the Fight against Cripplehood – 40 Years of Radiation Sterilisation and Tissue Banking in Poland";
- 7th Training Course on Radiation Sterilization and Hygienization;
- Conference on Problems of Waste Disposal;
- Expert Meeting on the Follow up of the Patients Involved in the Białystok Radiation Accident.

The international journal for nuclear research – NUKLEONIKA published by the INCT was mentioned on the SCI Journal Citation List with an impact factor IF = 0.5 distinctly higher than year ago.

MANAGEMENT OF THE INSTITUTE

MANAGING STAFF OF THE INSTITUTE

Director
Assoc. Prof. **Lech Waliś**, Ph.D.

Deputy Director for Research and Development
Prof. **Jacek Michalik**, Ph.D., D.Sc.

Deputy Director for Administration
Roman Janusz, M.Sc.

Accountant General
Barbara Kaźmirska

HEADS OF THE INCT DEPARTMENTS

- Department of Nuclear Methods of Material Engineering
  Assoc. Prof. **Lech Waliś**, Ph.D.
- Department of Structural Research
  Wojciech Starosta, M.Sc.
- Department of Radioisotope Instruments and Methods
  Prof. **Piotr Urbański**, Ph.D., D.Sc.
- Department of Radiochemistry
  Prof. **Jerzy Ostyk-Narbutt**, Ph.D., D.Sc.
- Department of Nuclear Methods of Process Engineering
  Prof. **Andrzej G. Chmielewski**, Ph.D., D.Sc.
- Department of Radiation Chemistry and Technology
  Zbigniew Zimek, Ph.D.
- Department of Analytical Chemistry
  Prof. **Rajmund Dybczyński**, Ph.D., D.Sc.
- Department of Radiobiology and Health Protection
  Prof. **Irena Szumiel**, Ph.D., D.Sc.
- Experimental Plant for Food Irradiation
  Assoc. Prof. **Wojciech Migdał**, Ph.D., D.Sc.
- Laboratory for Detection of Irradiated Foods
  Wacław Stachowicz, Ph.D.
- Laboratory for Measurements of Technological Doses
  Zofia Stuglik, Ph.D.

SCIENTIFIC COUNCIL (2003-2007)

1. Prof. **Grzegorz Bartosz**, Ph.D., D.Sc.
   University of Łódź
   • biochemistry
2. Assoc. Prof. **Aleksander Bilewicz**, Ph.D., D.Sc.
   Institute of Nuclear Chemistry and Technology
   • radiochemistry, inorganic chemistry
3. Prof. **Krzysztof Bobrowski**, Ph.D., D.Sc. (Chairman)
   Institute of Nuclear Chemistry and Technology
   • radiation chemistry, photochemistry, biophysics
4. **Sylwester Bułka**, M.Sc.
   Institute of Nuclear Chemistry and Technology
   • electronics

5. Prof. **Witold Charewicz**, Ph.D., D.Sc.
   Wrocław University of Technology
   • inorganic chemistry, hydrometallurgy
6. Prof. **Stanisław Chibowski**, Ph.D., D.Sc.
   The Maria Curie-Skłodowska University
   • radiochemistry, physical chemistry
7. Prof. **Andrzej G. Chmielewsk**i, Ph.D., D.Sc.
   Institute of Nuclear Chemistry and Technology
   • chemical and process engineering, nuclear chemical engineering, isotope chemistry
8. Prof. **Jadwiga Chwastowska**, Ph.D., D.Sc.
   Institute of Nuclear Chemistry and Technology
   • analytical chemistry
9. Prof. **Rajmund Dybczyński**, Ph.D., D.Sc.
   Institute of Nuclear Chemistry and Technology
   • analytical chemistry
10. Prof. **Zbigniew Florjańczyk**, Ph.D., D.Sc.
    (Vice-chairman)
    Warsaw University of Technology
    • chemical technology
11. Prof. **Leon Gradoń**, Ph.D., D.Sc.
    Warsaw University of Technology
    • chemical and process engineering
12. Assoc. Prof. **Edward Iller**, Ph.D., D.Sc.
    Radioisotope Centre POLATOM
    • chemical and process engineering, physical chemistry
13. Assoc. Prof. **Marek Janiak**, Ph.D., D.Sc.
    Military Institute of Hygiene and Epidemiology
    • radiobiology
14. **Iwona Kałuska**, M.Sc.
    Institute of Nuclear Chemistry and Technology
    • radiation chemistry
15. Assoc. Prof. **Marcin Kruszewski**, Ph.D., D.Sc.
    Institute of Nuclear Chemistry and Technology
    • radiobiology
16. Prof. **Marek Lankosz**, Ph.D., D.Sc.
    AGH University of Science and Technology
    • physics, radioanalytical methods
17. Prof. **Janusz Lipkowski**, Ph.D., D.Sc.
    Institute of Physical Chemistry, Polish Academy of Sciences
    • physico-chemical methods of analysis
18. **Zygmunt Łuczyński**, Ph.D.
    Institute of Electronic Materials Technology
    • chemistry
19. Prof. **Andrzej Łukasiewicz**, Ph.D., D.Sc.
    Institute of Nuclear Chemistry and Technology
    • material science
20. Prof. **Bronisław Marciniak**, Ph.D., D.Sc.
    Adam Mickiewicz University in Poznań
    • physical chemistry
21. Prof. **Józef Mayer**, Ph.D., D.Sc.
    Technical University of Łódź
    • physical and radiation chemistry
22. Prof. **Jacek Michalik**, Ph.D., D.Sc.
    Institute of Nuclear Chemistry and Technology
    • radiation chemistry, surface chemistry, radical chemistry
23. Prof. **Jerzy Ostyk-Narbutt**, Ph.D., D.Sc.
    Institute of Nuclear Chemistry and Technology
    • radiochemistry, coordination chemistry
24. **Jan Paweł Pieńkos**, Eng.
    Institute of Nuclear Chemistry and Technology
    • electronics
25. Prof. **Leon Pszonicki**, Ph.D., D.Sc.
    Institute of Nuclear Chemistry and Technology
    • analytical chemistry
26. Prof. **Sławomir Siekierski**, Ph.D.
    Institute of Nuclear Chemistry and Technology
    • physical chemistry, inorganic chemistry
27. Prof. **Sławomir Sterliński**, Ph.D., D.Sc.
    Central Laboratory for Radiological Protection
    • physics, nuclear technical physics
28. Prof. **Irena Szumiel**, Ph.D., D.Sc.
    Institute of Nuclear Chemistry and Technology
    • cellular radiobiology
29. Prof. **Jerzy Szydłowski**, Ph.D., D.Sc.
    Warsaw University
    • physical chemistry, radiochemistry
30. Prof. **Jan Tacikowski**, Ph.D.
    Institute of Precision Mechanics
    • physical metallurgy and heat treatment of metals
31. Prof. **Marek Trojanowicz**, Ph.D., D.Sc.
    Institute of Nuclear Chemistry and Technology
    • analytical chemistry
32. Prof. **Piotr Urbański**, Ph.D., D.Sc.
    (Vice-chairman)
    Institute of Nuclear Chemistry and Technology
    • radiometric methods, industrial measurement equipment, metrology
33. Assoc. Prof. **Lech Waliś**, Ph.D.
    Institute of Nuclear Chemistry and Technology
    • material science, material engineering
34. Assoc. Prof. **Andrzej Wójcik**, Ph.D., D.Sc.
    (Vice-chairman)
    Institute of Nuclear Chemistry and Technology
    • cytogentics

35. Prof. **Zbigniew Zagórski**, Ph.D., D.Sc.
    Institute of Nuclear Chemistry and Technology
    • physical chemistry, radiation chemistry, electrochemistry

36. **Zbigniew Zimek**, Ph.D.
    Institute of Nuclear Chemistry and Technology
    • electronics, accelerator techniques, radiation processing

HONORARY MEMBERS OF THE INCT SCIENTIFIC COUNCIL (2003-2007)

1. Prof. **Antoni Dancewicz**, Ph.D., D.Sc.
   • biochemistry, radiobiology

SCIENTIFIC STAFF

PROFESSORS

1. **Bobrowski Krzysztof**
   radiation chemistry, photochemistry, biophysics
2. **Chmielewski Andrzej G.**
   chemical and process engineering, nuclear chemical engineering, isotope chemistry
3. **Chwastowska Jadwiga**
   analytical chemistry
4. **Dybczyński Rajmund**
   analytical chemistry
5. **Leciejewicz Janusz**
   crystallography, solid state physics, material science
6. **Łukasiewicz Andrzej**
   material science
7. **Michalik Jacek**
   radiation chemistry, surface chemistry, radical chemistry
8. **Ostyk-Narbutt Jerzy**
   radiochemistry, coordination chemistry
9. **Piekoszewski Jerzy**
   solid state physics
10. **Pszonicki Leon**
    analytical chemistry
11. **Siekierski Sławomir**
    physical chemistry, inorganic chemistry
12. **Szumiel Irena**
    cellular radiobiology
13. **Trojanowicz Marek**
    analytical chemistry
14. **Urbański Piotr**
    radiometric methods, industrial measurement equipment, metrology
15. **Zagórski Zbigniew**
    physical chemistry, radiation chemistry, electrochemistry

ASSOCIATE PROFESSORS

1. **Bilewicz Aleksander**
   radiochemistry, inorganic chemistry
2. **Grigoriew Helena**
   solid state physics, diffraction research of non-crystalline matter
3. **Kruszewski Marcin**
   radiobiology
4. **Legocka Izabella**
   polymer technology
5. **Migdał Wojciech**
   chemistry
6. **Waliś Lech**
   material science, material engineering
7. **Wójcik Andrzej**
   cytogenetics
8. **Żółtowski Tadeusz**
   nuclear physics

SENIOR SCIENTISTS (Ph.D.)

1. **Bartłomiejczyk Teresa**
   biology
2. **Borkowski Marian**
   chemistry
3. **Buczkowski Marek**
   physics
4. **Cieśla Krystyna**
   physical chemistry
5. **Danko Bożena**
   analytical chemistry
6. **Dembiński Wojciech**
   chemistry

7. **Deptuła Andrzej**
   chemistry
8. **Dobrowolski Andrzej**
   chemistry
9. **Dudek Jakub**
   chemistry
10. **Dźwigalski Zygmunt**
    high voltage electronics, electron injectors, gas lasers
11. **Fuks Leon**
    chemistry
12. **Gniazdowska Ewa**
    chemistry
13. **Grądzka Iwona**
    biology
14. **Grodkowski Jan**
    radiation chemistry
15. **Harasimowicz Marian**
    technical nuclear physics, theory of elementary particles
16. **Jaworska Alicja**
    biology
17. **Kierzek Joachim**
    physics
18. **Krejzler Jadwiga**
    chemistry
19. **Kunicki-Goldfinger Jerzy**
    conservator/restorer of art
20. **Machaj Bronisław**
    electricity
21. **Mirkowski Jacek**
    nuclear and medical electronics
22. **Nowicki Andrzej**
    organic chemistry and technology, high-temperature technology
23. **Owczarczyk Andrzej**
    chemistry
24. **Owczarczyk Hanna B.**
    biology
25. **Palige Jacek**
    metallurgy
26. **Panta Przemysław**
    nuclear chemistry
27. **Pawelec Andrzej**
    chemical engineering
28. **Pawlukojć Andrzej**
    physics
29. **Pogocki Dariusz**
    radiation chemistry, pulse radiolysis
30. **Polkowska-Motrenko Halina**
    analytical chemistry
31. **Przybytniak Grażyna**
    radiation chemistry
32. **Ptasiewicz-Bąk Halina**
    physics
33. **Rafalski Andrzej**
    radiation chemistry
34. **Sadło Jarosław**
    chemistry
35. **Samczyński Zbigniew**
    analytical chemistry
36. **Skwara Witold**
    analytical chemistry
37. **Sochanowicz Barbara**
    biology
38. **Stachowicz Wacław**
    radiation chemistry, EPR spectroscopy
39. **Strzelczak Grażyna**
    radiation chemistry
40. **Stuglik Zofia**
    radiation chemistry
41. **Szpilowski Stanisław**
    chemistry
42. **Tymiński Bogdan**
    chemistry
43. **Warchoł Stanisław**
    solid state physics
44. **Wąsowicz Tomasz**
    radiation chemistry, surface chemistry, radical chemistry
45. **Wierzchnicki Ryszard**
    chemical engineering
46. **Wiśniowski Paweł**
    radiation chemistry, photochemistry, biophysics
47. **Wojewódzka Maria**
    radiobiology
48. **Zakrzewska-Trznadel Grażyna**
    process and chemical engineering
49. **Zimek Zbigniew**
    electronics, accelerator techniques, radiation processing

RADIATION CHEMISTRY
AND PHYSICS,
RADIATION TECHNOLOGIES

EPR STUDY OF RADIATION-INDUCED RADICALS IN AROMATIC CARBOXYLIC ACIDS CONTAINING THIOETHER GROUP. PART II.

Grażyna Strzelczak, Anna Korzeniowska-Sobczuk, Krzysztof Bobrowski

Sulfur-centred radicals and radical cations derived from aromatic sulfides play an important role in many chemical processes as: organic synthesis, and in environmental issues. Recently, sulfur-centred radicals derived from coinitiators have proven to be effective in photopolymerizations. Moreover, they are implicated in many biochemical processes, including those connected with the oxidative stress, aging, and with pathologies such as Alzheimer's disease.

In this report, we present the results of electron spin resonance (ESR) studies of radicals formed in γ-irradiated polycrystalline aromatic carboxylic acids containing thioether group in various position in relation to the aromatic ring and to the carboxylic function.

Four aromatic carboxylic acids containing thioether group: 4-(methylthio)benzoic acid – *p*-CH_3-S-C_6H_4-COOH (**1**), 4-(methylthio)phenylacetic acid – *p*-CH_3-S-C_6H_4-CH_2-COOH (**2**), α-(phenylthio)phenylacetic acid – C_6H_5-S-CH(C_6H_5)-COOH (**3**) and 2-(naphtylthio)acetic acid – $C_{10}H_9$-S-CH_2-COOH (**4**) were purchased from Aldrich and Lancaster.

The samples of polycrystalline acids were irradiated with doses of about 3 kGy in a ^{60}Co-source in liquid nitrogen.

The ESR measurements were performed using an X-band Bruker-300 spectrometer equipped with a cryostat and a variable temperature unit over the temperature range of 77-293 K.

Carbon dioxide (CO_2) was identified by a gas chromatography (GC) technique in samples exposed to γ-radiation.

The ESR spectra recorded at 95 K in (**1-3**) carboxylic acids were anisotropic singlets with g values: $g_{\|}$ = (2.024-2.013), and $g_{\perp}$ = (2.000-1.997). They were assigned to the monomeric sulfur radical cations (H_3C-$S^{+\bullet}$-C_6H_4-COOH), (H_3C-$S^{+\bullet}$-C_6H_4-CH_2-COOH), (C_6H_5-$S^{+\bullet}$-CH(C_6H_5)-COOH), respectively. In addition, a second singlet with g = 2.0068 and ΔH = 0.7 mT was assigned to the radical anions formed by an addition of electrons to the carboxyl groups (H_3C-S-C_6H_4-COOH)$^{\bullet-}$, (H_3C-S-C_6H_4-CH_2-COOH)$^{\bullet-}$, and (C_6H_5-S-CH(C_6H_5)-COOH)$^{\bullet-}$, respectively. As the temperature was increased over 150 K, in carboxylic acids (**1-3**) the spectra indicated presence of new anisotropic singlets with g values: $g_{\|}$ = (2.056-2.052), and $g_{\perp}$ = 2.000. These spectra were assigned to the thiyl-type radicals RS$^{\bullet}$ resulted from the fragmentation of the respective monomeric sulfur radical cations. Upon warming, sample (**1**) in addition to the anisotropic singlet, spectra recorded at 230-273 K indicated the triplet component with g = 2.005 and hyperfine splitting ΔH = 1.7 mT. This component was attributed to the α-(alkylthio)alkyl radicals, $H_2C^{\bullet}$-S-C_6H_4-COOH. These spectra are stable up to 293 K (Fig.1).

The spectrum observed for (**2**) at 230-273 K consists of a triplet with g = 2.0025 and hyperfine splitting a_H = 1.5 mT. This triplet was assigned to the H_3C-S-C_6H_4-$^{\bullet}CH_2$ radical resulted from decarboxylation process. Upon warming to 293 K, the spectrum consists of a doublet with g = 2.0025 and hyperfine splitting a_H = 1.3 mT assigned to the H-abstraction radical H_3C-S-C_6H_4-$^{\bullet}$CH-COOH (Fig.2).

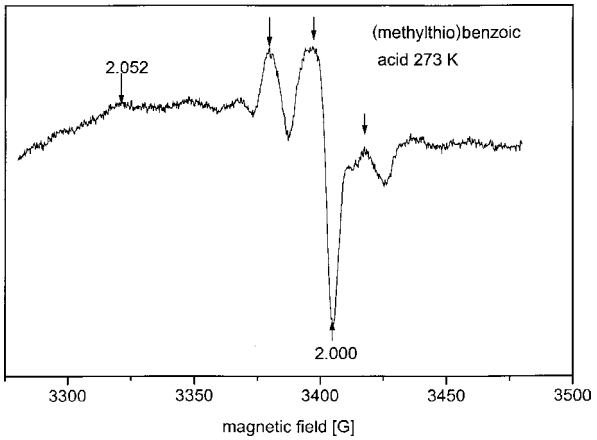

Fig.1. EPR spectrum recorded at 273 K in γ-irradiated (methylthio)benzoic acid at 77 K.

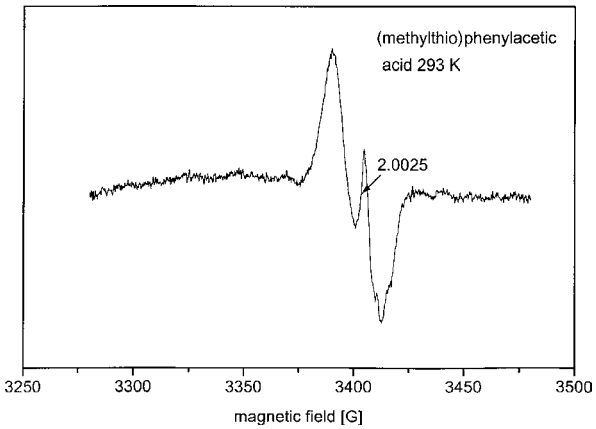

Fig.2. EPR spectrum recorded at 293 K in γ-irradiated (methylthio)phenylacetic acid at 77 K.

Warming the sample (**3**) to 180-273 K resulted in the appearance of a broad singlet with ΔH = 3.0 mT with g_{av} = 2.0027 containing 6 equally spaced lines with a_H = 0.6 mT (due to the interaction with 5 protons in the phenyl ring). This spectrum was assigned to C_6H_5-S-$C^{\bullet}$(C_6H_5)-COOH radical resulted from deprotonation of respective monomeric sulfur radical cation. The ESR spectrum recorded at 293 K indicated a doublet with g = 2.0025 and a_H = 1.5 mT. This spectrum was assigned to C_6H_5-S-$CH^{\bullet}$-(C_6H_5) radicals formed *via* decarboxylation process.

In contrast with the ESR spectra previously recorded for carboxylic acids (**1-3**) at 95 K, the ESR signal recorded in sample (**4**) consists of three lines

characterized by a high g anisotropy (g = 2.07, 2.056, and 2.042) which can be assigned to $g_{||}$-factors of sulfur-centered radicals. One can also recognize an anisotropic singlet assigned to the monomeric sulfur radical cation ($C_{10}H_9$-$S^{+\bullet}$-CH_2-COOH), and a second singlet assigned to the radical anion formed by an addition of an electron to the carboxyl group $(C_{10}H_9\text{-S-}CH_2\text{-COOH})^{\bullet-}$. At 293 K a weak triplet was recognized with g = 2.0025 and hyperfine splitting a_H = 1.6 mT, which can be assigned to the $C_{10}H_9$-S-$^{\bullet}CH_2$ radical resulted from decarboxylation process.

Carbon dioxide was identified and quantified in all polycrystalline samples of aromatic carboxylic acids studied and exposed to γ-radiation. The calculated yields of decarboxylation (expressed in G-units) are in the range of 0.2-3.5.

This work described herein was supported by the Polish State Committee for Scientific Research (KBN) – grant No. 3 T09A 037 19.

SPECTRAL AND CONDUCTOMETRIC PULSE RADIOLYSIS STUDIES OF RADICAL CATIONS DERIVED FROM *N*-ACETYL-METHIONINE METHYL ESTER

Krzysztof Bobrowski, Dariusz Pogocki, Gordon L. Hug[1/], Christian Schöneich[2/]

[1/] Radiation Laboratory, University of Notre Dame, USA

[2/] Department of Pharmaceutical Chemistry, University of Kansas, Lawrence, USA

In our previous report [1] we have shown that the sulfide radical cation of *N*-acetyl-methionine amide (*N*-Ac-Met-NH_2) might associate with the deprotonated amide nitrogen localized either N- or C-ter-

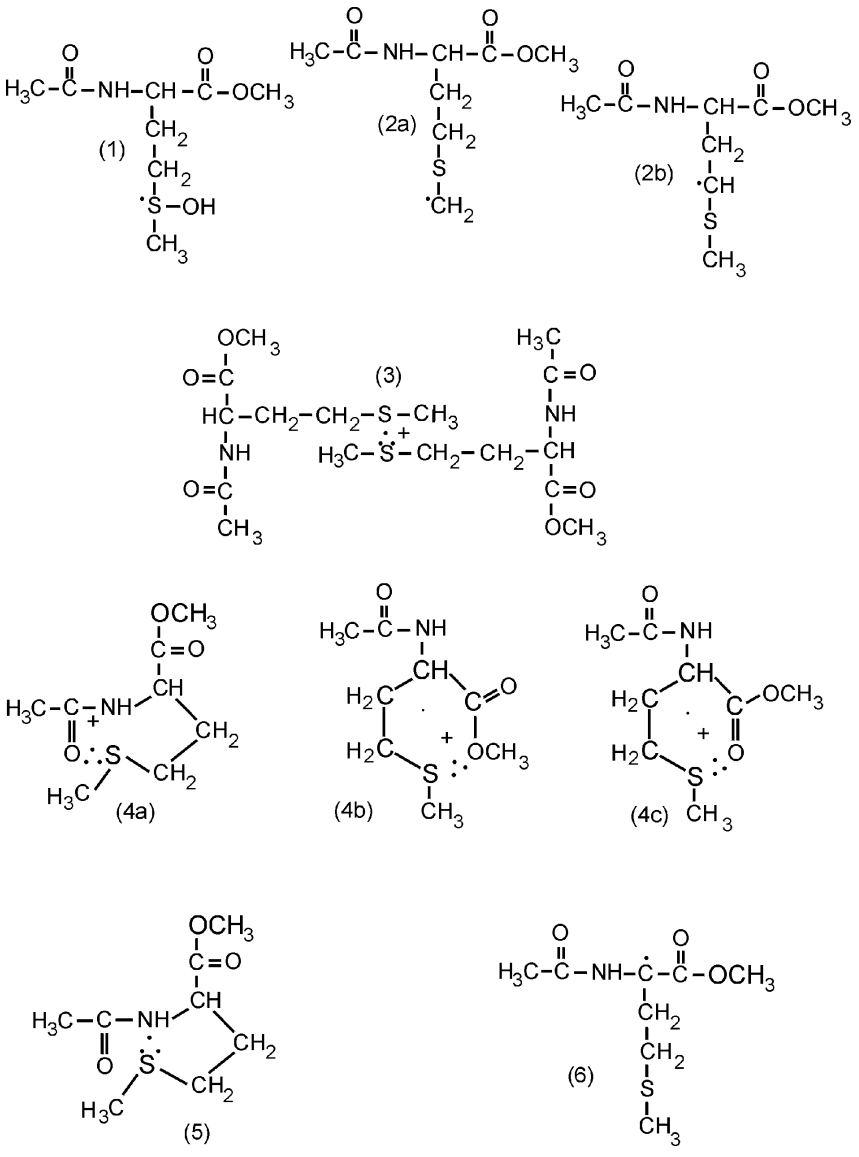

Chart 1.

minally to Met [2]. Mechanistically, the association with the C-terminal amide nitrogen would be easy to rationalize by a process involving first S-O bond formation followed by amide deprotonation and O-to-N migration of the sulfide radical cation resulting in the S-N bond formation, both bonds in thermodynamically favorable six-membered rings [1]. On the other hand, formation of the S-N bond with N-terminally localized nitrogen atom (although in a favorable five-membered ring) (Chart 1 – **5**) has to be preceded by the formation of the S-O bond in a seven-membered ring (Chart 1 – **4a**). In order to check whether such mechanism is possible, we have selected *N*-acetyl-methionine methyl ester (*N*-Ac-Met-OMe), a Met derivative lacking the C-terminal amide. In this case, only the possibility for the N-terminal S-N bond formation exists.

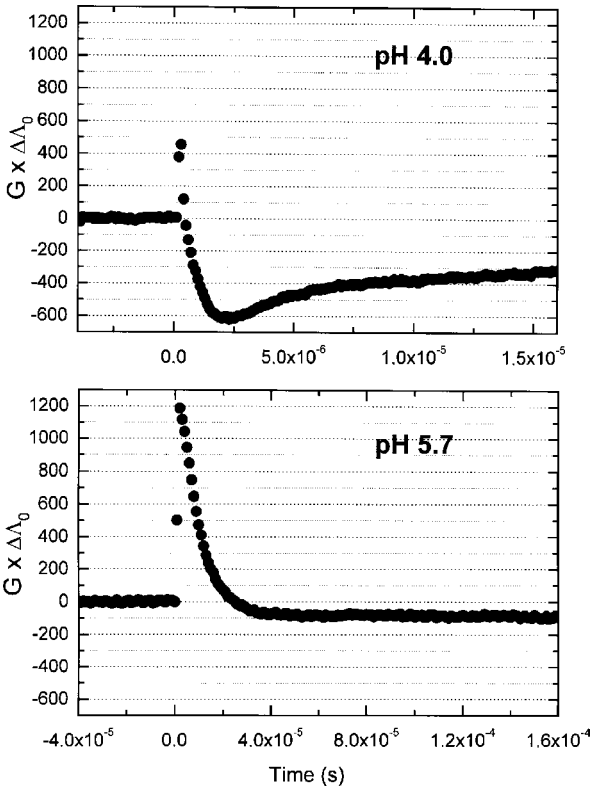

Fig.1. The equivalent conductivity changes represented as ($G \times \Delta\Lambda_0$) *vs*. time profile following the $^{\bullet}$OH-induced oxidation of *N*-acetyl-methionine methyl ester (0.2 mM) in N_2O saturated aqueous solutions at pH 4.0 and 5.7.

Time-resolved conductivity experiments with *N*-Ac-Met-OMe have shown decreasing amplitudes of negative conductivity with increasing pH (Fig.1). The different maximum loss of equivalent conductivity indicates a pH-dependent change in the yields of radical cations (Chart 1 – **3** and **4a,b,c**). Moreover, these yields are very comparable to those from *N*-Ac-Met-NH_2. This pH-dependent change in the yields of (**3**) and (**4a,b,c**) (Chart 1) would suggest that the S-N bond formation is generally possible with N-terminally localized nitrogen atom of the peptide bond. This was confirmed by time-resolved optical spectroscopy (*vide infra*).

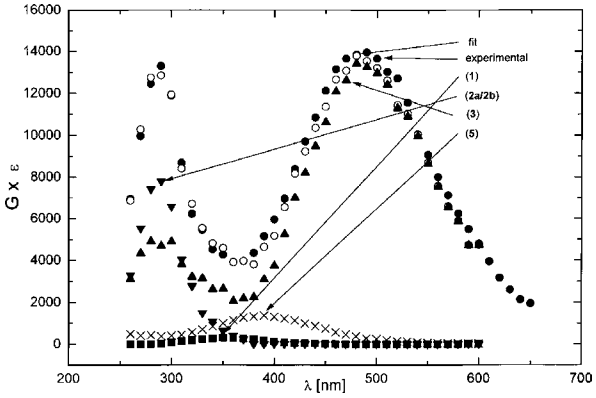

Fig.2. Resolution of the spectral components in the transient absorption spectra following the $^{\bullet}$OH-induced oxidation of *N*-acetyl-methionine methyl ester (0.2 mM) in N_2O saturated aqueous solutions at pH 4.0 taken 4 μs after the pulse.

The $^{\bullet}$OH-induced reaction pathways in *N*-Ac-Met-OMe have been characterized by the complementary pulse radiolysis measurements coupled to time-resolved UV-VIS spectroscopy. The optical spectrum recorded 2 μs after pulse irradiation is well deconvoluted into contributions from: the hydroxysulfuranyl radical (**1**), the two-α--(alkylthio)alkyl radicals (**2a,b**), the intermolecularly sulfur-sulfur three-electron bonded dimeric radical cation (**3**), and the intramolecular sulfur-oxygen bonded radical cations (**4a,b,c**) (Chart 1). The total yield of radical cations, $G_{3\,+\,4a,b,c} = 2.6$, is in a fairly good agreement with G(ions) = 2.4. Best results are obtained when deconvolutions take into account the simultaneous formation of (**4a,b,c**) and (**5**), yielding a perfect match between G(ions) = $G_{3\,+\,4a,b,c} = 2.4$. Importantly, at 4 μs after the pulse, species (**4a,b,c**) are replaced by species (**5**), which is evident from the deconvolution in Fig.2 and the agreement between G(ions) = 2.1 and $G_3 = 2.1$. For higher pH 5.7, in order to obtain the agreement between G(ions) measured in the time-resolved conductivity and G(ions) measured in the time-resolved optical measurements, deconvolution of the optical spectrum recorded 40 μs after pulse irradiation (Fig.3) requires the presence of (**5**), instead of (**4a,b,c**).

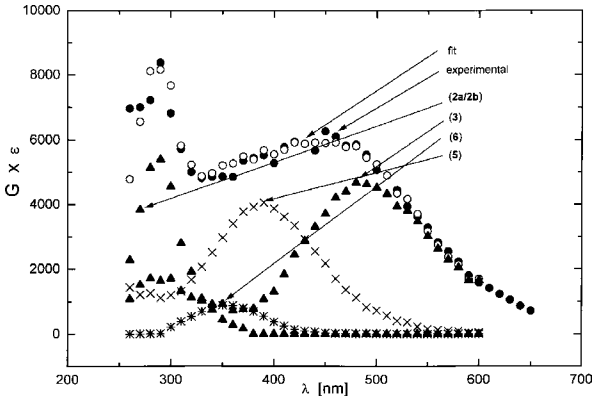

Fig.3. Resolution of the spectral components in the transient absorption spectra following the $^{\bullet}$OH-induced oxidation of *N*-acetyl-methionine methyl ester (0.2 mM) in N_2O saturated aqueous solutions at pH 5.7 taken 40 μs after the pulse.

In this report, by applying complementary time-resolved conductivity and UV-VIS spectrophotometric measurements in *N*-Ac-Met-OMe, we provide evidence that formation of the S-N bond involves N-terminally to Met residue located nitrogen atom in the peptide bond. Formation of the species (**5**) is preceded by the formation of the species (**4a**) (Chart 1).

This report is a part of the original paper [3] and was presented during 23th Radiation Chemistry Miller Conference and 1st International Meeting on Applied Physics APHYS-2003.

References

[1]. Bobrowski K., Pogocki D., Hug G.L., Schöneich Ch.: In: INCT Annual Report 2002. Institute of Nuclear Chemistry and Technology, Warszawa 2003, pp.23-25.
[2]. Schöneich Ch., Pogocki D., Wiśniowski P., Hug G.L., Bobrowski K.: J. Am. Chem. Soc., 122, 10224-10225 (2000).
[3]. Schöneich Ch., Pogocki D., Hug G. L., Bobrowski K.: J. Am. Chem. Soc., 125, 13700-13713 (2003).

SPECTRAL STUDIES OF RADICAL CATIONS DERIVED FROM (BENZYLTHIO)ACETIC ACID AND BENZYL METHYL SULPHIDE

Anna Korzeniowska-Sobczuk, Jacek Mirkowski, Krzysztof Bobrowski

Introduction

Chemistry of sulphur-centred radicals and radical cations derived from aromatic thioethers play an important role in many processes including those of organic synthesis [1], environmental [2], photo-induced polymerization [3], xenobiotic-glutathion conjugates [4, 5] and biological significance [6, 7]. An important feature of monomeric sulphur radical cations derived from aromatic thioethers is their propensity to form relatively stable monomeric radical cations because of the spin delocalization onto aromatic ring [8, 9]. On the other hand, monomeric sulphur radical cations derived from aliphatic thioethers form relatively stable dimeric radical cations with neutral parent molecules. These dimeric intermediates are characterized by two-center, three-electron bonds [10, 11].

In (benzylthio)acetic acid the thioether group is separated from the aromatic ring by the methylene group. Therefore, it might be expected that chemical properties of the monomeric sulphur radical cation derived from this acid should resemble those of the monomeric sulphur radical cations derived from aliphatic thioethers. Benzyl methyl sulphide was used as a model compound in order to eliminate decarboxylation, one of the potential reaction pathway in the decay of monomeric sulphur radical cations derived from (benzylthio)acetic acid [12].

Reaction of $^{\bullet}OH$ radicals with (benzylthio)acetic acid

Transient optical absorption spectrum (Fig.1) obtained on pulse radiolysis of N_2O-saturated neutral aqueous solution of (benzylthio)acetic acid is characterized by a strong absorption band with λ_{max} = 320 nm and two shoulders located in the range 280-300 and 350-390 nm. The absorption band with λ_{max} = 320 nm can be tentatively assigned to the Ph-CH_2-S-$CH_2^{\bullet}$ (**3ab**) and Ph-$CH_2^{\bullet}$ (**6ab**). A stronger shoulder can be assigned to Ph-CH_2-S-$CH^{\bullet}$-COOH (**5a**) and Ph-$CH^{\bullet}$-S-CH_2-COOH (**4a**) radicals. On the other hand, a weaker shoulder can be attributed both to hydroxycyklohexadienyl- (**7a**) and cyclohexadienyl-type radicals. However, no absorption band located in the region of 530-550 nm was observed that could be assigned to the monomeric sulphur radical cation (**2a**). The monomeric sulphur radical cation derived from (benzylthio)acetic acid seems to be characterized by a very short life-time.

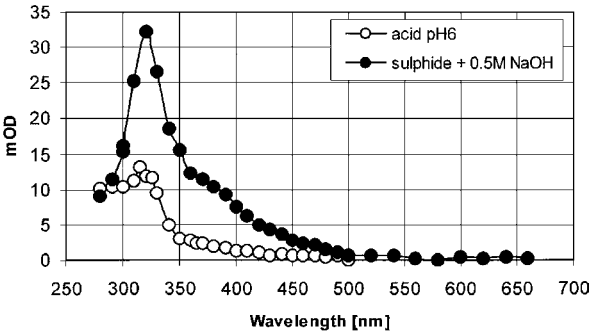

Fig.1. Transient absorption spectra recorded after 700 ns pulse irradiation of N_2O-saturated aqueous solutions containing 2 mM (benzylthio)acetic acid at pH 6.0 and 2 mM benzyl methyl sulphide + 5 M NaOH.

Reaction of $O^{\bullet-}$ radical anions with benzyl methyl sulphide

In N_2O-saturated strong alkaline solution e^-_{aq}, H and $^{\bullet}OH$ are converted into $O^{\bullet-}$ *via* the following reactions:

$$^{\bullet}OH + OH^- \leftrightharpoons O^{\bullet-} + H_2O$$
$$H^{\bullet} + OH^- \longrightarrow e^-_{aq}$$
$$e^-_{aq} + N_2O \longrightarrow N_2 + O^{\bullet-}$$

Oxide radical ions $O^{\bullet-}$ react preferentially with the aliphatic group by H-abstraction. Transient optical absorption spectrum obtained on pulse radiolysis of N_2O-saturated alkaline aqueous solution of benzyl methyl sulphide is characterized by a strong absorption band with λ_{max} = 320 nm. Comparison of transient absorption bands formed in aqueous solutions of benzyl methyl sulphide and (benzylthio)acetic acid allows assignment of the spectrum with λ_{max} = 320 nm to Ph-CH_2-S-$CH_2^{\bullet}$ (**3ab**) and Ph-$CH^{\bullet}$-S-CH_3 (**4b**) radicals (Fig.1).

Reaction of $^{\bullet}OH$ radicals with benzyl methyl sulphide

The pulse radiolysis of an N_2O-saturated aqueous solution containing 2 M $HClO_4$ and 2 mM benzyl methyl sulphide leads to spectra shown in Fig.2.

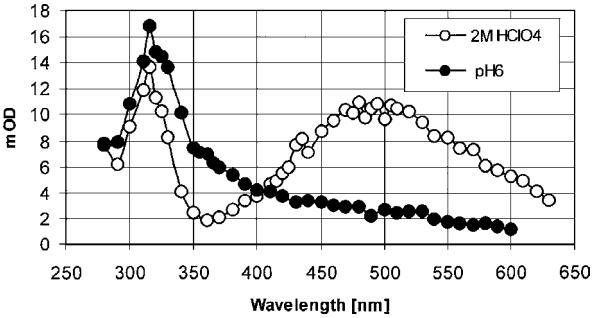

Fig.2. Transient absorption spectra recorded after 700 ns pulse irradiation of an N_2O-saturated aqueous solutions containing 2 mM benzyl methyl sulphide + 2 M $HClO_4$ and 2 mM benzyl methyl sulphide at pH 6.0.

The absorption band with λ_{max} = 320 nm was attributed accordingly to Ph-$\dot{C}H_2$-S-$CH_2^{\bullet}$ (**3ab**) and Ph-$CH^{\bullet}$-S-CH_3 (**4b**) radicals by comparison to spectra formed in benzyl methyl sulphide *via* reaction with $O^{\bullet-}$ radicals. The second absorption band with λ_{max} = 480 nm can be assigned to the dimeric radical cations (**5b**) since their yield is dependent on the concentration of sulphide. At neutral pH the absorption band with λ_{max} = 360 nm is attributed both to hydroxycyclohexadienyl- (**7b**) and cyclohexadienyl-type radicals.

Reaction mechanism

$^{\bullet}$OH induced oxidation mechanism of (benzylthio)acetic acid and benzyl methyl sulphide is identical in a primary stage. It occurs *via* two competitive addition pathways: to the thioether functionality and to the aromatic ring (Scheme 1) that lead to **1a**, **1b** and **7a**, **7b** radicals respectively. At low pH radicals **1a** and **1b** undergo proton-catalyzed elimination of water resulting in the formation of sulphur monomeric radical cations (**2a**, **2b**). The monomeric sulphur radical cations derived from (benzylthio)acetic acid (**2a**) are very unstable. They undergo a very fast decarboxylation that leads to α-(alkylthio)alkyl radicals (**3ab**). Moreover, based on the analysis of stable products the monomeric sulphur radical cations fragmentation and deprotonation. These reactions lead to benzyl radicals (**6ab**) and α-(alkylthio)alkyl radicals (**4a** and **5a**) respectively. On the other hand, monomeric sulphur radical cations (**2b**) derived from benzyl methyl sulphide undergo either dimerization with parent sulphide molecules (at high sulphide concentration) that leads do dimeric sulphur radical cations (**5b**) or deprotonation that leads to α-(alkylthio)alkyl radicals (**3ab** and **4b**).

Conclusion

Monomeric sulphur radical cations derived from (benzylthio)acetic acid are very unstable since they undergo a very fast decarboxylation. Monomeric sulphur radical cations derived from benzyl methyl sulphide are stabilized as intermolecular three-electron bonded dimeric radical cations or undergo deprotonation to respective α-(alkylthio)alkyl radicals.

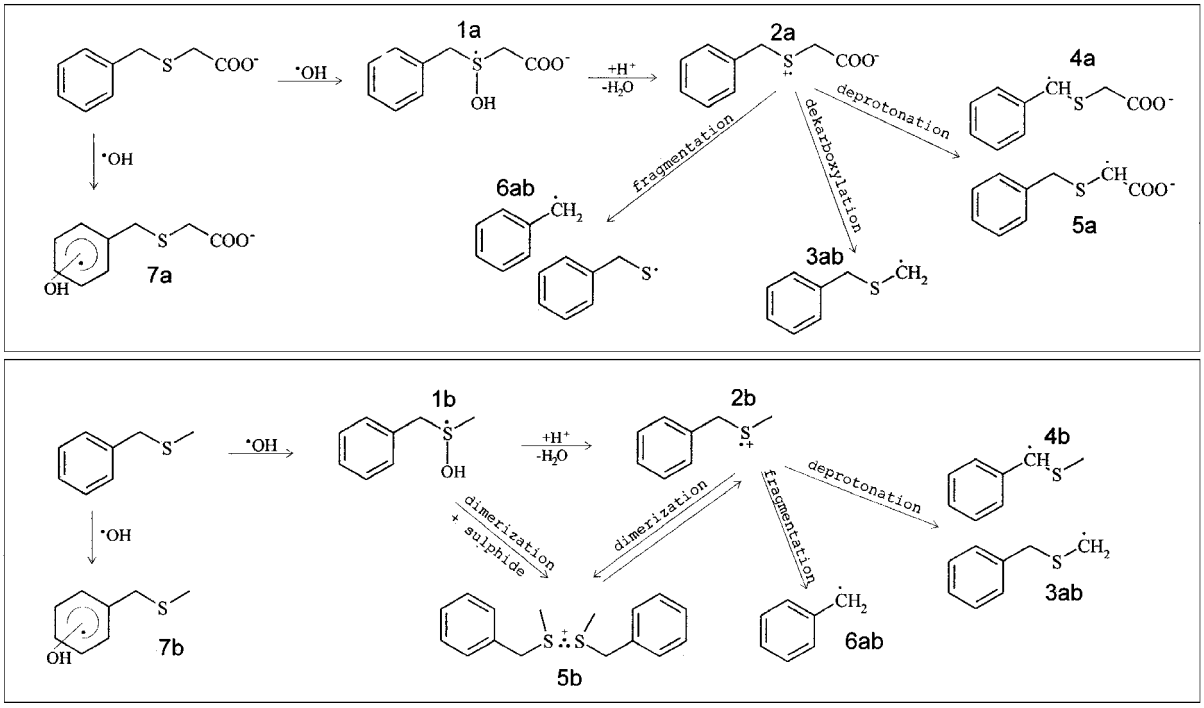

Scheme 1.

This work described herein was supported by the Polish State Committee for Scientific Research (KBN) – grant No. 3 T09A 037 19.

References

[1]. Chatgilialoglu C., Bertrand M.P., Ferreri C.: In: S-centered radicals. Ed. Z.B. Alfassi. John Wiley & Sons Ltd., Chichester 1999, pp.311-354.

[2]. Tobien T., Cooper W.J., Nickelesen M.G., Pernas E., O'Shea K.E., Asmus K.-D.: Env. Sci. Technol., 34, 1286-1291 (2000).

[3]. Wrzyszczynski A., Filipiak P., Hug G.L., Marciniak B., Paczkowski J.: Macromolecules, 33, 1577-1582 (2000).

[4]. Seńczuk W.: Toksykologia. Wydawnictwo Lekarskie PZWL, 2002, pp.149-152.

[5]. Monks T.J., Lau S.S.: Chem. Res. Toxicol., 10, 1296-1313 (1997).

[6]. Ozaki S., de Montelano O.: J. Am. Chem. Soc., 117, 7056-7064 (1995).
[7]. Stubbe J.A., van der Donk W.A.: Chem. Rev., 98, 705-762 (1998).
[8]. Asmus K.-D.: In: S-centered radicals. Ed. Z.B. Alfassi. John Wiley & Sons Ltd., Chichester 1999, pp.141-191.
[9]. Korzeniowska-Sobczuk A., Hug G.L., Carmichael I., Bobrowski K.: J. Phys. Chem. A, 106, 9251-9260 (2002).
[10]. Asmus K.-D.: Nukleonika, 45, 3-10 (2000).
[11]. Asmus K.-D.: In: Sulphur-Centered Reactive Intermediates in Chemistry and Biology. Eds. C. Chatgilialoglu, K.-D. Asmus. Plenum Press, New York 1990, Vol.197, pp.155-172.
[12]. Korzeniowska-Sobczuk A., Hug G.L., Bobrowski K.: In: INCT Annual Raport 2001. Institute of Nuclear Chemistry and Technology, Warszawa 2002, pp.19-21.

CESR IN SMALL SILVER PARTICLES

Marek Danilczuk, Jarosław Sadło, Anders Lund[1/], Hirohisa Yamada[2/], Jacek Michalik

[1/] Department of Physics and Measurements Technology, Linköping University, Sweden
[2/] National Institute for Material Science, Tsukuba, Japan

Electron paramagnetic resonance (EPR) spectroscopy has been used to study of conduction electron spin resonance (CESR) in small silver particles stabilized in dehydrated Ag-rho zeolite. Silver particles were produced during hydrogen reduction at different temperatures and diameter of the stabilized particles was calculated based on the Kawabata theory [1].

Metallic nanoparticles are of special interest because of quantum size effects which distinctly modify their physical and electronic properties. When the percentage of surface atoms becomes comparable to the total number of atoms in cluster, the states density changes can lead to the changes of properties from conducting to superconducting or semiconducting.

Transition metal clusters supported on silica or zeolites are active in numerous chemical processes of heterogeneous catalysis. The studies on cluster nuclearity and uniformity became especially important since it was found that the catalytical activity and selectivity depends on cluster size. Different experimental techniques such as scanning electron microscopy (SEM), X-ray diffraction (XRD), infrared radiation (IR) and electron spin resonance (ESR) have been used for that purpose [2-5].

The ESR studies of γ-irradiated silver zeolites proved that the nuclearity of stabilized Ag clusters depends on several factors as silver loading, framework porosity, total cation capacity, degree of dehydratation and others [6-9].

Recently, we carried out CESR measurements on silver, platinum and palladium nanoclusters in mesoporous materials. Kawabata's theory which relates the CESR linewidth to the diameter of metal particles has been used to calculated the nuclearity of silver clusters [10]. Pulsed and continuous wave (cw) ESR techniques were used to study silver metallic nanoparticles in amorphous SiO_2 and crystalline TiO_2 oxides [11-12].

The NaCs-rho zeolite synthesized by a modified Robson's method [13] in cationic form was exchanged three times with 20% solution of NH_4NO_3 followed by calcination at 573 K in air for 20 h to prepare the protonic form of zeolite. The H-rho was ion exchanged with $AgNO_3$ water solution for 24 h in the dark at room temperature. The zeolite powder was then repeatedly washed with distillated water to remove excess of silver and subsequently dried in air at room temperature. Then the samples were dehydrated in a vacuum line increasing gradually the temperature to 573 K. After dehydratation the zeolite samples were reduced with 40 kPa of hydrogen in the temperature range 323-873 K.

The EPR spectra were recorded with an X-band Bruker ESP 300 spectrometer equipped with a liquid helium cryostat which enables to control the temperature of the tested sample in the range 4-300 K. The room temperature ESR spectra were checked for zeolite samples at two stages of preparation – first after dehydratation and second during hydrogen reduction at increasing temperature. In the dehydrated Ag-rho sample, before hydrogen reduction, no ESR signal was detected. However, after hydrogen reduction at 323 K a narrow symmetric ESR singlet of low with no hyperfine structure was recorded. Its intensity increased with temperature of reduction reaching maximum at 723 K. The ESR spectra of Ag-rho reduced at 723 K and recorded at 4 and 300 K are shown in Fig.1.

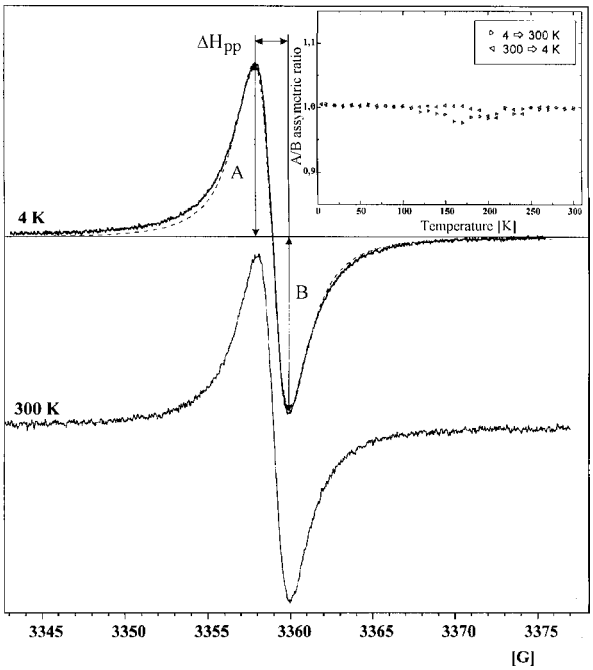

Fig.1. The ESR spectra of Ag-rho recorded at 4 and 300 K and temperature dependence of asymmetric ratio (inset).

The experimental spectra were simulated assuming the Lorentzian lineshape. The lineshape and symmetry of the ESR singlet do not depend on temperature in the range 4-300 K. Asymmetric ratio A/B (which is defined as the ratio of the peak high of maximum (A) to the peak height at minimum (B), both measured with respect to the zero line of the resonance derivative) is equal to 1 (Fig.1, inset). This indicates that electron diffusion does not occur and skin depth is much grated than the particle dimension.

As is shown in Fig.2, the line width (Fig.2a) which exhibits very small changes with temperature – ΔH_{pp} decrease from 0.210 mT at 300 K to 0.199 mT at 4.2 K. Similarly, the g factor of ESR singlet does not depend on temperature and is equal to 2.0026 in the whole temperature range (Fig.2b).

In standard ESR first measurements, the derivative of the imaginary part of the paramagnetic susceptibility $\chi_{(ESR)}/dH$ is recorded as a function of the external magnetic field. Thus, the double integrate of EPR signal is directly proportional to the

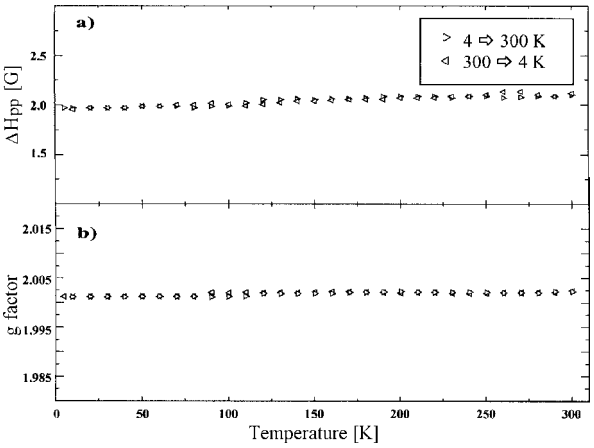

Fig.2. Temperature dependence of line width ΔH_{pp} (a) and g factor (b).

paramagnetic susceptibility. In the temperature range of 4-300 K, the singlet intensity is practically temperature independent. This means that the sample exhibits Pauli – like temperature relationship – independence of paramagnetic susceptibility, which is characteristic for metallic behavior. Small variation of the ESR intensity in this temperature region can be accounted of the changes of the resonator Q factor.

Based on these results, we assign the ESR singlet shown in Fig. 1 to the resonance of conduction electrons (CESR) in small silver clusters showing quantum size effect.

High stability of silver particles (ESR signal is stable over year) suggests that silver clusters are effectively isolated inside rho zeolite which makes them unusually stable. Since the line width of CESR signal is not changed with the reduction of temperature, it is postulated that bigger silver clusters are not formed.

The basic properties of small metal clusters are determined by the discrete energy spacing between adjacent levels. Observation of CESR has been reported in a relatively small numbers of papers. Usually, even microparticles of metals are large enough, so the conduction-electron energy levels are quasi continuous. For heavy metals the spin relaxation times of conduction electrons are very short which makes CESR lines very broad and difficult or impossible to detect. However, Dyson [14] suggests that for very small metallic particles classical scattering mechanism should be modified. For particles with diameter smaller than rf skin depth, the conduction electron is scattered by the surface of a particle with probability of a spin flip given by Δg_{∞}^2. In contrast, Kubo [15] postulates that the relaxation mechanism in very small metallic particles can be quenched due to discreetness of the conduction electron energy levels. As a result, the electronic properties of small metallic particles are changed and the observed CESR lines are very narrow.

According to the Kawabata's theory [1], when $\hbar\omega_z/\delta << 1$ and $\hbar/\tau_s\delta << 1$ are satisfied, a quantum size effect can be expected and the observed line width of conduction electrons is inversely proportional to the size of metallic particles and given by:

$$\Delta H_{pp} \cong \frac{\hbar\omega_z}{(\gamma_e\delta\tau_s)d} = \frac{V_F(\Delta g)^2 h\nu_e}{\delta\gamma_e d}$$

where: V_F – Fermi velocity of the conduction electrons, Δg – bulk metal g shift from $g_e = 2.0023$, $h\nu_e$ – electron Zeeman energy, δ – electronic level spacing, γ_e – magnetogyric ratio, ω_z – Zeeman frequency, d – particle diameter and τ_s – relaxation time (is given by $d/V_F(\Delta g)^2$).

Based on the observed line width and using $\Delta g = -1.9\cdot10^{-2}$ [16] and $V_F = 1.39\cdot10^6$ ms^{-1} for silver, we estimated the diameter of silver particles stabilized in Ag-rho zeolite as 0.6 nm.

The characteristics of CESR signal in reduced Ag-rho zeolite is very similar to the nature of CESR of small silver particles stabilized earlier in AlMCM-41 mesoporous materials.

References

[1]. Kawabata A.: J. Phys. Soc. Jpn., 29, 902 (1970).
[2]. Kim Y., Seff K.: J. Am. Chem. Soc., 100, 175 (1978).
[3]. Hemrschmitdt D., Haul R.: Ber. Bunsen-Ges. Phys. Chem., 84, 902 (1980).
[4]. Morton J.R., Preston K.F.: J. Magn. Reson., 68, 121 (1986).
[5]. Jacobs P.A., Uytterhoeven J.B., Beyer H.: J. Chem. Soc., Farday Trans., 75, 56 (1979).
[6]. Michalik J., Zamadics M., Sadlo J., Kevan L.: J. Phys. Chem., 97, 10440 (1993).
[7]. Sadlo J., Wasowicz T., Michalik J.: Radiat. Phys. Chem., 45, 909 (1995).
[8]. Wasowicz T., Michalik J.: Radiat. Phys. Chem., 37, 427 (1991).
[9]. Michalik J.: Appl. Magn. Reson., 10, 507 (1996).
[10]. Michalik J., Brown D., Jong-Sung Yu, Danilczuk M., Jeong Yeon Kim, Kevan L.: PCCP, 3, 1705 (2001).
[11]. Mitrikas G., Trapalis C.C., Kordas G.: J. Chem. Phys., 111, 8098 (1999).
[12]. Mitrikas G., Deligiannakis Y., Trapalis C.C., Boukos N., Kordas G.: J. Sol-Gel. Sci. Technol., 13, 503 (1998).
[13]. Robson H.E.: US Patent No. 3 904 738.
[14]. Dyson F.J.: Phys. Rev., 98, 349 (1955).
[15]. Kubo R.: J. Phys. Soc. Jpn., 17, 975 (1962).
[16]. Beuneu F., Monod P.: Phys. Rev. B, 18, 2422 (1978).

RADIATION-INDUCED OXIDATION OF DIPEPTIDE FRAGMENTS OF ENKEPHALINS

Gabriel Kciuk, Jacek Mirkowski, Krzysztof Bobrowski

Enkephalins (Chart 1), the class of opioid peptides, are of great interest because of their role as neurotransmitters or neuromodulators. The aromatic amino acids (tyrosine – Tyr and phenylalanine – Phe) and methionine (Met) residues are especially

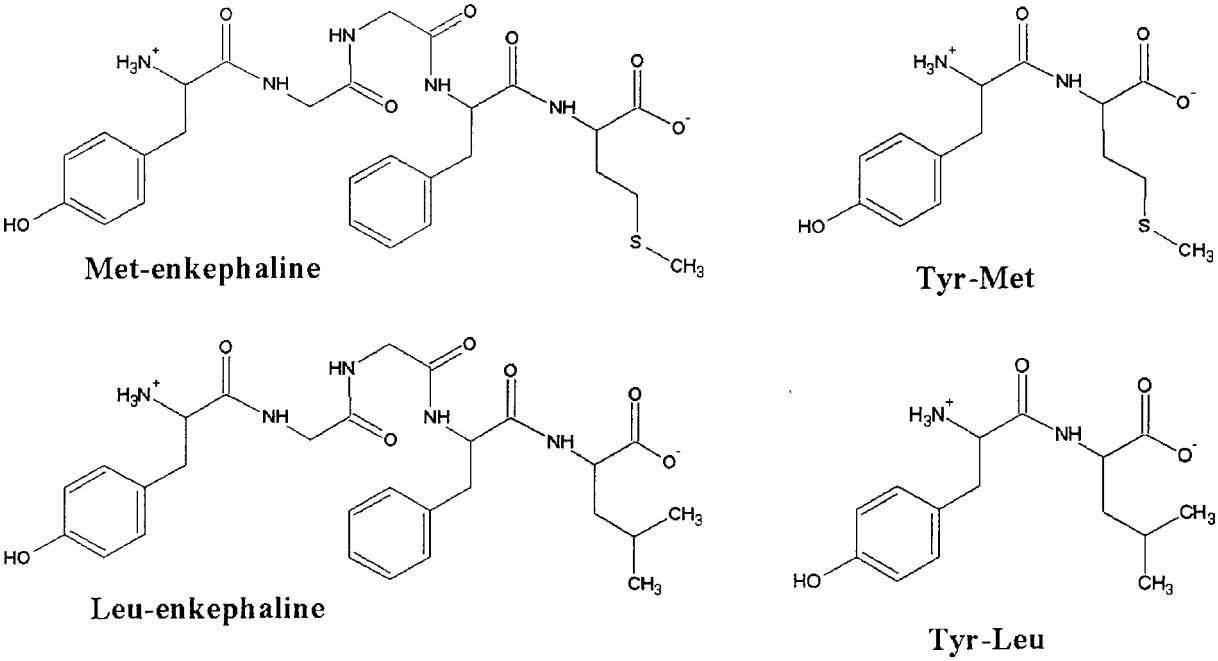

Chart 1.

susceptible to oxidation in these peptides. In the case of enkephalins functional changes upon oxidation might appear to be connected with activity, and to be of pathophysiological significance.

For better understanding of processes occurring in enkephalins, oxidation of the following dipeptides that mimick their fragments (Tyr-Met and Tyr-Leu) has been studied. Based on the rate constants of hydroxyl radicals ($^{\bullet}OH$) with individual aminoacids ($k = 1.2\times10^{10}$ [$M^{-1}s^{-1}$] for Met; $k = 1.3\times10^{10}$ [$M^{-1}s^{-1}$] for Tyr; and $k = 1.7\times10^{9}$ [$M^{-1}s^{-1}$] for leucine – Leu) for the similar experimental conditions (pH, dose) one can predict higher radiation chemical yield of tyrosyl radicals (TyrO$^{\bullet}$) in Tyr-Leu in comparison with Tyr-Met (Chart 1).

On the other hand, one can expect similar radiation chemical yields of TyrO$^{\bullet}$ in both dipeptides when azide radical ($^{\bullet}N_3$) has been used as one-electron oxidant. This is due to the redox potential of $^{\bullet}N_3$ ($E_0 = 1.33$ V) which allows selective oxidation of Tyr residues.

According to expectations, transient absorption spectra (with three absorption maxima at $\lambda = 290$, 390 and 405 nm) recorded in neutral aqueous solutions containing sodium azide (NaN_3) and Tyr-Leu or Tyr-Met (Fig.1) have been assigned to TyrO$^{\bullet}$. Moreover, intensities of absorption observed at the respective three maxima were similar. This confirms similar radiation chemical yields of TyrO$^{\bullet}$ expected in both dipeptides.

Contrary to the earlier predictions, TyrO$^{\bullet}$ are formed in Tyr-Met with substantial higher radiation chemical yields as compared with Tyr-Leu (Figs.2 and 3) when Tyr-Leu and Tyr-Met have been oxidized by $^{\bullet}OH$. Moreover, formation of TyrO$^{\bullet}$ in Tyr-Met occurs predominantly in a fast single kinetic step, contrary to Tyr-Leu where for-

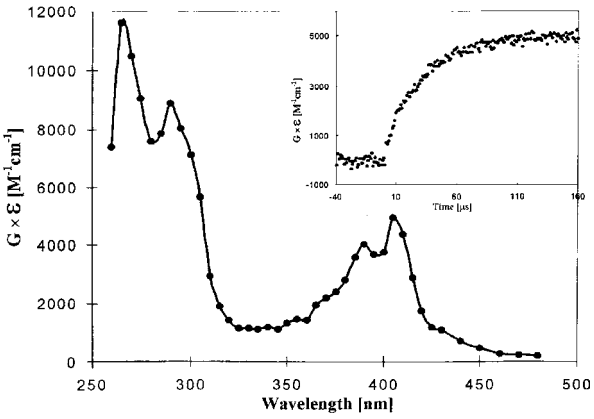

Fig.1. Transient spectrum recorded 140 µs after pulse irradiation of an N_2O-saturated aqueous solution containing 0.2 mM Tyr-Met and 0.1 M NaN_3 at pH 6.5. Inset: experimental kinetic trace recorded at $\lambda = 405$ nm (absorption maximum for tyrosyl radical).

mation of TyrO$^{\bullet}$ occurs in two kinetically distinguished steps (insets in Fig.2).

The following conclusions can be drawn:

- transformation of the primary radical site located on the Met residue to the TyrO$^{\bullet}$, as a result of electron transfer from the Tyr residue to the oxidized Met residue, is a predominant source of TyrO$^{\bullet}$ in Tyr-Met

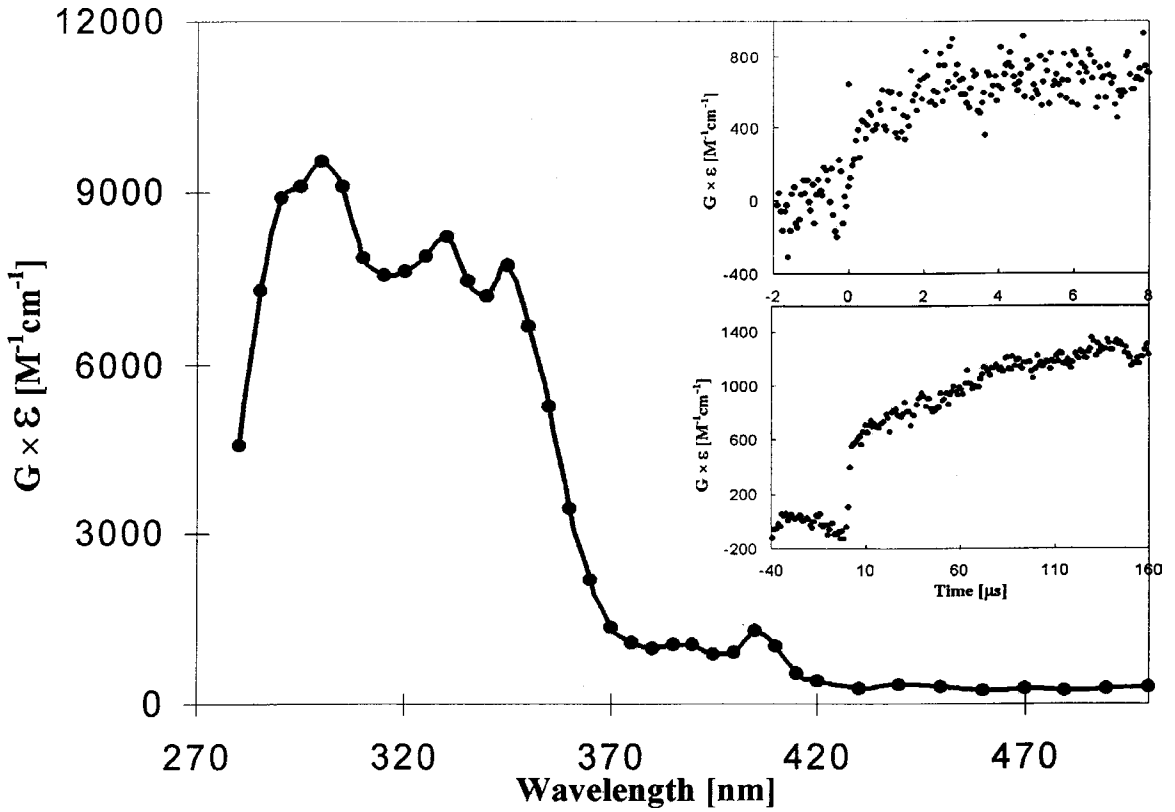

Fig.2. Transient spectrum recorded 140 μs after pulse irradiation of an N_2O-saturated aqueous solution containing 0.2 mM Tyr-Leu at pH 6.2. Insets: experimental kinetic traces recorded at λ = 405 nm (absorption maximum for tyrosyl radical) for various time windows.

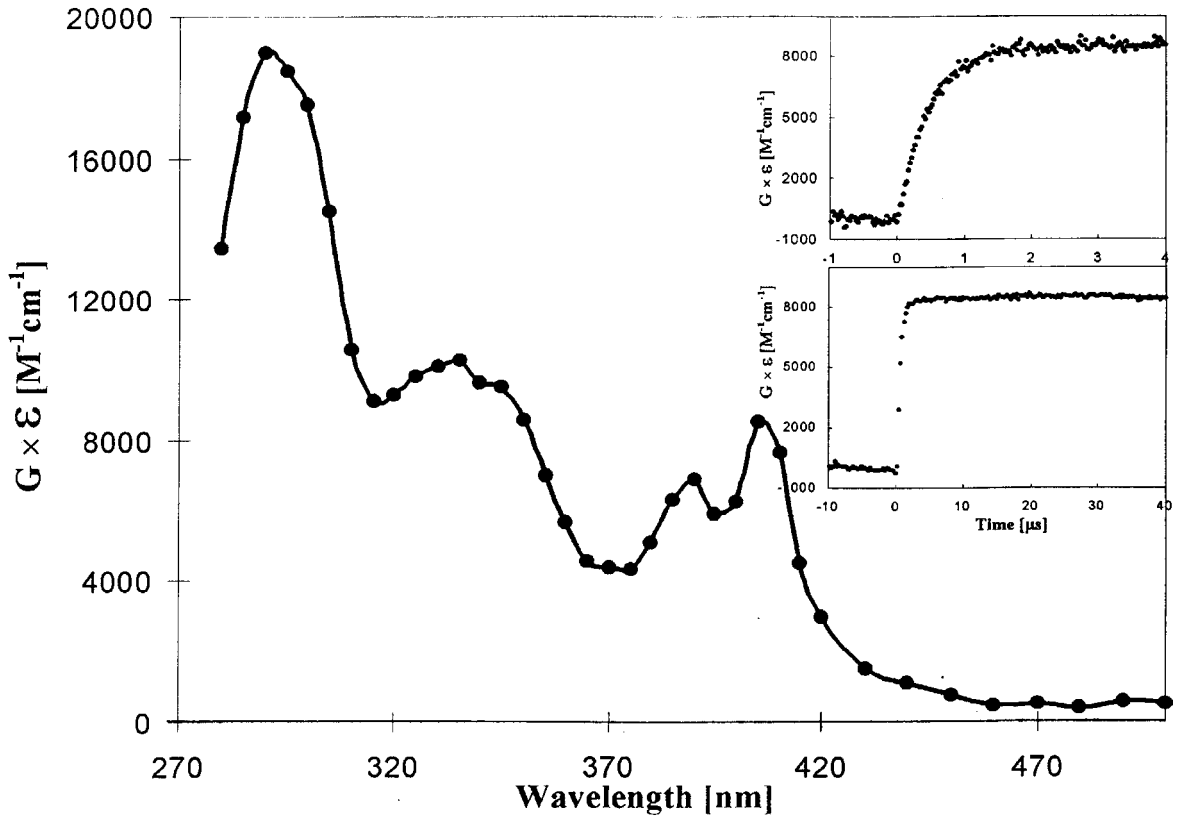

Fig.3. Transient spectrum recorded 140 μs after pulse irradiation of an N_2O-saturated aqueous solution containing 0.2 mM Tyr-Met at pH 6.5. Insets: experimental kinetic traces recorded at λ = 405 nm (absorption maximum for tyrosyl radical) for various time windows.

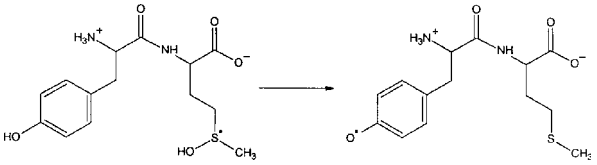

- dehydration of the hydroxycyklohexadienyl radical derived from Tyr seems to be of minor importance as a source of TyrO$^\bullet$ in Tyr-Met and Tyr-Leu.

References

[1]. Enkephalins and Endorphins. Stress and the Immune System. Eds. N.P. Plotnikoff, E.R. Faith, A.J. Murgo, R.A. Good. Plenum Press, New York 1998.

[2]. Ram M.S., Stanbury D.M.: Inorg. Chem., 24, 4233-4234 (1985).

[3]. Kciuk G., Mirkowski J., Bobrowski K.: In: INCT Annual Report 2001. Institute of Nuclear Chemistry and Technology, Warszawa 2002, pp.23-24.

[4]. Stadtman E.: In: Free Radicals, Oxidative Stress, and Antioxidants. Ed. T. Özben. Plenum Press, New York 1998, pp.131-143.

[5]. Adams. J.D., Odunze I.N.: Free Radical Biol. Med., 10, 161-169 (1991).

[6]. Markersbery W.R.: Free Radical Biol. Med., 23, 134-147 (1997).

[7]. Davies M.J., Dean R.T.: Radical-mediated protein oxidation. From Chemistry to Medicine. Oxford University Press, Oxford 1997.

THE ROLE OF CYSTEAMINE IN THE γ-RADIOLYSIS OF DNA. PART I. EPR STUDIES AT CRYOGENIC TEMPERATURES

Ewa M. Kornacka, Grażyna K. Przybytniak

In the present paper, we report the effects of cysteamine on the production of radical intermediates generated radiolytically in DNA at cryogenic temperatures as examined by electron paramagnetic resonance (EPR), together with their transformation at temperatures elevated above 77 K. Mechanisms can vary due to the influence of thiol on the indirect and direct actions of ionising radiation. In the first (indirect) process, the effect named "protection" prevents any attack of reactive species able to transfer damage to DNA by scavenging the species, as under irradiation of solvents (water) or solid matrices they could be formed in the vicinity of DNA. The "repair" can also appear and correct in a secondary process the damage already done to biomolecules by the reactive species. In the latter (direct) process of radiation, thiols are capable of correcting some direct radiation-induced damage to biomolecules *via* the "repair" effect [1].

Experimental EPR spectra were recorded at 77 K directly after irradiation and on annealing to higher temperatures. The changes of the superposed signals were detected at the same concentrations of cysteamine in the presence and absence of oxygen. The collected spectra were analysed using isolated signals obtained separately in frozen aqueous solutions in order to estimate the participation of some components in the overall radical population.

The $^\bullet$OH radical, formed on radiolysis in crystalline ice of a frozen aqueous solution of DNA at 77 K, decays in this phase below 140 K without crossing the phase barrier, and is therefore not considered as a damaging agent to DNA [2]. Its concentration in the applied system is *ca*. 50% at 77 K and has been subtracted before further analysis and not displayed in figures. The other identified radicals such as thymyl ($^\bullet$TH), peroxyl (DNAOO$^\bullet$) and thiyl (CyaS$^\bullet$) radicals, being mostly secondary species, appear at various elevated temperatures.

The results of the quantitative analysis of experimental EPR spectra shown in Fig.1 have been obtained in experiments performed under air (A), and under anoxic conditions (B) at 0, 10 and 100 mM concentrations of cysteamine in the temperature range 77-240 K.

At 77 K we can observe the protection of DNA on addition of the thiol, *i.e*. the lowering of the DNA radical concentration and the formation of CyaS$^\bullet$. The influence of thiol under cryogenic conditions, despite restrained diffusion, is possible, because on cooling, while the system becomes compartmentalised into phases, all additives are frozen out from the crystalline sphere of water and then condensed close to DNA surrounded by a glassy hydration layer. Additionally, the cysteamine positive charge +1 at physiological pH ($H_3N^+CH_2CH_2SH$) also enables condensation in the vicinity of the polyanionic DNA helix [3]. The protection of DNA is *ca*. 5% at the 10 mM concentration of cysteamine and *ca*. 27% at 100 mM of CyaSH under the influence of oxygen. A slightly smaller DNA protection, 22%, is observed at 100 mM CyaSH under anoxic conditions. These results are shown together with the formation of the thiyl radical upon annealing and subsequently its decays above 190 K. The fast decay of the $^\bullet$TH is accompanied by the rapid growth of DNA peroxyl radicals under oxic conditions.

In the present studies, in the presence of oxygen, the maximum concentration of thymyl radical, *i.e*. the octet contribution in the EPR spectrum at higher temperatures for 0 and 10 mM CyaSH, is about half of that observed under anoxic condition due to the effective oxidation of radical anions and $^\bullet$TH. Simultaneously, at elevated temperatures, relative participation of the singlet component increases considerably as a result of raising the relative participation of guanine radical cation. Obviously, this product shows a lower reactivity towards O_2 as confirmed earlier by Steenken [4]. As seen in Fig.1, more than 30% of DNA radi-

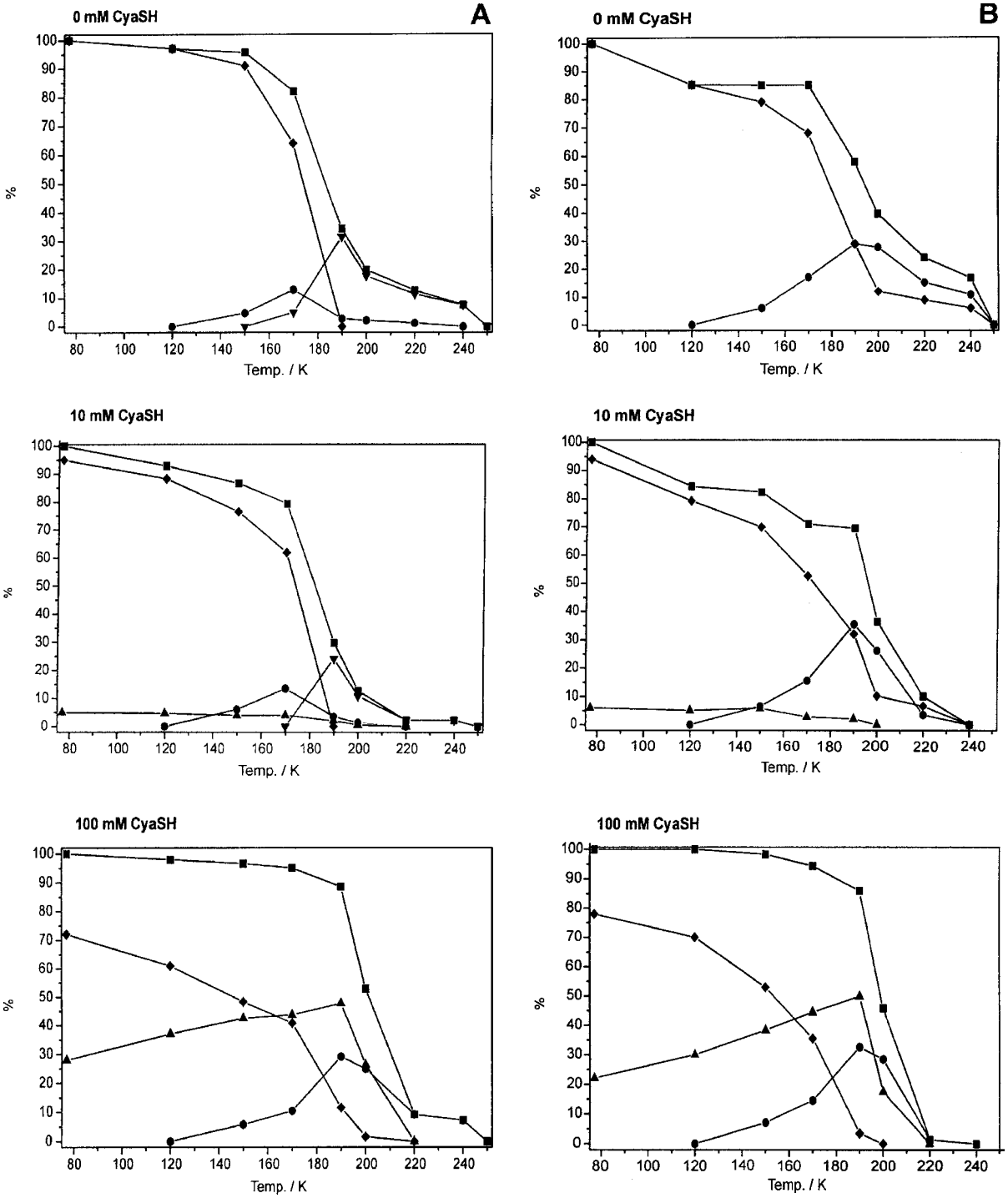

Fig.1. Relative concentrations of DNA and cysteamine radicals in frozen aqueous solutions in equilibrium with air (A, left column), and in deoxygenated system (B, right column), on irradiation at 77 K and upon annealing, without addition of cysteamine, and in presence of 10 and 100 mM of cysteamine: (■) total radicals (excluding $^{\bullet}$OH), (◆) DNA radicals except $^{\bullet}$TH (and DNAOO$^{\bullet}$, left column), (▼) DNAOO$^{\bullet}$ and (●) $^{\bullet}$TH, (▲) CyaS$^{\bullet}$.

cals can convert to peroxyl radical on warming if CyaSH is absent, only 20% in presence of 10 mM CyaSH and, at a concentration of 100 mM CyaSH, DNAOO$^{\bullet}$ is not detected.

In both systems, in the presence of 100 mM CyaSH, the first recorded spectra consist of the dominating doublet and signal of CyaS$^{\bullet}$. On warming the samples to 190 K, the amount of thiyl radical increases gradually as a result of the transfer of paramagnetic centres from DNA to cysteamine. Both effects, *i.e.* hole scavenging and other repair processes at higher temperatures, diminish the concentration of DNA radicals by almost 50%. Under aerated conditions the influence of the thiol is comparable, and no peroxyl radicals and higher thiyl radical contribution were detected. This indicates a high reactivity of the thiol or a thiyl radical towards molecular oxygen or peroxyl radicals [5].

As shown earlier, the level of $^{\bullet}$TH participation can serve as an indicator of the generation of all products formed *via* the reductive pathway. The

relationship between the curves presented in Fig.1 shows that the $^{\bullet}$TH level remains unchanged. Therefore, we can conclude that cysteamine is not involved in reactions with electron-excess species. This is clearly connected with the fact that thiols, being good electron donors, are active towards electron-loss and inactive towards electron-gain centres. Consequently, at high concentrations, CyaSH protects and repairs almost all DNA oxidative damage [6]. Another very important role of the thiol is the elimination of oxygen species from the system, which inhibits fixation of damage by the oxidation pathway.

References

[1]. Wang W., Sevilla M.D.: Int. J. Radiat. Biol., 66, 6, 683-695 (1994).
[2]. Ambroż H.B., Kemp T.J., Kornacka E.M., Przybytniak G.K.: Radiat. Phys. Chem., 53, 491-499 (1998).
[3]. Smoluk G.D., Fahey R.C., Ward J.F.: Radiat. Res., 114, 3-10 (1988).
[4]. Steenken S.: Free Rad. Res. Comms., 16, 6, 349-379 (1992).
[5]. Lal M.: Radiat. Phys. Chem., 43, 6, 595-611 (1994).
[6]. Ambroż H., Kornacka E., Przybytniak G.: Radiat. Phys. Chem., in press.

THE ROLE OF CYSTEAMINE IN THE γ-RADIOLYSIS OF DNA. PART II. GEL-ELECTROPHORESIS STUDIES

Ewa M. Kornacka, Grażyna K. Przybytniak

Studies of the influence of cysteamine on damage to DNA by ionising radiation, using gel-electrophoresis at ambient temperatures, enabled us to draw some conclusions as to the most probable reaction pathways in the complicated system of DNA/thiol/oxygen [1].

Examination of the numbers of radiation-induced strand lesions of plasmid DNA, single strand breaks (ssb) and double strand breaks (dsb) were performed using the gel electrophoresis method. All experiments were carried out in the presence of oxygen; samples were kept in equilibrium with air. Irradiation was performed at room temperature and at 77 K [2].

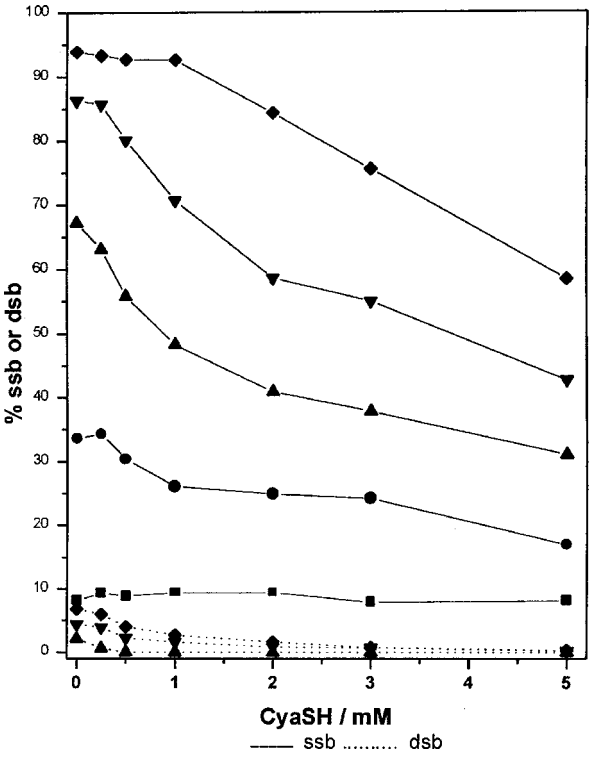

Fig.1. Single and double strand breaks of plasmid DNA as a function of CyaSH concentration, irradiated at ambient temperature to a dose of: (■) 0 Gy, (●) 10 Gy, (▲) 50 Gy, (▼) 100 Gy, (◆) 200 Gy.

Under the conditions of allowed diffusion (ambient temperature irradiation) at absorbed doses of radiation of 0-200 Gy, the addition of cysteamine up to 5 mM causes a distinct lowering of ssb (circular form) and also some decrease of dsb (linear form); the latter appears at higher doses. The reduced amounts of lesions due to the presence of CyaSH are shown in Fig.1 for ssb and dsb. Such relationships indicate for protection and repair of DNA breaks by cysteamine.

Figure 2 illustrate similar dependencies as shown in Fig.1 but on irradiation at 77 K. Note that 10^2 times higher radiation doses are needed under cryogenic irradiation to cause comparable damage to those observed at room temperature.

Comparison of all the results obtained from electrophoresis experiments shows a much higher positive influence of the thiol when diffusion becomes possible (ambient temperature) and a noticeably non-linear dependence on increasing thiol concentration. Because of repeated experiments, we believe that the non-linearity is genuine. We applied similar procedures previously and did not observe such behaviour [3].

Generally, it can be observed that the efficiency of the thiol is diminished under restricted diffusion at cryogenic irradiation temperatures. In the room temperature experiments, the results seem to indicate a higher affinity of cysteamine than DNA to oxygen or reactive oxygen spieces – ROS (protection) or an effective role of the thiol in the repair of DNA-peroxide species [4]. This means that the thiol is able to consume oxygen before it can attack DNA or to deactivate DNA-peroxyl radicals without a chain break, as was shown above in our electron paramagnetic resonance (EPR) studies. Under cryogenic conditions at higher radiation doses, the increased amount of CyaSH added sometimes did not lower but even increased the damage to DNA, especially dsb. The increase of dsb formation in non-diffusion system under irradiation would suggest that resulting thiol/oxygen or thiol/DNAOO$^{\bullet}$ secondary species are able to transfer the damage to another nearby DNA strand

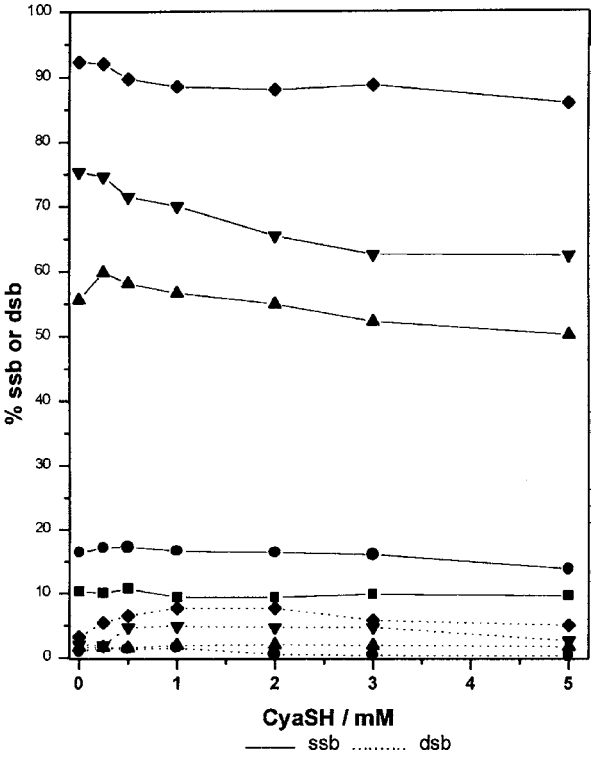

Fig.2. Single and double strand breaks of plasmid DNA as a function of CyaSH concentration, irradiated at 77 K to a dose of: (■) 0 kGy, (●) 1 kGy, (▲) 5 kGy, (▼) 10 kGy, (◆) 20 kGy.

that results in a dsb, thus forming the linear form of the plasmid, which produces the most lethal consequence for a living cell. Dsb, if not repaired chemically or in an enzymatic process, causes cell death [5].

The EPR and electrophoresis experiments require the application of different conditions, e.g. concentrations of the ingredients, which have to be adjusted to the method of further examination. The electrophoresis experiments are performed solely in aerated systems with irradiation carried out at ambient or cryogenic temperatures while the EPR method allows for aerated and oxygen-free systems, although the temperature of irradiation has to be cryogenic as the paramagnetic transients (without using the spin-trapping technique) are thermally unstable. However, it creates the possibility of examining secondary processes on gradual warming of the samples.

The results obtained using both methods confirm the non-linear effect of the concentration of cysteamine in damaging DNA due to the competitive reactions in irradiated DNA/thiol/oxygen systems as discussed above and the considerable influence of oxygen on the extent of damage. Evidently, during the irradiation of plasmid DNA, the influence of oxygen on primary processes under cryogenic conditions is lower, as the system consists of only oxygen dissolved in the solution before freezing and no diffusion at 77 K is possible. The oxygen is then consumed in the system and further radiolysis proceeds under oxygen-free conditions. As $DNAOO^{\bullet}$ is formed in the presence of O_2 as revealed by EPR, it would suggest that protection of the biomolecules by cysteamine is mainly due to consumption of oxygen and not to the deactivation of $DNAOO^{\bullet}$. The DNA peroxyl radicals definitely increase the possibility of secondary reactions with a neighbouring DNA strand that is manifested by increase of dsb.

References

[1]. Spear N., Aust S.D.: Arch. Biochem. Biophys., 324, 1, 111-116 (1995).
[2]. Spotheim-Maurizot M., Charlier M., Sabattier R.: Frontiers in Radiation Biology. Ed. E. Riklis. Balaban Publishers, VCH, Wienheim 1990, pp.493-502.
[3]. Ambroż H.B., Bradshaw T.K., Kemp T.J., Kornacka E.M., Przybytniak G.K.: J. Photochem. Photobiol. A, 142, 9-18 (2001).
[4]. Becker D., Summerfield S., Gillich S., Sevilla M.D.: Int. J. Radiat. Biol., 65, 5, 537-548 (1994).
[5]. Held K.D., Biaglow J.E.: Radiat. Res., 139, 15-23 (1994).

NEW TYPE OF PARAMAGNETIC SILVER CLUSTER IN SODALITE: Ag_8^{7+}

Jarosław Sadło, Jacek Michalik, Marek Danilczuk, Hirohisa Yamada[1/], Yuichi Michiue[1/], Shuichi Shimomura[1/]

[1/] National Institute of Material Science, Tsukuba, Japan

Ultrafine metal particles have attracted a considerable interest as a distinct state of matter with unique physical and chemical properties. The studies of size-dependent properties of clusters are important with respect to fundamental knowledge concerning the transition from atom to bulk properties, the catalytical activity and the relation to optical and electronic material development. During the past two decades silver agglomeration in molecular sieves reduced by hydrogen or ionizing radiation was extensively studied mostly using electron paramagnetic resonance (EPR) as an experimental method.

Generally, in zeolites two pathways of silver agglomeration were proposed. The first one was observed in gamma-irradiated AgNaCs-rho zeolite, where agglomeration process initiated by radiolytic formation of silver atoms Ag^0 involves the reaction of silver atoms or clusters with Ag^+ cations leads to the successive formation of silver dimers Ag_2^+, trimers Ag_3^{2+} and tetramers Ag_4^{3+} [1]. The final tetramers are very stable and can be observed above 100°C. The agglomeration pathway is the same for a broad range of silver loadings whereas the clustering rate is controlled by the annealing temperature and Ag^+ loading.

The second pathway of silver agglomeration was observed in dehydrated zeolite A with high silver loadings (Ag_xNa-A, $x \geq 6$). In this case, directly

after irradiation at 77 K, a seven-line EPR multiplet, assigned to a silver octahedral hexamer Ag_6^{n+}, is recorded [2]. As the mobility of the silver species at the liquid nitrogen temperature is negligible, it was postulated that paramagnetic hexamer is formed from diamagnetic silver hexamer by electron capture during radiolysis at 77 K. The proposed mechanism assumes that silver agglomeration is initiated by autoreduction of Ag^+ and proceeds by the reaction of Ag^0 atoms with Ag^+ cations until a diamagnetic hexamer is formed.

Another type of silver cluster was recorded in sodalite with oxalate guest anion, synthesized at 95°C. In this case, the EPR signal consists of 6 lines and was assigned to Ag_5^{n+} silver pentamer [3].

In this work, we have been studying silver agglomeration in gamma-irradiated microcrystals of Ag-sodalite with hydroxyl guest anion.

The building block of the sodalite structure is a cubooctahedron of corner-connected tetrahedra or a sodalite cage which is also a component of zeolites A, X and Y. The unit cell of sodalite consists of two cages with single cage stoichiometry $Na_4X(AlSiO_4)_3 \cdot 2H_2O$ where X represents a negative ion (e.g. hydroxyl or halogen) and has tetrahedral coordination with four sodium cations as the nearest neighbours. The sodalite frameworks structure is presented in Fig.1.

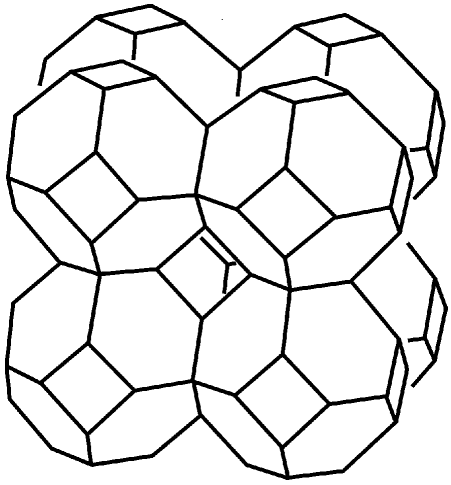

Fig.1. The framework structure of sodalite.

The sodium sodalite crystals were prepared hydrothermally by the modified procedures described earlier [4]. Starting materials were a mixture of Al_2O_3, SiO_2 and NaOH with stoichiometric sodalite composition with an excess amount of sodium (molar ratios: $2SiO_2$:Al_2O_3:16NaOH:aqua). The reaction mixtures were sealed in gold tubes of 7 mm diameter and 100 mm lengths packed in a rapid-quench type high-pressure vessel. The vessel was kept in a furnace at 773 K and 100 MPa for 40 days. After quenching to room temperature, the crystals were separated and washed with distilled water. Finally, the crystals were dried at 373 K for one day. Silver-containing sodalite (Ag-SOD) was prepared by a melt ion-exchange of a mixture containing the parent sodium sodalite crystals and excess amount of silver nitrate. The mixture was heated in a mortar in the dark to 503 K for 24 h. The products were filtered in the dark through a 0.45 μm membrane filter, washed with distilled water and dried in air at ambient temperature.

The chemical compositions of Ag-SOD were determined by inductively coupled plasma spectroscopy – ICP (SEIKO HVR 1700). The phase identification of the synthesized materials were carried out by both powder X-ray diffraction with CuKα radiation (RIGAKU RINT 2200) and single-crystal X-ray diffraction (Rigaku AFC7R four-circle diffractometer). The cell dimension was obtained by a least-squares refinement at diffraction angles of 25 selected reflections.

After synthesis, colorless, transparent crystals with dimensions up to 100 μm have been obtained. Both powder X-ray diffraction photograph and single-crystal X-ray analysis identified the materials as pure sodalite phases with a high degree of crystallinity. The obtained dimension of the cubic cell 0.8784(3) nm is typical for the sodalite lattice. Diffraction intensities were also checked whether the sample has the Laue class m-3m, which is identical to that of the original sodalite. After silver loading the crystals changed their color to brick red. ICP analysis showed that the Ag:Na:Si:Al molar ratio is 7.97:0.03:6.45:5.22, indicating that sodium is almost fully exchanged by silver.

EPR spectra of Ag-SOD irradiated at 77 K and annealed at various temperatures are shown in Fig.2. At 110 K the major EPR signal is an isotropic nine-line multiplet with $g_{iso} = 1.987$ and hyperfine splitting of 8.3 mT assigned to Ag_8^{n+} cluster

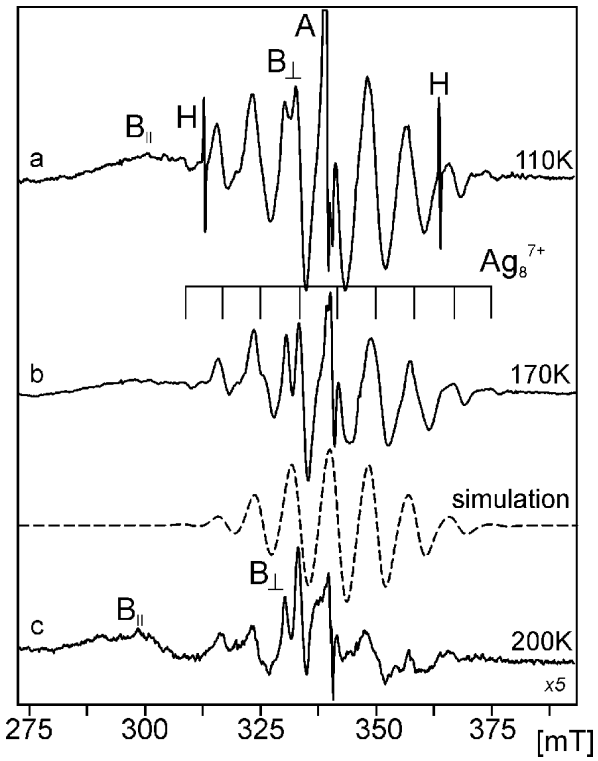

Fig.2. EPR spectra of Ag-sodalite gamma-irradiated at 77 K and recorded at: a) 110 K, b) 170 K and c) 200 K. Dashed line represents simulated spectrum of .

(Fig.2a). The octamer signal is overlapped with anisotropic doublet B ($A_\perp = 2.8$ mT, $g_\perp = 2.045$, $g_{||} = 2.284$) representing divalent silver cations

Ag^{2+}. Two other signals do not represent silver species: a singlet A with g = 2.003 is due to centers induced radiolytically in the silicoaluminum framework and a doublet of narrow H lines (A_{iso} = 50.7 mT, g_{iso} = 2.002) derives from hydrogen atoms. At 170 K signals A and H decay and then the Ag_8^{n+} multiplet is recorded practically without any interference from other signals. Owing to that it is possible to compare the experimental and simulated spectra of Ag_8^{n+}. The dashed line in Fig.2 shows that the shape and line intensity ratios in both spectra are similar provided that our assignment of the EPR nonet to octamer silver clusters is correct. At higher temperatures, Ag_8^{n+} signal decays quickly and it is barely recorded at 200 K.

Till now, the biggest radiation-induced silver cluster identified in molecular sieves was silver hexamer located in sodalite cage of zeolite A. A silver octamer Ag_8^{n+} was previously reported in hydrogen reduced Ag-A zeolite, but its spin Hamiltonian parameters (A_{iso} = 5.2 mT, g = 2.025, [5]) were completely different than the parameters of silver octamer stabilized in sodalite crystals. Especially the difference between g values is significant. All Ag_n^{n-1} clusters have g values in the range 1.970-2.000 considerably smaller than the g value of the free electron that equals 2.0023. Based on g value we tentatively assign a nine-line multiplet to Ag_8^{7+} clusters. Then silver octamer reported earlier [5] would have a different charge.

The fact that the multiplet spectrum of Ag_8^{7+} is observed directly after irradiation at 77 K univocally proves that silver agglomeration proceeds according to the second pathway described above. During sodalite dehydration Ag^+ cations migrate and agglomerate in such a way that some cages are loaded with 8 Ag^+ leaving the others empty. Such arrangements of close cations constitute the perfect trapping sites for electrons generated during low temperature radiolysis. The studies of electron traps in frozen solutions proved that the traps can be rearranged structurally even at low temperature in order to minimize the energy of the system. The rearrangement of Ag^+ around trapped electron should change the spin density on silver nuclei and observed hyperfine splittings. In the temperature range 110-170 K we did not record any changes in the value of silver hyperfine splitting. This prompts us to assume that preexisting traps of eight Ag^+ cations do not rearrange after electron trapping or the structural changes proceed rapidly at 77 K.

Earlier, in gamma-irradiated polycrystalline Ag-SOD, we observed an EPR multiplet with similar hyperfine splitting (A_{iso} = 8.2 mT) which was assigned to Ag_6^{5+} hexamer [6]. In those samples, additionally to the multiplet the doublet of Ag^0 atoms was recorded all over temperature range. The present results indicate that other interpretation of EPR multiplet in polycrystalline samples is possible. Because Ag^0 doublet could overlap with the weak outer lines of EPR nonet (hfs = 8.3 mT), Ag_8^{7+} cluster might be also stabilized in polycrystalline Ag-SOD samples. The additional studies will be undertaken to prove that hypothesis.

References

[1]. Michalik J., Sadlo J., Yu J.-S., Kevan L.: Colloids Surf. A, 115, 239-247 (1996).

[2]. Morton J.R., Preston K.F.: J. Magn. Reson., 68, 121-128 (1986).

[3]. Sadło J.: Paramagnetic Silver Clusters in Molecular Sieves. Ph.D. Thesis, 2000 (in Polish).

[4]. Bye K.L., White E.A.D.: J. Cryst. Growth, 6, 355-356 (1970).

[5]. Grobet P.J., Schoonheydt R.A.: Surf. Sci., 156, 893-898 (1985).

[6]. Michalik J., Sadlo J., Danilczuk M., Perlinska J., Yamada H.: Stud. Surf. Sci. Catal., 142, 311-318 (2002).

SOME SUBSTITUTED THIOETHERS ARE ABLE TO SPONTANEOUSLY REDUCE Cu^{II} IMIDAZOLE COMPLEXES. A POSSIBLE IMPLICATION FOR THE COPPER-RELATED NEUROTOXIC PROPERTIES OF ALZHEIMER'S AMYLOID β-PEPTIDE

Katarzyna Serdiuk[1/], Jarosław Sadło, Małgorzata Nyga, Dariusz Pogocki

[1/] Pedagogical University of Częstochowa, Poland

The amyloid β-peptide (βA) dependence formation of free radicals and reactive oxygen species has been identified as an important pathway of Alzheimer's disease pathology. To some extent neurotoxicity of βA seems to correlate with its ability to both formation of free radicals and spontaneous reduction of complexed copper, whose concentration in the amyloid plaques reaches 400 μM [1].

The involvement of Met^{35} in copper reduction by βA is an important, although not completely understood, phenomenon. It has been postulated that N-terminally bonded Cu^{II} is reduced by the electron originating from the C-terminal methionine (Met) residue [2-4]. However, the direct oxidation of thioether sulfur of Met^{35} by copper appears unfavorable based on the reduction potentials of the $\beta A(Cu^{I}/Cu^{II})$ and $MetS^{\bullet+}$/Met couples. In normal conditions the difference between the reduction potentials of $\beta A(Cu^{I}/Cu^{II})$ (0.5-0.55 V *vs*. Ag/AgCl) [4] and $MetS^{\bullet+}$/Met (1.26-1.5 V *vs*. Ag/AgCl) [5-8], is about ~0.7-1.0 V, thus equilibrium (1) should be shifted to far left-hand side [9].

$$MetS + \beta A(Cu^{II}) \rightleftharpoons \beta A(Cu^{I}) + MetS^{\bullet+} \quad (1)$$

However, products of reaction can be efficiently removed from equilibrium (1), which can be, therefore, dragged to the right-hand side. One of poss-

ible mechanisms of removing $MetS^{\bullet+}$ from the equilibrium is the formation of α-(alkylthio)alkyl radicals (αS) in reaction (2):

$$MetS^{\bullet+} + B \rightarrow Met(\alpha S)^{\bullet} + BH^{+} \quad (2)$$

Therefore, in this work we studied spontaneous reactions leading to α-(alkylthio)alkyl radicals, which may influence equilibrium (1), accelerating oxidation of the Met residue in peptides.

We designed a system, in which complexes of Cu^{II} with imidazole (Im) mimic cupric site of βA. The fifth fold excess of imidazole over Cu^{2+} guarantee that at least 95% of copper is complexed as $Cu(Im)_4^{2+}$-type complex, whose spectral and redox characteristic is well known ($\lambda_{max} \approx 590$ nm ($\varepsilon = 53 \pm 2$ $M^{-1}cm^{-1}$) [10] and $E^0(Cu^{II}/Cu^{I}) \leq 0.2$ V and $E^0(Cu^{I}/Cu^{0}) \leq 0.6$ V *vs.* SCE – saturated calomel electrode) [11]. On the other hand, the Met residue was mimicked by organic thioethers (I-IV) substituted in the α position. Such substitution should significantly influence the rate of formation α-(alkylthio)alkyl radicals in the reactions of deprotonation and decarboxylation, and therefore in some cases facilitate the reduction of $Cu(Im)_4^{2+}$.

(I) $HO_2CCH_2SCH_2CO_2H$
(II) $HO_2CCH_2CH_2SCH_2CH_2CO_2H$
(III) $CH_3SCH_2CO_2H$
(IV) $CH_3SCH_2CO_2NH_2$

The reduction of $Cu(Im)_4^{2+}$ by thioethers was investigated in an air or argon saturated aqueous solution containing 1.5×10^{-2} M $CuCl_2$, $(4.5\text{-}7.5)\times10^{-2}$ M Im, and $(0.32\text{-}1.5)\times10^{-2}$ M of thioethers at pH 5.87-6.04, incubated at 37 and 50°C. For all thioethers we monitored the decay of the UV-VIS absorption and the electron spin resonance (ESR) signal of paramagnetic Cu^{II}. For the compounds I-III the yield of decarboxylation was measured applying head-space gas-chromatography.

In the argon saturated samples containing thioethers I and III efficient decarboxylation was observed (Fig.1). Whereas in the air saturated solution the yield of CO_2 was decreased by *ca.* 30% compare to argon saturated solutions. For thioether II, the yield of decarboxylation was negligible in both air and argon saturated solutions. The oxidation of thioethers I and III in the argon saturated solutions was accompanied by precipitation of copper mirror on the surface of the reactor, visible after *ca.* 300 h of incubation at 50°C. Simultaneously, during the incubation of $Cu(Im)_4^{2+}$ with thioethers I, III and IV we observed the decay of the ESR signal (Fig.2) together with the decay of the UV-VIS absorption of $Cu(Im)_4^{2+}$. In all cases

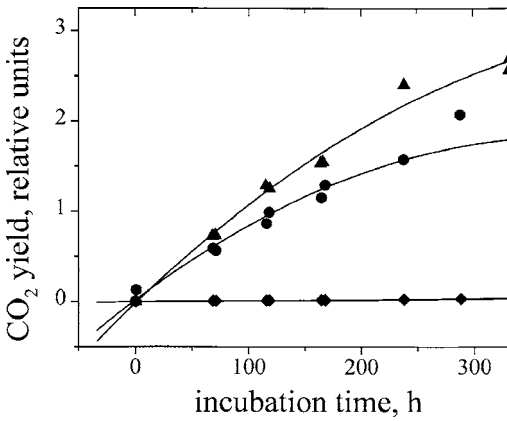

Fig.1. The yield of CO_2 as a function of the incubation time at 50°C in aqueous solutions containing 0.75×10^{-2} M thioether, 1.5×10^{-2} M $CuCl_2$ and 7.5×10^{-2} M Im: triangle – thioether I in argon saturated solution, circle – thioether I in air saturated solution, diamond – thioether III in argon saturated solution.

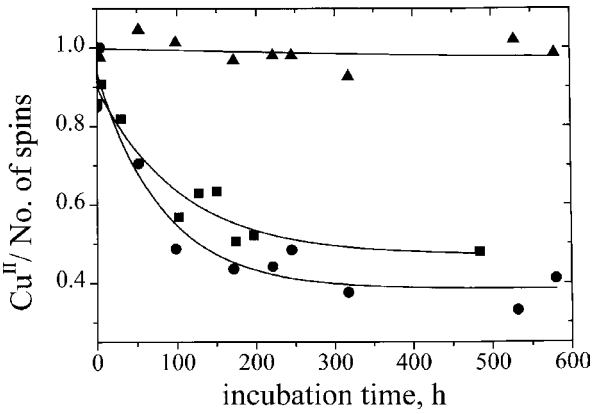

Fig.2. The ESR signal changes (represented as number of spins Cu^{II}) *vs.* incubation time at 50°C in argon saturated solutions containing the thioethers: square – thioether I 0.75×10^{-2} M, $CuCl_2$ 1.5×10^{-2} M, Im 4.5×10^{-2} M; circle – thioether IV 0.75×10^{-2} M, $CuCl_2$ 1.5×10^{-2} M, Im 4.5×10^{-2} M; triangle – $CuCl_2$ 1.5×10^{-2} M, Im 4.5×10^{-2} M.

where decay of $Cu(Im)_4^{2+}$ is observed (thioethers I, III, IV), the density functional theory (DFT) calculations show that decarboxylation or deprotonation of thioether sulfide radical-cation leads to the formation of resonance stabilized radicals ($E_s \approx 10$ kcal/mol for $III^{\bullet}$ and $E_s \approx 19$ kcal/mol for $IV^{\bullet}$). Whereas, for thioether III, where one may expect decarboxylation leading to the formation of alkyl radicals ($E_s \approx 0$), neither decarboxylation nor $Cu(Im)_4^{2+}$ reduction was observed.

The significant differences observed in the yield of $Cu(Im)_4^{2+}$ reduction between air and argon saturated solutions, and the lack of metallic copper precipitation in the presence of oxygen, suggest that oxygen takes part in the process. The presence of oxygen in solution can be a reason of partial reversibility of copper reduction.

The mechanism shown in Scheme 1 is a preliminarily attempt to rationalize current observation for thioether I. This requires, however, additional experimental support.

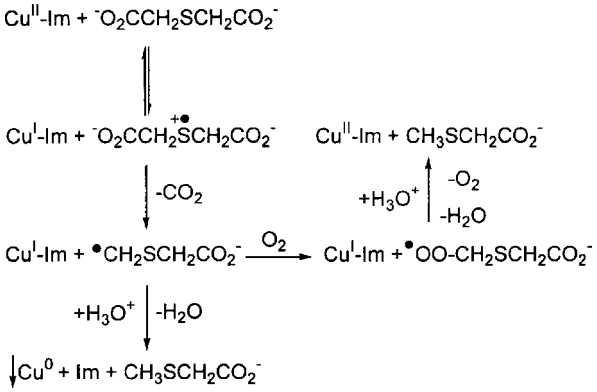

Scheme 1.

The α-carboxylate substituted thioethers are able to spontaneously reduce $Cu(Im)_4^{2+}$, since the process is "driven" by irreversible decarboxylation of S-centered radical-cation. Release of CO_2 is accompanied by an increase of entropy and thus is thermodynamically favored. Similarly, α-amide substituted thioethers can reduce $Cu(Im)_4^{2+}$, taking advantage of stabilization of arising α-(alkylthio)alkyl radicals by the capto-dative effect.

The future of this project is to design a system, in which the influence of factors like the proton acceptors concentration, ionic strength, molecular oxygen concentration, and pH on the reduction of cupric complexes by thioethers can be investigated as these factors vary upon the oxidative stress and inflammation accompanying Alzheimer's disease.

References

[1]. Pogocki D.: Acta Neurobiol. Exp., 63, 131-145 (2003) with all references cited therein.
[2]. Varadarajan S., Kanski J., Aksenova M., Lauderback C., Butterfield D.A.: J. Am. Chem. Soc., 123, 5625-5631 (2001).
[3]. Rauk A., Armstrong D.A., Fairlie D.P.: J. Am. Chem. Soc., 122, 9761-9767 (2000).
[4]. Huang X. *et al.*: J. Biol. Chem., 274, 37111-37116 (1999).
[5]. Merényi G., Lind J., Engman L.: J. Phys. Chem., 100, 8875-8881 (1996).
[6]. Engman L., Lind J., Merényi G.: J. Phys. Chem., 98, 3174-3182 (1994).
[7]. Huie R.E., Clifton C.L., Neta P.: Radiat. Phys. Chem., 92, 477 (1991).
[8]. Sanaullah, Wilson S., Glass R.S.: J. Inorg. Biochem., 55, 87-99 (1994).
[9]. Schöneich Ch.: Arch. Biochem. Biophys., 397, 370-376 (2002).
[10]. Edsall J.T., Falsenfeld G., Goodman D.S., Guard F.R.N.: J. Am. Chem. Soc., 76, 3054-3061 (1954).
[11]. Li N.C., White J.M., Dood E.: J. Am. Chem. Soc., 76, 6219-6223 (1954).

POLY(SILOXANEURETHANES) AS SCAFFOLDS FOR TISSUE ENGINEERING

Izabella Legocka, Monika Celuch, Jarosław Sadło

Sterilization process using the radiation method may be connected with some structural changes of the polymer material. So, the optimization of sterilization process parameters and at the same time optimization of chemical structures of polymer materials selected to meet specific requirements for biomedical applications are very important.

The main scope of the presented study is to observe and understand the influence of sterilization process by the radiation method on chemical and structural changes of experimental segmented poly(siloxaneurethanes) (PSU) designed for medical scaffolds for tissue engineering.

It is known that under irradiation conditions free radicals in polymers are formed. Kinetics of initiation and decaying of these radicals as a function of structure of segmented PSU was investigated.

One of the area of our interest are polymers designed for tissue engineering as scaffold tissue. Such polymers should meet basic requiments:

- to make it possible cells adherence to scaffold surface, that means that there should be achieved optimal hydrophobic-hydrophilic surface balance;
- to make it possible growing new cells, so no toxic substances should be produced;
- to have adequate mechanical properties.

All the above parameters of polymeric scaffolds should be held after radiation sterilization.

Very interesting polymers owing to their useful properties are polyurethanes and segmented PSU. They have a chemical structure which can be modified in a very large range. The mentioned polymers are characterized by:

- very good mechanical properties;
- possibility of frothing which indicates that their macrostructure is useful for mechanical cells settling;
- good chemical resistance;
- surface structure which can be relatively easy modified.

Table 1. Chemical composition of selected PSU.

Number of sample	Chemical structure of samples			
	NCO/OH ratio	oligosiloxanediol		
1519	2:1	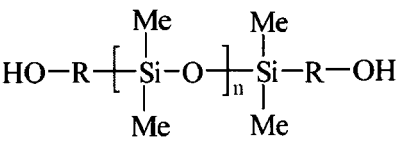	n=30	R= -$(CH_2)_6$-
1515	3.5:1		n=30	R= -$(CH_2)_6$-
1461	2:1		n=40	R= -$(CH_2)_3$-O-$(CH_2)_2$-
1463	3.5:1		n=40	R= -$(CH_2)_3$-O-$(CH_2)_2$-
1518	2:1		n=10	R= -$(CH_2)_6$-
1522	3.5:1		n=10	R= -$(CH_2)_6$-
1456	3.5:1		n=20	R= -$(CH_2)_3$-O-$(CH_2)_2$-

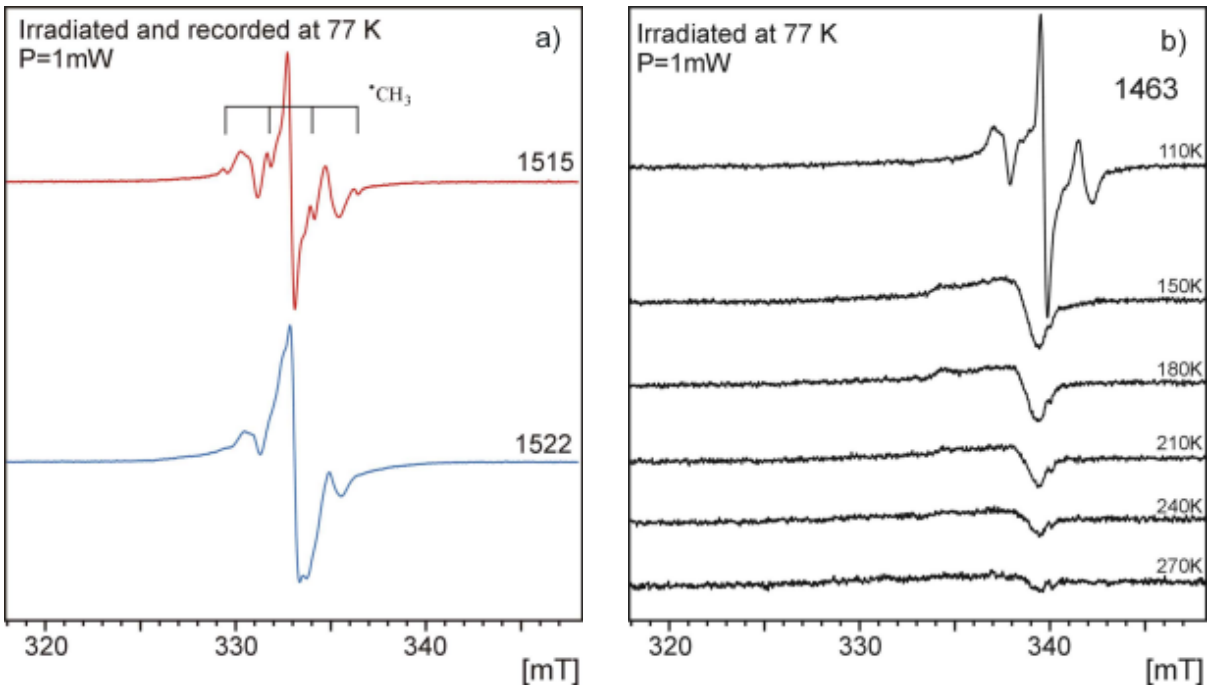

Fig.1. ESR spectrum for samples irradiated at a temperature of 77 K and recorded: a) at temperature 77 K; b) at different temperatures in the range 110-270 K.

They predict that these polymers could be good scaffolds provided that they will be resistant to irradiation at a sterilization dose level.

Materials: poly(siloxaneurethanes) – block copolymers consisting of rigid segments (IPDI – isophorone diisocyanate for all samples) and flexible ones (oligosiloxanediols), (Table 1); phenylalanine – a modifier and probably scavenger of free radicals.

Conditions of irradiation:

- The films of samples packed in double sterilization pouches were irradiated with a standard dose of 28 kGy used for sterilization at room temperature.
- The samples were irradiated using the accelerator type LAE 13/9 with nominal energy of 10 MeV. Some samples, which had to be irradiated at temperature of liquid nitrogen were irradiated using a ^{60}Co gamma ray source named Minejola 1000.
- During irradiation none inert gas was applied.

Methods of investigations: ESR – electron spin resonance (apparatus Bruker-300), temperature of measurement: ambient, 77 K and 77-270 K; FTIR-ATR (apparatus Bruker); DRS – diffuse reflection spectrophotometry (apparatus Perkin Elmer Lambda-9); SFE – surface free energy (apparatus goniometer Krüss-G10).

ESR spectrum shows no signals at ambient temperature. Signals with different intensity from paramagnetic species were observed for samples irradiated at 77 K (Fig.1a). These signals disappeared

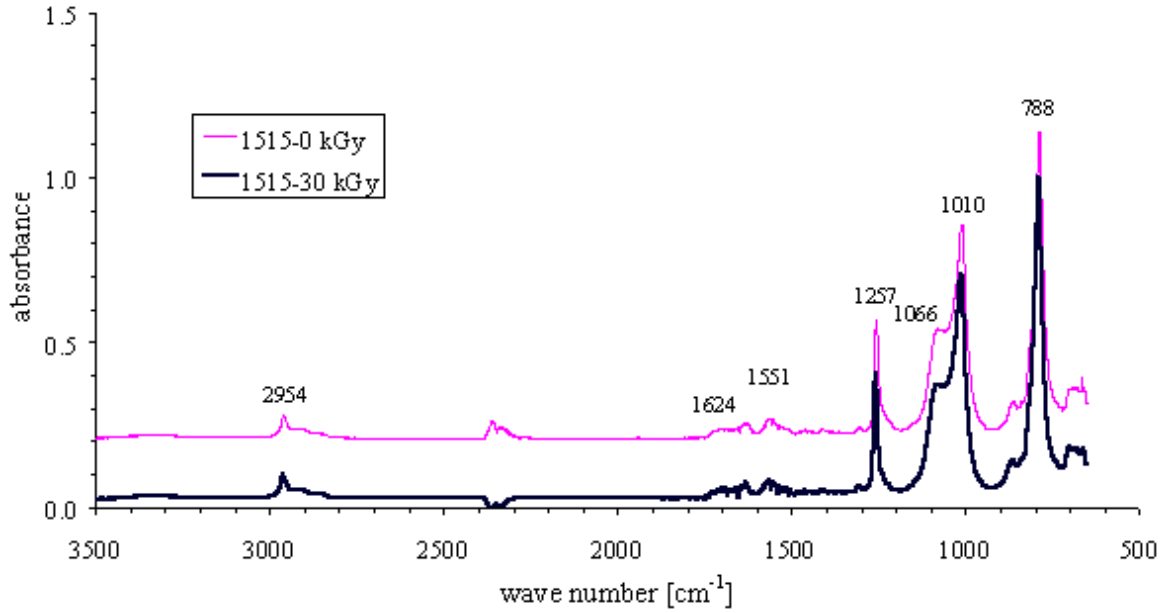

Fig.2. Comparison of FTIR-ATR spectrum of samples No. 1515 before and after sterilization.

Table 2. Comparison of the contact angle θ values in different solvents for selected PSU before and after irradiation (*).

Number of sample	Contact angle θ [°]							
	diiodomethane		formamide		ethylene glycol		aqua	
1456	72.62	74.44*	96.39	98.40*	87.17	89.95*	**105.79**	**109.00***
1461	78.84	79.62*	98.42	101.10*	92.15	99.93*	**110.78**	**113.02***
1463	72.07	73.85*	92.99	95.34*	84.86	90.27*	**101.08**	**108.81***
1515	280.04	69.58*	88.08	91.61*	84.32	83.94*	**105.23**	**108.10***
1519	80.06	81.22*	98.54	103.19*	94.24	99.02*	**108.94**	**108.34***

with an increase of temperature (Fig.1b). At the same time no differences in IR spectra were observed (Fig.2). It means, no changes in chemical structure of irradiated samples were observed. This can be a result of fast recombination process of radical forms created under irradiation.

More hydrophobic surfaces of the samples of PSU after sterilization process may be unsuitable as medical scaffold for tissue engineering.
And so, we have started to study modification of this type of PSU with additives-modifiers of surface properties and scavengers like phenylalanine.

Table 3. Comparison of the SFE values obtained different methods for selected PSU before and after irradiation (*).

Number of sample	Owens-Wendt's method						Acid-base method	
	SFE [mN/m]		γ^p [mN/m]		γ^d [mN/m]		SFE [mN/m]	
1456	**21.89**	**20.66***	0.47	0.23*	21.42	20.43*	**22.36**	**21.17***
1461	**18.35**	**17.81***	0.26	0.13*	18.09	17.69*	**18.49**	**19.23***
1463	**22.87**	**20.97***	1.15	0.23*	21.72	20.75*	**22.97**	**21.46***
1515	**23.85**	**23.25***	0.35	0.14*	23.51	23.11*	**23.87**	**23.08***
1519	**17.97**	**17.53***	0.50	0.65*	17.46	16.87*	**18.49**	**19.69***

The changes of the value of contact angle θ (Table 2) and surface free energy (Table 3) of irradiated samples are probably induced by the recombination of radicals. Recombination can lead to partial crosslinking of the polymer chains and finally to phase separation.

References

[1]. Lewanowska-Szumieł M., Kałuska I.: Polimery w Medycynie, XXV, 1-2 (1995).
[2]. Zhand Y.-Z., Bjursten L.M., Freji-Larsson C., Kober M., Wesslen B.: Biomaterials, 17, 2265-2272 (1996).
[3]. Jagur-Grodziński J.: e-Polymers, 012 (2003).

INFLUENCE OF CARBOXYLIC ACIDS ADDITION TO POLYPROPYLENE ON ITS PROPERTIES UNDER STERILIZATION DOSE OF ELECTRON BEAM

Izabella Legocka, Zbigniew Zimek, Monika Celuch, Krzysztof Mirkowski, Andrzej Nowicki

Polypropylene (PP) main features are as follow: low price, friendly environmental behavior, easy processing and recycling, rather good performance. It meets requirements suitable for many customers. Polypropylene materials are used often for medical disposable manufacturing. Radiation sterilization of medical devices made of PP has been actively carried out, but with some limitation. The degradation effect is observed at the dose required for product sterility which influences properties of the product [1-6].

This year, the following studies have been initiated to formulate new grade of PP composites for medical devices with a suitable long time stability of mechanical parameters:

- introducing nucleating and stabilizing agents to obtain products with more complex and better mechanical properties,
- introducing additives which could promote crosslinking process of PP compositions and improve its mechanical strength,
- introducing polymer chain bonding stabilizers and taking advantage of functionalized polymers and increasing protective effect on a long time scale,
- introducing nanosized particles (MMT) to ob-

tain products with significantly higher mechanical and thermal properties and protection against oxidative destruction to stop or delay the process of chain degradation caused by radicals located in a PP matrix. The selected products could be appropriate during the preparation of composite materials as well as nanocomposites, which are more suitable to be filled and characterized by new properties as compared to pure PP.

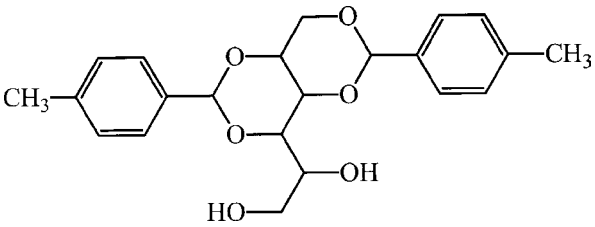

Fig.1. Structure of Irgaclear DM.

The following materials and chemicals were used in this study:
- homopolypropylene Malen P J601 (PP-J601) – produced by PKN "Orlen",
- copolymer propylene/ethylene Moplen PLZ 841 – produced by Montell Polyolefins,
- Irgaclear DM – produced by Ciba (Fig.1),
- Irganox 1081 – produced by Ciba (Fig.2),

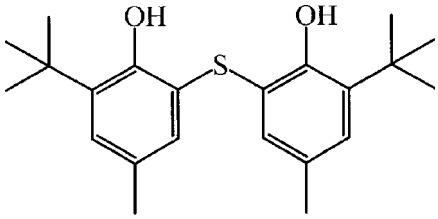

Fig.2. Structure of Irganox 1081.

- maleic anhydride (MA) – produced by POCh (Fig.3),
- itaconic acid (IA) – produced by Fluka (Fig.4).

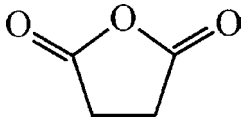

Fig.3. Structure of maleic anhydride.

Samples for testing were prepared as follows:
- Composition of polymers with additives was prepared using the Brabender Plasti-Corder PLV151 at a rotation speed of 60 to 90 rpm in the temperature range 180-235°C (0.3-1.0% of Irgaclear was added to PP as master batch concentrate, 0.2% of stabilizer was also added).
- From the obtained products the plates were pressed at 190-230°C with dimensions 140x120x1 mm.

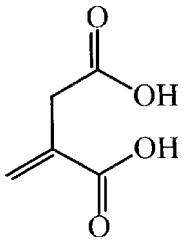

Fig.4. Structure of itaconic acid.

- Irradiation of the samples was conducted with a high energy electron beam, 10 MeV, in the LAE 13/9 accelerator, using the standard sterilization dose 28 kGy.

The following analytical methods were used:
- Melt flow index (MFI) was determined on a plastometer from Zwick under standard conditions.
- Mechanical properties (tensile stress, stress at yield, relative elongation at stress) were investigated using an universal testing machine Instron 5565 type, using samples of dimensions 1BA according to PN-EN ISO527 standard, at a speed of 25 mm/min.

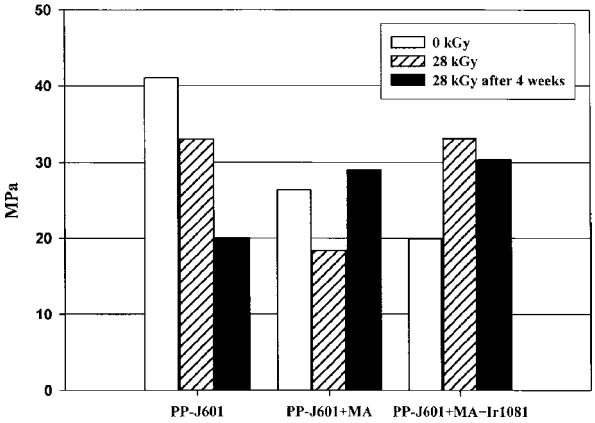

Fig.5. Modification of polypropylene with maleic anhydride. Tensile stress of samples.

- Viscosities were measured at elevated temperatures in the melt using a Brookfield CP2000+ apparatus.
- ESR (electron spin resonance) investigations were provided on a Bruker 300 spectrometer at ambient temperature in air.

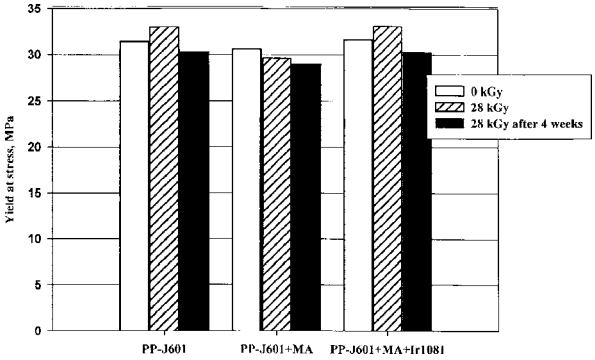

Fig.6. Modification of polypropylene with maleic anhydride. Yield at stress of samples.

Former results of our investigation have been presented in [7]. In short, the main results were as follows:
- Mechanical properties such as tensile stress and Young's modulus show that the addition of nucleating agent results in increasing these parameters.
- The nucleated homopolymer before and after irradiation process in comparison with the copolymer is characterized by a higher Young's modulus and tensile stress, but the elongation is dramatically low.

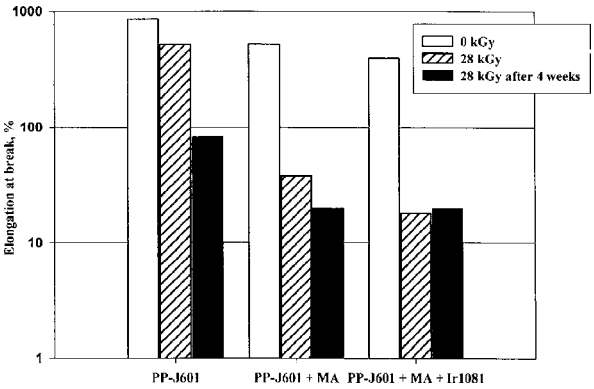

Fig.7. Modification of polypropylene with maleic anhydride. Elongation at break of samples.

Obtained results may lead us to the conclusion that the addition of nucleating agent increases the degree of crystallinity of samples. Higher values of stress at break and lower values of elongation are observed. This can be the reason for large stiffness.

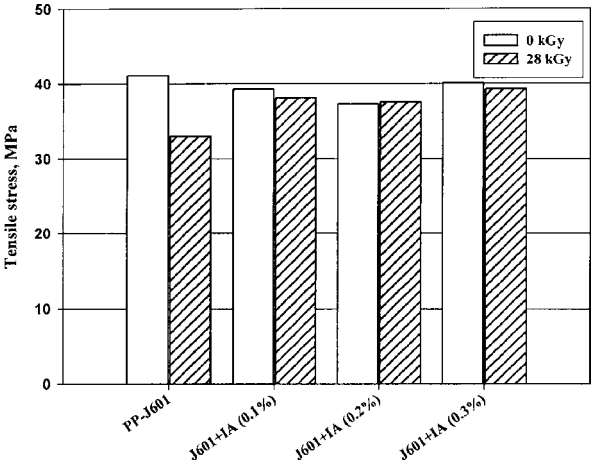

Fig.8. Modification of polypropylene with itaconic acid. Tensile stress of samples.

At this moment, we cannot conclude if the addition of nucleating agent (containing aromatic rings) protects PP against the destruction during radiation sterilization.

In this year, we are concerning with the method of grafting or functionalization of PP with different compounds containing reactive groups, which can be further used to change various properties and to improve resistance against irradiation.

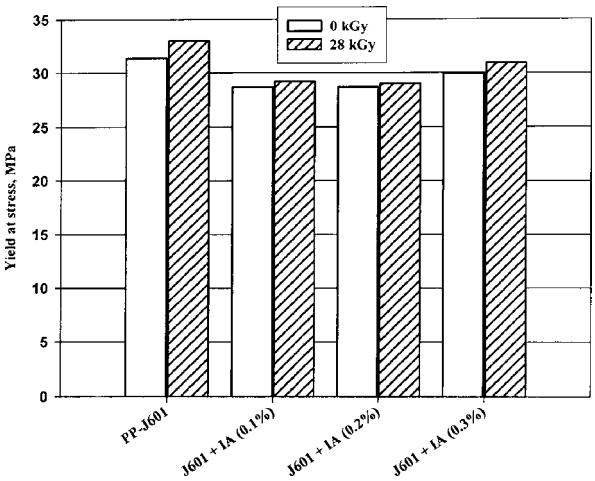

Fig.9. Modification of polypropylene with itaconic acid. Elongation at break of samples.

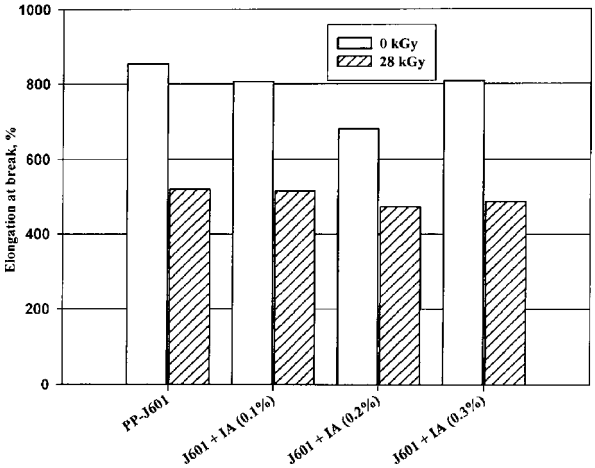

Fig.10. Modification of polypropylene with itaconic acid. Yield at stress of samples.

At the same time, the reactive functions of the pendant groups such as hydroxy-, carboxy-, anhydride in the grafted or funcionalized polymers can react with suitable antioxidants. Such a binding antioxidant with the matrix of a polymer can prolong its protective effect.

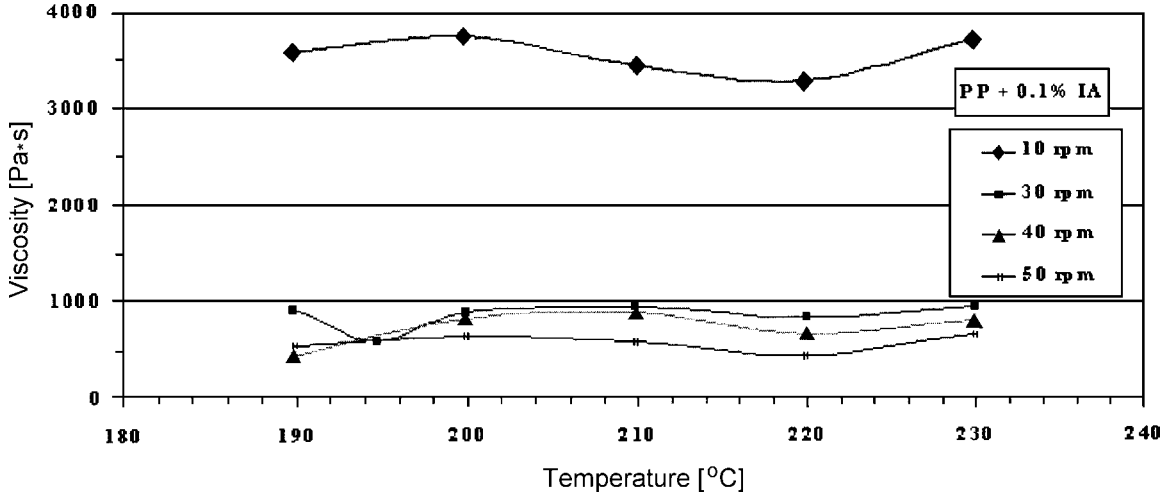

Fig.11. Viscosity *vs*. temperature for polypropylene with 0.1% of itaconic acid at various shear rate.

In this part of work the following compositions were prepared: PP+MA, PP+MA+antioxidant, PP + IA.
All operations were conducted as previously described.

For the compositions with added MA, tensile stress of the irradiation modified PP was lower than for a pure polymer, but its value increased after seasoning (Fig.5). Stress at yield shows that the addition of a modifier with an antioxidant results in increasing that parameter also after seasoning (Fig.6). Elongations of the modified PP are significantly lower as compared with an unmodified polymer (Fig.7). However, immediate and after seasoning elongation values did not change.
All these results may be caused by crosslinking.

Mechanical properties such as tensile stress of the compositions with IA, show that the addition of IA (all amount content) results in increasing that parameter (Fig.8). No differences were observed in elongation at yield after irradiation of the samples (Fig.9), but at the same time stress at yield was lower (Fig.10).

Some changes of viscosity *vs*. shear rate have been observed (Fig.11).

The curves of viscosity show peaks with a minimum value at 220°C. At higher temperatures the viscosity are increasing. This means that the addition of IA may create a crosslinking process of PP under irradiation.

Results of mechanical properties such as: higher stress at yield, lower elongation at break and character of the viscosity curves show that the application of IA as a PP modifier can allow to obtain a partly crosslinked structure of the studied compositions.

References

[1]. Bojarski J., Bułhak Z., Burlińska G., Zimek Z.: Radiat. Phys. Chem., 46, 801 (1995).
[2]. Thorat H.B., Prabhu C.S.: Radiat. Phys. Chem., 51, 215 (1998).
[3]. Kadir Z.A., Yoshii F., Makuuchi K.: Die Angew. Makromol. Chem., 174, 131 (1990).
[4]. Maeco C., Gomez M.A., Ellis G., Arribas J.M.: J. Appl. Polym. Sci., 84, 1669 (2002).
[5]. Kotek J., Raab M., Baldrian J., Grellmann W.: J. Appl. Polym. Sci., 85, 1174 (2002).
[6]. Shamshad A., Basfar A.: Nucl. Instrum. Meth. Phys. Res. B., 151, 169 (1999).
[7]. Legocka I., Bojarski J., Zimek Z., Mirkowski K., Nowicki A.: In: INCT Annual Report 2002. Institute of Nuclear Chemistry and Technology, Warszawa 2003, pp.40-42.

IRREVERSIBLE RADIOLYTIC DEHYDROGENATION OF POLYMERS – THE KEY TO RECOGNITION OF MECHANISMS

Zbigniew P. Zagórski, Wojciech Głuszewski

Detachment of gaseous hydrogen from polymers at ambient temperature is unknown in the conventional polymer chemistry. In the latter, gaseous hydrogen can appear only over polymers heated to high temperatures, well above the melting or decomposition temperature. Free H_2 formation is incorporated in that case in the thermal degradation process. At not so high temperature, the hydrogen can appear as water or as products of reaction with additives, e.g. peroxides applied for conventional crosslinking of polymers.

On the other hand, in the radiolytic decomposition at room temperatures and also under cryogenic conditions, hydrogen is the main constituent of the gas phase above polymers. Hydrogen dominates over the concentration of low molecular weight debris of the degraded polymer. That phenomenon occurs only in the case of neat polymers, but those dissolved, e.g. in water, exceptionally only do release hydrogen in the result of radiolysis. In the case of polymer solutions, the solvent is absorbing the most of energy and its reactive products are entering the reaction with macromolecules. For instance, gelatin in aqueous solution [1] shows during irradiation many different products of reaction with water radiolysis intermediates. Also the crosslinking of gelatin into collagen-like supramolecular entities occurs, but without release of gaseous hydrogen. However, H_2 appears with the yield of 0.45/100 eV in radiolysis of aqueous solution of polymers as the product of multi-ionization spurs in water, not involved in reactions with dissolved polymer and not destroyed by radical products of H_2O, being used for reactions with the polymer.

During 2003, we have systematically investigated the problem, referring to different types of polymers, including biopolymers. The analytical method to be applied for hydrogen determination is obviously gas chromatography already applied successfully to the determination of radiation yield of multi-ionization spurs in alanine, from the yield of carbon dioxide [2]. However, the link between irradiation and the gas chromatography (GC) operation, developed for that purpose cannot be applied for the case of hydrogen. The integration of irradiation and the GC determination, for the case of solid polymers involved a special approach to the specific technique of electron beam (EB) irradiation of cells closed with septa and consideration of different solubility of hydrogen in a variety of polymers, resulted in new procedures. Three milliliter glass vials, closed by septa, are filled only in one third with the sample and only this part is irradiated with a straight beam of electrons from the linear electron accelerator LAE 13/9 [3], leaving the rubber septa intact. This technique allows application of small doses of radiation energy, by triggering single pulses. The Figure 1 shows the arrangement of the cell in the beam, positioning is secured by a laser beam.

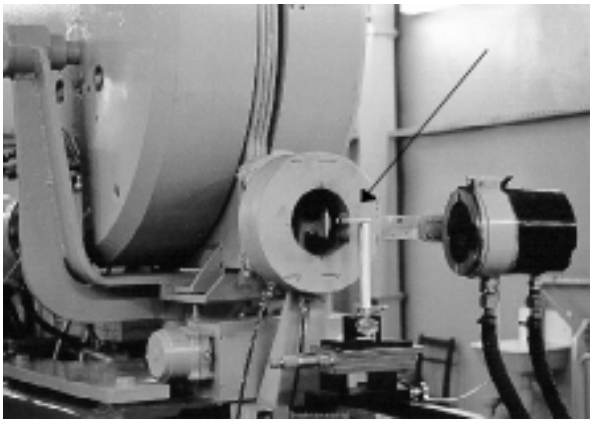

Fig.1. The vial with irradiated sample at the electron-exit window of the accelerator. The red spot on the cell is from laser beam used for positioning of the object in the electron beam.

Application of higher, kilogray doses proved to be more convenient by conventional, technological irradiation on the conveyor, by the bent beam of electrons. The septa are covered with a thick hood made of lead in this case. Experiment with an empty vial did not show the presence of hydrogen, what has demonstrated no significant irradiation of septa made of rubber. This technique was applied for high doses only; application of this mode for low doses of radiation yields erratic doses, because of the structure of the beam. That limitation has been recognized already before the construction of the machine [4] and cannot be avoided due to the pulsing regime of the accelerator action and scanning frequency of 5 Hz.

The application of the developed technique to the particular polymer was always preceded by a study of kinetics of the release of hydrogen, as well as of its distribution between the sample and the gas phase. The behaviour of different polymers, even of comparable surface area of the sample, is, in this respect, different.

Several types of commercial polymers and biopolymers have been investigated. Irradiation by the EB produced by the most reliable, versatile, oldest linear accelerator LAE 13/9 in the Department of Radiation Chemistry and Technology of the Institute of Nuclear Chemistry and Technology has been applied. All samples were of geometry and size securing the homogeneity DUR = 1.2 of dose distribution. The split dose technique has been applied to avoid the warming of samples higher than by 35 K [5]. Goals of investigations were various: There were applied aspects involved, e.g. one of the applications was devoted to the simulation of radiolytic effects in elastomers, contaminated with α-emitters, investigated from the point of view of storage of radioactive waste [6].

Basic aspects of radiation chemistry of polymers became involved, when the H_2 radiation yields were confronted with the composition of commercial polymers and with the effects of polymer irradiation. As concerns the composition: The spectrum of additives present in commercial polymers is very wide – otherwise the processing of polymers for their application in industry and household would have been impossible. Comparatively pure polymers, *i.e.* obtained directly from the polymerization line, after basic purification from catalysts and unwanted isomers, are used in basic research only. That was the case with polypropylene used by A. Rafalski in his Ph.D. thesis [7]. That kind of polymer yields important results concerning its radiation chemistry, in spite of the fact that it can be processed, e.g. into films, after addition of stabilizers only.

Consideration of G_{H2} radiation yields as a part of complete radiation chemistry of polymers, had permitted to draw important conclusions. The majority of commercial polymers show a typical curve of hydrogen yield *vs*. the dose, with a visibly lower yield at the beginning of the curve. After that initial step, the growth of hydrogen production is linear with dose (Fig.2). Production of hydrogen from a neat polymer, polypropylene, is linear from

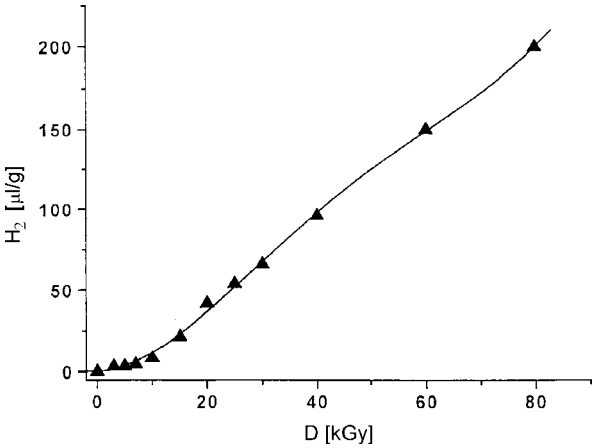

Fig.2. Hydrogen detachment from high-tech polymer (hydrogenated nitrile butadiene rubber) of complicated radiation-induced crosslinking system.

the beginning (Fig.3). Evidently the mechanism of radiolysis of commercial polymer at the beginning of irradiation is different. Leaving the full discussion to the detailed publications, we can explain the phenomenon by the consumption of additives present in polymers, by intermediate species of radiolysis. The degree of crosslinking *vs*. the dose is usually parallel to the hydrogen-detachment curve, *i.e.* at the beginning the crosslinking cannot

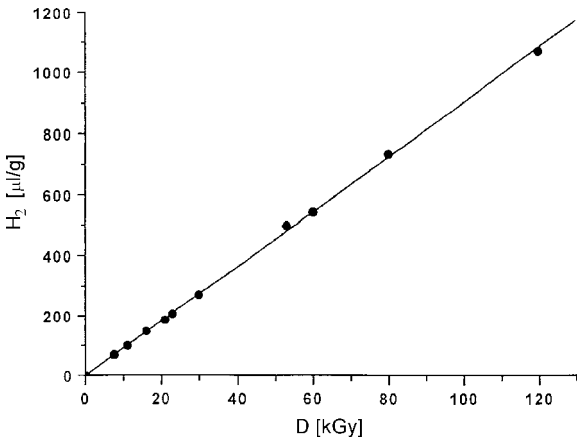

Fig.3. Radiolytic hydrogen production from virgin polypropylene without additives (as taken from the production line at Płock-Orlen Works, Poland).

occur. The additive which is present next to the chain, is winning here the competition for the positive hole (h^+). The loser is the energetically favourable site where two chains of the polymer are sufficiently close together. At subsequent higher doses, the meeting sites of two chains, the irradiated and unirradiated chain are only places where the transfer of h^+ stops, to release hydrogen and form the crosslinking bond. Comparison of hydrogen yields *vs*. dose is the vital part of the future work, because crosslinking of polymers shows also the effect of diminished yield at starting doses of irradiation [8, 9].

If the polymer-additive has aromatic groups, and that is usually the case, or the polymer is a mixture or co-polymer aliphatic-aromatic, the energy transfer to aromatic moieties results in dissipation of absorbed energy in single ionization steps. The ionizing energy is changing into emission of visible light, and/or changing into molecular vibrations manifested as chemically ineffective heat. The main source of hydrogen in the zone of low dose irradiated, protected polymers are multi-ionization spurs which occur also in random sites, but cannot be transferred. The result is an immediately broken chain of the polymer and sometimes additional formation of low molecular weight debris of the polymer from sites around the scission point.

The initial, low degradation zone of radiolysis is welcomed, if the polymer is irradiated for the sake of sterility, with a minimum degree of degradation. The unavoidable degradation, caused by 20% of deposited energy in multi-ionization spurs, can be reduced by proper additives to the polymer. The present incorporation of hydrogen determination in irradiated synthetic polymer matches other phenomena observed in irradiated polymers, as reported at the recent IMRP Chicago 2003 Conference [9] and the Conference on Advances in Radiation Chemistry of Polymers organized in 2003 by the International Atomic Energy Agency at the University of Notre Dame [10]. A new approach to radiolysis of polymers is also a supplement to the successful radiation crosslinking specifically of polyethylene, which started on the commercial scale 50 years ago [11].

The behaviour of biopolymers is in general different. The radiation yield of hydrogen is lower, and the starting part of the curve does not show the pre-step like in C-H polymers with additives. As an example, Fig.4 shows the radiolytic hydrogen generation curve of two kinds of keratin. The radiation chemistry of biopolymers as a part of our hydrogen research is not as advanced as in the case of synthetic polymers yet, but it seems to be more important in 2004.

In conclusion, our investigations of radiation yields of hydrogen release from irradiated polymers have shown important regularities. In general, the detachment of H_2 is an irreversible reaction, a substantial element of definite degradation, not sufficiently stressed until now. It is not well accepted by specialists in polymers, where such reaction is not existent, except for the fragment of

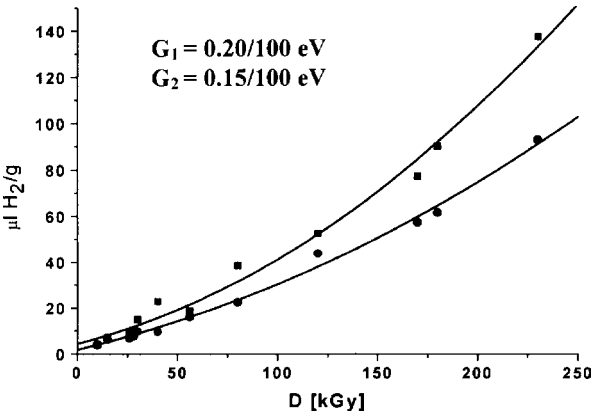

Fig.4. Radiation-induced hydrogen production from two kinds of keratin.

the thermal degradation. The irreversibility of dehydrogenation of biopolymers is specially important because it means the loss of any functions belonging to life processes. The radiation damage of biopolymers in aqueous solutions is very often repaired, because radiation-induced reactions start with the main constituent of the system, *i.e*. with radiolysis of water. Biopolymers in solution are not the object of direct radiolysis but of the attack of reactive species of water radiolysis. Radiolysis of the same biopolymers in the dry state starts with direct ionization actions on macromolecules with completely different chemical reactions. The dehydrogenation occurring in dry forms of life, like in the case of spores of bacteria, means immediate, irreversible destruction already by low doses of radiation.

References

[1]. Zagórski Z.P.: Radiat. Phys. Chem., 34, 839-847 (1989).
[2]. Zagórski Z.P.: Radiat. Phys. Chem., 56, 559-565 (1999).
[3]. Zagórski Z.P.: Radiat. Phys. Chem., 22, 409-418 (1983).
[4]. Zagórski Z.P.: Postępy Techniki Jądrowej, 12, 601-608 (1968), (in Polish).
[5]. Zagórski Z.P.: Thermal and electrostatic aspects of radiation processing of polymers. In: Radiation Processing of Polymers. Eds. A. Singh, J. Silverman. Hanser Publishers, Munich 1992, pp.271-287.
[6]. Zagórski Z.P., Dziewinski J., Conca J.: Radiolytic effects of plutonium. In: Plutonium Futures – the Science. Ed. G.D. Jarvinen. American Institute of Physics, 2003, Conference Proceedings, Vol.673, pp.336-338.
[7]. Rafalski A.: Unstable products of radiolysis of polypropylene. Ph.D. Thesis. Instytut Chemii i Techniki Jądrowej, Warszawa 1998 (in Polish).
[8]. Bik J., Głuszewski W., Rzymski W.M., Zagórski Z.P.: Radiat. Phys. Chem., 67, 421-423 (2003).
[9]. Zagórski Z.P.: EB crosslinking of elastomers, how does it compare with radiation crosslinking of other polymers? Contribution S-185 to the International Meeting on Radiation Processing, Chicago 2003, p.279.
[10]. Zagórski Z.P.: Radiation chemistry of spurs in polymers. IAEA Consultants Meeting (CT) on "Advances in Radiation Processing of Polymers" at Radiation Laboratory, University of Notre Dame, USA, 13-17 September 2003, to be published as IAEA TECDOC, 2004.
[11]. Zagórski Z.P.: Postępy Techniki Jądrowej, 46, (4) 10-16 (2003), (in Polish).

DEGRADATION OF PESTICIDE 2,4-D BY γ-RADIATION COMBINED WITH HYDROGEN PEROXIDE

Przemysław Drzewicz, Anna Bojanowska-Czajka, Wojciech Głuszewski, Grzegorz Nałęcz-Jawecki[1/], Józef Sawicki[1/], Edward Listopadzki[2/], Marek Trojanowicz

[1/] Department of Environmental Health Sciences, Medical University of Warsaw, Poland

[2/] Roktita-Agro S.A., Brzeg Dolny, Poland

The least expensive source of hydroxyl radicals is Fenton process, however, its drawback is side-production of iron-containing sludge and slow rate of H_2O_2 reduction by Fe(II) [1, 2]. Also inexpensive photolytic reduction of hydrogen peroxide to hydroxyl radicals in aqueous solutions has certain limitations. Its rate is highest for UV irradiation at 210 to 230 nm [3], however, this process has to compete with absorption of many other organic compounds present in wastes. Hydroxyl radicals are also produced during ozonation in the presence of H_2O_2, which provides more efficient decomposition of organic compounds than in the absence of hydrogen peroxide, however also this reaction is considered as slow [4].

An increase of efficiency of degradation of organic compounds for combined γ-irradiation and electron beam irradiation with hydrogen peroxide was observed by Gehringer *et al*. [5] for tetrachloroethylene (PCE) and 1,2,2-trichloroethylene (TCE). A similar observation was reported for degradation of chloroform by γ-irradiation with H_2O_2 [6]. Recently, in radiation-reduced degradation of polyvinyl alcohol it was found that at a certain dose rate there was an optimal dosage of H_2O_2 to facilitate the degradation and above which H_2O_2 dosage reduced the degradation efficiency [7]. Chloroalkanes react faster with hydrated electron and with hydrogen radical than with hydroxyl radicals. In spite of the fact that oxygen is a scavenger of hydrated electron and H radical, the presence of oxygen in irradiated solution enhances degradation of chlorinated ethylenes [8] and trihalomethanes (THMs) [9]. Additionally, oxygen is involved in further radical chain reactions of chlorinated alkanes. Wu *et al*. [6], have found that concentration of oxygen in irradiated solution is constant during γ-irradiation of chloroform in the presence of hydrogen peroxide.

The hydrogen peroxide reacts with $H^\bullet$ (k (20°C) = 2.4×10^{10} $M^{-1}s^{-1}$) and with e_{aq} (k (20°C) = 1.5×10^{7} $M^{-1}s^{-1}$) as follows [10]:

$$e^-_{aq} + H_2O_2 \longrightarrow {}^\bullet OH + OH^- \quad (1)$$

$$H^\bullet + H_2O_2 \longrightarrow {}^\bullet OH + H_2O \quad (2)$$

In the presence of excess of hydrogen peroxide in solution it can scavenge the hydroxyl radicals with rate constant k (20°C) = 3.1×10^{10} $M^{-1}s^{-1}$ [10], according to the reactions:

$$^\bullet OH + H_2O_2 \longrightarrow H_2O + HO_2^{\bullet-} \quad (3)$$

$$2\ HO_2^{\bullet-} \longrightarrow H_2O_2 + O_2 \quad (4)$$

The total effect of reactions (3) and (4) is the following process:

$$^\bullet OH + H_2O_2 \longrightarrow 2\ H_2O + O_2 \quad (5)$$

The estimation of optimum amount of hydrogen peroxide needed in order to enhance a given process is difficult, as it is involved in numerous reactions with radicals formed during radiolytic degradation of target compounds. Additional problem is self-decomposition of hydrogen peroxide to water and oxygen, which depends on pH. The first order rate constant of self decomposition of hydrogen peroxide is $2.29\text{x}10^{-2}$ min^{-1} at pH 7 and $7.4\text{x}10^{-2}$ min^{-1} at pH 10 [11]. In order to decrease the rate of decomposition of hydrogen peroxide to oxygen and water, it is usually carried out in solution of pH 5.

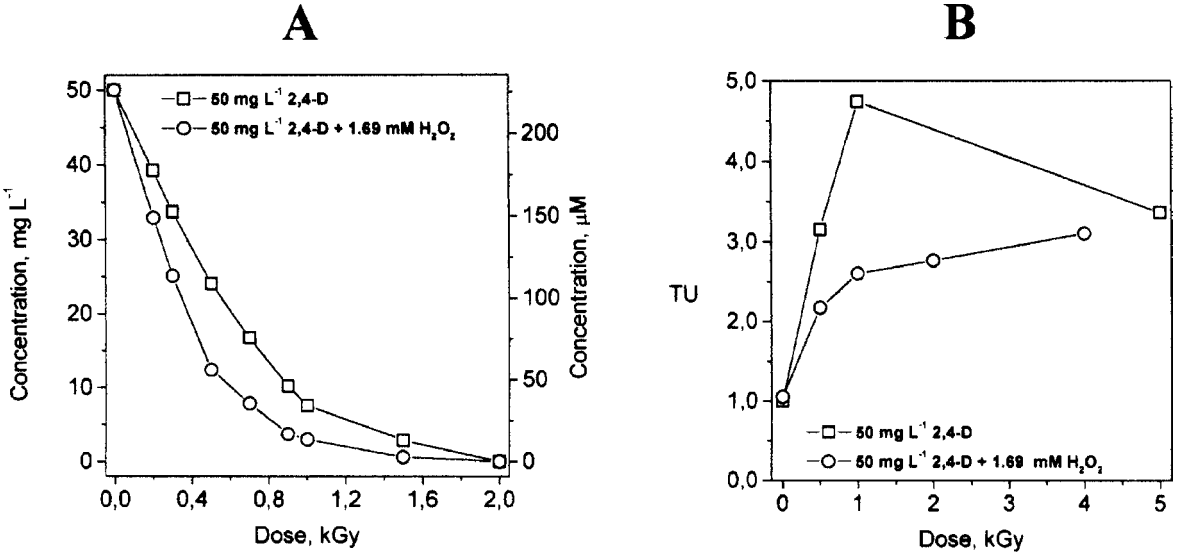

Fig.1. Effect of addition of 1.69 mM hydrogen peroxide on decomposition of 50 mg L^{-1} 2,4-D by γ-irradiation (A) and changes of toxicity of the same irradiated solution measured by Microtox test (B).

Although it was reported that hydrogen peroxide does not react with 2,4-dichlorophenoxyacetic

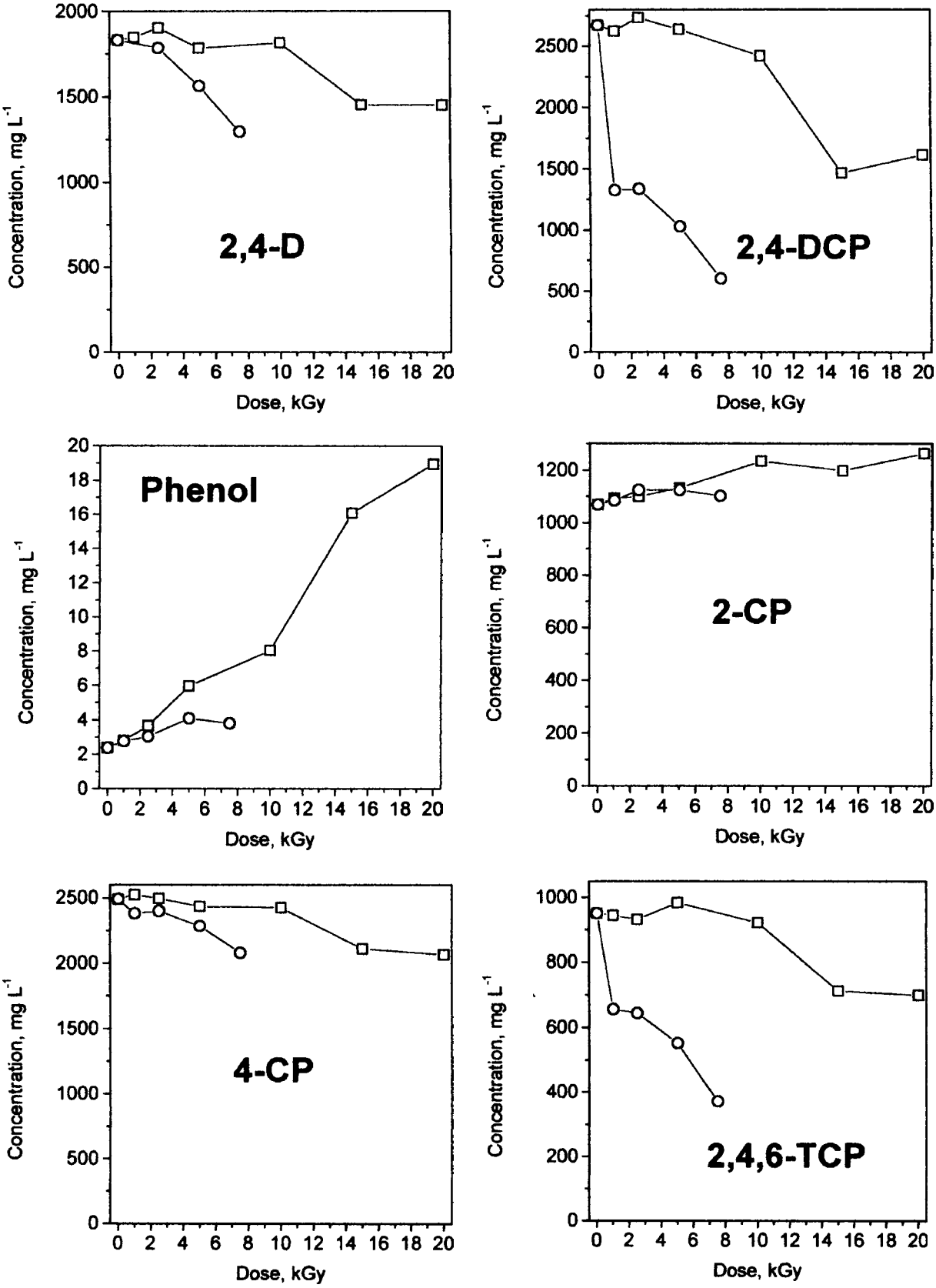

Fig.2. Degradation of selected organic pollutants by γ-irradiation in industrial wastes from synthesis of 2,4-D observed without addition of hydrogen peroxide (□) and in the presence (○) of 39 mM hydrogen peroxide in irradiated solutions.

acid (2,4-D) [12], and also with products of its decomposition, phenol and chlorophenols [13], in several radical reactions taking place during decomposition of 2,4-D oxygen is involved [14], hence the subject of this work was to examine the effect of hydrogen peroxide on the decomposition of 2,4-D.

Irradiation of the examined aqueous samples was carried out in a Russian cobalt source "Issle-

dovatel" with a dose-rate of 1.76 kGy/h. Aqueous solutions of herbicide were irradiated in 300 ml Winkler bottles (commonly used for dissolved oxygen measurements) without deaeration. Analytical determination of 2,4-D and products of its irradiation was carried out using reversed-phase high performance liquid chromatography (HPLC) in a Shimadzu setup with a diode array detector and using a column Luna ODS2, 5 μm, 250x4.6 mm and a guard column from Phenomenex (Torrance, CA, USA). The sample injection volume was 20 μL. As eluent the solution containing 2 g/L of citric acid in a mixture of water, methanol and acetonitrile in volume ratio 65:35:5 was used, at a flow rate of 1 mL/min.

tion stage was taken in which chemical oxygen demand (COD) value was 79.2 gL^{-1} and pH 8. In this sample, HPLC measurements allowed to identify and quantitate 2-chlorophenol (2-CP), 4-chlorophenol (4-CP), 2,6-dichlorophenol (2,6-DCP), 2,4-dichlorophenol (2,4-DCP), 2,4,6-trichlorophenol (2,4,6-TCP) and 2,4-dichlorophenoxyacetic acid at levels shown in Fig.2. The addition of 39 mM hydrogen peroxide to irradiated waste for all mentioned pollutants causes their more efficient decomposition compared to irradiation without H_2O_2. Some of these compounds, e.g. phenol or dichlorophenols, are products of degradation of higher chlorinated compounds hence increase of their content with increase of applied dose is observed. This

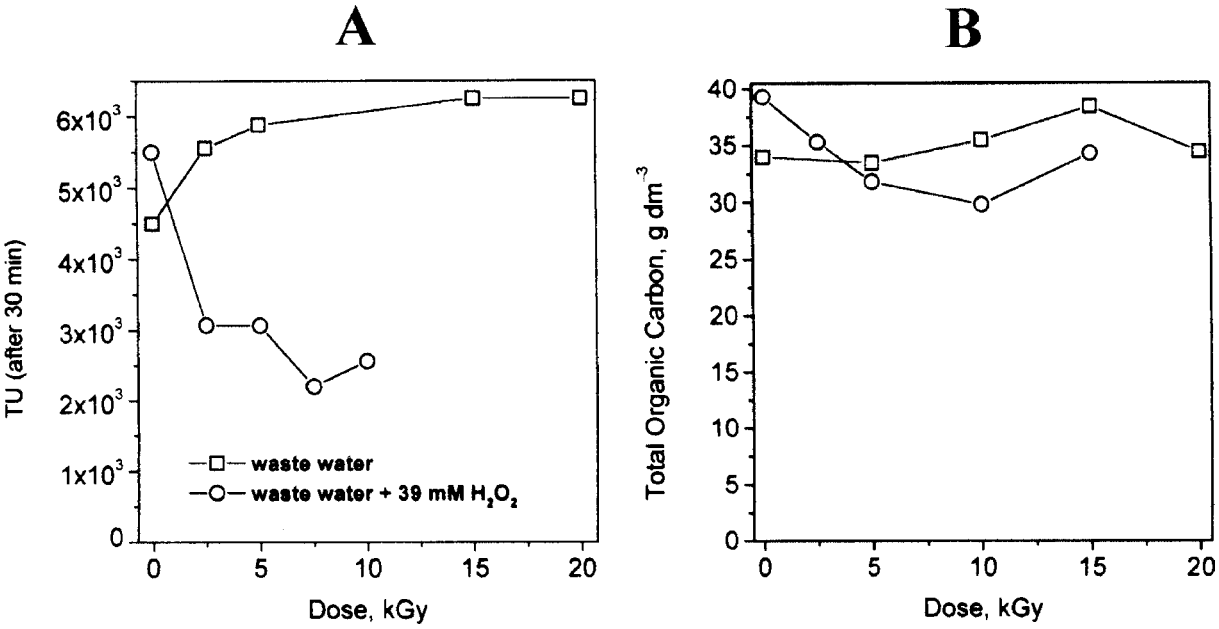

Fig.3. Changes of toxicity (A) and total organic carbon (B) observed during irradiation of wastes from production of 2,4-D in the absence (□) and in the presence (○) of 39 mM hydrogen peroxide in irradiated solutions.

It was found that addition of 1.69 mM H_2O_2 to irradiated solution at pH 7 allows to decrease the γ-irradiation dose to decompose 95% of 2,5-D at initial concentration 50 mg L^{-1} from 2 to 1 kGy (Fig.1A). Simultaneously, 50% lower toxicity of irradiated solution was observed (Fig.1B). This illustrates the fact that during irradiation the hydrogen peroxide added is an additional source of oxygen and hydroxyl radicals that results in more efficient degradation of 2,4-D and their products.

The effect of the presence of hydrogen peroxide to irradiated samples was also examined for samples of industrial wastes from production of 2,4-D. The synthesis of 2,4-D proceeds in three stages, the first being by chlorination of phenol yelding 2,4-dichlorophenol (2,4-DCP). Then in alkaline medium a condensation of 2,4-DCP with chlorooacetic acid is carried out, and 2,4-D formed is precipitated as sodium salt. Finally, 2,4-D is transformed into acid form and purified. Wastes produced in synthesis of 2,4-D, beside organic pollutants, contain also a substantial level of sodium chloride (about 0.1 gL^{-1}), which can be recycled industrially after removal of organic pollutants. For irradiation studies, the waste from the condensa-

effect, however, is evidently reduced in the presence of hydrogen peroxide. The waste irradiated in the presence of hydrogen peroxide exhibits also significantly lower toxicity than in the absence of H_2O_2 (Fig.3A), although the addition of H_2O_2 does not affect the level of total organic carbon in irradiated solutions (Fig.3B).

Although it was shown to be effective in the discussed case, the addition of hydrogen peroxide to irradiated solutions containing organic pollutants is less efficient than electron beam irradiation in the presence of ozone [15], hydrogen peroxide is a less expensive reagent for industrial use than ozone. Further increase of efficiency of radiolytic degradation of organic pollutants in the presence of H_2O_2 requires both careful optimisation of chemical conditions of irradiation (pH, concentration of H_2O_2) as well as preliminary chemical neutralization of wastes prior to irradiation.

References

[1]. Walling C., Goosen A.: J. Am. Chem. Soc., 95, 2987-2991 (1973).
[2]. De Laat J., Gallard H.: Environ. Sci. Technol., 33(16), 2726-2732 (1999).

[3]. Beltran F.J., Ovejero G., Acedo B.: Water Res., 27(6), 1013-1021 (1993).
[4]. Sehested K., Corfitzen H., Holcman J., Hart E.J.: J. Phys. Chem., 96, 1005-1009 (1992).
[5]. Gehriger P., Eschweiler H.: Radiat. Phys. Chem., 65, 379-386 (2002).
[6]. Wu X.Z., Yamamoto T., Hatashita M.: Bull. Chem. Soc. Jpn., 75, 2527-2532 (2002).
[7]. Zhang S.J., Yu H.Q.: Water Res., 38, 309-316 (2004).
[8]. Gehringer P., Proksch E., Eschweiler H., Szinovatz W.: Radiat. Phys. Chem., 35, 456-460 (1990).
[9]. Cooper W.J., Cadavid E.M., Nickelsen M.G., Lin K., Kurucz C.N., Waite T.D.: J. Am. Water Works Assoc., 85, 106-112 (1993).
[10]. Christensen H., Sehested K., Logager T.: Radiat. Phys. Chem., 43, 527-531 (1994).
[11]. Chu W.: Chemosphere, 44, 935-941 (2001).
[12]. Sun Y. Pignatello J.J.: J. Agric. Food Chem., 41, 1139-1142 (1999).
[13]. De A.K., Chaudhuri B., Bhattacharjee S., Dutta B.K.: J. Hazard. Mater., 64, 91-104 (1999).
[14]. Zona R., Solar S., Sehested K., Holcman J., Mezyk S.P.: J. Phys. Chem. A, 106, 6743-6749 (2002).
[15]. Drzewicz P., Trojanowicz M., Zona R., Solar S., Gehringer P.: Radiat. Phys. Chem., 69, 281-287 (2004).

STABILITY OF THE EPR SIGNAL PRODUCED BY IONIZING RADIATION IN SPICES AND SEASONINGS

Katarzyna Lehner, Wacław Stachowicz

It has been proven experimentally that under the action of ionizing radiation on dried spices, herbs and seasonings a specific signal is observed in electron paramagnetic resonance (EPR) spectroscopy. This EPR signal is usually quite stable at room temperature. It is identified in EPR by two weak satellite lines distanced about 6 mT and located from both, low field and high field sides of a strong central line with g = 2.003. The central signal alone appears also in the most of spices, herbs and seasonings which were not exposed to the action of radiation. It is generally accepted that this strong signal is derived from semi-quinone radical which is usually present in many foods of rural origin. Two satellite lines belong presumably to cellulose radical produced by radiation which give rise in EPR to a triple line. However, the appearance of a strong semi-quinone EPR signal in both irradiated and non-irradiated spices makes it impossible to observe the central line of a much weaker cellulose born triplet in the EPR spectra due to the overlapping of the latter [1].

The detection of two satellite lines distanced *ca*. 6 mT appearing in the neighborhood of a strong singlet is a proof of radiation treatment of foods (Fig.). The method has been standardized and validated through several inter-laboratory trials organized at international level [2, 3]. The results of trials were fully positive. Consequently, the method has been approved as one of the European Standards for the detection of irradiated foods numbered EN 1787. It has also a status of the Polish Standard PN-EN 1787 [4].

The stability of the cellulose radical in dried foods is relatively high at room temperature, but it depends strongly on the cellulose structure inside the product and its moisture content. The location of cellulose radicals inside the crystalline network of cellulose is decisive. Thus, from a practical point of view it is very important to have the knowledge on the stability of these radicals in various products when kept in typical storage conditions. Obviously, to meet the requirement of a reliable detection method of radiation treatment in foods, the EPR signal of cellulose radical must be stable enough to be measurable longer than lasts the validity period of a product for consumption.

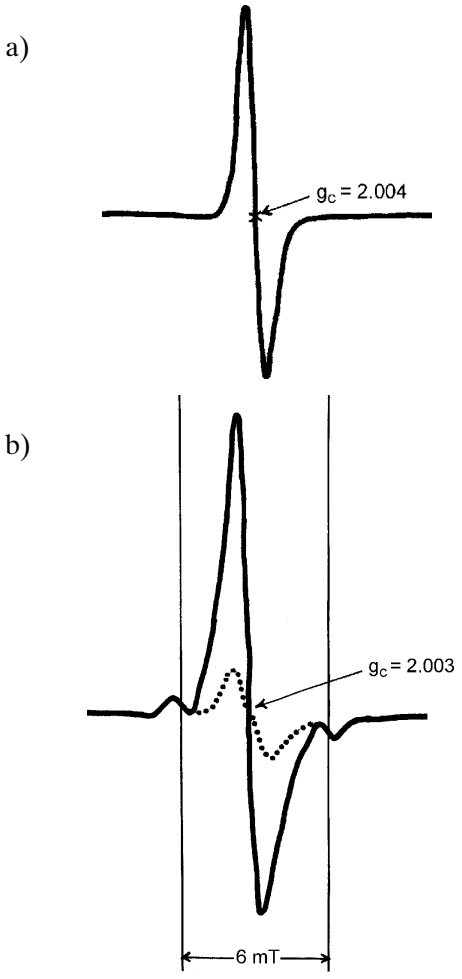

Fig. EPR spectra (first derivative) of pistachio nut: a) non-irradiated and b) irradiated with 7 kGy of gamma rays. a) 2.004 denotes g_c of the EPR signal assigned to the semi-quinone radical. b) Positions of both satellite lines of a triplet assigned to the cellulose radical are marked with vertical lines. The distance between both lines is 6 mT. Dashed line indicates the expected localisation of central line belonging to the cellulose radical overlapped by a strong signal of the semi-quinone radical. 2.003 denotes g_c of superposed central line.

This is the decisive criterion of the applicability of the method for the detection of irradiation in different foods and condiments.

As to our knowledge, there is unavailable full information on the stability of cellulose radicals which could be useful to predict the applicability of the method for the detection of irradiation in different spices. The aim of present study is to eliminate this gap.

Twenty six different spices available in the market have been examined. All are listed in Table. The samples were irradiated with a dose of 7 kGy of gamma rays from the INCT ^{60}Co irradiator "Issledovatel". The measurements have been done with the use of an EPR-10 MINI spectrometer installed in the Laboratory for Detection of Irradiated Foods of the Institute of Nuclear Chemistry and Technology. The EPR examination of the samples has been accomplished during 14 months from the date of irradiation. The results of measurements are comprehended in Table. As seen, there are only a few spices in which radiation induced cellulose radical survives longer than 3 months. Fortunately, such popular spices as red pepper, curry, onion and chili belong to this group. However, the results obtained with black pepper were not satisfactory enough.

On the other side, the Table indicates those spices which are not appropriate for EPR examination since cellulose radicals are not effectively stabilized in them. The general conclusion from the study is that in respect to spices the EPR method for the detection of radiation treatment based on the identification of cellulose radicals although standardized should be treated as a typical screening method only. In other words, the detection of cellulose radical is

Table. Stability of EPR signals (two satellite line) assigned to cellulose radical in spices irradiated with the dose of 7 kGy. Storage of samples at room temperature (18÷23°C).

Spice	Storage time after irradiation										
	1 day	1 week	fortnight	1.5 month	bimester	2.5 month	3 months	6 months	11 months	12 months	14 months
marjoram[1]	–	–	–	–	–	–	–	–	–	–	–
saffron[3]	–	–	–	–	–	–	–	–	–	–	–
basil[1]	±	–	–	–	–	–	–	–	–	–	–
oregano[1]	±	–	–	–	–	–	–	–	–	–	–
nutmegapple[3]	+	±	–	–	–	–	–	–	–	–	–
ginger[3]	±	±	–	–	–	–	–	–	–	–	–
fennel[1]	+	+	–	–	–	–	–	–	–	–	–
curcuma[3] (turmeric)	+	+	–	–	–	–	–	–	–	–	–
lovage[1]	+	±	–	–	–	–	–	–	–	–	–
white pepper[3]	±	±	±	–	–	–	–	–	–	–	–
rosemary[1]	+	+	±	–	–	–	–	–	–	–	–
caraway[2]	+	+	+	±	–	–	–	–	–	–	–
cayene pepper[3]	+	+	+	±	–	–	–	–	–	–	–
parsley[1]	+	+	+	±	–	–	–	–	–	–	–
tarragon[1]	+	+	+	+	±	–	–	–	–	–	–
pimento[2]	+	+	+	+	±	–	–	–	–	–	–
cloves[2]	+	+	+	+	+	–	–	–	–	–	–
juniper[2]	+	+	+	+	+	+	–	–	–	–	–
black pepper powder[3]	+	+	+	+	±	±	±	–	–	–	–
black pepper corns[2]	+	+	+	+	±	±	±	–	–	–	–
charlock[2] (white mustard)	+	+	+	+	+	+	+	±	–	–	–
curry[3]	+	+	+	+	+	+	+	+	±	–	–
laurel leaf[1] (bay leaf)	+	+	+	+	+	+	+	+	±	–	–
sweet paprika[3]	+	+	+	+	+	+	+	+	+	–	–
hot paprika[3]	+	+	+	+	+	+	+	+	+	+	–
onion[4]	+	+	+	+	+	+	+	+	+	+	±
chili[3]	+	+	+	+	+	+	+	+	+	+	±

[1] leafs, caulis; [2] seeds, fruits, flowers; [3] powder; [4] granulate.

a 100% proof of irradiation, while the lack of the corresponding EPR cellulose signal does not mean necessarily that sample was non-irradiated.

References

[1]. Goodman B.A., McPhail D.B., Duthie D.M.L.: J. Sci. Food Agric., 47, 101-111 (1989).

[2]. Raffi J.: ESR Inter-comparison Studies on Irradiated Foodstuffs. BCR-Information 1992. Report EUR/13630/en.

[3]. Raffi J. *et al.*: Int. J. Food Sci. Technol., 27, 111-124 (1992).

[4]. PN-EN 1787: Artykuły Żywnościowe: Wykrywanie napromieniania żywości zawierającej celulozę; metoda spektroskopii EPR. June 2001.

DETECTION OF RADIATION TREATMENT OF POWDERED PAPRIKA ADMIXED TO COTTAGE CHEESE

Kazimiera Malec-Czechowska, Wacław Stachowicz

Cottage cheese belongs to a group of condiments characterised by a short storage time. The product is consumed without thermal treatment and for that reason must meet high microbiological quality ensuring safety for the consumers. The additives of a natural origin *i.e.* spices and herbs admixed to improve the taste are very often characterised by a high level of microbial contamination. For that reason, to avoid the danger of development of food born diseases, they are proposed to undergo radiation treatment.

According to the requirements of the Directive 1999/2/EC and in agreement with the Decree issued by the Minister of Health on 15th January 2003, all foods treated with ionising radiation and/or produced with the admixing of irradiated components must be labelled [1, 2].

The aim of the study undertaken in the Laboratory for Detection of Irradiated Foods of the Institute of Nuclear Chemistry and Technology (INCT) in the frames of the Polish Committee for Scientific Research (KBN) grant No. 6 P0 6T 026 21 was

Table. Results of TL measurements on silicate minerals isolated from one control sample of cottage cheese containing 0.1% by weight of non-irradiated paprika and test samples of different (from 0.1 to 0.5% by weight) content of powdered paprika irradiated with 7 kGy of gamma rays.

No.	Product and its code	Percentage of paprika irradiated with 7 kGy	TL intensity Glow 1 (214-284°C)	TL intensity Glow 2 (214-284°C)	Glow 1/Glow 2 (214-284°C)	$(\text{Glow 1/Glow 2})_{av} \pm SD$
1	Cream cheese SOK	0.1 (non-irradiated)	1226 249 1894	881073 140572 915233	0.001 0.002 0.002	0.0017 ± 0.0006
		0.1	2535885 2748127 4854232	1555341 1856842 4221071	1.63 1.48 1.15	1.42 ± 0.25
		0.25	55168 1215124 843215	30203 826615 481837	1.83 1.47 1.75	1.68 ± 0.19
		0.50	15508641 6184483 1510370	7566518 2786451 937343	2.05 2.22 1.61	1.96 ± 0.31
2	Cottage cheese natural SP	0.1 (non-irradiated)	4898 10154 7248	5079685 3485136 6124321	0.0009 0.003 0.001	0.0016 ± 0.0012
		0.1	1960295 2153083 1724851	1308702 1251792 1165440	1.50 1.72 1.48	1.57 ± 0.13
		0.25	3506361 2754813 5128512	1807991 1700501 3465210	1.94 1.62 1.48	1.68 ± 0.24
		0.50	4289587 4419107 6453275	2482311 2951405 3708779	1.73 1.50 1.74	1.66 ± 0.14

to prove the application of the thermoluminescence (TL) method for the detection of irradiated components contained in non-irradiated condiments.

In the present communication, the results of the TL measurements on silicate minerals isolated from non-irradiated cottage cheese with varying content of irradiated paprika are presented. The grounded red paprika was irradiated with a dose of 7 kGy in a ^{60}Co gamma cell "Issledovatel" installed in the Department of Radiation Chemistry and Technology of the INCT. Test samples of cottage cheese obtained from two producers were modified by adding a defined amount of irradiated paprika to each sample. In parallel, the sample of cheese containing 0.1% by weight of non-irradiated paprika was prepared, too.

In order to isolate silicate minerals from test samples, the matrix was hydrolysed with 1 M KOH solution in methyl alcohol. The process was conducted in a round flask equipped with a serpentine cooler in a water bath at 60°C during 1.5 h. The solution was decanted while mineral fraction taken from the button of a flask and placed with a Pasteur pipette in a test-tube. A further purification procedure of mineral fraction was undertaken according to PN EN 1788 standard [3].

The TL measurements were done with a TL reader, model TL-DA-15 (Risoe National Laboratory, Denmark). The measuring conditions were as in our earlier works [4, 5].

In enclosed Table, the results of measurements are comprehended. The intensities of TL Glow 1 were calculated within the range of temperature from 214 to 285°C. This temperature range is routinely used in the lab and was estimated in accordance with the requirements given in Annex 1 to PN EN 1788. The TL intensities of minerals treated with a normalising dose of 1 kGy (Glow 2) are given, too. The ratios Glow 1/Glow 2 for each sample were calculated and included in the Table. The ratios were found higher than 0.1 with those samples that contained 0.50, 0.25 and 0.1% of irradiated paprika by weight. On the other side the ratios were significantly lower that 0.1 if minerals isolated from non-irradiated paprika were examined.

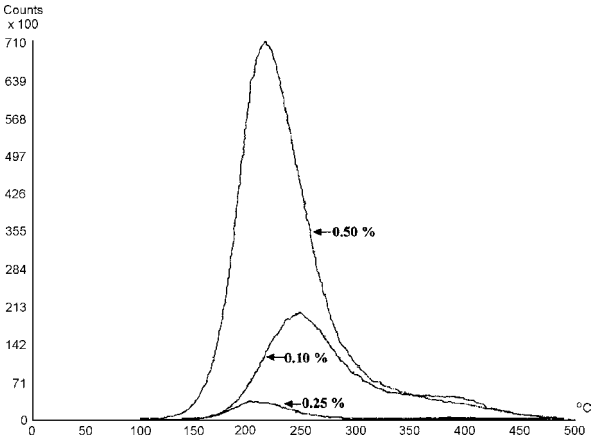

Fig.1. TL Glow 1 curve of silicate minerals isolated from test sample of cream cheese SOK with different content of powdered paprika irradiated with 7 kGy of gamma rays.

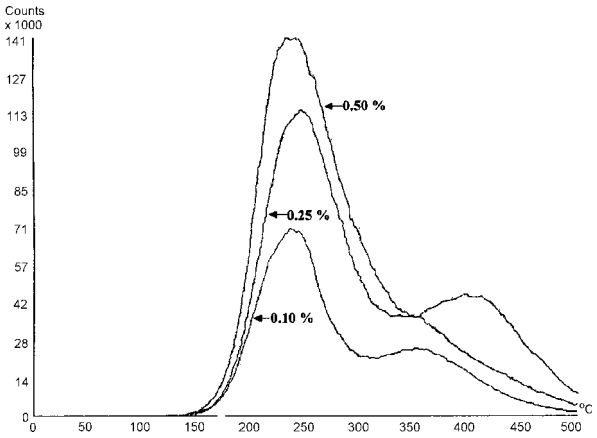

Fig.2. TL Glow 1 curve of silicate minerals isolated from test sample of cottage cheese natural SP with different content of powdered paprika irradiated with 7 kGy of gamma rays.

In Figs.1 and 2 the Glow 1 curves recorded with silicate minerals isolated from test samples of two varieties of cottage cheese (cream cheese SOK and cottage cheese natural SP) with equal contents of irradiated paprika are presented. The recorded shape of Glow 1 curves is typical for irradiated products with the maximum within the range of temperature 150 and 250°C.

The presented results show that the TL method is suitable for the detection of the admixture of irradiated paprika to non-irradiated cottage cheese under condition that its content is 0.1% by weight or higher.

Taking advantage of obtained results, similar TL studies were undertaken on commercial cottage cheese containing typically pepper, herbs, dried mushrooms and dehydrated vegetables. The results of the measurements show conclusively that in the production of these condiments the irradiated additives are quite common. Twelve samples of different products purchased in the market were examined while 8 of them contained irradiated stuff.

References

[1]. Directive 1999/2/EC of the European Parliament and of the Council of 22 February 1999 on the approximation of the Member States concerning foods and food ingredients treated with ionising radiation. Off. J. European Communities L 66/16-23 (13.03.1999).

[2]. Rozporządzenie Ministra Zdrowia z dnia 15 stycznia 2003 r. w sprawie warunków napromieniowania środków spożywczych, dozwolonych substancji dodatkowych lub innych składników żywności, które mogą być poddane działaniu promieniowania jonizującego, ich wykazów, maksymalnych dawek napromieniowania oraz wymagań w zakresie znakowania i wprowadzania do obrotu. Dz. U. Nr 37, poz. 327.

[3]. Standard PN EN 1788:2002. Foodstuffs – Thermoluminescence detection of irradiated food from which silicate minerals can be isolated.

[4]. Malec-Czechowska K., Strzelczak G., Dancewicz A.M., Stachowicz W., Delincée H.: Eur. Food Res. Technol., 216, 157-165 (2003).

[5]. Malec-Czechowska K., Stachowicz W.: Nukleonika, 48, 3, 127-132 (2003).

THE INFLUENCE OF GAMMA IRRADIATION ON FUNCTIONAL PROPERTIES OF STARCH; GELATINISATION, CREATION OF THE COMPLEXES WITH CETYLTRIMETHYLAMMONIUM BROMIDE AND FILM FORMATION

Katarzyna Stefaniak, Krystyna Cieśla

Starch and a number of its connections (so called complexes) with surfactants and lipids are more and more widely applied as a food additive but also in a number of industries. In particular, the interest increased during the last years in the preparation of starch-surfactant systems with modified properties. Functional properties of starches and their complexes (for example ability to form gels or films and the resulting product properties) depend on the structure of starch granules. In regard to the known influence of irradiation on starch structure, these properties can be modified by ionising radiation. Our previous studies carried out by differential scanning calorimetry (DSC) [1, 2] and rheology showed the differences between gelatinisation and amylose-lipid complex structure taking place in the irradiated and non-irradiated potato, wheat, and corn starches.

At present, studies were carried out dealing with the influence of gamma irradiation on gelatinisation of potato and wheat starch. For this purpose we have adopted methods of swelling power measurements and analysis of the soluble starch polysaccharide using of the blue iodine method [3]. Moreover, the method was adopted for syntheses of the complexes between the selected samples of potato starch and cetyltrimethylammonium bromide (CTAB) [4]. The potato starch was selected because this starch of B-type do not contain native lipids connected to the polysaccharide chains. The attempts were carried out to prepare films using the synthesised products and pure starches.

Potato starch (laboratory extracted), was used as well as wheat starch and cetyltrimethylammonium bromide (both Sigma product). Irradiations were carried out with ^{60}Co radiation at a dose rate of 0.82 Gys^{-1} in a gamma cell "Issledovatel" in the Department of Radiation Chemistry and Technology of the Institute of Nuclear Chemistry and Technology. Solid native potato starch and dense water suspensions were irradiated applying doses of 0, 5, 10, 20 and 30 kGy. Wet samples were lyophilised afterwards at ambient temperature. Solid native wheat starch was irradiated with 0, 1, 2, 5, 10, 20, 30 kGy.

Starch suspensions (2.4%) were prepared and heated during 1 h at selected temperature. The resulting products were centrifuged at 2200 turns per min and the volume of gels was determined. The solution was separated from gel and used for detection of the soluble starch (free amylose) applying the blue iodine method. The complex absor-

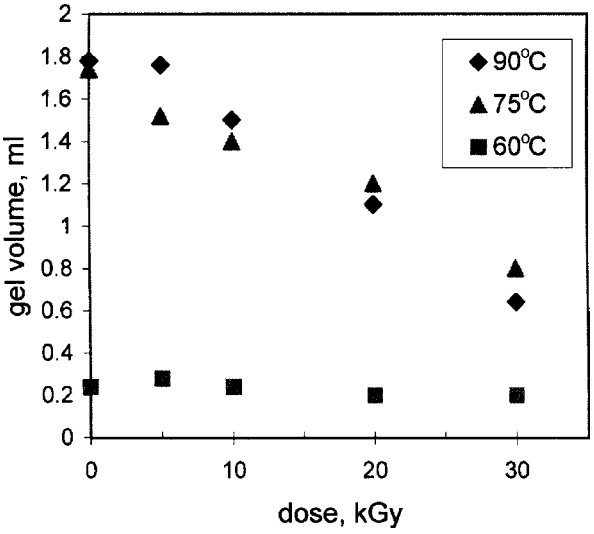

Fig.1. Volume of gel obtained after 1 h of heating at 60, 75 and 90°C of 3 ml of the suspension (concentration equal to 2.4%) of the potato starch irradiated using various doses.

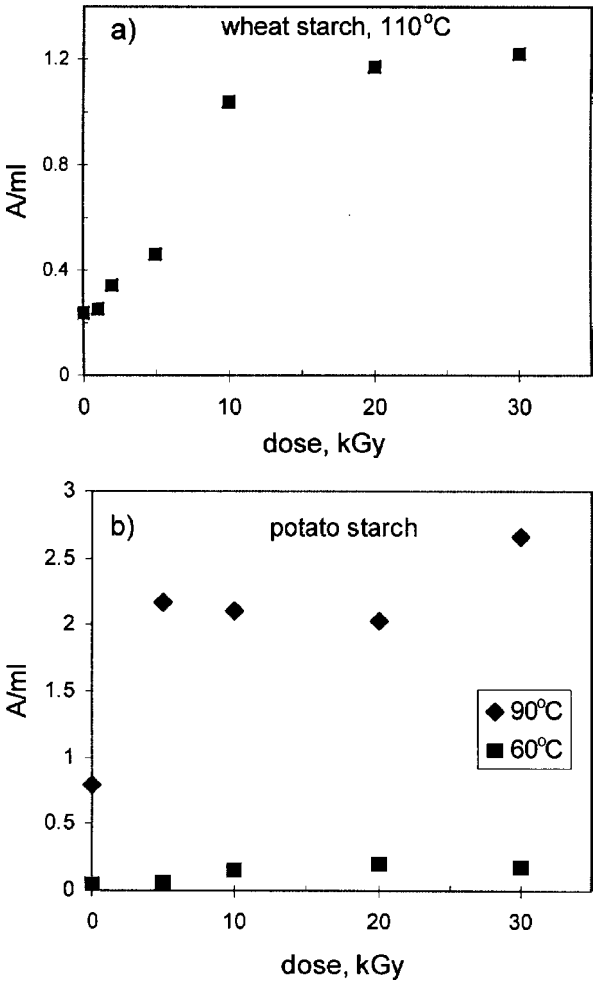

Fig.2. Dose dependence of the maximum absorbance of the blue iodine complexes (expressed in means of 1 ml): a) wheat starch heated at 110°C; b) potato starch heated at 60, 75 and 90°C.

bance in UV region were related to 1 ml of the solution.

The experiments were carried out dealing with the syntheses of complexes between the reference potato starch and CTAB. 1% water solution containing CTAB was introduced into hot 1% starch gels during vigorous stirring at 70°C and heated for a required time at 70°C and afterwards at 90°C. The CTAB to starch weight ratio was equal to 0.2 and 0.1. The product was then centifuged and gel fraction was separated from the residual solution. In the first stage of experiments, the influence was tested of the amount of CTAB introduced to the samples as well as time of heat treatment on the amount of residual free CTAB. On the basis of these preliminary results, the conditions were selected for further complex preparation. Then, the syntheses were performed using the potato starch irradiated with a 30 kGy dose. The preliminary evaluation was done of the properties of the products (solutions, gels and films) obtained after connection of CTAB to the non-irradiated and irradiated starch as well as those obtained using of pure starches.

A larger amount of gel as well as a larger amount of free amylose in solutions are detected when a higher temperature was applied for gel creation [3]. Swelling power of starch decreases when the irradiation dose increases (Fig.1), as expected due to degradation taking place in starch. Simultaneously, free amylose appears in solution. The larger was irradiation dose applied, the larger intensity of the blue iodine complex was observed (the examples are shown for potato and wheat starch in Fig.2). Moreover, as a result of the differences in the structure of short starch chains, the maximum of the complex absorption is shifted to the smaller wavelengths (Fig.3). These results were

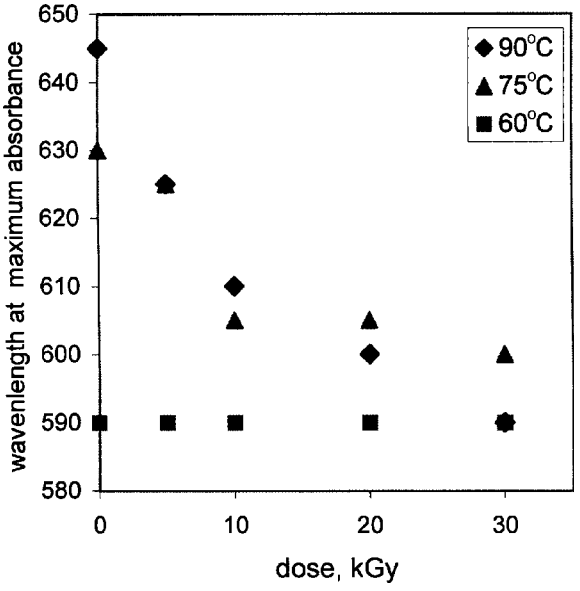

Fig.3. Dose dependence of the wavenlength of the maximum absorbance of the blue iodine complex of potato starch created on the way of 1 h heating at 60, 75 and 90°C.

obtained both in the case of the samples irradiated in solid state as well as in solutions. The results obtained for the solid native irradiated potato starch have, however, reveal better regularity as compared to the samples irradiated in suspensions and subjected to the additional treatment apart from irradiation.

It can be stated that 3.5 h of total heat treatment at 70-90°C suffices to connect all CTAB at $m_{CTAB}/m_S = 0.1$. No free CTAB was detected in the product by X-ray diffraction. At $m_{CTAB}/m_S = 0.2$ free CTAB was present in the product after heat treatment under the same conditions (Fig.4, curves 2 and 4). When, however, treatment time increases, more CTAB might be connected to starch. As a result, no free CTAB was noticed after heat treatment prolonged till 5.75 h (Fig.4, curve 3). Only gel fraction was found after centrifugation of this product.

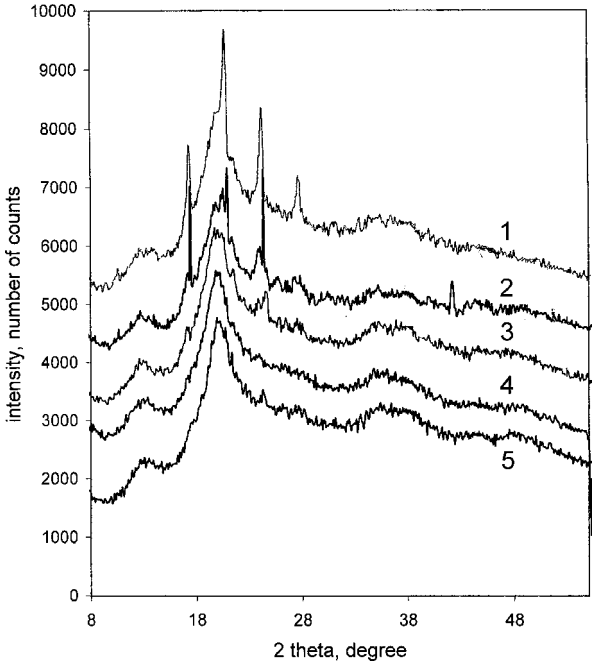

Fig.4. X-ray diffraction pattern of the product obtained on the way of treatment of the reference potato starch with CTAB applying various conditions: curve 1 – $m_{CTAB}/m_S = 0.2$, heating at 70°C during 55 min and 15 min at 90°C; curve 2 – $m_{CTAB}/m_S = 0.2$, 1.5 h at 70°C and 2 h at 90°C; curve 3 – $m_{CTAB}/m_S = 0.2$, 1.5 h at 70°C and 4.25 h at 90°C; curve 4 – $m_{CTAB}/m_S = 0.1$, 1.5 h at 70°C and 2 h at 90°C, curve 5 – pure starch, 1.5 h at 70°C and 2 h at 90°C.

Gels obtained after additions of CTAB were more dense than those prepared using the pure starches. Similarly as in the case of pure starch, only a small amount of gel was created after heating of the starch irradiated with a 30 kGy dose. The films were obtained then from the solution and gel fractions (after separation) as well as from total solutions. The solutions were carefully filtered before further operations. X-ray diffraction patterns do not show any presence of free CTAB in the products. No special differences can be stated – apart from those which can be attributed to the different drying time – on the basis of our preliminary X-ray diffraction data between the patterns of the films obtained starting from the particular fractions and those obtained from the irradiated

and non-irradiated samples, as well as from the complexes and pure starches (Fig.3).

The difference between consistency of the products obtained after connection of surfactant to the irradiated and control starch results from the currently found decrease in swelling power of our potato starch (in 2.5 times) and the essential increase in the amount of short soluble polysaccharide chains (in at least 4 times). Decreased viscosity of the starch-lipid system might appear profitable for preparation of the hydrophobic coatings characterised by improved adhesion to the surface.

References

[1]. Cieśla K., Eliasson A.-C.: Radiat. Phys. Chem., 64, 137-148 (2002).
[2]. Cieśla K., Eliasson A.-C.: Radiat. Phys. Chem., 68, 933-940 (2003).
[3]. Eliasson A.-C.: Starch/Stärke, 37, 411-415 (1985).
[4]. Eliasson A.-C.: Carbohydr. Res., 172, 83-95 (1988).

GAMMA IRRADIATION INFLUENCE ON PHYSICAL PROPERTIES OF MILK PROTEINS

Krystyna Cieśla, Stephane Salmieri[1/], Monique Lacroix[1/], Cahn Le Tien[1/]

[1/] Canadian Irradiation Center, Research Laboratories in Sciences Applied to Food, INRS-Institute Armand Frappier, University of Quebec, Laval, Canada

Gamma irradiation was found to be an effective method for improvement of both barrier and mechanical properties of the edible films and coatings based on calcium and sodium caseinates alone or combined with some globular proteins [1, 2]. It is well known that properties of films are determined by properties of the initial solutions and gels – the intermediate products created during film formation. Properties of all solutions, gels and final films depends, however, on the tertiary structure of proteins. Accordingly, good knowledge of the processes and products resulting from the particular steps of preparation together with recognition of the radiation effect is expected to help in further optimisation of the preparation conditions applying ionising radiation.

Our previous studies concerned films prepared using non-irradiated and irradiated solutions of calcium caseinate (CC)-whey protein isolate (WPI)-glycerol (1:1:1). At present [3], the studies were carried out concerning gamma irradiation influence on the physical properties of solutions and gels in relation to the functional properties of the films obtained using the control and the irradiated solutions. Apart from the studies carried out at ambient temperature, the route of gel creation was examined during heating and cooling in the range 20-90°C. The results were related to modification of proteins conformation concluded on the basis of FTIR (Fourier transform infrared spectroscopy) spectra and interaction with calcium ions.

Calcium caseinate (New Zealand Milk Product Inc.) and whey protein isolate (BiPro Davisco) and chemical grade glycerol were used. Irradiation of solutions was carried out with gamma rays from Co-60 applying a dose of 32 kGy at a dose rate of 7 Gys^{-1}. The solutions were dissolved till 5% (total proteins mass). The control of non-irradiated solutions, were also prepared. Parts of these solutions were used directly in viscosity measurements, while the other parts were heated before measurements for 45 min at a temperature of 90°C. pH values of all the solutions, irradiated and control were in the range of 6.6-6.8.

Viscosity measurements were carried out applying a Brookfield viscometer type LVDV-II+ (Brookfield Engineering Laboratories Inc., USA) with a close tube system enabling to create a circulating water bath by connecting the water jacket to the bath inlet and outlet ports. At first, the experiments were carried out at ambient temperature applying several shear rates (selected in regard to good reproducibility and reliability of the data as well as a linear dependence of a shear stress upon a shear rate). Four measurements were done for each composition and the average values were calculated for viscosity and shear stress. The further experiments (four repetitions) were carried out at a selected constant shear rate during dynamic heating and cooling in the range of 25-90°C.

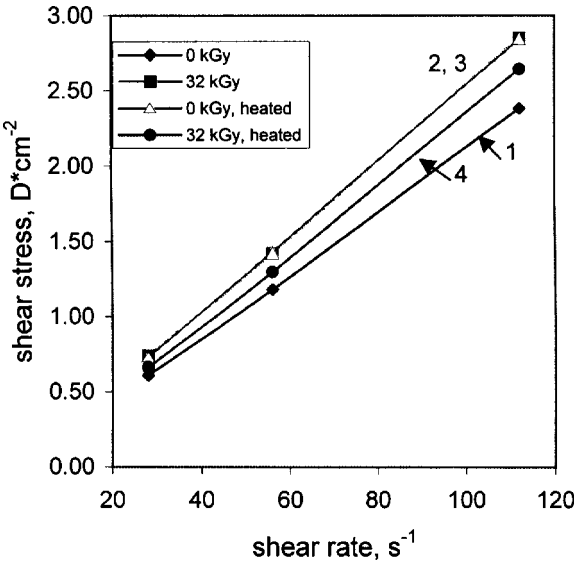

Fig.1. Comparison of dependence of shear stress on shear rate, obtained in the case of: 1 – control solution, 2 – solution irradiated with a 32 kGy dose, 3 – heated at 85°C for 45 min, 4 – irradiated with 32 kGy and heated at 85°C for 45 min. The values of shear stress determined at a shear rate of 122.3, 61.2 and 30.6 s^{-1}, respectively, were equal to 2. 38, 1.18, 0.61 (curve 1); 2.84, 1.43, 0.73 (curve 2); 2.85, 1.42, 0.74 (curve 3); 2.64, 1.30, 0.66 (curve 4).

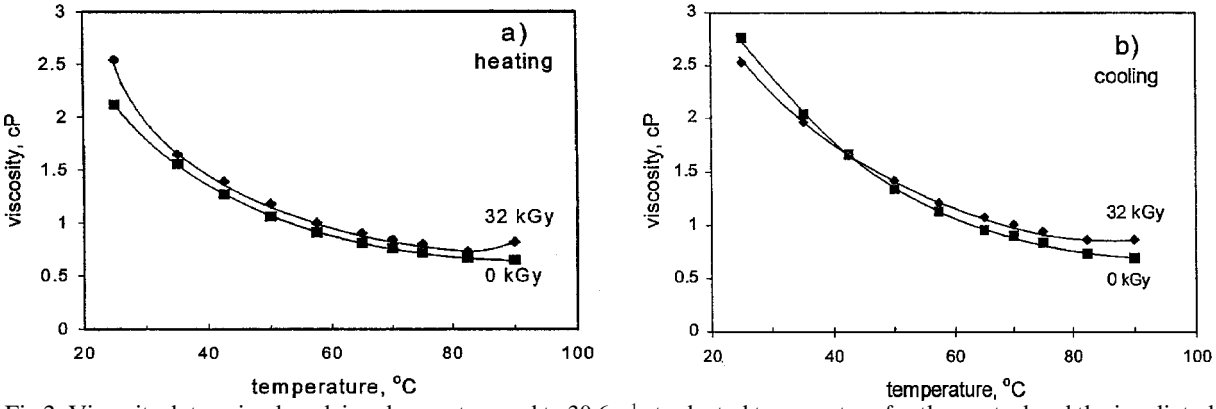

Fig.2. Viscosity determined applying shear rate equal to 30.6 s^{-1} at selected temperature for the control and the irradiated CC-WPI solutions during: a) dynamic heating with an average rate of 2.4°C min^{-1}, b) cooling with an average rate of 1.9°C min^{-1}.

The films were prepared using the gelatinised solutions and examined accordingly to the procedures described earlier [1]. In particular, water vapour permeability (WVP) and mechanical properties like a puncture strength, deformation and viscoelastic properties were determined. Two replicas of ten samples were tested for both film types.

FTIR spectra were measured applying the total reflectance method and a Perkin-Elmer Spectrum One Spectrophotometer equipped with Universal ATR Sampling Accesory with a diamond crystal. The average spectrum was calculated on the basis of 3-4 measurements. The method based on analysis of the second derivative of the amide I band at 1630 nm was applied in purpose to examine the proteins conformation [4, 5].

Gel formation, binding of calcium ions and gel fracture strength measurements were realised accordingly to the procedure described by Ressounay *et al.* [2]. Nine repetitions were performed for each compositions.

A Stevens LFRA Texture Analyser Model TA/100 (USA) was applied for mechanical measurements. The SAS statistical package was applied to analyse statistically the results dealing with gel fracture strength and functional properties of the films. The Student's *t*-test was used and paired-comparison. Differences between means were considered significant when $p \leq 0.05$.

The increase in viscosity of solutions was found after irradiation connected to radiation induced crosslinking. This is shown by the higher values of shear stress recorded at the same shear rate for the irradiated solution than for the initial one (Fig.1, curves 1 and 2). The lower viscosity values were detected, however, after heating of the irradiated solutions than after heating of the non-irradiated ones regarding to differences in structure of gels (Fig.1, curves 3 and 4). This happens because viscosity of the initial solution increases, while that of the irradiated one decreases after heat treatment. As a result, different temperature-viscosity curves were recorded for the irradiated and non-irradiated samples during heating and cooling (Fig.2). As a result, the irradiated gels are less viscous than the non-irradiated ones. Creation of less stiff but better ordered gels after irradiation arises probably from reorganisation of aperiodic helical phase and β-sheets, in particular from increase in the amount of β-strands, detected by FTIR. It is confirmed by a stronger interaction with calcium ions, possibly in the case of the higher content of β-strands and leading to creation of the more dense network.

Presence of the better ordered protein conformations in gels obtained from irradiated solutions leads to production of the more "crystalline" films. These films are characterised by improved barrier properties and mechanical resistance and higher rigidity than those prepared from the non-irradiated solutions (Table).

Table. Fracture strength of the gels treated with calcium salt and the functional properties of the films.

Dose [kGy]	Fracture stength of gels with Ca^{2+} [N]	Tensile strength [Nmm^{-1}]	Deformation [mm]	Viscoelasticity	WVP [x10 g·mm/m^2·d mm·Hg]
0	48.0 ± 4.7	53.9 ± 2.6	4.46 ± 0.29	0.524 ± 0.01	168.6 ± 10.1
32	413 ± 30.5	77.4 ± 3.2	4.07 ± 0.35	0.561 ± 0.01	114.9 ± 9.6

The financial support of the International Atomic Energy Agency (fellowship of K. Cieśla, C6/POL/01003P) is kindly acknowledged.

References

[1]. Brault D., D'Aprano G.D., Lacroix M.: J. Agric. Food Chem., 45, 2964-2969 (1997).
[2]. Ressouany M., Vahon C., Lacroix M.: J. Agric. Food Chem., 46, 1618-1623 (1998).
[3]. Cieśla K., Salmieri S., Lacroix M., Le Tien C.: Gamma irradiation influence on physical properties of milk proteins. Radiat. Phys. Chem., in press.
[4]. Byler D.M., Susi H.: J. Ind. Metrol., 3, 73-88 (1988).
[5]. Lefevre T., Subirade M.: Biopolymers, 54, 578-586 (2000).

RADIOCHEMISTRY
STABLE ISOTOPES
NUCLEAR ANALYTICAL METHODS
GENERAL CHEMISTRY

INFLUENCE OF RELATIVISTIC EFFECTS ON HYDROLYSIS OF THE HEAVY METAL CATIONS

Maria Barysz[1/], Jerzy Leszczyński[1/], Barbara Zielińska, Aleksander Bilewicz

[1/] Department of Quantum Chemistry, Faculty of Chemistry, Nicolaus Copernicus University, Toruń, Poland

The process of hydrolysis is related to the interaction between the oxygen in the water molecule and the metal cation as shown in the following reaction [1]:

$$M(H_2O)_x^{n+} \rightarrow M(H_2O)_{x-1}(OH)^{(n-1)+} + H^+$$

Therefore, the tendency to hydrolyze increases with increasing oxidation state of the cation and decreasing ionic radius. This is understandable because with decreasing M-O distance, the polarizing effect of smaller cation on the O-H bond in the aqua ligand increases, which, in turn results in easier loss of the proton from the hydrated cation. The ability to hydrolysis has been discussed in many papers in terms of the charge (Z) and ionic radii (r_i) of the cation. According to all of these the hydrolytic ability will increase with decreasing radius of the outermost shell in the ion. The models work very well as far as not too heavy metals are hydrolysed. Unexpectedly, for 1+ cations of Group 11, 2+ cations of Group 12, and 3+ cations of Group 13 the heaviest members in each group (Au^+, Hg^{2+} and Tl^{3+}, respectively) hydrolyze much more easy than their lighter congeners. Table 1 presents the first hydrolysis constants

$$K_{1h} = \frac{[M(OH)(OH_2)_{x-1}^{(n-1)+}][H^+]}{[M(OH_2)_x^{n+}]}$$

and ionic radii of the cations of metal Group 11, 12 and 13.

Some models for the explanation of this phenomenon have been proposed but none of them appears to be sufficiently adequate and complete [l, 7]. On the other hand, certain empirical correlations between experimental data and parameters which characterize cations suggest that a successful model of the phenomenon must explicitly include relativistic effects. For heavy ions these effects should be important for predicting the structure and strength of the cation-water complexes. The present paper aims at showing the role of the relativistic effects on the structure and energetics of these complexes and their ability to release protons.

From the side of experimentalists, the model of hydrolysis should be as close as possible to "chemical reality". From the computational point of view, the selected model must be small enough that the corresponding calculations can be carried out in a reasonably short time and with available resources. The analysis of the experimental data and their correlations with the ion parameters indicate that most of the observed effect should be reflected in a model consisting of the heavy metal cation and a single water molecule: $M^{n+}...OH_2$. During hydrolysis such a system will release one proton, $Me\text{-}OH_2 \rightarrow Me\text{-}OH^{(n-1)+} + H$. The efficiency of hydrolysis is, therefore expected to be reflected by the strength of the O-H bond in the

Table 1. Ionic radii [2] for CN = 6 and pK_{1h} for cations of Groups 11, 12 and 13. The pK_{1h} for Au^+ from [3], other pK_{1h} values from [4].

Cation	r_i [pm]	pK_{1h}	Cation	r_i [pm]	pK_{1h}	Cation	r_i [pm]	pK_{1h}
Cu^+	77	-	Zn^{2+}	74	8.96	Ga^{3+}	62.0	3.6
Ag^+	115	12	Cd^{2+}	95	10.08	In^{3+}	80.0	4.0
Au^+	137	3.8	Hg^{2+}	102	3.40	Tl^{3+}	88.5	0.6

The Cu^+ and Au^+ aqua ion is known to be unstable in aqueous solution, especially under alkaline conditions. However, gold(I) solutions in mixtures of acetonitrile and dilute mineral acids have been used to determined a first hydrolysis constant of Au^+ [3]. Similar deviation from the expected hydrolysis strength was also observed for the Ra^{2+} cation [5] of the Group 2 and the Rf^{4+} cation of the Group 4 [6].

complex. Among such parameters one can choose, e.g. the equilibrium OH bond length (d_{OH}) and the stretching force constant for this bond (K_{OH}). In addition to the determination of these parameters for the series of the Group 11 and 12 cation-water complexes, we wish to investigate the importance and role of the relativistic treatment of the problem. To rationalize the variation of the heavy metal cation hydrolysis in terms of relativistic effects,

Table 2. The geometry data and Me...O and O-H force constants for aqua cations of Group 11 obtained from nonrelativistic (nrel) and relativistic (rel) MP2 calculations.

Cation	M-O [pm]		O-H [pm]		K(M-O) [a.u.]		K(O-H) [a.u.]	
	nrel	rel	nrel	rel	nrel	rel	nrel	rel
CuH_2O^+	190.86	187.58	97.235	97.351	0.0948	0.1066	1.026	1.017
AgH_2O^+	226.57	220.52	97.103	97.187	0.05266	0.06079	1.036	1.0290
AuH_2O^+	233.46	207.92	97.113	97.685	0.0522	0.1084	1.037	0.9913

parallel relativistic and nonrelativistic calculations will be carried out at the same level of theory with respect to the electron correlation effects. The details of the calculations is described in [8]. The geometry data and Me...O and O-H force constants obtained from nonrelativistic and relativistic MP2 calculations for Group 11 and 12 are presented in Tables 2 and 3.

The nonrelativistic studies predict that for both series of complexes the length of the Me...O bond will systematically increase with nuclear charge (Z) of the singly or doubly positive metal cation. Simultaneously, the force constant data show the decrease k O-H. Both these features of the interacting $Me(H_2O)^+$ and $Me(H_2O)^{2+}$ systems lead to the conclusion that the nonrelativistic theory predicts weakening of the Me...O bond interaction with increasing cation nuclear charge. For the OH bond the nonrelativistic theory shows that the metal cation has hardly any effect on its length. However, the O-H force constants systematically increase with increasing cation nuclear charge. Hence, according to the nonrelativistic calculations, the hydrolytic ability will decrease with an increase of Z. This conclusion essentially agrees with the result of the extrapolation of the experimental data for the two lighter cations in each Group and disagrees with the experimental values for Au^+ and Hg^{2+}. This disagreement is expected to be explained by including the relativistic effects.

Indeed, our relativistic calculations show markedly different pattern of changes. The optimized Me...O distance from relativistic calculations is found to increase first and then either to decrease (Au^+ in comparison with Ag^+) or to remain at almost the same value (Hg^{2+}) as for its predecessor (Cd^{2+}). The maximum values of d_{Me-O} are reached for the central element in the given Group. This pattern is accompanied by that of changes in the Me...O force constant. First, on passing from Cu^+ to Ag^+ one observes some decrease of the relativistic values of k_{Me-O}. Then, on replacing Ag^+ by Au^+ one finds that this force constant significantly increases to become almost the same as the value calculated for $Cu(H_2O)^+$. Exactly the same regularities are observed for the Group 12 cations. Both Cu and Ag (Zn and Cd) are relatively light elements and the relativistic contribution to the calculated parameters of the Me...O bond is not of primary importance. However, Au (Hg) are heavy enough to make the relativistic contributions significantly large. It is due to relativistic effects that the Au...O and Hg...O bonds are shortened in comparison with nonrelativistic data.

The increase of k_{Me-O} in Au^+ and Hg^{2+} complexes rather than its lowering unambiguously shows that the relativistic effects significantly strengthen the corresponding Me...O bonds. This also exemplifies how misleading could be the extrapolation of data for light systems to the high values of Z. Moreover, as shown by the relativistic results of Tables 2 and 3, the increase of k_{Me-O} is accompanied by the decrease of the relativistic values of k_{O-H} in Au^+ and Hg^{2+} complexes. Hence, because of the definitely relativistic character of these two ions, the O-H bonds in their complexes will be weakened and will be likely to dissociate. This explains why the pK_{1h} value for the Hg^{2+} hydrolysis is lower than that for Cd^{2+} (Table l), although that for Cd^{2+} is higher than the pK_{1h} value for Zn^{2+}. Similar trends are expected for the coinage metals. It is also of interest to elucidate the mechanism of the relativistic effect upon the calculated parameters in terms of the electronic structure of the investigated complexes and its changes upon including the relativistic contributions in the hamiltonian. It is known that the relativistic effects lead to the stabilization of s shells and to some extent also to the stabilization of p shells whereas the d electronic shells are energetically destabilized. The relativistic lowering of the orbital energy of the valence s orbital brings its energy closer to the energies of the occupied orbitals in the water molecule and will increase the amount of the charge transfer between Me^{m+} and H_2O. Simultaneously, the destabilization of the d shell will increase the overlap between d orbitals of the metal ion and orbitals of H_2O. Both these effects will lead to the relativistic increase of the strength of the Me...O interaction (bond). In a similar way the relativistic increase of the Me...O interaction shifts the electronic charge in the water molecule towards the metal ion and makes the O-H bond weaker than in the nonrelativistic case.

Obviously, the present model study of the metal hydrolysis is highly simplified and to complete understanding of this process one may need to study more sophisticated models with several water molecules in the complex. However, the importance of the relativistic effects on their structure is already well seen from the calculations reported in this paper.

Table 3. The geometry data and Me...O and O-H force constants for aqua cations of Group 12 obtained from nonrelativistic (nrel) and relativistic (rel) MP2 calculations.

Cation	M-O [pm]		O-H [pm]		K(M-O) [a.u.]		K(O-H) [a.u.]	
	nrel	rel	nrel	rel	nrel	rel	nrel	rel
ZnH_2O^{2+}	184.62	183.03	98.923	98.923	0.174	0.182	0.92	0.912
CdH_2O^{2+}	211.07	207.36	98.394	98.394	0.121	0.131	0.956	0.943
HgH_2O^{2+}	219.53	205.78	98.394	99.452	0.113	0.154	0.961	0.881

References

[1]. Baes C.F., Jr., Messmer R.E.: The Hydrolysis of Cations. Krieger Publishing Company, Malabar, Fl. 1986.
[2]. Shannon R.D.: Acta Crystal., A32, 751 (1976).
[3]. Kissner R., Welti G., Geier G.: J. Chem. Soc., Dalton Trans., 1773 (1997).

[4]. Smith R.M., Martell A.E.: Critical Stability Constants. Vol..4. Plenum Press, New York 1976, pp.1-12.
[5]. Zielińska B., Bilewicz A.: Hydrolysis of Ra^{2+}. In preparation.
[6]. Bilewicz A., Siekierski S., Kacher C.D., Gregorich K.E., Lee D.M., Stoyer N.J., Kadkhodayan B., Kreek S.A., Lane M.R., Sylwester E.R., Neu M.P., Mohar M.F., Hoffman D.C.: Radiochim. Acta, 75, 121 (1996).
[7]. Moriyama H., Kitamura A., Fujiwara K., Yamana H.: Radiochim. Acta, 87, 97 (1999).
[8]. Barysz M., Leszczyński J., Bilewicz A.: submitted to J. Phys. Chem.

BINDING OF METAL-^{211}At COMPLEXES TO BIOMOLECULES – A NEW METHOD FOR PREPARATION OF ASTATINE RADIOPHARMACEUTICALS

Marek Pruszyński, Aleksander Bilewicz, Bogdan Wąs[1/], Barbara Petelenz[1/], Mirosław Bartyzel[1/], Małgorzata Kłos[1/]

[1/] H. Niewodniczański Institute of Nuclear Physics, Polish Academy of Sciences, Kraków, Poland

In the field of radioimmunotherapy, the choice of a radioisotope depends on the type of disease to be treated. The decay energy of the nuclide and the type the emitted particles are directly related to the tissue penetration and cell killing ability. Aiming at therapeutic applications, many radiometals are under investigation, most notably the Auger emitter ^{67}Ga ($t_{1/2}$=3.3 d), the α particle emitters ^{211}At ($t_{1/2}$ = 7.2 h), ^{212}Bi ($t_{1/2}$ = 1 h), ^{213}Bi ($t_{1/2}$ = 45.6 m), ^{225}Ac ($t_{1/2}$ = 10 d), and the β particle emitters ^{90}Y ($t_{1/2}$ = 64 h), ^{188}Re ($t_{1/2}$ = 16.7 h), ^{153}Sm ($t_{1/2}$ = 46.8 h), ^{177}Lu ($t_{1/2}$ = 6.7 d), ^{67}Cu ($t_{1/2}$ = 2.6 d), ^{105}Rh ($t_{1/2}$ = 36 h), ^{47}Sc ($t_{1/2}$ = 3.3 d), and ^{109}Pd ($t_{1/2}$ = 13.5 h) [1]. Solid tumors have been successfully treated with β emitters whose β particle emissions have a tissue range of several millimeters. This relatively large tissue range is not optimal for treatment of single cells or small clusters of cells which are targets of treatment in micrometastatic disease, leukemias, and lymphomas. Treatment of these diseases may be more efficient with α emitters, which combine high cytotoxicity and a short tissue range. In view of this, a considerable effort has been placed in the development of radiopharmeceuticals based on the α emitters: ^{211}At, ^{212}Bi, ^{213}Bi and ^{225}Ac. Unfortunately, the half-life of both ^{212}Bi and ^{213}Bi is short, which may limit potential applications. Actinium ^{225}Ac has also limited applicability, due to its series decay (^{221}Fr→ ^{217}At→ ^{213}Bi→ ^{213}Po→ ^{209}Pb→ ^{209}Bi) where the first intermediate product can easily diffuse from the biomolecule. Actually, the most promising is ^{211}At.

Astatine ^{211}At decays *via* two branches (^{211}At, EC→^{211}Po, α, $t_{1/2}$ = 0.5 s, and ^{211}At, α→^{207}Bi, EC/β^+, $t_{1/2}$ = 33.4 y) to the stable ^{207}Pb. High energy α particles with mean energy of 6.4 MeV are emitted in the decay, corresponding to a mean range in human tissue of 65 μm. Therefore, this nuclide may be optimal for treatment of micrometastases. Additionally, the EC branch gives rise to high intensity Po X-rays (76.863 keV, 19.7% and 79.290 keV, 33.1%) making ^{211}At easy to follow with a γ camera [2].

In the past, ^{211}At labelled immunoconjugates have been synthesized and evaluated for their therapeutic potential. Proteins labelled with ^{211}At by direct electrophilic astatination turned out unstable *in vivo* by virtue of the rapid loss of ^{211}At following administration. Better stabilization, but still not fully satisfactory, has been observed for biomolecules labelled by electrophilic astato-destannylation of *N*-succinimidyl-3-(trimethyl stannyl) benzoate. In view of this, finding an alternative way of binding astatine into radiopharmaceuticals was of primary importance.

In this short note we present preliminary results of our studies on labelling biomolecules *via* a metal cation bridge between ^{211}At and the biomolecule. As potential metal cations which should form strong complexes with At^- ligand, Pd^{2+}, Bi^{3+}, Cu^{2+} and Hg^{2+} were selected. In the first step of work, stability constants of the Hg-At^+ bindings were determined.

The isotope ^{211}At was obtained in the AIC-144 cyclotron at the H. Niewodniczański Institute of Nuclear Physics, *via* the nuclear reaction ^{209}Bi(α,2n)^{211}At. The targets of pure metallic bismuth molten on a 0.1 mm thick copper foil (*ca*. 50 mg cm^{-2} of Bi), protected with a 2 mg cm^{-2} thick aluminium foil, were activated during 1 h with the 30 MeV and 1 μA internal beam of α particles.

A home-made apparatus for the separation of ^{211}At from a metallic target was inspired by that described in [3]. The separation of ^{211}At was carried out under argon at a gas flow of 120 cm^3 min^{-1}. After 15 min of flushing, the apparatus with argon, the activated target was placed in a quartz

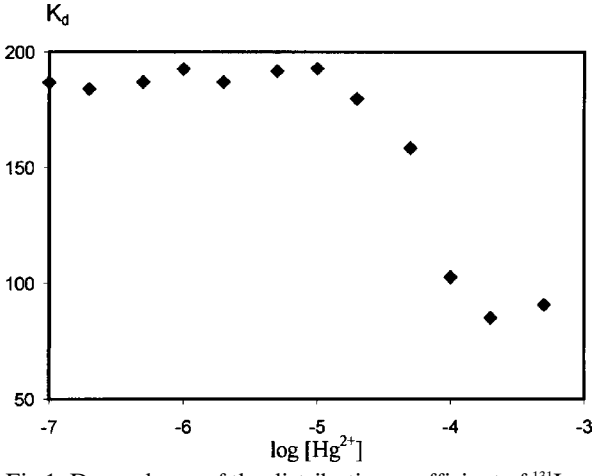

Fig.1. Dependence of the distribution coefficient of ^{131}I on the concentration of Hg^{2+} in the solution (Dowex 1 anion exchanger).

tube inside the resistance furnace. After switching the heating on, the desired temperature of 650°C was achieved during 30 min and kept constant dur-

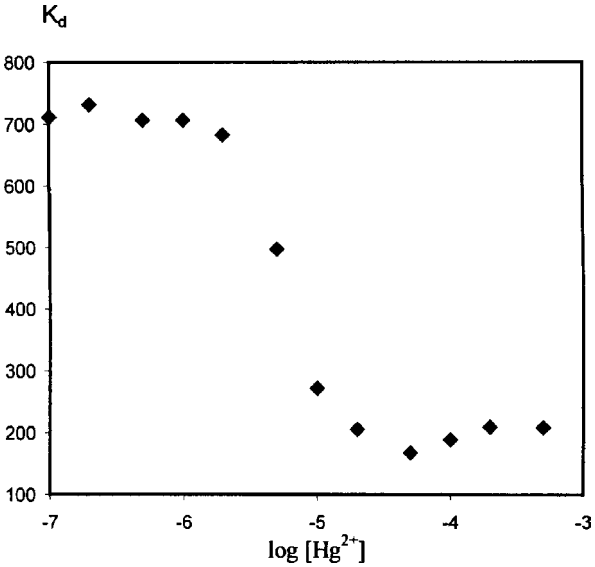

Fig.2. Dependence of the distribution coefficient of ^{211}At on the concentration of Hg^{2+} in the solution (Dowex 1 anion exchanger).

ing further 15 min. The evolved ^{211}At was collected in a cold trap consisting of a polyethylene tube of 1 mm inner diameter, immersed in ethanol cooled with liquid nitrogen down to the temperature between -55 and -50°C. The obtained ^{211}At was dissolved in 100 µl of Na_2SO_3 + $NaNO_3$ solution.

The ion exchange method based on the various partitions of $HgAt^+$ and At^- on anion exchange resin was used for complexation studies. The distribution coefficient values were determined using batch technique in 0.1 M $NaNO_3$ solutions with 0.001 M Na_2SO_3 as reducing agent.

From the plotted relationship between the $\log K_d$ and $\log[Hg^{2+}]$ values (Figs.1 and 2), the first stability constants have been determined for $HgAt^+$ and, for comparison, also for HgI^+. The inflection points on the curves indicate that the $\log K_1$ is 5.4 for $HgAt^+$ and 4.1 for HgI^+. These values reflect formation of a strong bonding between At^- and Hg^{2+}, which indicates that the method of labelling biomolecules *via* a cation bridge between ^{211}At and the biomolecule is promising for preparation of astatine radiopharmaceuticals.

References

[1]. Chappell L.L., Deal K.A., Dadachova E., Brechbiel M.W.: Bioconjug. Chem., 11, 510 (2000).
[2]. Johnson E.L. *et al*.: Nucl. Med. Biol., 22, 45 (1995).
[3]. Koziorowski J., Lebeda O., Weinreich R.: Appl. Radiat. Isot., 50, 527 (1999).

HYDROLYSIS OF ACTINIUM

Barbara Zielińska, Aleksander Bilewicz

According to most of the hydrolysis models, the degree of hydrolysis should decrease down of each Group in the Periodic Table due to increasing radius of the outermost shell of the cations. Unexpectedly, for 1+ cations of Group 11, for 2+ cations of Group 12, and for 3+ cations of Group 13 the heaviest members in each group (Au^+, Hg^{2+} and Tl^{3+}, respectively) hydrolyse more strongly than their lighter neighbours in the Groups (Ag^+, Cd^{2+} and In^{3+}, respectively) [1]. Also hydrolysis of Ra^{2+} is the same as Ba^{2+} in spite of that the ionic radius of Ra^{2+} is by 6 pm larger than that of Ba^{2+} cation [2].

The knowledge of the first hydrolysis constant of Ac^{3+} is crucial for understanding the reason of the unexpected strong hydrolysis of the heaviest cations. Unfortunately, only few data on hydrolytic behaviour of Ac^{3+} are available in the literature and, moreover, they are at variance. Ziv and Szestakova [3] report that pH of precipitation of $Ac(OH)_3$ is 8.61. On the contrary, it has been reported that no hydrolytic reactions take place up to pH = 10.4. By electromigration method the overall hydrolytic constant $\log \beta_3$ = -31.9 has been determined [4].

Studies on hydrolytic behaviour is also important from the point of view of applications of new therapeutic radiopharmaceuticals based on ^{225}Ac [5-7]. Some biochemical studies have shown that the hydrolysis of Ac^{3+} leads to formation of protein complexes which accumulate in tumour cells [4]. The aim of the present work was to study the

Table. First hydrolysis constants and ionic radii (CN = 6 [8]) for group 3 metal cations.

Cation	r_i [pm] CN=6	pK_{1h} (literature [1])	pK_{1h} (this work) (μ=1 mol dm^{-3})
Sc^{3+}	74.5	4.94	
Y^{3+}	90.0	8.61	
La^{3+}	103.2	9.33	9.0 ± 0.1
Ac^{3+}	112	-	9.4 ± 0.1

hydrolysis of actinium in comparison with the hydrolysis of lighter homologues in Group 3. The Ac^{3+} cations exist only in submicroamounts, therefore the simple potentiometric method cannot be applied for determination of hydrolysis constants. The ion exchange method, elaborated in our laboratory, based on the different partition of the Ac^{3+} and $AcOH^{2+}$ cations on the strong acidic cation exchanger was used. This method permits to work with extremely dilute Ac^{3+} radioactive solutions. As radiotracer we used ^{228}Ac ($t_{1/2}$ = 6.13 h) which emits a strong γ-ray of 911 and 966 keV.

The distribution coefficients of $^{228}Ac^{3+}$ and $^{140}La^{3+}$ between the strong acidic cation exchanger and 1 molar aqueous sodium perchlorate solutions buffered with 0.05 M $NH_3/HClO_4$ have been determined by batch technique. Table presents Shannon [8] ionic radii and the determined values

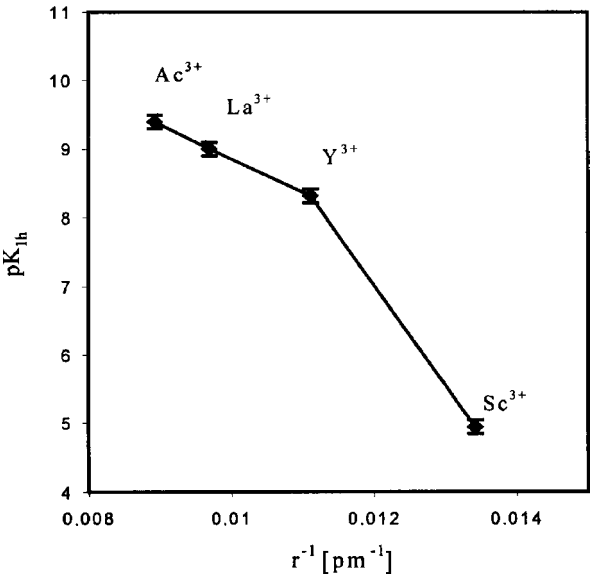

Fig. Dependence of pK_{1h} for cations of Group 3 on r^{-1}.

of the first hydrolysis constant together with literature values for Sc^{3+}, Y^{3+} and La^{3+}, determined by the potentiometric method for comparison. The values presented in Table were used for illustration of the dependence of pK_{1h} on $1/r_i$. Figure was prepared by assuming that the difference between the hydrolysis constant for La^{3+} determined for $\mu = 0.3$ mol dm^{-3} (literature value) and for $\mu = 1$ mol dm^{-3} (our value) 0.3 unit is the same for Y^{3+}.

The function is linear for Y^{3+}, La^{3+} and Ac^{3+} while the hydrolysis of Sc^{3+} is much higher than expected. The strong hydrolysis of Sc^{3+} is probably connected with low coordination number (CN = 4) of Sc^{3+} in aqua ion. The linearity of the function $\log K_{1h}$-$1/r_i$ is in agreement with electrostatic model of hydrolysis [9]. However, this relation is at variance with the tendency observed in other groups of Periodic Table where heaviest cations hydrolyse either equally (Ra^{2+}) or more strongly (Au^{+}, Hg^{2+}, Tl^{3+}) than their lighter homologues in the Group.

The Ac^{3+} hydrolytic behaviour could be explain on the basis of recently performed quantum relativistic and nonrelativistic calculations of Ac^{3+} interaction with water [10]. The calculated Ac^{3+}-O distance in aqua ion (245 pm) is larger than for La^{3+}-O distance (234 pm), therefore according to electrostatic models of hydrolysis Ac^{3+} should hydrolyse more weakly than La^{3+}. It should be noted that the same results were obtained by relativistic and nonrelativistic calculations, which indicates the absence of influence of relativistic effect on Ac^{3+}-O bonding and for Ac^{3+} hydrolysis.

References

[1]. Smith R.M., Martell A.E.: Critical Stability Constants. Vol.4. Plenum Press, New York 1976, pp.1-12.
[2]. Zielińska B., Bilewicz A.: Hydrolysis of actinium. J. Radioanal. Chem., in press.
[3]. Ziv D.M., Shestakova I.A.: Radiokhimiya, 7, 175 (1965).
[4]. Kulikov E.V., Novgorodov A.F., Schumann D.: J. Radioanal. Nucl. Chem. Lett., 164, 103 (1992).
[5]. McDevitt M.R., Ma D., Lai L.T., Simon J., Borchardt P., Frank R.K., Wu K., Pellegrini V., Curcio M.J., Miederer M., Bander N.H., Scheinberg D.A.: Science, 294, 1537 (2001).
[6]. McDevitt M.R., Ma D., Simon J., Frank R.K., Scheinberg D.A.: Appl. Radiat. Isot., 57, 841 (2002).
[7]. Chappell L.L., Deal K.A., Dadachova E., Brechbiel M.W.: Bioconjug. Chem., 11, 510 (2000).
[8]. Shannon R.D.: Acta Crystallogr., A32, 751 (1976).
[9]. Baes C.F., Jr., Messmer R.E.: The Hydrolysis of Cations. Krieger Publishing Company, Malabar, Fl. 1986.
[10]. Mochizuki Y., Tatewaki H.: Chem. Phys., 273, 135 (2001).

KINETICS OF HYDROLYSIS AND LIQUID-LIQUID DISTRIBUTION OF TRIS(THENOYLTRIFLUOROACETONATE)THALLIUM(III)

Jerzy Narbutt, Jadwiga Krejzler

Hydrolytic properties of certain metal ions make many of their complexes in aqueous solution unstable against substitution of water and/or hydroxide ion for the original ligands. However, if such complexes (labelled with radionuclides) are inert, they remain in solution intact for a time long enough to use them as radioactive indicators. When hydrolysis proceeds in the time-scale of minutes to hours, exact measurements require correction for ligand replacement. On the other hand, inertness is an important feature of metal complexes, in particular metal-essential radiopharmaceuticals. That is because no excess of the ligand is available *in vivo* to stabilize the original complex against ligand exchange, the more that other potential ligands (e.g. amino acids) compete for the central metal ion in the molecule.

Kinetics of ligand exchange in metal complexes was widely studied using either spectroscopic methods or radioactive indicators [1]. The latter method requires the chemical separation of different labelled species. In this work a new method is described, developed for the determination of both the rate of hydrolysis of neutral metal chelates in aqueous solution and their partition constants in two-phase systems [2], based on the continuous solvent-extraction separation of the original complex from the products of its hydrolysis. Partition constant, P_0, defined as the ratio of the concentrations of a given complex in the organic and aqueous phase at equilibrium, is the measure of lipophilicity of metal complexes, which is an important characteristic of certain radioactive indicators, in particular radiopharmaceuticals [3].

The aim of the present work was to study this new method in more detail, including the effect of pH on the rate of hydrolysis. Tris(thenoyltrifluoroacetonate)thallium(III) – $Tl(tta)_3$ (ML_n), neutral

chelate of suitable lipophilic-hydrophilic properties, was selected for studies. Due to strong hydrolysis of the thallium(III) ion [4], direct determination of P_0 of its neutral complexes is not possible, because their equilibrium concentration in the aqueous phase can hardly be reached. In fact, thallium(III) can be extracted by numerous chelating extractants, but the reliable P_0 values of the chelates are scarce [5]. However, the slowed down kinetics of hydrolysis of thallium(III) in its chelates makes it possible to extrapolate the kinetic data to the zero time. The appropriate kinetic equation was therefore derived and compared with experimental data.

The distribution of thallium(III) between an organic and an aqueous phase was studied in back-extraction experiments with the organic phase previously loaded with $Tl(tta)_3$ labelled with ^{204}Tl. Usually ML_n is the only form of the metal in the organic phase, however, coordinatively unsaturated chelates can also form self-adducts, $ML_n(HL)_j$, with an excess of the extractant, HL. The total concentration of the metal in the organic phase is then equal to:

$$[M]_{org} = [ML_n]_{org}(1 + \sum_{j=1}^{m} \beta_{n,j}[HL]^j) \qquad (1)$$

where $\beta_{n,j}$ are association constans of successive self-adducts, $ML_n(HL)_j$ in the organic phase.

The organic phase with the initial metal concentration $[M]_{org,0} = 1 \div 5 \times 10^{-5}$ mol dm^{-3}, was obtained by extraction of thallium(III) from a slightly acidic aqueous phase (H_2SO_4, pH 2.5÷3) to 0.1 mol dm^{-3} Htta in toluene. It was found that the toluene $Tl(tta)_3$ solution was kinetically inert, nevertheless it was always prepared fresh, immediately before further back extraction to a fresh thallium-free aqueous phase, pH-adjusted and containing an excess of strongly oxidizing ammonium persulfate to stabilize incoming thallium(III) chelate [2]. Equal volumes of the phases ($V_{org} = V_{aq}$) were shaken, and the aliquots of both were collected in several minutes intervals for measurements of specific activities, proportional to the total concentrations of M in each phase: $[M]_{org}$ and $[M]_{aq}$. The distribution ratio, $D = [M]_{org}[M]_{aq}^{-1}$, decreased with time. After a fast drop within the first 3-5 min, a further continuous decrease in D was observed, with pH-dependent moderate rates. It was assumed that the fast process observed at t < 10 min was the transfer of the neutral chelate from the organic to the aqueous phase, while the slow decrease corresponded to the hydrolysis of the neutral chelate in the aqueous phase. The rate of the hydrolysis is proportional to the concentration of ML_n in the aqueous phase (the first-order reaction). However, because the partition equilibrium has already been established, the decrease in $[ML_n]_{aq}$ is being continuously compensated (in part) by the transfer of ML_n from the organic phase. Therefore, both $[ML_n]_{org}$ and $[ML_n]_{aq}$ are the transient values depending on time, t. The total change in $[ML_n]_{aq}$ is equal to:

$$-\frac{d[ML_n]_{aq}}{dt} = -\frac{d[ML_n]_{hydrolysis}}{dt} + \frac{d[M]_{org}}{dt} \qquad (2)$$

After substituting $-d[ML_n]_{hydrolysis}/dt = k[ML_n]$ and $P = P_0(1 + \sum_{j=1}^{m} \beta_{n,j}[HL]^j)$ and integrating eq. (2) we obtain for $V_{org} = V_{aq}$:

$$\ln[ML_n]_{org} = \ln[\overline{ML_n}]_{org} - \frac{k}{P+1}t \qquad (3)$$

where is the extrapolated to t = 0 virtual concentration of ML_n in the organic phase, and k is the rate constant of ML_n hydrolysis. Equations (3) and (1) allow for the experimental determination of P and k, however assuming that the hydrolysis products (including e.g. colloidal hydroxides) remain in the aqueous phase evenly distributed within it, we have $d[M]_{aq} = -d[M]_{org}$, and eq. (3) can be transformed into the more convenient form:

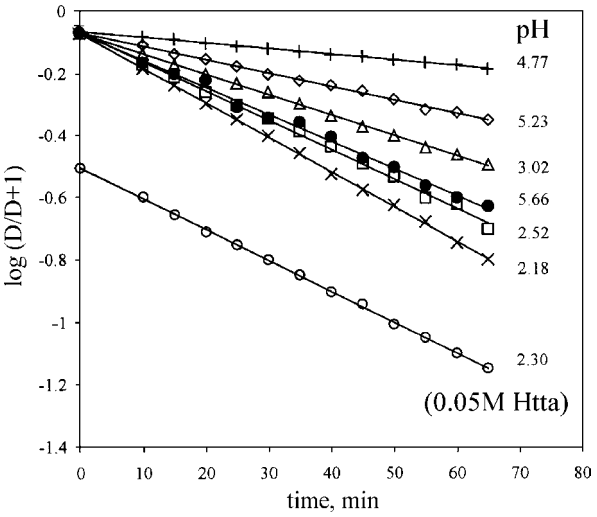

Fig.1. Back extraction of $Tl(tta)_3$ from toluene (0.1 M Htta) to water (0.1 M $NaClO_4$) at 25.0°C; the dependence of log{D/(D+1)} on time at various pH (the data for pH 3.50 and 3.90 not shown for clarity). The lowest line corresponds to 0.05 M Htta.

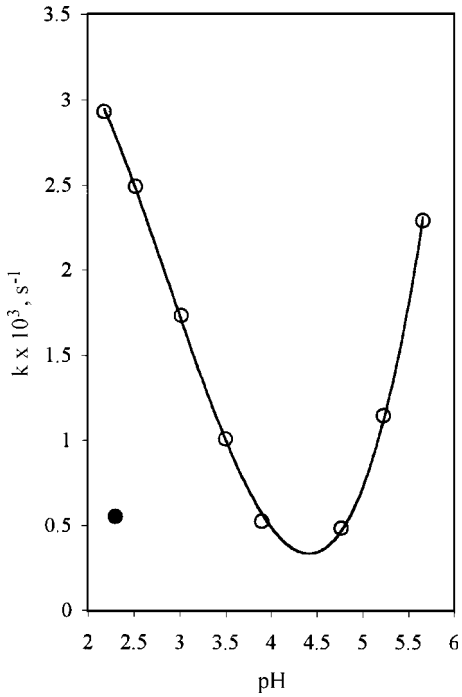

Fig.2. The pH dependence of the hydrolysis constant of $Tl(tta)_3$ at 25.0°C. Open circles correspond to 0.1 M Htta; solid circle – to 0.05 M Htta.

$$\ln\left(\frac{D}{D+1}\right) = \ln\left(\frac{P}{P+1}\right) - \frac{k}{P+1}t \qquad (4)$$

By plotting the set of experimental ln{D/(D+1)} values *vs*. time (Fig.1) we calculate P and k directly from the intercept and slope. The experimental data, collected in the pH range of 2.2 to 5.6, determine a bunch of straight lines of different slopes but of the same intercept from which P = 5.87 ± 0.30 was obtained. In more acidic solutions (pH < 2) the slopes are still higher but the dependences (not shown in Fig.1) are no more linear and do not converge to the same intercept. The different intercept of the lowest line, corresponding to 0.05 M Htta and pH 2.30, gives P = 0.454. This strong dependence of P on the extractant concentration confirms that extraction of self-adducts with m > 1 takes place.

The dependence of k on pH, with the minimum at 4.3 < pH < 4.5 (Fig.2), similar to that observed for other metal chelates [1], may be interpreted in terms of acid-catalysed and base hydrolysis of the chelate. The rate determining step would be the release of HL molecule(s) from the self-adducts (which is confirmed by the lower k at less concentrated Htta; Fig.2) and/or formation of an inner-sphere hydrate of the chelate in the aqueous phase. The succeeding steps: protonation (low pH) and deprotonation (pH > 4.5) of the hydrated chelates; should be fast. The decrease in $[HL]_{org}$ at low pH, due to formation of protonated H_2L^+ in the aqueous phase, accelerates the hydrolysis. This is probably the reason of non-linear drop of the function (4) values at pH < 2. The work is in progress.

References

[1]. Basolo F., Pearson R.G.: Mechanisms of Inorganic Reactions. A Study of Metal Complexes in Solution. John Wiley & Sons, Inc., New York 1958, pp.104, 152-154.
[2]. Narbutt J., Czerwiński M., Krejzler J.: Eur. J. Inorg. Chem., 3187 (2001).
[3]. Packard A.B., Kronauge J.F., Brechbiel M.W.: In: Metallopharmaceuticals II. Diagnosis and Therapy. Eds. M.J. Clarke and P.J. Sadler. Springer, 1999, p.66.
[4]. Baes C.F., Jr., Mesmer R.E.: The Hydrolysis of Cations. Krieger Publ. Co., Malabar, Fl. 1986, pp.328-333.
[5]. Sekine T., Hasegawa Y.: Solvent Extraction Chemistry. Marcel Dekker Inc., 1977, p.516.

TRICARBONYL(N2-METHYL-2-PYRIDINECARBOTHIOAMIDE)CHLORO--RHENIUM(I) AS A RADIOPHARMACEUTICAL PRECURSORS

Leon Fuks, Ewa Gniazdowska, Wojciech Starosta, Monika Zasępa, Józef Mieczkowski[1/], Jerzy Narbutt

[1/] Department of Chemistry, Warsaw University, Poland

Progress in coordination chemistry, observed in the last three decades, is due to the dominant role of the γ-emitting ^{99m}Tc in diagnostic nuclear medicine and to potential applications of the β/γ-emitting ^{188}Re in tumor therapy [1, 2]. In a great number of currently applied or studied radiopharmaceuticals containing ^{99m}Tc or ^{188}Re these elements appear in their higher oxidation states. However, tricarbonyl complexes of monovalent technetium and rhenium have recently received more attention [3]. These soft metal cations of d^6 electronic configuration show an increased kinetic inertness and lower affinity for ligands with hard donor oxygen atoms, readily present in the blood. This characteristics protects the complexes *in vivo* against ligand exchange.

The aim of our studies is to synthesize and physicochemically characterize tricarbonyl complexes of technetium and rhenium with derivatives of thiopicolinic acid amide as bidentate ligands. Due to the presence of two soft donor atoms in the ligand molecules: sulfur and aromatic nitrogen; their Tc(I) and Re(I) chelates were expected to be exceptionally stable, therefore good candidates for radiopharmaceuticals. Tricarbonyl(N2-methyl-2-pyridinecarbothioamide)chlororhenium(I), $Re(CO)_3(L)Cl$ (**1**) was synthesized and studied as the first compound in the series.

The N2-methyl-2-pyridinecarbothioamide ligand, $C_5H_4NCSNHCH_3$ (**2**) (Fig.1) was synthesized from a mixture of α-picoline, *N*-methyformamide and sulphur, according to the general procedure described in [4]. Crude product was dissolved in chloroform and purified chromatographically on silica gel, then recrystallized twice from ethyl acetate (m.p. 75÷79°C, yield 40%). The com-

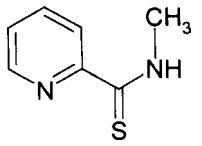

Fig.1. Stick formula of N2-methyl-2-pyridinecarbothioamide (**2**).

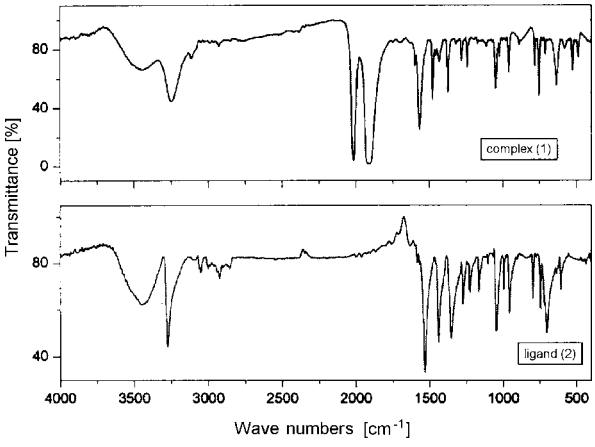

Fig.2. FT-IR spectrum of the title complex (**1**) and ligand (**2**).

Table 1. Unit cell parameters of the $Re(CO)_3(L)Cl$ complex (**1**).

Crystal system	triclinic
Space group	P1(bar)
Unit cell dimensions	a = 7.827(2) Å b = 7.974(2) Å c = 10.903(2) Å α = 77.35(3)^0 β = 84.39(3)^0 γ = 88.12(3)^0 V = 660.7(2) Å^3
Z	2

position of the final product was confirmed by elemental analysis, ^{1}H-NMR and ^{13}C-NMR.

The title complex **1** ($Re(CO)_3(L)Cl$), where L = **2**, was obtained, following a general synthetic procedure worked out at the Paul Scherrer Institute in Villigen, Switzerland [5]. Commercial $Re(CO)_5(H_2O)Cl$ and a small excess of **2** were dissolved in argon saturated tetrahydrofuran and stirred for 48 h. The orange residue obtained after evaporation of the solvent was dissolved in a 1:1 v/v mixture of *n*-pentane/dichloromethane, filtered, dissolved in a small amount of methanol and analyzed by thin-layer chromatography (TLC). Fourier-tranform infrared spectroscopy (FT-IR) and X-ray diffraction studies were also made. Crystals suitable for the X-ray diffraction analysis were obtained after evaporation of methanol and slow crystallization from a methanol/dichloromethane mixture (1:1); m.p. = 209°C.

Infrared spectra of the solid species **1** and **2** were registered as a KBr pellet within the 4.000-400 cm^{-1} range (Fig.2). All the main bands of **2** can be found in the spectrum of **1**, as well as two characteristic peaks of the coordinated CO vibrations (2015 and 1913 cm^{-1}) which confirm the existence of the typical tricarbonylrhenium(I) core.

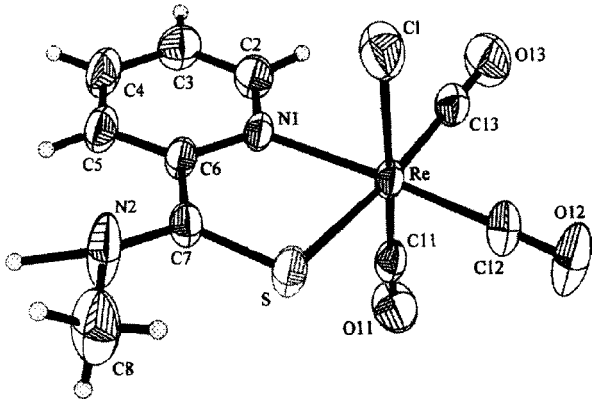

Fig.3. Molecular structure of the title complex $Re(CO)_3(L)Cl$ (**1**).

The molecular and crystal structure of **1** was determined based on single cystal X-ray reflections measured at room temperature, processed using profile analysis, and corrected for Lorentz factor and polarization effects. Non-hydrogen ions were

Table 2. Selected bond lengths and angles in the $Re(CO)_3(L)Cl$ complex (**1**).

Bond lengths [pm]		Angles [deg]			
Re-C11	189.3(7)	C13-Re-Cl	89.5(3)	N1-C6-C5	121.3(6)
Re-C12	191.8(8)	C12-Re-Cl	92.9(3)	N1-C6-C7	117.1(5)
Re-C13	189.8(7)	S-Re-Cl	85.99(9)	C5-C6-C7	121.5(6)
Re-N1	219.6(5)	C11-Re-Cl	177.1(2)	C4-C5-C6	119.0(7)
Re-S	244.5(2)	C11-Re-C13	89.1(3)	N1-C2-C3	123.3(7)
Re-Cl	247.5(2)	C11-Re-C12	89.6(3)	C3-C4-C5	119.2(7)
C11-O11	115.5(9)	C11-Re-N1	93.9(3)	N2-C7-C6	118.3(6)
C12-O12	113.0(10)	C11-Re-S	95.3(2)	N2-C7-S	120.8(5)
C13-O13	115.2(9)	N1-Re-Cl	83.8(2)	C6-C7-S	121.0(5)
C6-N1	135.2(8)	C12-Re-N1	172.7(3)	C7-N2-C8	124.1(7)
C6-C5	140.1(9)	C13-Re-C12	89.2(3)	C2-C3-C4	118.8(7)
C6-C7	147.2(8)	C12-Re-S	94.4(2)	C2-N1-C6	118.3(6)
C5-C4	138.1(11)	N1-Re-S	79.02(15)	C2-N1-Re	120.3(5)
C2-N1	133.8(8)	C13-Re-N1	97.2(3)	C6-N1-Re	121.4(4)
C2-C3	137.4(11)	C12-Re-N1	172.8(3)	C7-S-Re	101.1(2)
C4-C3	137.9(12)				
S-C7	167.1(6)				
C7-N2	131.3(8)				
N2-C8	145.4(11)				

located by direct methods using SHELXLS program [6] and then hydrogen atoms were found by successive Fourier syntheses. The unit cell parameters are listed in Table 1. The molecular structure of **1** is presented in Fig.3. As it was expected, the ligand **2** coordinates rhenium *via* pyridine nitrogen and sulfur atoms, forming a five-membered ring with the metal. Selected bond lengths and angles are presented in Table 2. Detailed data on the structure of the $Re(CO)_3(C_5H_4NCSNHCH_3)Cl$ complex reported in this paper have been deposited with Cambridge Crystallographic Data Center under the code number CCDC 224857.

An interesting feature of the determined structure of **1** is a shift of the "keto-enol" equilibrium in the coordinated ligand **2**. The most important parameter describing the difference between both structures is the distance between C(7)-N(2) atoms. The length of a single C-N bond is about 150 pm, while that for the double C=N bond shortens to about 120-130 pm [7]. The experimental value of 131.4 pm suites well to the "enolic" form of the ligand engaged in the complex formation.

Lipophilicity is an important characteristics of radiopharmaceuticals, which influences their biodistribution. It is usually determined as logP in the system isooctanol/water (partition constant P is the ratio of the concentrations of the same chemical species in the organic and aqueous phases at equilibrium). The P values for both **1** and **2** were preliminarily determined by solvent extraction from aqueous solutions (pH 4.6) to isooctanol. UV determinations (in the range of 260-300 nm) of the concentrations of **1** and **2** in the aqueous phase, initial and at equilibrium, gave $\log P_1 = 1.3$ and $\log P_2 = 0.6$. The work is in progress.

The work was supported by the Polish State Committee for Scientific Research (KBN) in the frame of the Research Contract No. 4 TO9A 11023.

References

[1]. Dilworth J.R., Parrott S.J.: Chem. Soc. Rev., 27, 43-55 (1998).
[2]. Volkert W.A., Hoffman T.J.: Chem. Rev., 99, 2269-2292 (1999).
[3]. Alberto R., Schibli R., Waibel R., Abram U., Schubiger A.P.: Coord. Chem. Rev., 190-192, 901-919 (1999).
[4]. Neuere Methoden der Präparativen Organischen Chemie. Band III. Verlag Chemie, 1961, p.30.
[5]. Fuks, L., Gniazdowska, E.: unpublished results (2002).
[6]. Sheldrick G.M.: Acta Cryst., A 46, 467 (1990).
[7]. Gillespie R.J., Popelier P.A.: Chemical Bonding and Molecular Geometry. Oxford University Press, NY-Oxford 2001, pp.25-38.

IMPROVED SYNTHESIS OF 3,4,5-TRIS(DIETHYLENEOXY)BENZOIC ACID

Ewa Gniazdowska, Jerzy Narbutt, Holger Stephan[1/], Hartmut Spies[1/]

[1/] Institute of Bioinorganic and Radiopharmaceutical Chemistry, Forschungszentrum Rossendorf, Dresden, Germany

^{99m}Tc and ^{188}Re radionuclides are widely used in nuclear medicine both for diagnostics [1] and therapy [2]. Progress in supramolecular chemistry led, in the recent years, to the synthesis of perfectly branched molecules – dendrimers [3]. Because of the unique molecular architecture of dendrimers, their physical and chemical properties significantly differ from those of linear and hyperbranched polymers. These specific properties make dendrimers suitable for a variety of technological uses in particular for biomedical applications [4-7].

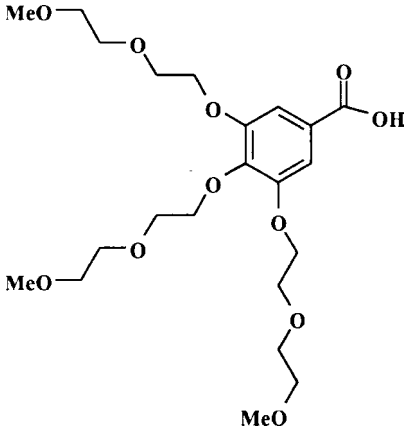

Fig.1. Structure of 3,4,5-tris(diethyleneoxy)benzoic acid – the model dendron.

The aim of this work was to elaborate conditions for efficient synthesis of a model dendron – 3,4,5-tris(diethyleneoxy)benzoic acid (Fig.1), to get a skill for the synthesis of the target dendron 3,4,5-tris(tetraethyleneoxy)benzoic acid. This precursor shall be coupled on 2-aminobenzothiole known as a suitable chelating unit for technetium and rhenium. Such oligoethyleneoxy-substituted dendritic 2-aminobenzothiols are expected to produce highly stable technetium and rhenium complexes having the required solubility properties for *in vivo* application.

At the first stage, monomethyldiethyleneglycol monotosylate (**1**) was synthesized – eq. (1) [8] (yield ~87%) of high purity, checked by thin-layer chromatography – TLC (Silica Gel, chloroform/methanol v/v = 97:3, $R_f = 0.76$).

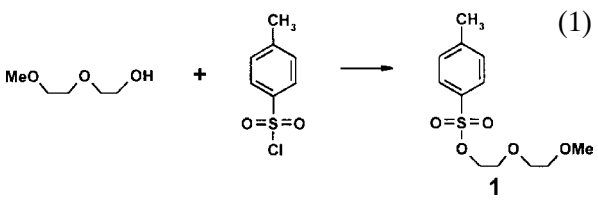

(1)

Then, 3,4,5-tris(diethyleneoxy)methyl benzoate (**2**) was obtained from **1** in Williamson's reaction – eq. (2):

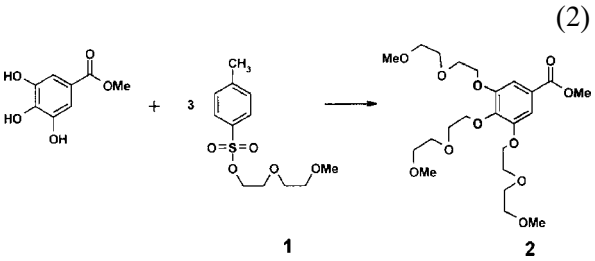

The literature procedure [6] has been modified according to [9]. Thus, the reaction was performed as follows: finely ground potassium carbonate (10 eq.) and **1** (3.5 eq.) were added consecutively to a solution of trihydroxybenzoate methylester (1 eq.) in methylisobutyl ketone. Then 5 mol% tetrabutylammonium bromide was added as a phase transfer catalyst and the heterogenous mixture was heated under reflux (117°C, 5 h, argon). The crude product, obtained after filtering of wet potassium carbonate and solvent evaporation, was dissolved in dichloromethane, washed consecutively with water, 1 M HCl, water, and finally the solvent was evaporated. After column chromatography (Silica Gel 60, 230-400 mesh, Merck), using chloroform as an eluent, compound **2** was obtained in a high yield (~82%) and high purity (~98% by gas-liquid chromatography-mass spectrometry – GLC-MS: m/z → 490, TLC on silica gel using chloroform/methanol, v/v = 97:3, solution as an eluent gave one spot with R_f = 0.61). This new procedure provided a higher yield and much shorter reaction time than those described in the literature [6].

Table. Selected group frequencies of 3,4,5-tris(diethyleneoxy)benzoic acid.

Wave number [cm^{-1}]	Functional group/assignment
3400-2800 (broad)	hydroxygroup, H-bonded O-H stretch
2824-2919	methyl ether O-CH_3, C-H stretch
1724	carboxylic acid, C=O stretch
1586	aromatic ring C=C-C stretch
1429	acids, O=C-OH
1324	acids, O=C-OH
1199	sceletal C-C vibrations
1102	alkyl substituted ether, C-O stretch
848	aromatic C-H out-of-plane bend

The title compound, 3,4,5-tris(diethyleneoxy)benzoic acid, has been obtained by hydrolysis of **2** (1 eq.) with water-LiOH (1.5 eq.)/methanol solution (v/v = 1:3). The compound was characterized by TLC, IR ATR (Table, Fig.2) and ^{1}H-NMR ($CDCl_3$, δ = 3.35, s,3H, (OCH_3)$_2$; 3.52-3.88, m,18H, (OCH_2); 4.22, m,6H, Ar-(OCH_2CH_2O)$_3$; 7.31, s,2H, Ar-H; Fig.3).

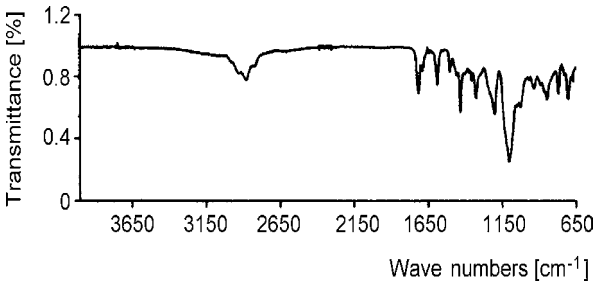

Fig.2. IR ATR spectrum of 3,4,5-tris(diethyleneoxy)benzoic acid.

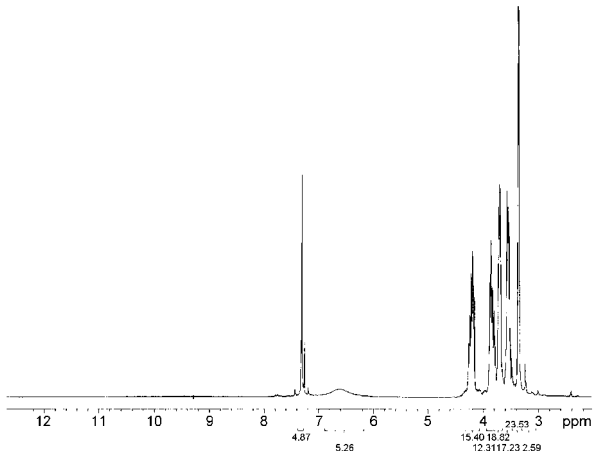

Fig.3. ^{1}H-NMR spectrum of 3,4,5-tris(diethyleneoxy)benzoic acid in $CDCl_3$.

The work is a part of the common Polish-German project "Nanoscalic metallodendrimers based on radioactive rhenium aminobenzenethiolate complexes". The authors thank Dr. Zygmunt Matacz (Department of Chemistry, Warsaw University of Technology) for the GLC-MS analysis.

References

[1]. Dilworth J.R., Parott S.J.: Chem. Soc. Rev., 27, 43-55 (1998).
[2]. Volkert W.A., Hoffman T.J.: Chem. Rev., 99, 2269-2292 (1999).
[3]. Zeng F., Zimmerman S.C.: Chem. Rev., 97, 1681-1712 (1997).
[4]. Kim Y., Zimmerman S.C.: Curr. Opin. Chem. Biol., 2, 733-742 (1998).
[5]. Liu M., Kono K., Frèchet J.M.J.: J. Controlled Release, 65, 121-131 (2000).
[6]. Baars M.W.P.L., Kleppinger R., Koch M.H.J., Yeu S.-L., Meijer E.W.: Angew. Chem., 112, 7, 1341-1344 (2000).
[7]. Stiribia S.-E., Frey H., Haag R.: Angew. Chem., 114, 1383-1390 (2002).
[8]. Ouchi M., Inoue Y., Liu Y., Nagamune S., Nakamura S., Wada K., Hakushi T.: Bull. Chem. Soc. Jpn., 63, 1260-1262 (1990).
[9]. Vekemans J.A.J.M. (Laboratory of Macromolecular and Organic Chemistry TU/e, Eindhoven, the Netherlands): private information.

PLATINUM(II) AND PALLADIUM(II) COMPLEXES WITH THIOUREA – QUANTUM CHEMICAL AND STRUCTURAL STUDIES

Leon Fuks, Marcin Kruszewski, Nina Sadlej-Sosnowska[1/], Krystyna Samochocka[2/], Wojciech Starosta

[1/] National Institute of Public Health, Warszawa, Poland

[2/] Department of Chemistry, Warsaw University, Poland

The long-standing interest in platinum(II) complexes, especially in *cis*-$[PtCl_2(NH_3)_2]$ (*cis*-diamminedichloroplatinum(II), clinically known as *cis*platin and abbreviated as CDDP), originates from the well-established anticancer activity of these compounds. Today, *cis*platin is commonly used in clinical therapy and is considered as a successful drug in the therapy of the testicular and ovarian carcinomas, as well as of numerous tumor kinds of the head and neck [1-3]. Although the nephrotoxicity of CDDP can be effectively inhibited, other severe toxic side effects of the therapy have been found. The latter have stimulated intensive research towards the design of new platinum (and other metals) chemotherapeutic agents [4-6]. Structure of the *cis*platin is illustrated in Scheme 1.

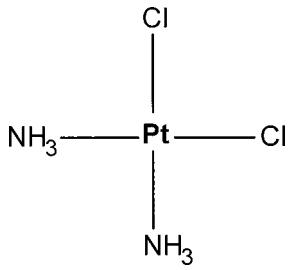

Scheme 1. Structure of the *cis*-diamminedichloroplatinum(II), *cis*platin.

In order to obtain compounds with superior chemotherapeutic index in terms of increased bioavailability, higher cytotoxicity and lower side-effects than *cis*platin, basic physico-chemical prop-

Table 1. Selected experimentally found values (exp) for the bond lengths [pm] and angles [deg] together with these calculated theoretically (calc).*

	$[Pt(tu)_4]Cl_2$		$[Pd(tu)_4]Cl_2$	
	exp	calc	exp	calc
M(1)-S(1)	232.60(19)	243.4	230.52(19)	243.7
M(1)-S(2)	231.27(12)	243.5	233.87(21)	243.7
M(1)-S(3)	233.29(19)	243.4	234.15(23)	243.7
M(1)-S(4)	232.73(21)	243.5	232.80(20)	243.7
S(1)-C(1)	172.61(87)	179.1	172.09(81)	179.1
S(3)-C(3)	173.50(77)	179.1	172.34(82)	179.1
S(2)-C(2)	170.77(73)	179.2	175.83(89)	179.1
S(4)-C(4)	174.14(74)	179.2	173.78(84)	179.1
M(1)-Cl(1)	1020.9		1236.1	
M(1)-Cl(2)	606.6		976.1	
S(1)-M(1)-S(2)	83.53(07)	95.45	86.72(08)	95.11
S(1)-M(1)-S(3)	176.10(07)	180.01	175.76(08)	180.00
S(2)-M(1)-S(3)	98.10(07)	84.56	93.42(08)	84.89
S(1)-M(1)-S(4)	92.33(08)	84.56	89.76(07)	84.89
S(2)-M(1)-S(4)	174.97(07)	179.99	174.17(08)	180.00
S(3)-M(1)-S(4)	83.53(07)	95.43	90.41(07)	95.11
C(1)-S(1)-M(1)	109.72(32)	109.71	110.40(27)	110.49
C(3)-S(3)-M(1)	110.66(27)	109.78	108.36(31)	110.50
C(2)-S(2)-M(1)	110.84(2)	109.76	111.50(29)	110.46
C(4)-S(4)-M(1)	105.69(26)	109.78	110.00(25)	110.50
Cl(1)-M(1) Cl(2)	72.74		69.34	

* MPW1PW.

Fig.1. Experimentally found molecular structure of the title complex $[Pt(tu)_2]_4Cl_2$ together with atom labelling.

erties together the toxicity against standard tumor cell lines must be investigated for numerous compounds. In this paper, we present the results of our preliminary investigations of the $M(tu)_4Cl_2$ complexes ($M = Pt^{2+}$ or Pd^{2+}), because in addition to the detoxicant properties, thiourea (tu) derivatives are poor ligands and their facile substitution under mild conditions turned already different transition metal complexes into useful precursors to other compounds exhibiting therapeutic properties in aqueous solutions, e.g. $[Tc^{III}(tu)_6]Cl_3$ or $[Re^{III}(tu)_6]Cl_3$ [7-11].

Structures of $Pt(tu)_4Cl_2$ and $Pd(tu)_4Cl_2$, crystallographically nearly isomorphic, consist of complex cations $M(tu)_4^{2+}$ and two uncoordinated chloride anions, each. Metal and four sulfur atoms in the cation exhibit square planar coordination. However, the S-M-S angles appeared to be distorted from the ideal values of 90 or 180°. Simultaneously, a slight tetrahedral distorsion about the central metal has been determined. Chloride anions, occupying non-axial positions relative to the plane of the metal and four sulfurs, show long metal-chloride distances indicating only of the van der Waals interactions. The latter contribute to the packing by forming an extensive network of hydrogen bonds, in which hydrogen atoms of the NH_2 groups are involved. So, results obtained in the presented paper (Table 1, Fig.1) remain in sufficient agreement with those obtained already for the divalent platinum [12, 13] and palladium [14, 15]. If we consider the structures for similar complexes of $M(tu)_4Cl_2$ (literature and presented here for the relevant Pt(II) or Pt(II) cation) certain differences can be found only in the M-Cl distances and directions. For example, the shortest experimentally found here Pt-Cl distance and Cl-Pt-Cl angle appeared to be about 606 pm and 73° in relation to the 377 pm and 130° (literature data [12, 13]).

Results presenting the main optimized interatomic distances and angles are included in Table 1. Data obtained for the bond lengths are overestimated by about 4-6% in relation to the experimental atom distances. On the contrary, both calculated and experimental values of the bond angles are much alike. In our opinion, the discrepancy between the corresponding values for the atom distances can be related to the similarity, but not equality, established for the covalent radii, r_{cov}, and the radii of the outermost shells in the atoms, $r_{max,out}$

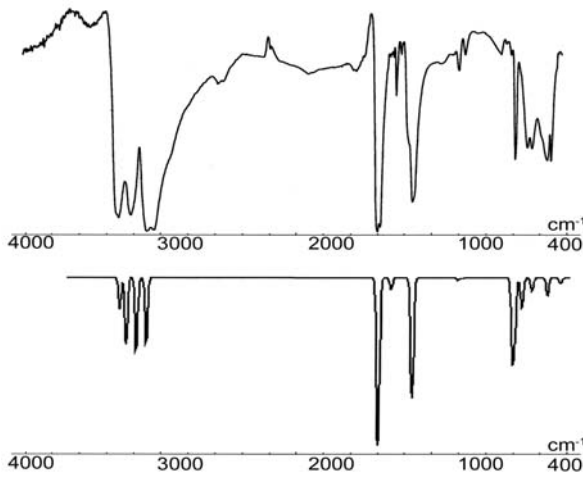

Fig.2. Experimentally found (upwards) and theoretically calculated (bottom) vibrational spectra for the title complex $[Pd(tu)_2]_4Cl_2$.

(e.g. 103 *vs*. 110 pm for sulfur, 70 *vs*. 76.5 pm for nitrogen or even 77 *vs*. 92 pm for carbon) [16].

Registered and theoretically simulated vibrational spectra of the title species are shown in Fig.2. Selected FT-IR (Fourier-transform infrared spectroscopy) bands recorded for the ligand as well as

Table 2. Selected IR frequencies [cm^{-1}].

	δ_{CN}	β_{SCNN}	ν_{CS}	ν_{CS}	ν_{CN}	δ_{NH}	δ_{NH}	ν_{NH}	ν_{NH}
$S=C(NH_2)_2$									
experimental	488	631	735	1414	1473	1512	1618	3276	3379
calculated	484	629		1437	1509	1669	1703	3652	3808
$[Pt(tu)_2]_4Cl_2$									
experimental	472	650	708	1455	1462	1500	1622	3273	3808
calculated	555	666	743	1394	1458	1618	1714	3619	3757
	$[Pd(tu)_2]_4Cl_2$								
experimental	471	627	712	1402	1438	1504	1630	3269	3352
calculated	543	669	741	1449	1457	1616	1724	3619	3757

for the title complexes, ν (cm^{-1}) are listed in Table 2 together with their assignment. The assignment was made according to [17-19] and the references cited therein.

In the presented investigations, we were primarily interested in determining the performance of the theory by calculating the vibrational frequencies of the investigated species and comparing them with the experimental values. Calculated structures of the investigated complexes that more or less accurately reproduce the experimental spectra, are the best test of the applied basis set applied to the description of structural or thermodynamic properties in comparison with the X-ray-determined geometry. The latter can be affected by crystal packing, intermolecular interactions, *etc*. Because the spectrum recorded for thiourea in KBr pellets by Stewart and by Peyronel [17, 18] is rather at variance – the authors concluded that this fact may indicate that the pellet spectra depend on too many factors which cannot always be controlled or exactly reproduced.

Cytotoxicity of the investigated complexes (mouse lymphoma cell line L1210) was estimated *in vitro* by means of the relative growth test as described earlier [20]. No significant toxicity of the investigated complexes was found: the 50% inhibition dose (ID_{50}) values are about 1400 $mmol \cdot cm^{-3}$ for both $[Pt(tu)_2]_4Cl_2$ and $[Pd(tu)_2]_4Cl_2$. Standard *cis*platin, in turn, shows the ID_{50} being about 2 $mmol \cdot cm^{-3}$.

References

[1]. Platinum and Other Metal Coordination Compounds in Cancer Chemotherapy. Ed. M. Nicolini. Nijhoff 1988.
[2]. Metal Ions in Biological Systems. Eds. H. Sigel, A. Sigel. Dekker, NY 1980, vol.11.
[3]. Metal Complexes in Cancer Chemotherapy. Ed. B.K. Keppler. Verlag Chemie, Weinheim 1993.
[4]. Reedijk J.: Chem. Rev., 99, 2499 (1999).
[5]. Bradner W.T., Rose W.C., Hauftalen J.B.: Antitumor Activity of Platinum Analogs. In: Cisplatin: Current Status and New Developements. Eds. A.W. Prestayko, S.T. Crooke, S.K. Carter. Academic Press, NY 1980, pp.171-182.
[6]. Christian M.C.: Sem. Oncol., 19, 720 (1992).
[7]. Bandoli G., Mazzi U., Spies H., Munze R., Ludwig E., Ulhemann E.: Inorg. Chim. Acta, 132, 177 (1987).
[8]. Abrams M.J., Davison A., Faggiani R., Jones A.G., Lock C.J.L.: Inorg. Chem., 23, 3284 (1984).
[9]. Kremer C., Kremer E.: J. Radioanal. Nucl. Chem., Lett., 175, 445 (1993).
[10]. Tkac P., Kopunec R., Skraskova S.: J. Radioanal. Nucl. Chem., 258, 215 (2003).
[11]. Omori T.: Topics in current chemistry. In: Technetium and Rhenium. Vol.176. Springer-Verlag, Berlin 1996, p.267.
[12]. Girling R.L., Chatterjee K.K., Amma E.L.: Inorg. Chim. Acta, 7, 557 (1973).
[13]. Arpalahti J., Lippert B., Schollhorn H., Thewalt U.: Inorg. Chim. Acta, 153, 51 (1988).
[14]. Berta D.A., Spofford W.A., Boldrini P., Amma E.L.: Inorg. Chem., 9, 136 (1970).
[15]. Ooi S., Kawase T., Nakatsu K., Kuroya H.: Bull. Chem. Soc. Jpn., 33, 861 (1960).
[16]. Siekierski S., Burgess J.: Concise Chemistry of the Elements. Horwood Publisching, Chichester 2002.
[17]. Stewart J.E.: J. Chem. Phys., 26, 248 (1957).
[18]. Peyronel G., Pignedoli A., Malawasi A.: Spectrochim. Acta, 40A, 63 (1984).
[19]. Coates J.: Interpretation of Infrared Spectra, A Practical Approach. In: Encyclopedia of Analytical Chemistry. Ed. R.A. Meyers. John Wiley & Sons, Chicester 2000, pp.10815-10837.
[20]. Samochocka K., Kruszewski M., Szumiel I.: Chem.-Biol. Interact., 105, 145 (1997).

PRELIMINARY RESULTS OF FRACTIONATION OF GALLIUM ISOTOPES IN THE DOWEX 50-X8/HCl SYSTEM

Wojciech Dembiński, Irena Herdzik, Witold Skwara, Ewa Bulska[1/], Agnieszka Wysocka[1/]

[1/] Faculty of Chemistry, Warsaw University, Poland

The role of isotopically pure materials in the microelectronic industry is recently growing because of their higher thermal conductivity and lower crystal lattice noise in comparison with the materials of natural isotope composition. These phenomena are best recognized for silicon, however the isotopically-engineered materials of gallium and indium can also effectively increase the performance and reliability of the devices used in wireless communication, optoelectronics, semiconductor lasers, high frequency integrated circuits, *etc*. [1-3].

The career of isotopically-engineered materials depends mostly on the isotope separation cost, *i.e*. on the effectiveness of isotope enrichment methods. This motivated us to undertake studies in the field of isotope chemistry of such elements as gallium and indium in order to select chemical systems characterized by high isotope separation factors, as well as to add a new data to the knowledge on the recently discovered relation between the chemical isotope effect and the specific properties of isotope nuclei such as nucleus volume, shape and charge distribution [4, 5]. The systems like liquid-liquid extraction, ion exchange chromatography, red-ox systems with amalgams are here of interest. Till now, no separation data of gallium and indium isotopes in chemical exchange reactions have been published.

At the beginning stage of our work, we examined the separation of gallium isotopes, $^{69}Ga/^{71}Ga$, by band elution chromatography, using a cation exchanger Dowex 50-X8, as stationary phase and hydrochloric acid as effluent. The following parameters of the process were studied in order to obtain appropriate number of theoretical plates, column height and diameter, grain-size of ion exchanger, flow of effluent, number of cycles.

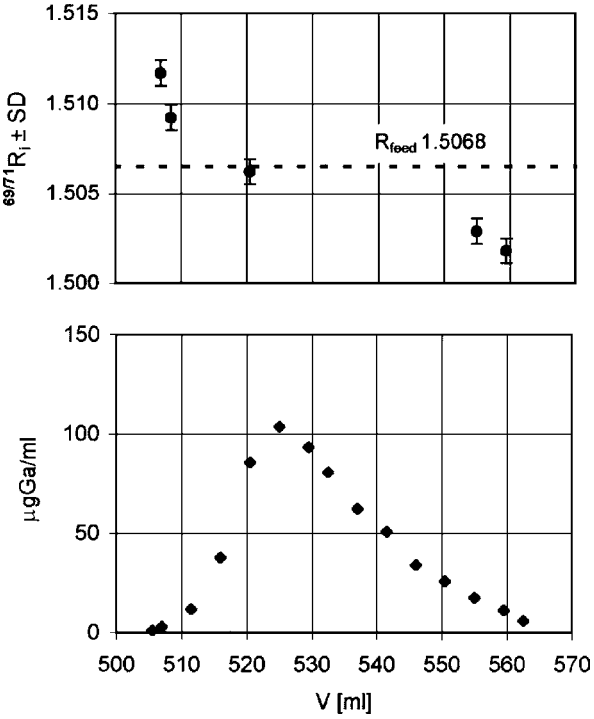

Fig. Band profile and local isotope ratio for DOWEX 50-X8, 400 mesh/2 M HCl. Column: h = 100 cm, d = 0.5 cm; effluent flow: 0.13 ml/min; band: 2.7 mg Ga.

The band profile was controlled by determination of gallium in consecutive fractions by the atomic absorption method with flame atomization.

Isotope ratio (R) in selected fraction was determined by an inductively coupled plasma mass spectrometer Perkin Elmer, Elan 6100 DRC.

The chromatogram and the local isotope ratios from the experiment performed with 2 M HCl is shown in Fig. It revealed that in the studied system the lighter isotope, ^{69}Ga, is enriched in the front part of the band and the heavier isotope, ^{71}Ga, is enriched in the rear part of the band. This means that the lighter isotope is preferentially fractionated to the solution phase. The value of unit enrichment factor in the system is expected to be of the order of magnitude $10^{-4} \div 10^{-5}$, as follows from the recalculation of the data by Glueckauf theory [6, 7].

The work is in progress.

This work is supported by the Polish State Committee for Scientific Research (KBN) – grant No. 4 T09A 057 25.

References

[1]. Ma Tso-Ping: US Patent No.5,442191.
[2]. Ruf T., Henn R., Assen-Palmer M., Gmelin E., Cordona M., Pohl H., Devayatych G., Sennikov P.: Solid State Commun., 115(5), 110 (2000).
[3]. Chmielewski A., Dembiński W., Trznadel G.: Postępy Techniki Jądrowej, 44(1), 26-36 (2001), (in Polish).
[4]. Bigeleisen J.: J. Am. Chem. Soc., 118, 367 (1996).
[5]. Dembiński W., Poniński M., Fidler R.: Sep. Sci. Technol., 29(11), 1693 (1998).
[6]. Glueckauf E.: Trans. Faraday Soc., 51, 34 (1955).
[7]. Glueckauf E.: Trans. Faraday Soc., 54, 1203 (1958).

A CHROMATOGRAPHIC INVESTIGATION OF DYES EXTRACTED FROM COPTIC TEXTILES FROM THE NATIONAL MUSEUM IN WARSAW

Jowita Orska-Gawryś, Marek Trojanowicz, Katarzyna Urbaniak-Walczak[1/], Jerzy Kehl[1/], Izabella Surowiec[2/], Bogdan Szostek[3/], Marek Wróbel[4/]

[1/] National Museum in Warsaw, Poland
[2/] Department of Chemistry, Warsaw University, Poland
[3/] DuPont Haskell Laboratory for Health and Environmental Sciences, Newark, USA
[4/] Geological Bureau GEONAFTA, Warszawa, Poland

Introduction

The aim of this work was the chemical identification of natural substances used for dying of Coptic textiles from the collection of National Museum in Warsaw, which was part of the comprehensive research programme, including chemical, microbiological, and mechanical investigations on the preparation of complete documentation of natural dyes used in the examined textiles. Results of this work will be used to establish the most appropriate conservation conditions and can also be helpful in dating or elucidating the place of origin of the examined archaeological objects.

Ancient dyestuffs originate from extracts of plants, insects and molluscs. Dyes can be extracted directly from these natural species or can be obtained after various chemical pre-treatments such as complexation with metals, hydrolysis or oxidation. Although the literature on the chemical examination of historical textiles is quite extensive [1-10], limited attention was paid to Coptic textiles. The investigation based on chemical reactions of dyes in textiles from Christian burials in Egypt dating from the 4th to the 6th century was pioneered by Pfister in the 1930ies [11]. The first high performance liquid chromatography (HPLC) examination of extracts from four Coptic objects dating from the 3rd to the 8th century was reported by Wouters [8]. From his later works [9, 12], one can conclude that natural dyes with different compositions were used at different periods of time. For example, in the Byzantine period, the proportion of madder to kermes in Egyptian textiles was 95/5, and in the early Arabic period, the proportion of madder to lac dye was 50/50.

In the present study, HPLC with three methods of detection – diode-array UV-VIS (DAD), fluorescence (FLD), and mass spectrometry (MS) –

was used to identify individual chemical components of anthraquinone, indigoid, and flavonoid dyes in extracts from fibres of different colours taken from Coptic textiles. Elemental analysis us-

Table 1. Components found in extracts from threads taken from selected Coptic textiles.

Sample (date, colour, fibre)	Compounds identified	Method of detection					Natural dyes identified
		DAD (1) hydrolyzate	DAD (2) hydrolyzate	DAD (3) pyridine extract	FLD hydrolyzate	MS hydrolyzate	
AD 6th yellow wool	Luteolin	43%	58%			+	Madder (Rubia tinctorum), Flavonoid yellow dye*
	Apigenin	4%	8%			+	
	Alizarin	44%	29%			+	
	Purpurin	9%	5%		+	+	
	Kaempferol				+		
	Quercetin				+		
	Rhamnetin					+	
	Xanthopurpurin					+	
AD 4th brown wool	Alizarin	10%	42%			+	Madder (Rubia tinctorum), Indigotin, Tannins, Flavonoid yellow dye*
	Purpurin	90%	41%		+	+	
	Munjistin		8%		+		
	Ellagic acid		4%				
	Indigotin	<1%					
	Kaempferol				+		
	Quercetin				+		
	Rhamnetin				+	+	
	Luteolin		5%			+	
	Apigenin					+	
	Indirubin					+	
	Xanthopurpurin					+	
AD 7th-9th dark blue wool	Alizarin	45%	14%			+	Madder (Rubia tinctorum), Flavonoid yellow dye**, Indigotin
	Purpurin	21%	35%		+	+	
	Indigotin	22%	51%				
	Indirubin	12%				+	
	Kaempferol				+		
	Luteolin					+	
	Xanthopurpurin					+	
AD 7th-9th green wool	Luteolin	75%	27%			+	Madder (Rubia tinctorum), Flavonoid yellow dye*, Indigotin, Tannins
	Apigenin					+	
	Alizarin	16%				+	
	Kaempferol				+		
	Quercetin				+		
	Rhamnetin				+	+	
	Ellagic acid		64%		+	+	
	Indigotin	9%	9%				
	Indirubin					+	
	Xanthopurpurin					+	
AD 7th-9th black wool	Alizarin	58%	48%			+	Madder (Rubia tinctorum), Flavonoid yellow dye*, Indigotin, Tannins
	Purpurin	42%				+	
	Indigotin			+			
	Indirubin	<1%		+		+	
	Luteolin		10%			+	
	Ellagic acid		42%				
	Kaempferol				+		
	Quercetin				+		
	Rhamnetin				+		

Table 1. contd.

Sample (date, colour, fibre)	Compounds identified	Method of detection					Natural dyes identified
		DAD (1) hydrolyzate	DAD (2) hydrolyzate	DAD (3) pyridine extract	FLD hydrolyzate	MS hydrolyzate	
Unknown date red silk	Alizarin	4%				+	Armenian cochineal (Porphyrophora hamelii), Lac dye (Laccifer lacca), Madder (Rubia tinctorum), Flavonoid yellow dye**, Indigotin, Tannins
	Purpurin	11%				+	
	Carminic acid	41%	87%		+	+	
	Ellagic acid	21%	13%				
	Laccaic acid A	13%					
	Laccaic acid B	2%					
	Gallic acid	2%					
	Luteolin	5%				+	
	Apigenin	1%				+	
	Indigotin			+			
	Kaempferol				+		
	Quercetin				+		
	Xanthopurpurin					+	
Uknown date red wool	Alizarin	60%	64%			+	Madder (Rubia tinctorum), Flavonoid yellow dye**, Tannins
	Purpurin	40%	35%		+	+	
	Ellagic acid		1%				
	Luteolin					+	
	Apigenin					+	
	Xanthopurpurin					+	
	Monochloroalizarin					+	
	Dichloroalizarin					+	

* Most probably of weld or Rhamnus source.
** Postulated weld.

ing scanning electron microscope and energy dispersive X-ray spectrometry (SEM-EDS) technique was performed to identify mordants on threads from Coptic textiles.

Experimental section

Extraction procedure was applied earlier and described in [13].

HPLC and LC/MS instrumentation

The separations for diode array and fluorescence detections were carried out with two HPLC systems from Shimadzu (Kyoto, Japan) consisting of an injection valve with a 20 μL loop, a column oven CTO-10AS, a photo diode array detector SPD-M10A, a spectrofluorometric detector RF-10A, a system controller SL-10A, Shimadzu chromatographic software Class-VP, a gradient pump LC-10AT, and a phase mixer FCV-10AL in the first, and two HPLC pumps model LC10 AD and a degasser DGU-14A in the second system. With the first HPLC system UV-VIS detection was applied, with the second, UV-VIS and fluorometric detections.

For mass spectrometry detection two different LC/MS systems were employed. Two different systems were used because of availability of the systems at the time the samples were analysed and the second system (System II) had an in-line DAD detector while the first system (System I) only had a single wavelength detector. As far as the mass spectrometers used in these systems are concerned, they have very similar capabilities and sensitivity. Initially, the work was started on a triple quadrupole mass spectrometer Quattro LC (Micromass, Manchester, United Kingdom) equipped with a Z-spray API ESI (Atmospheric Pressure Ionization, ElectroSpray Ionization) source, interfaced with HP 1100 HPLC system (Agilent, Palo Alto, CA, USA) and in-line variable wavelength ultraviolet detector (Agilent, Palo Alto, CA, USA) (System I). The work was continued on a triple quadrupole mass spectrometer Quattro Micro (Micromass, Manchester, United Kingdom) equipped with Z-spray API ESI source or APCI source, combined with a 2795 Waters HPLC system (Waters, Milford, MA, USA) and in-line Model 2996 PDA ultraviolet detector (Waters, Milford, MA, USA) (System II).

SEM-EDS analysis

Elemental analysis of Coptic threads was done using an electron microprobe LINK-ISIS coupled to a scanning electron microscope JSM-630 from JEOL (Peabody, USA). Three techniques were used. Point analysis was made on 40 samples of Coptic threads. Because of significant differences in elemental composition within one sample, three point analysis from different areas of the thread

were made for each sample. Line analysis of one sample and area analysis of another one were also made. Line and area analyses were carried out in scanning mode in order to observe a change in element content along the cross-section of the fibre. All determinations were performed with an accelerating voltage of 20 keV and a beam current of 10^{-9} A. Duration of point, line and area analysis was 200 s, 20 min and 2 h, respectively. All samples were rinsed three times with distilled water and coated with spectrally pure carbon before analysis.

Results and discussion

Identification of dyes by chromatography

Investigations based on UV-VIS identification of compounds were carried out in three stages. First, chromatographic measurements were made on purified dyes and natural dyeing substances collected from various sources. Then HPLC data were recorded for extracts of dyes from contemporary dyed fibres, which were dyed with dyestuff extracted from raw material purchased from Kremer. Finally, the extracts from fibres taken from ancient Coptic objects were analysed under two sets of chromatographic conditions as described in the experimental section. Identification of dyes extracted from the objects was based on retention times and on UV-VIS spectra recorded for sample extracts and standards.

Fifty six hydrochloric acid/ethanol/water extracts and 16 pyridine extracts from threads from Coptic textiles were examined. The peak area absorbance values at 255 nm were used to determine the relative amounts (in percent) of dyes identified in each extract. This wavelength provides sufficient sensitivity for the detection of all compounds identified. It is also widely used in the literature as a reference wavelength for comparing results obtained for different extracts from natural dyes and archaeological threads. It was noticed that the relative sensitivity of the DAD detection, *i.e.* the relative amounts of dyes identified for each extract, varied depending on the gradient of eluent used, even if the same extraction method was applied. It was probably due to the different eluent background in applied gradients. Frequently, the fluorescence detection can provide better selectivity and detectability than UV-VIS detection. Often, a post- or pre-column derivatization is needed to achieve that. Methanolic solutions of Al(III), Ga(III), In(III) and Zn(II) salts were tested as post-column complex-forming reagents for enhancing the fluorescence signal of the investigated dyes. Among these, Ga(III) proved to be the best one and 10 mM solution of this cation was used for fluorescence detection of some plant extracts and 56 water/methanol extracts from Coptic textiles. Fluorescence detection with Ga(III) solution as the post-column reagent proved to be more sensitive than UV-VIS for the detection of purpurin, rhamnetin, quercetin, gallic acid, kaempferol and munjistin. DAD, however, was more sensitive for the determination of carminic acid, ellagic acid, luteolin, alizarin, apigenin, lawson and indigoid dyes.

The chromatographic and mass spectrometric behaviour was investigated for selected dye compounds of flavonoid-, anthraquinone- and indigo--type. Most of the investigated compounds can be ionised with the positive and negative ion electrospray ionisation.

Mass spectrometric detection, using different scanning modes of a triple quadrupole mass spectrometer, combined with the UV detection was demonstrated to be a powerful approach for the detection and identification of dyes in extracts from archaeological textiles. This approach is extremely useful in cases where a limited amount of precious sample is available and a maximum amount of information is attempted to be gained about the samples. MS detection additionally provides selectivity that is hard to obtain with UV detection. This is advantageous for complex sample matrices and for resolution of overlapping chromatographic peaks. In this case, the mass spectrometer is set up to monitor signal for characteristic parent-daughter ion transitions for pre-selected group of compounds (MRM mode), allowing their selective and sensitive detection and providing additional confidence of compound identity, besides the retention time match. The UV detection was not sufficient to detect these compounds for this sample.

Full scan MS with different ionisation modes, combined with simultaneous UV detection is often sufficient to identify the main components. Individual components can be easily identified by plotting traces for molecular ions of investigated compounds and matching the retention time of the peak with that of the standard. In addition, the data from the full scan mode can be used to flag the parent ions of unknowns showing up either on the UV trace or MS trace and subject them to further structure elucidation effort by collecting their daughter ion spectra. Comparison of results for UV-VIS, fluorescence and MS detections for some of the extracts from Coptic threads is shown in Table 1.

X-ray spectroscopic determination of inorganic mordants

Calcium, oxygen, aluminium, silicon, and magnesium were found in all samples in point analysis mode. These elements, together with phosphorus (found in 36 samples), potassium (18 samples), sodium (24 samples) and chlorine (9 samples) can be associated with contaminants from the archaeological sites and it is not possible to conclude if they are chemical elements of the mordants. Sulphur was detected in all samples, which is not surprising since this element is found in animal fibres. Its occurrence in two flax fibres is very interesting and can probably indicate the use of a mordant. Iron was found in 26 samples and its presence can indicate the use of mordant during dyeing procedure or that the sample was buried in an iron-rich soil. Zinc, reported to be used for weld to obtain yellow colours, was found in 7 samples. In all of them weld or at least kaempferol were identified. Copper and chromium were found in one brown sample on which madder, weld and indigotin were

Table 2. Examples of elemental composition of Coptic threads obtained by X-ray spectroscopy.

Thread			Elemental composition	
Date	Colour	Fibre		
4th-5th	Violet	Wool	Ca, Mg, O, Al, Si, S	N
4th	Brown	Wool	Ca, Mg, O, Al, Si, S	N
5th	Brown	Wool	Ca, Mg, O, Al, Si, S	N, Fe, Na, Cl, Cu, Cr
5th	Black	Wool	Ca, Mg, O, Al, Si, S	P, Fe, Cl, K, Ti
5th	Violet	Wool	Ca, Mg, O, Al, Si, S	P, N, Fe, Na, Cl, K
7th-9th	Green	Linen	Ca, Mg, O, Al, Si, S	P, N, Na
7th-8th	Yellow	Silk	Ca, Mg, O, Al, Si, S	P, Fe, Na, Cl
Unknown	Red	Silk	Ca, Mg, O, Al, Si, S	N, P
Unknown	Blue	Linen	Ca, Mg, O, Al, Si, S	Fe
8th-9th	Dark blue	Wool	Ca, Mg, O, Al, Si, S	P, N, Na, Zn
8th-9th	Black	Wool	Ca, Mg, O, Al, Si, S	N, Zn
7th-9th	Dark blue	Wool	Ca, Mg, O, Al, Si, S	P, N, Fe, Na, Zn
7th-9th	Green	Wool	Ca, Mg, O, Al, Si, S	P
7th-9th	Yellow	Wool	Ca, Mg, O, Al, Si, S	P, N, Fe, K
7th-9th	Black	Wool	Ca, Mg, O, Al, Si, S	N, Na
7th-9th	Orange	Wool	Ca, Mg, O, Al, Si, S	P, N, Fe, Na, K, Zn

identified by HPLC analysis. Titanium was found in one black thread, dyed with madder, weld, indigotin and tannins. These elements are not mentioned in the literature as having been used by Copts as mordants. Tin was not detected in any of the investigated samples, although it is said that its salts could be used in ancient Egypt as mordants. Results of point analysis for some of the samples are shown in Table 2.

References

[1]. Wouters J., Verhecken A.: J. Soc. Dyers Colour., 107, 266-269 (1991).
[2]. Cardon D., Colombini A., Oger B.: Dyes History Archaeol., 8, 22-31 (1989).
[3]. Walton P., Tylor G.: Chromatogr. Analysis, 17, 5-7 (1991).
[4]. Wouters J.: Dyes History Archaeol., 10, 17-21 (1991).
[5]. Derksen G.C.H., van Beek T.A., de Groot E., Capelle A.: J. Chromatogr. A, 816, 277-281 (1998).
[6]. Fischer Ch.H., Bischof M., Rabe J.G.: J. Liq. Chromatogr., 13, 319-331 (1990).
[7]. Nowik W.: Analysis, 24, 7, M37-M40 (1996).
[8]. Wouters J.: Stud. Conserv., 30, 119-128 (1985).
[9]. Wouters J.: Dyes History Archaeol., 13, 38-45 (1994).
[10]. Wouters J., Maes L., Germer R.: Stud. Conserv., 35, 89-92 (1990).
[11]. Pfister R.: Teinture et alchimie dans l'Orient Hellénistique. Seminarium Kondakovianum VII, Prague 1935, pp.1-59.
[12]. Wouters J.: Dye analysis of Coptic textiles. In: Koptisch Textiel. De Moor, Zottegem 1993, pp.53-64.
[13]. Orska-Gawryś J., Urbaniak-Walczak K., Surowiec I., Kehl J., Rejniak H., Trojanowicz M.: In: Annual Report 2001. Institute of Nuclear Chemistry and Technology, Warszawa 2002, pp.73-76.

THE STUDY ON THE INFLUENCE OF TEMPERATURE ON ION EXCHANGE SEPARATIONS OF ANIONS AND THE STABILITY OF ANION EXCHANGE COLUMNS IN ISOCRATIC ION CHROMATOGRAPHY

Krzysztof Kulisa, Rajmund Dybczyński

Establishing of conditions and parameters influencing the quality of chromatographic separations of mixtures of ionic species in aqueous solutions is essential for the accurate and reliable chromatographic analysis. The column temperature is a valuable parameter for optimizing ion chromatographic separations of inorganic anions. Influence of column temperature on separation processes was investigated to a greater extent for classical ion exchange chromatography [1-3] as well as several high performance liquid chromatography (HPLC) techniques, such as reversed phase chromatography [4-6], ion-pair chromatography [7, 8], normal phase HPLC [9], ion exchange chromatography [10-11] and occasionally for ion chromatography [12-14]. The comprehensive studies on the thermodynamics

Table. Examples of changes of values of separation factor (α) and the resolution (R_s) for selected pairs of inorganic anions. Column – Ion Pac AS9SC. Eluents – 1.5 mM $NaHCO_3$, 10 mM $NaHCO_3$ and 1.7/1.8 mM $NaHCO_3/Na_2CO_3$.

$SO_4^{2-} - SO_3^{2-}$

T [°C]	10 mM $NaHCO_3$		1.7/1.8 mM $NaHCO_3/Na_2CO_3$	
	$\alpha_{SO_3}^{SO_4}$	$R_s^{SO_3-SO_4}$	$\alpha_{SO_3}^{SO_4}$	$R_s^{SO_3-SO_4}$
10	1.28	2.14	1.31	1.42
25	1.29	2.02	1.34	1.53
35	1.29	1.86	1.40	1.83
40	1.31	1.87	1.40	2.12

$Br^- - Cl^-$

T [°C]	1.5 mM $NaHCO_3$		10 mM $NaHCO_3$		1.7/1.8 mM $NaHCO_3/Na_2CO_3$	
	α_{Cl}^{Br}	R_s^{Cl-Br}	α_{Cl}^{Br}	R_s^{Cl-Br}	α_{Cl}^{Br}	R_s^{Cl-Br}
10	1.87	5.33	2.28	3.31	2.68	4.20
25	1.43	4.81	2.20	3.06	2.55	5.22
35	1.23	2.50	2.11	3.00	2.50	4.61
40	1.01	0.46	2.03	2.71	2.47	4.43

1.5 mM $NaHCO_3$

T [°C]	$IO_3^- - F^-$		$IO_4^- - F^-$	
	$\alpha_F^{IO_3}$	$R_s^{F-IO_3}$	$\alpha_F^{IO_4}$	$R_s^{F-IO_4}$
10	2.46	2.81	2.02	2.32
25	1.92	1.76	2.04	2.38
35	1.59	1.32	1.64	1.55
40	1.01	0.52	1.06	0.54

$I^- - PO_4^{3-}$

T [°C]	10 mM $NaHCO_3$				1.7/1.8 mM $NaHCO_3/Na_2CO_3$	
	$\alpha_{PO_4}^{I}$	$\alpha_I^{PO_4}$	$R_s^{PO_4-I}$	$R_s^{I-PO_4}$	$\alpha_{PO_4}^{I}$	$R_s^{PO_4-I}$
10	1.31	-	2.11	-	2.08	5.23
25	1.25	-	1.65	-	2.10	4.89
35	1.08↑	-	0.77↑	-	1.71	3.90
40	-↓	1.09	-↓	1.55	1.35	2.30

$I^- - SO_4^{2-}$

T [°C]	10 mM $NaHCO_3$		1.7/1.8 mM $NaHCO_3/Na_2CO_3$			
	$\alpha_{SO_4}^{I}$	$R_s^{SO_4-I}$	$\alpha_{SO_4}^{I}$	$\alpha_I^{SO_4}$	$R_s^{SO_4-I}$	$R_s^{I-SO_4}$
10	1.09	0.81	1.38	-	2.70	-
25	1.36	2.55	1.11↑	-	0.93↑	-
35	1.58	4.71	-↓	1.07	-↓	0.90
40	1.80	5.11	-	1.33	-	3.31

↑↓ – change of elution order.

of ion exchange processes with the use of special type "agglomerated" ion exchange resins applied in ion chromatography, however, were practically not carried out so far.

This study was carried out in order to evaluate the effect of column temperature on ion exchange equilibria of low capacity "agglomerated" anion exchange resins of type Dionex Ion Pac, and to investigate the changes of basic chromatographic parameters such as retention time t_R, column efficiency N (peak broadening), peak asymmetry A_s, capacity factor k, selectivity coefficient K, separation factor α and the resolution R_s according to column temperature changes. One could expect, that the "agglomerated" type ion exchangers of low exchange capacity (10-30 μeq/g) and short diffu-

sion paths for exchanging ions which are applied in ion chromatography, could be strongly affected by changes of column temperature similarly as the ion exchangers of greater ion exchange capacities used in classical ion exchange chromatography. The studies were carried out with the use of a commercially available ion chromatograph Dionex 2000i/SP and three anion exchange columns: Ion Pac AS5, Ion Pac AS9SC and Ion Pac AS4A with different degrees of hydrophobicity of quaternary ammonium functional groups and different exchange capacities (within the range of 10-30 μeq/g). A hydrogen carbonate (1.5 and 10 mM $NaHCO_3$), hydrogen carbonate-carbonate buffer (1.7 mM $NaHCO_3$/1.8 mM Na_2CO_3) solutions (pH range 8.15-9.97) as well as NaOH solutions (0.5, 1, 3, 5, 10, 20 and 30 mM, pH range 9.61-11.85) were used as a mobile phase. Changes of chromatographic parameters were established as a function of column temperature in the range of 10-55°C for Ion Pac AS5 and AS9SC anion exchange columns and 10-40°C for Ion Pac AS4A column for many inorganic anions such as: F^-, Cl^-, ClO_3^-, ClO_4^-, IO_3^-, BrO_3^-, Br^-, NO_2^-, NO_3^-, I^-, PO_4^{3-}, SO_3^{2-}, SO_4^{2-}, WO_4^{2-}, MoO_4^{2-}, $S_2O_3^{2-}$, SCN^-, AsO_4^{3-}, SeO_4^{2-}. Columns were maintained at each temperature chosen before elution process during the period of *ca*. 0.5 h to stabilize thermal conditions of each experiment.

It was established that the chromatographic parameters investigated, such as column efficiency, peak asymmetry, capacity factor, selectivity coefficient and the resolution for different anions may increase or decrease with the change of column temperature. Thermal stability of the investigated anion exchange resin beds was good at temperature below 40°C. Above this limit, the symptoms of partial ion exchange bed degradation were observed when Ion Pac AS5 and AS9SC anion exchange columns were used [15]. As a consequence, column exchange capacities rapidly decreased as well as column efficiencies, which caused the rise of peak broadening and asymmetry as well as lowering of retention times of separated anions. Changes of chromatographic parameters caused by ion exchange bed degradation were irreversible. During the studies with the use of Ion Pac AS4A column, the range of column temperatures from 10 to 40°C was applied and NaOH of varied concentration as a mobile phase. This time no symptoms of ion exchange bed degradation were observed during the experiments and the nominal ion exchange capacity was maintained. Elevated column temperature (up to 40°C) caused usually the rise of column efficiency for investigated anions for all columns studied. Changes of column temperature induced changes of selectivity between separated anions. For several pairs of anions (e.g. $I^- - PO_4^{3-}$, $I^- - SO_4^{2-}$, $Br^- - Cl^-$, $SO_4^{2-} - SO_3^{2-}$; AS9SC column) significant changes of separation factors α and the resolution R_s have been observed (Table). Sometimes, appropriate changes of α and R_s enabled better separation of chosen ion-pair at elevated or lowered temperature than at the ambient.

The values of standard thermodynamic functions (ΔH, ΔS and ΔG) for ion exchange reactions were calculated for the temperature range investigated.

References

[1]. Dybczyński R.: Anal. Chim. Acta, 29, 369-372 (1963).
[2]. Dybczyński R.: J. Chromatogr., 14, 79-96 (1964).
[3]. Dybczyński R.: J. Chromatogr., 13, 155-170 (1967).
[4]. Snyder L.R.: J. Chromatogr., 179, 167-172 (1979).
[5]. Melander W.R., Bor-Kuan C., Horvath C.J.: J. Chromatogr., 185, 99-109 (1979).
[6]. Głód B., Alexander P.W., Zu L.C., Haddad P.R.: Anal. Chim. Acta, 306, 267-272 (1995).
[7]. Terweij-Groen C.P., Kraak J.C.: J. Chromatogr., 138, 245 (1977).
[8]. Lammers N., Zeeman J., de Jong G.J.: J. High Resolut. Chromatogr. and Chromatogr. Comm., 4, 444 (1981).
[9]. Inno K., Hirata Y.: J. High Resolut. Chromatogr. and Chromatogr. Comm., 5, 85 (1982).
[10]. Baba Y., Yoza N., Ohashi S.: J. Chromatogr., 348, 27-37 (1985).
[11]. Fortier E., Fritz J.S.: Talanta, 34, 4, 415-418 (1987).
[12]. Hatsis P., Lucy C.A.: J. Chromatogr., 920, 3-11 (2001).
[13]. Hatsis P., Lucy C.A.: Analyst, 126, 2113-2119 (2001).
[14]. Paull B., Bashir W.: Analyst, 128, 335-344 (2003).
[15]. Dybczyński R., Kulisa K.: Chromatographia, 57, 475-484 (2003).

SPECIATION ANALYSIS OF INORGANIC ARSENIC AND ANTIMONY IN MINERAL WATERS AND SALINAS BY ATOMIC ABSORPTION SPECTROMETRY AFTER SEPARATION ON THE THIONALIDE SORBENT

Jadwiga Chwastowska, Witold Skwara, Elżbieta Sterlińska, Jakub Dudek, Leon Pszonicki

Arsenic and antimony belong to strongly toxic elements and their presence in the environment and, particularly, in the food and healing products are limited at a very low concentration level. Moreover, the toxicity of these elements is dependent on their oxidation stage, As(III) is more toxic than As(V). The toxicity distribution and the physiological behaviour of Sb(III) and Sb(V) are less known as those for arsenic, however, one assumes they are similar [1]. The inorganic species of As(III) and As(V) are most abundant in waters. They may be partially detoxified by the biological activity and transformed into organoarsenic compounds, however, their concentration is at an ultratrace level and in most cases they are undetectable [2]. Various analytical methods are used for speciation analysis of these elements at a trace concentration level, as it is mentioned for antimony in the review

of Smichowski *et al*. [3]. Mass spectrometry with inductively coupled plasma ionisation (ICP-MS) hyphenated with hydride generation technique is considered as the most satisfactory detection system for these elements. A shortcoming of the ICP-MS method is the expensive equipment and relatively high cost of its exploitation. Therefore, its application is economically justified only in laboratories making continuously a large number of determinations. Many authors used atomic absorption spectrometry (AAS) with various types of atomisation after preliminary separation and preconcentration of analytes [4-8].

The aim of the presented work was to elaborate a method for speciation analysis of arsenic and antimony in mineral waters and in salinas used in medicine and in industry. In this method, As(III) and Sb(III) are separated from a sample and determined by graphite furnace AAS (GF AAS). The total amounts of arsenic and antimony are determined directly in the sample by hydride generation AAS (HG AAS). The concentrations of As(V) and Sb(V) are calculated as the difference between these two results.

In the speciation analysis, the chelating sorbents are used very often for separation and preconcentration of trace elements. They are able, under carefully selected conditions, to react only with one form of the chosen element. The sorbents with thiol groups show particularly large affinity to the heavy elements. Therefore, the sorbents obtained by fixation on the solid polymeric bed such reagents as dithizone, dithiocarbaminates and thionalide are used for quantitative sorption of trace elements from various types of waters. We have prepared and tested the sorbents with thionalide and with the thiocarbaminates of ammonium, sodium and zinc. The thionalide sorbent was found to be most effective.

The preparation of the thionalide sorbent and its analytical properties were described previously [9]. Now, we estimated its sorption efficiency of As(III) and Sb(III) as a function of the solution acidity, amount of sorbent in the column, optimum flow rate, type and amount of eluent and the separation effectiveness of As(III) from As(V) and of Sb(III) from Sb(V). For a 100 ml analytical sample the following parameters of the separation process were found as optimal: 1.5 M hydrochloric acid solution, column diameter – 0.4 cm, amount of sorbent – 0.2 g, flow rate – 0.8 ml·min^{-1} and 10 ml of acetone used as eluent. The quality of the simultaneous separation of As(III) and Sb(III) from As(V) and Sb(V) and from the matrix elements was tested on the basis of the synthetic water similar in composition to the natural one with the addition of known amounts of both the elements. The recovery in the eluent solution of As(III) was in the range 92-96% and of Sb(III) in the range 98-100%. The presence of As(V) and Sb(V) in the test solution does not affect the results obtained for both the elements on the oxidation stage (III). It indicates that only the elements in the oxidation stage (III) are present in the eluent, *i.e*. both the forms of the elements to be determined are very good separated.

Magnesium in 1 M nitric acid solution, used as modifier, was added into the acetone effluent from the column in such amount that its concentration in the final solution was equal to 300 μm·ml^{-1}. In this solution, As(III) and Sb(III) were determined by GF AAS in the graphite tube with pyrolytic platform using Smith-Hieftje non-specific absorbance correction. The parameters of the atomisation and measurement processes are given in Table. The low detection limit of the determinations for the 100 ml sample is 0.3 μg·l^{-1} for both the elements and relative standard deviation (RDS) is equal to 5% (n = 5).

The total concentration of arsenic and antimony was determined directly from the analysed sample by continuous HG AAS using reduction by 1% $NaBH_4$ in 1% NaOH solution and the same spectral lines as those given in Table. The low detection limit of these determinations is 0.5 μg·l^{-1} for arsenic and 0.8 μg·l^{-1} for antimony. RSD for the determination of both the elements is equal to 3% (n = 5). The concentrations of As(V) and Sb(V) is calculated as the difference between the total concentrations and the concentrations of As(III) and Sb(III).

Table. Atomisation parameters used in the GF AAS determinations.

Element	Spectral line [nm]	Pyrolysis temperature [°C]	Atomisation temperature [°C]
As	193.7	800	2400
Sb	217.6	800	2200

The described method was applied for the analysis of various mineral waters and salinas used for therapeutic purposes.

References

[1]. Mok W.M., Wai C.M.: Anal. Chem., 59, 233 (1987).
[2]. Munoz O., Velez D., Montoro R., Arroyo A., Zamorano M.: J. Anal. At. Spectrom., 15, 711 (2000).
[3]. Smichowski P., Madrid Y., Camara C.: Fresenius J. Anal. Chem., 360, 623 (1998).
[4]. Garboś S., Bulska E., Hulanicki A.: At. Spectrosc., 21, 128 (2000).
[5]. Elsayed M., Björn E., Frech W.: J. Anal. At. Spectrom., 15, 697 (2000).
[6]. Marlon de Morales Flores E., Pereira dos Santos E., Barin J.S., Zanella R., Dressler V.L., Bittencourt C.F.: J. Anal. At. Spectrom., 17, 819 (2002).
[7]. Chamsaz M., Arbab-Zavar M.H., Nazari S.: J. Anal. At. Spectrom., 18, 1279 (2003).
[8]. Sayago R., Recamales M.A.F., Gomez-Ariza J.L.: J. Anal. At. Spectrom., 17, 1400 (2002).
[9]. Chwastowska J., Żmijewska W., Sterlińska E.: Anal. Chim. Acta, 276, 265 (1993).

ANALYSIS OF SOME METALLIC ALLOYS USING STANDARDLESS X-RAY FLUORESCENCE SPECTROMETRY

Józef L. Parus[1/], Wolfgang Raab[2/], Joachim Kierzek

[1/] Radioisotope Centre POLATOM, Świerk, Poland

[2/] International Atomic Energy Agency, Vienna, Austria

Wave-length X-ray spectrometry (WDXRF) is a very powerful method for the quantitative elemental composition analysis. The main advantage of this method is a wide range of the analysed elements and the relative freedom from spectral inteferences. Nowadays, there are available software packages enabling a fast semiquantitative analysis with a minimum effort used for calibra-

Table. Certified and determined by WDXRF composition of 13 metallic reference materials.

Element	Concentration [%]									
	Certified value	WDXRF	Certified value	WDXRF	Certified value	WDXRF	Certified value	WDXRF	Certified value	WDXRF
	Solder-Silver LTS-33X		Solder Tin/Lead TL-11X		Solder Tin/Lead TLSB-3		Solder Tin/Silver TS-4X			
Cu	0.073	0.106	0.0078				0.10	0.12		
Ag	2.86	3.01	0.010		0.13	0.17	4.0	4.1		
Cd			0.092		0.13	0.15				
Sn	8.88	10.46	11.62	13.88	48	53.80	***95.60***	95.38		
Sb	0.21	0.19	0.21	0.20	0.68	0.68	0.13	0.09		
Pb	***87.97***	85.94	***88.16***	85.34	***50.58***	44.39	0.043	0.11		
Bi	0.0072		0.034	0.041	0.48	0.45	0.10	0.10		
	High speed steel JSS 608-5		High speed steel SS 483		Nickel-chromium steel 8001 A		Gunmetal BNF C71X10		Phosphor bronze 554	
Al					0.50	0.42	0.005		0.005	
Si	0.277	0.21	0.11	0.12	0.11		0.005		0.038	
P	0.0129		0.019				0.015		0.41	0.57
V	1.196	1.30	0.54	0.59						
Cr	4.062	4.27	3.31	3.42	20.24	21.07				
Mn	0.312	0.34	0.29	0.31	1.12	1.09	0.043	0.040		
Fe	***66.56***	66.74	***82.23***	81.63	***44.93***	44.28	0.044	0.047	0.022	0.019
Co	9.186	9.09	1.94	1.94	1.01	0.99				
Ni	0.0545			0.134	31.0	30.81	2.1	2.19	0.22	0.0223
Cu	0.0320			0.123	0.055	0.087	***83.81***	85.94	87.40	87.37
Zn							4.0	3.78	0.22	0.22
Mo	0.564	0.516	0.17	0.15	0.48	0.444				
W	16.944	17.47	10.8	11.45						
Sn				0.036			3.8	3.74	11.3	11.11
Sb				0.016			0.057	0.045		
Pb							6.0	3.94	0.34	0.27
Bi							0.056	0.037		
	Ni-Co-Cr alloy W901		Ni-Co-Cr alloy W1055		Nickel alloy BS 500B		Titanium alloy Ti 685			
Mg	0.018		0.028	0.037	0.020	0.029				
Al	1.52	1.04	4.71	4.08	2.87	2.28	6.25	5.96		
Si	0.52	0.39	0.54	0.37	0.10		0.23	0.04		
Ti	2.24	2.36	1.01	1.04	0.50	0.53	***87.98***	88.18		
Cr	20.9	20.91	16.25	16.39	0.08	0.088				
Mn	0.57	0.59	0.22	0.24	0.66	0.72				
Fe	0.61	0.60	0.60	0.61	1.19	1.19	0.036	0.035		
Co	17.10	16.85	18.9	18.90	0.08	0.072				
Ni	***55.96***	56.76	***52.91***	53.77	64.21	65.27				
Cu	0.11	0.11	0.10	0.13	30.11	29.75				
Mo	0.27	0.20	4.48	4.26	(0.03)	0.008	0.53	0.52		
Zr							4.98	5.11		

tion. The well-known suppliers of X-ray wave-length dispersive spectrometers usually offer a package for the semiquantitative X-ray analysis. One of such packages is the Uniquant developed by W. de Jongh [1, 2] formerly a coworker of Philips. We tested the performance of the Uniquant IV for analysis of samples of various types.

Uniquant is a computer program for a semiquantitative analysis of elements in the atomic number range from fluorine (Z = 9) to uranium (Z = 92). It is calibrated before use with pure elements (metal foils) or simple compounds in the form of discs. Based on the measured intensities of analytical lines, the program calculates the coefficients of calibration curves corrected by influence factors of 5 selected elements disturbing the linearity of calibration curves. These corrections can be adjusted for a particular type of samples. The sample itself can be a solid disc, a piece of metal having a flat surface or a powder filling a well-defined part of the circle. The sample area must be defined before the measurement eventually together with the undetermined part of sample when only some elements are to be analyzed.

The characteristic X-ray intensities of all elements (Z from 9 to 92) are measured using the LiF 220, Ge 111 and TIAP crystals. The background is also measured in 5 points to determine the shape of the continuum under analytical lines. The measurement time for each line is equal to about 10 s. The total measurement time is about 20 min and the total analysis time is less than 25 min for a completely unknown sample. We selected 13 certified metallic reference materials in form of discs each of at least 28 mm diameter. The discs were only washed with ethanol before the measurement. All measurements were carried out on the Philips 1480 sequential X-ray spectrometer in vacuum using a 6-position sample changer. It is equipped with a Rh-target tube.

The results of analysis are shown in Table. The certified and calculated from Uniquant the percent contents of element are put together. The results in italics are the difference obtained by subtraction from 100% the sum of all certified elements. The materials measured are of a very different composition and can be grouped as follows: lead solder alloys (3), tin-silver alloy (1), high speed steels (2), bronses (2), nickel alloys (4), titanium alloy (1). Only the results for lead and tin (3 samples) are unsatisfactory. The lead content is too high and tin too low. The sum of both elements is close to the certified values. The source of discrepansies can be twofold: 1) the calibration function for lead is wrong (too low the calibration curve slope) or 2) the surface of calibration standard is enriched in lead due the smearing properties of this element. This problem should be studied in more detail. The results for the rest of samples of a very different composition are rather satisfactory. Particularly the results for many minor elements of all samples are good. Only in the case of the very light elements (magnesium to sulfur) the determination limit is above 0.1%. For the heavier elements it is at the level of about 0.05%.

It can be concluded that the Uniquant program is a very useful tool for a fast and sufficiently accurate analysis of multielement metallic samples. Any prior information about the qualitative sample composition is not required although the knowledge of the matrix when it is composed from very light elements (Z from 1 to 8) can be helpful (for example, boron or beryllium oxides, hydrated compounds).

References

[1]. de Jongh W.K.: X-Ray Spectrom., 2, 151 (1973).
[2]. de Jongh W.K.: X-Ray Spectrom., 8, 52 (1979).

LEAD IN CENTRAL EUROPEAN 18th CENTURY COLOURLESS VESSEL GLASS

Jerzy J. Kunicki-Goldfinger, Joachim Kierzek, Aleksandra J. Kasprzak[1/], Piotr Dzierżanowski[2/], Bożena Małożewska-Bućko, Anna Misiak

[1/] National Museum in Warsaw, Poland
[2/] Faculty of Geology, Warsaw University, Poland

The introduction of lead compounds as the separate raw materials to the batches for colourless vessel glass have been known, with only a few exceptions, since the second half of the 17th century.

Since 1998, over 1000 glass items originated from the 17th-20th centuries have been examined by the use of energy dispersive X-ray fluorescence (EDXRF) [1-3]. Most of them were originated from the 18th century central European glasshouses and were colourless, glass vessels. Selected group of them was also analysed by the electron probe microanalysis (EPMA). As for the last method, a detection limit for PbO was 0.043%.

Twenty two glasses that contained PbO in the range of ~22-30% have been found among the examined items. This group covered mainly objects that had been attributed to German, Polish or Russian glass centres. This PbO concentration range as well as the level of remaining glass constituents was found to be consistent with English lead glass characteristics.

Among all remaining 18th century colourless glass objects, the highest PbO content (~13%) has been enclosed in the case of a medallion with portrait of Augustus III, the King of Poland, which was glued to a goblet (1 half of 18th century, Dresden or Naliboki). The goblet glass contained ~8%

Table. Composition of 18th century central European glass, analysed using EPMA [wt%].

1	2	3	4	5	6	7	8	9	10	11	12	13
Object	Altmünden *c.* 1720 Goblet	Dresden *c.* 1740 Goblet	Germany 1st half of 18th century Plaque	Zechlin *c.* 1740 Goblet	Zechlin *c.* 1740 Goblet	Zechlin *c.* 1738-47 Goblet	Naliboki *c.* 1740 Goblet	Naliboki *c.* 1740 Flute	Naliboki *c.* 1740 Goblet	Lauenstein 2nd half of 18th century Goblet	Naliboki *c.* 1790 Goblet	Bohemia 1st half of 18th century Lid
Museum	National Museum in Wrocław	National Museum in Warsaw	National Museum in Wrocław	Museum Palace Wilanów	National Museum in Wrocław	Museum Palace Wilanów	National Museum in Warsaw	Museum Palace Wilanów	National Museum in Wrocław	National Museum in Warsaw	National Museum in Warsaw	National Museum in Poznań
Inv. No.	II.811	23.222	II.340	Wil 74a	1473	Wil 49	211599	Wil 3540	II.249	SZSmag82	34066/3	Rz 1245/2
SiO_2	72.88	66.38	69.50	76.77	75.22	76.78	70.04	68.85	69.31	75.57	67.49	73.15
Al_2O_3	0.15	< 0.11	0.11	< 0.11	0.20	< 0.11	0.92	0.73	0.73	0.23	0.94	0.31
Na_2O	0.18	0.53	< 0.14	0.43	0.44	0.50	< 0.14	< 0.14	< 0.14	1.89	0.99	0.55
K_2O	16.43	15.42	20.17	14.66	16.11	15.10	19.69	20.50	20.79	12.29	18.11	14.17
CaO	0.39	5.10	3.42	2.10	3.05	2.21	4.78	5.32	5.24	7.50	9.34	9.48
MgO	< 0.17	< 0.17	< 0.17	< 0.17	< 0.17	< 0.17	< 0.17	< 0.17	< 0.17	< 0.17	0.24	< 0.17
As_2O_3	1.26	2.41	2.57	2.27	1.99	1.67	1.84	1.81	1.67	0.77	0.86	1.21
PbO	**9.48**	**8.91**	**5.73**	**2.70**	**2.63**	**2.27**	**2.09**	**2.01**	**1.85**	**0.99**	**0.44**	**0.36**
MnO	0.05	0.03	0.07	0.06	0.05	0.05	0.12	0.12	0.14	0.06	0.48	0.05
B_2O_3	< 0.4	0.63	< 0.4	0.76	0.34	0.40	< 0.4	< 0.4	< 0.4	< 0.4	< 0.4	< 0.4
Cl	< 0.18	0.38	< 0.18	<0.18	< 0.18	< 0.18	< 0.18	< 0.18	< 0.18	0.22	< 0.18	< 0.18
BaO	< 0.04	< 0.04	< 0.04	< 0.04	< 0.04	< 0.04	0.02	< 0.04	0.02	< 0.04	0.03	< 0.04
Fe_2O_3	0.07	0.08	0.04	< 0.03	0.04	0.03	0.19	0.13	0.12	0.07	0.13	0.04
TiO_2	0.08	< 0.02	0.04	0.09	0.12	0.07	0.08	0.07	0.07	0.03	0.06	0.04
SrO	0.02	0.04	0.03	0.04	0.04	0.03	0.02	0.03	0.03	0.02	0.03	0.04
ZrO_2	< 0.01	< 0.01	< 0.01	0.03	0.03	< 0.01	0.01	0.02	< 0.01	< 0.01	< 0.01	< 0.01
K_2O/CaO	42.3	3.0	5.9	7.0	5.3	6.8	4.1	3.9	4.0	1.6	1.9	1.5
As_2O_3/CaO	3.2	0.5	0.8	1.1	0.7	0.8	0.4	0.3	0.3	0.1	0.1	0.1

For all samples: $P_2O_5 < 0.4$, $SO_3 < 0.4$, $Sb_2O_3 < 0.02$, CuO < 0.03, $Rb_2O < 0.08$, $Y_2O_3 < 0.04$, ZnO < 0.04.

PbO. Also ~8% PbO has been found in the case of another similar medallion.

Bearing in mind only vessels, the highest PbO level (~11%) has been found in a Saxon goblet from *c*. 1720-1740. Considering lead variables in glasses that contain PbO < 11%, no evident further border levels of the element concentration, which could be associated with certain groups of ware regarding to their origin or dating, have appeared. To confirm this observation, technological studies according to the recipe used in each case were done. As regards to the 18th century glassware, provenance studies should be always proceeded by a glass technological interpretation. It was already emphasised in previous papers that chemical composition of the glasses melted according to different technology in one glasshouse might be more differentiated than chemical composition of glasses fabricated by the same (or similar) technology in different glasshouses. During the discussed period, three main technological types of vessel glass, which had not been coloured intentionally, occurred (ordinary, white and crystal). Differentiating of crystal glasses made in certain glasshouses has been found not to be difficult if their chemical composition would have been known. Not always was it possible considering white glasses and nearly impossible regarding ordinary glasses. Therefore, beside the familiarity with the basis glass composition that reflects recipe used, the knowledge about the levels of certain minor and trace elements (e.g. Fe, Ba, Ti, Zr, Rb, Y, Sr) that were introduced to glass as the contamination of the raw materials, is essential for such deeper studies. Obviously, geochemical studies and archival surveys constitute necessary and supplementary approach to such provenance studies. In the course of the discussed project, all these steps were carried out. It allowed us to re-attribute part of the examined vessels, although the attribution of Baroque vessel glass frequently remains uncertain due to the lack of certain comparable fabric.

Significant lead content was found both among crystal and white glasses. The majority of examined crystal glass items contained lead and in the case of white glass, minority of the examined vessels did.

Thanks to the EDXRF results, all glasses that contained PbO > 0.1% were selected. This group covered 161 items, without English origin objects. Some of them were subjected to quantitative analysis by the use of EPMA. In Table, in the columns 2-10, the composition of a few different crystal glasses is shown. The composition of white glasses is given in the columns 11-13. Independently of the origin of items, crystal glass differs from white glass by the ratios of K_2O/CaO and As_2O_3/CaO. As for the crystal one, they amount to the higher values (respectively, > ~4 and > ~0.3). As for the white glass, they remain below ~2 and ~0.1, respectively. As a rule, PbO concentration is higher in the case of crystal glasses, although these sets of crystal and white glasses overlap considering lead content. Among the examined leaded crystal glasses, the PbO concentration exceeded ~0.4%. In the case of white glass, the value did not exceed ~2%. Therefore, it seems that lead concentration knowledge does not constitute a sufficient feature to differentiate leaded crystal and leaded white glass. The obtained results does not allow us to point out the border content of lead, that could help us to find out the white glasses, which contain lead only as a contamination. On the other hand, it seems possible to find this limit concentration of lead in the case of crystal glass, although for this purpose further studies are still required.

Among the glasses that contained PbO in the range ~7-11%, the majority of items were Saxon (Dresden) glasses. That group contained also a few objects of other attributions, among other the goblet (~11% PbO) engraved by F. Gondelach (*c*. 1710). The compositions of these glasses differed from the compositions of the examined ones, which were attributed to well known Saxon, Brandenburgian, Bohemian, Silesian, Polish, Lithuanian or Russian glass production centres. But their German provenance should be strongly considered.

The group of glasses that contain PbO < 6% covered the crystal of Zechlin, Potsdam and Naliboki origins, as well as one goblet manufactured in Lauenstein and an one-side engraved plaque of an unknown origin. Saxon glasses have been occurring exceptionally (their PbO contents were slightly over 2%), but their attribution was uncertain. Among the objects attributed to Bohemian and Silesian glass centres, a group of white glasses that contained lead (PbO < 1.5) has been also enclosed. Most of them were originated from the middle of the century.

Summing-up: it should be stressed that a significant amount of lead has been found only in part of all the examined glassware. Lead compounds as a raw material for the production of colourless vessel glass was introduced in central European glassmaking at the beginning of the 18th century. Then, its usage was restricted only to a few glass production centres.

References

[1]. Kunicki-Goldfinger J., Kierzek J., Kasprzak A., Małożewska-Bućko B.: Non destructive examination of 18th century glass vessels from central Europe. 6th International Conference on "Non-Destructive Testing and Microanalysis for the Diagnostics and Conservation of the Cultural and Environmental Heritage", Rome, Italy, 1999. AIPnd and ICR, Roma 1999, vol.II, pp.1539-1552.

[2]. Kunicki-Goldfinger J., Kierzek J., Kasprzak A., Małożewska-Bućko B.: X-Ray Spectrom., 29, 4, 310-316 (2000).

[3]. Kunicki-Goldfinger J., Kierzek J., Kasprzak A., Małożewska-Bućko B.: Analyses of 18th century central European colourless glass vessels. Annales du 15e Congrès de l'Association Internationale pour l'Histoire du Verre, New York – Corning 2001. AIHV, Nottingham 2003, pp.224-229.

INFLUENCE OF LOW-TEMPERATURE PLASMA DISCHARGE ON SURFACE PROPERTIES OF THIN PET FILM

Danuta Wawszczak, Wojciech Starosta, Marek Buczkowski, Bożena Sartowska

Low-temperature plasma can be a source of chemically active particles (excited or ionized molecules, radicals, metastable atoms) which are produced as a result of collisions of atoms or molecules with electrons and also with neutral particles. Nowadays, interest in practical application of plasma arrangements is becoming bigger and bigger. Such arrangements can be applied for manufacturing semiconducting or magnetic materials, introducing coatings, modification of physical and chemical properties of polymers [1-3]. Some works in the above last direction were undertaken in the Institute of Nuclear Chemistry and Technology a few years ago [4, 5].

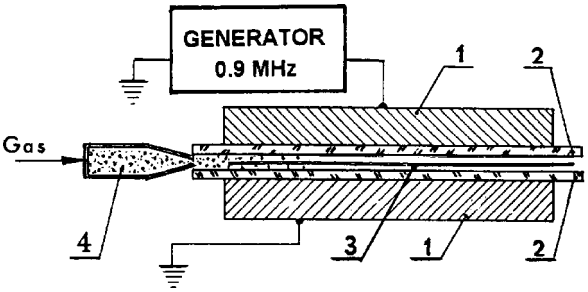

Fig.1. A scheme of the high frequency dielectric barrier discharge set-up: 1 – electrodes, 2 – dielectric plates, 3 – sample, 4 – nozzle.

In this work, results of low-temperature plasma modification of surface properties in case of a polyester (PET) film has been described. For such plasma modification, the PET film Estrofol ET type (produced by Nitron-Erg, Poland) 12 μm thick has been taken. Investigations have been aiming at:

- checking how wettability is changed after plasma treatment and what is the stability of such changes *vs*. storage time;
- checking if it is possible introducing polymer layers after plasma treatment (e.g. from aqueous solution of acrylic acid) on the film surface.

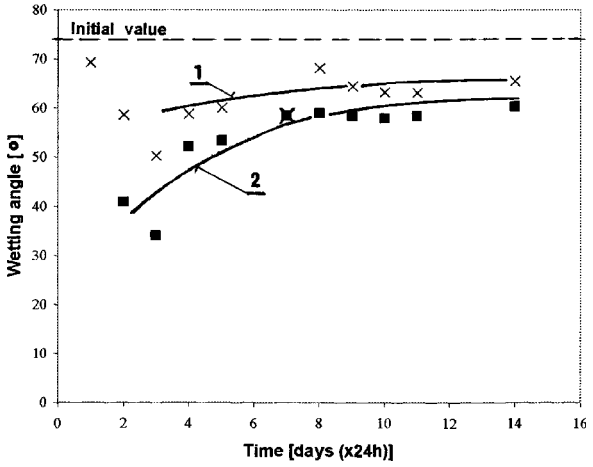

Fig.2. Wetting angle *vs*. storage time for PET film treated with argon plasma in high frequency barrier discharge (time of treating: 1 – 1 min; 2 – 5 min).

For plasma modification described above, high frequency dielectric barrier type discharge set-up has been designed and put into operation. This set-up can works under atmospheric pressure in a

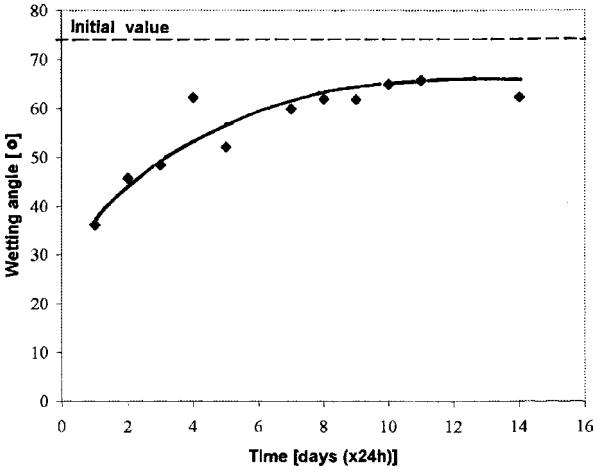

Fig.3. Wetting angle *vs*. storage time for PET film treated with helium plasma in high frequency barrier discharge (time of treating – 1 min).

gas flow regime. A scheme of the set-up is given in Fig.1. The set-up consist of two aluminium, planar electrodes (plates of 10x10 cm size each) on that alundum plates (1 mm thickness of each) are mounted. At both sides of these plates there are two narrow glass plates which give a slit of 1.5 mm. A sample of PET film was mounted between electrodes. Working gas was introduced to the slit and then high voltage discharge with frequency 0.9 MHz was generated.

For wettability determination, a method for measuring the slope of a small water drop from a micro-pipette on the film surface has been applied. As a result a wetting angle is obtained. Results of treatment of the PET film sample in argon plasma at different time (1 and 5 min) are given in Fig.2. Direct measurements after plasma treatment were

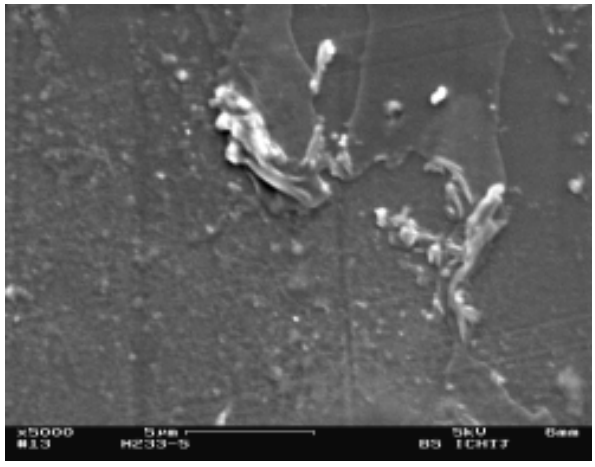

Fig.4. SEM photograph of acrylic acid layer on a PET film after high frequency plasma discharge with argon as working gas (magnification 5000x).

practically impossible because of very fast spreading of water drops. Values of wetting angle increase *vs*. storage time reaching stabilization after 10 days. After such storage time in comparison with initial value of wetting angle (74°), obtained results are following: 65° (decreasing by 12%) after 1 min of treatment and 60° (decreasing by 19%) after 5 min of treatment. Results for the same sample treatment in helium plasma are given in Fig.3. In this case for time treatment 1 min, the value of wetting angle after two days was lower than in case of argon plasma treatment but after 10 days of storage time, the stable values of wetting angle were similar.

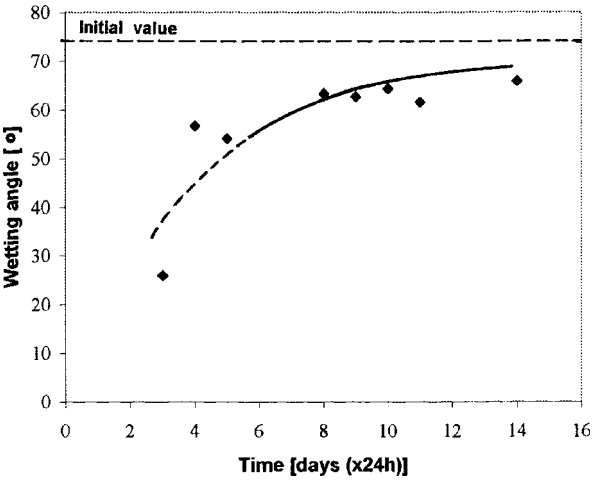

Fig.5. Wetting angle *vs*. storage time for PET film covered by acrylic acid layer after high frequency plasma discharge.

For determination of changes on the film surface after experiments with plasma coating of polymer layers, scanning electron microscopy – SEM (DSM 942 Zeiss-Leo type), method has been used. In Fig.4, the result of introducing acrylic acid on the surface of PET film is given. Working gas was argon with addition of acrylic acid vapours from aqueous solution. In this Fig., it is seen a plasma polymer layer on the film surface. The obtained layer was not satisfactorily uniform and homogeneous. Wetting angle after two days was rather small (about 40°) but after 10 days this value was equal to 67° (by 9% less than initial value), (Fig.5).

We can say that after helium or argon plasma treatment with high frequency (0.9 MHz) barrier discharge, the PET film samples become more hydrophilic. After 10 days the wetting angle reaches a stable value of 12 or 19% (depending on plasma treatment time) less than in the case of initial value. It is possible in the described set-up to obtain a polymer layer from a solution of acrylic acid, however, this method should be worked out in further investigations.

References

[1]. Jeong J., Park J., Henins I., Babayan S., Tu V., Selwyn G., Ding G., Hicks R.: J. Phys. Chem. A, 104, 8027-8032 (2000).
[2]. Nedelmann H., Weigel T., Hicke H.G., Muller J., Paul D.: Surf. Coat. Technol., 973-980 (1999).
[3]. Kunhardt E.E.: IEEE Trans. Plasma Sci., 28, 1, 189-200 (2000).
[4]. Starosta W., Buczkowski M., Sartowska B., Żółtowski T., Wawszczak D.: In: INCT Annual Report 2001. Institute of Nuclear Chemistry and Technology, Warszawa 2002, p.79.
[5]. Sartowska B., Buczkowski M., Starosta W.: Mater. Chem. Phys., 81, 352-355 (2003).

APPLICATION OF LOW-TEMPERATURE PLASMA AND RADIATION TREATMENT FOR CHANGING PROPERTIES OF POLYPROPYLENE MEMBRANES

Marek Buczkowski, Danuta Wawszczak, Wojciech Starosta, Bożena Sartowska

Polymer membranes are often being used as barriers in arrangements for electrochemical processes, which are important in galvanic cells or batteries. Using membranes for such purposes often requires modification of their surface and volume properties. This work has been focused on changing properties of polypropylene (PP) membranes that can be used as electrochemical separators in cells [1-3].

Samples of PP membranes (Celgard® type) have been treated with electrical discharge barrier type in a planar system in the atmosphere of different gases. A scheme of the applied set-up is given in Fig.1. This is two-electrode set-up: the lower electrode (2) is a duralumin plate on which there is a thin dielectric plate made of alundum (3); the upper electrode is a thin-walled stainless steel pipe (4) with a row on small holes through which flows working gas. This system of electrodes is in a casing made of plexiglass (5). High voltage pulses from

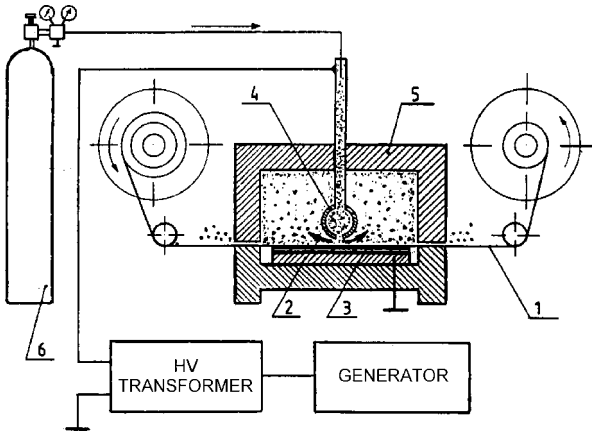

Fig.1. A scheme of the set-up for surface treatment of polymer membranes or films with barrier discharge: 1 – strip of polymer membrane, 2 – lower electrode, 3 – alundum dielectric plate, 4 – upper electrode, 5 – plexiglass casing, 6 – gas cylinder.

a transformer at a frequency of 0.25 kHz generate linear discharge between the upper electrode and dielectric surface in the atmosphere of working gas. In this volume, a strip of a membrane (1) is being moved by the system of rollers.

Table. Comparison of wetting angle for virgin film and after plasma treatment in different gases atmosphere.

Kind of working gas	Value of wetting angle
Without treating	99.4°
Ar	80.8°
Synthetic air	78.1°
O_2	76.5°
N_2	61.3°

Within the confines of experiments, discharges have been made in the atmosphere of such working gases as: Ar, synthetic air, O_2, N_2. After double-side discharge treatment of a strip of the membrane, a wetting angle was determined as a mean value of at least five measurements. Results of the above measurements are given in Table. In the second line of this Table, an initial value of wetting angle (99.4%) for Celgard® membrane without treatment is given. A scanning electron micro-

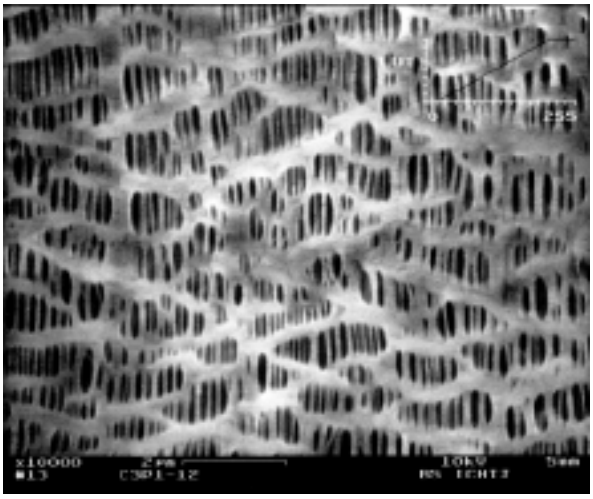

Fig.2. SEM photograph of initial PP Celgard® membrane surface (magnification 10 000x).

scope – SEM (DSM 942 Zeiss-Leo type) was used for checking membranes surfaces during experiments. A typical view of the initial membrane surface is given in Fig.2 and after plasma treatment (discharge in N_2) – in Fig.3. It is seen that practically there is no difference in the structure of the membrane after plasma treatment (seen in SEM photographs with magnification 10 000x).

In further experiments, samples of Celgard® membrane have been treated with swift electron beam from a linear accelerator of energy 10 MeV at the Department of Radiation Chemistry and Technology of the Insitute of Nuclear Chemistry and Technology. Two doses were applied: 40 and

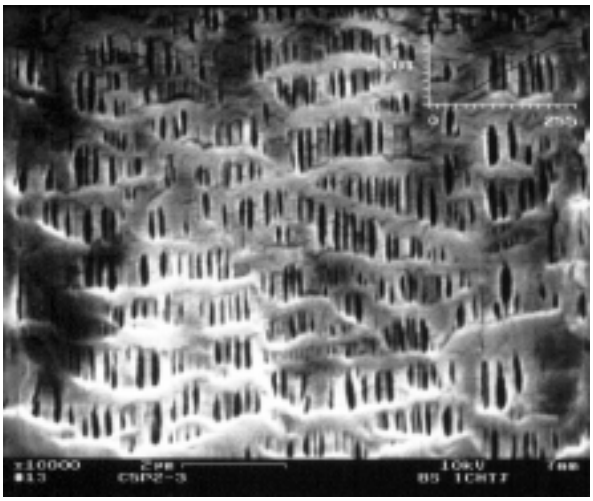

Fig.3. SEM photograph of PP Celgard® membrane surface after treatment with barrier discharge in N_2 atmosphere (magnification 10 000x).

70 kGy. For the first dose, the wetting angle was practically the same, for the higher dose – was equal to 91.9°. In both the above cases electrolytic resistance has been decreased significantly.

We can say that electrical barrier discharge under atmospheric pressure with different working gases as: Ar, synthetic air, O_2, N_2 improves hydrophilic properties of PP Celgard® membrane. The biggest decrease of the wetting angle (by 38%) was in the case of using N_2 as working gas.

Treatment PP Celgard® membrane with 10 MeV swift electron beam causes decrease of electrolytic resistance, which is profitable for the application of such membrane, and from the other hand – decreases mechanical strength. Choosing a proper dose of radiation treatment should be a compromise between two above effects.

References

[1]. Kawahara J., Nakano A., Kinoshita K., Harada Y., Tagami M., Tada M., Hayashi Y.: Plasma Sources Sci. Technol., 12, S80-S88 (2003).
[2]. Matsuyama H., Teramoto M., Hirai K.: J. Membr. Sci., 99, 139-147 (1995).
[3]. Lewis H., Jackson P., Salkind A., Danko T., Bell R.: J. Power Sources, 96, 128-132 (2001).

CARBONATE IMPURITIES REMOVAL FROM $LiNi_XCo_{1-X}O_2$ LAYERED OXIDES BY LOW-TEMPERATURE TREATMENT WITH NITRIC ACID AND HYDROGEN PEROXIDE

Andrzej Deptuła, Tadeusz Olczak, Wiesława Łada, Bożena Sartowska, Fausto Croce[1/], Angelo Di Bartolomeo[2/], Aldo Brignocchi[2/]

[1/] Department of Chemistry, University "La Sapienza", Rome, Italy

[2/] Italian Agency for the New Technologies, Energy and Environmental (ENEA), C.R.E. Casaccia, Rome, Italy

The layered oxides have received considerable attention as the positive electrode materials in high--energy density lithium and lithium-ion batteries. Within this frame $LiNiO_2$ and $LiCoO_2$ oxides and their solid solutions have been extensively studied, as they (and the $LiMn_2O_4$ spinels) are the only known materials able to intercalate reversibly lithium at high cell voltage (3.5-4 V). Recently, the solid solutions such as $LiNi_xCo_{1-x}O_2$ have attracted attention as alternative cathodes to the state of art $LiCoO_2$ in commercial rechargeable lithium-ion batteries. These materials are comparable in performances to $LiCoO_2$, however their cost is radically considerably lower [1]. The solid state reaction routes commonly utilized to synthesize this kind of materials have the drawback of the necessity of high-temperature synthesis. However, just Tarascon *et al*. [2, 3] produced finer particles of $LiNiO_2$ and $LiCoO_2$ with a higher cell capacity. Recently wet processing, especially various sol-gel procedures, have been used also for mixed $LiNi_xCo_{1-x}O_2$ layered oxides [4-7].

In our previously published works [4, 7, 8], we reported the preparation of the entire family of the mixed oxides $LiNi_xCo_{1-x}O_2$, in which x ranges from 0 to 1 by the Complex Sol-Gel Process (CSGP). The main feature in this process is application of a very strong complexing agent (ascorbic acid – ASC) for the preparation of sols. In all samples prepared with ASC we observed that thermal treatment of those gels is a very complex process, which involves foaming, self-ignition, and sometimes formation of the carbonates. Presence of the carbonates impurities is not surprising in samples prepared by organic precursors, but using similar techniques we synthesized carbonates free $LiCoO_2$ [8] and $Li_xMn_2O_{4\pm\delta}$ [9] exhibit very good electrochemical properties. Moderate results for the nickel containing layered oxides $LiNi_xCo_{1-x}O_2$ [8], are evidently connected with presence of the carbonates. It has been previously reported by some of the present authors that carbonates hinder the formation of High Temperature Superconductors [10]. In the above cited papers the description of a new processing (this proprietary procedure IChTJ has been patented [11]) is given for removal of the carbonates from ceramics by low-temperature treatment with nitric acid. We believe that this processing could be effectively applied for other systems.

In the present study, we have pursued the goal to try to apply this processing for decarbonization of the layered oxides $LiNi_xCo_{1-x}O_2$, synthesized using CSGP.

Table. Carbonates content ($\%CO_3$) of the samples.

Sample	$\%CO_3$	Sample characterization
$LiNiO_2$	15	very hard shard
$LiNiO_{0.75}Co_{0.25}O_2$	14	hard shard
$LiNiO_{0.5}Co_{0.5}O_2$	3	hard shard
$LiNiO_{0.25}Co_{0.75}O_2$	1	shard
$LiCoO_2$	0	powder

The CSGP, described in details in [8], we have used to prepare $LiNi_xCo_{1-x}O_2$ (x = 0, 0.25, 0.5, 0.75, 1). Briefly, the starting sols were prepared from xNi^{2+}; (1-x) Co^{2+}-acetate-ascorbic acid aqueous solutions by alkalizing with LiOH and ammonia. Gels after described in [8] thermal treatment in air atmosphere were finally heated for 24 h at 750°C. After careful milling, samples (generally 20 g) were placed in a Buchi RE 121 Rotavapor baker. To a sample concentrated nitric acid was carefully (~1 ml/min) sucked to reach pH = 1. Concentrated hydrogen peroxide was introduced in a similar way.

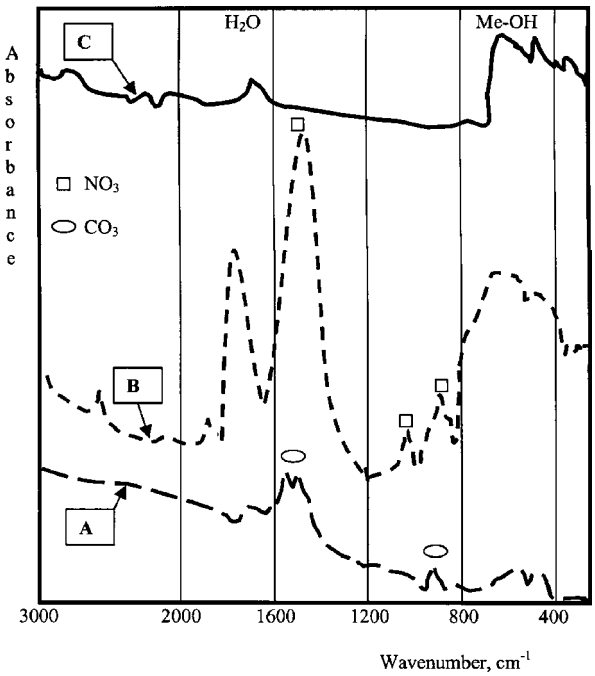

Fig.1. Infrared spectra of precursors for $LiNi_{0.75}Co_{0.25}O_2$ synthesis in various stages of processing: A – sample before treatment (Table); B – sample A after treatment with $HNO_3+H_2O_2$ and drying at 200°C for 24 h; C – sample B after final heating at 750°C for 1 h.

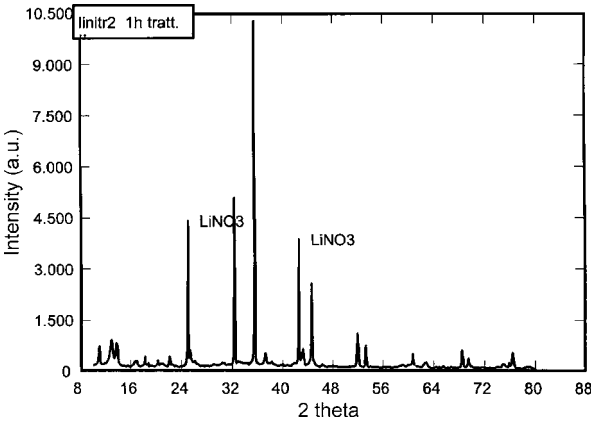

Fig.2. XRD of patterns of dried at 200°C gel $LiNio_{0.75}Co_{0.25}O_2$.

After evaporation to dryness under reduced pressure at 80°C, samples were transferred to a furnace and dried for 24 h at 200°C. The samples were then heated at a rate of 3°C/min to 750°C (soaked 1 or 24 h) with visual observation of the process. All thermal treatments were effectuated in a programmed Carbolite furnace type CSF 1200. The X-ray diffraction (XRD) measurements were taken by Cu K_α Philips Diffraction System and a scanning electron microscopy (SEM) measurements were taken by Zeiss DSM 942. The infrared (IR) measurements were effectuated by a Perkin Elmer Model 983 Spectrometer using the potassium bromide pellet technique. The carbonate concentrations were determined by the internal standardization [12] using sodium nitride and ν_2 carbonate bands at 875 cm^{-1}. This method, never used by other authors for similar materials, is very specific and accurate for carbonates determination.

The carbonate content and characterization of are shown in Table. The data confirmed our former

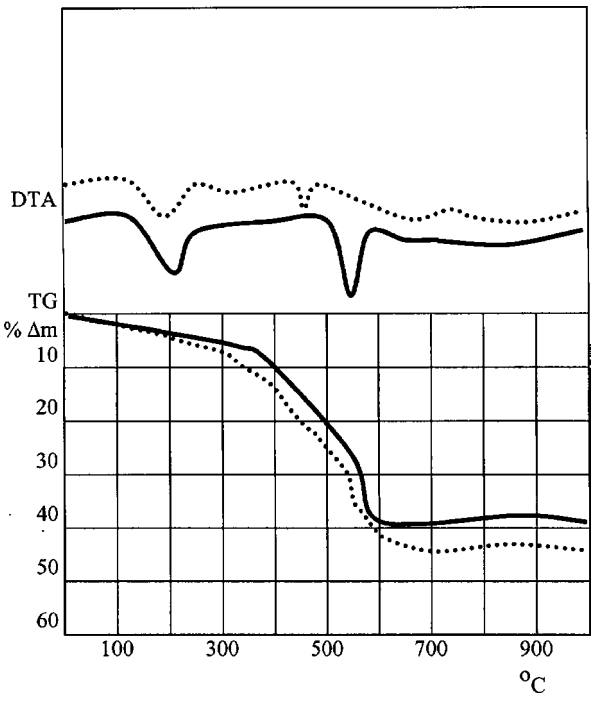

Fig.3. TG (thermogravimetry) and DTA (differential thermal analysis) traces of decarbonizated gels after drying for 24 h at 200°C: — $LiNi_{0.75}Co_{0.25}O_2$, $LiNiO_2$.

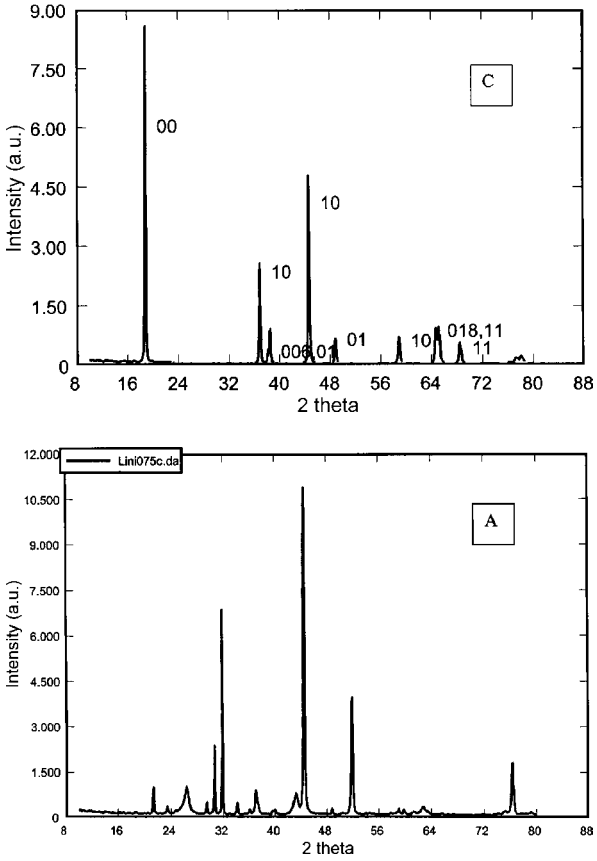

Fig.4. XRD patterns of $LiNi_{0.75}Co_{0.25}O_2$ samples before (A) and after (C) decarbonization.

observations [7, 8] that for materials containing nickel, very hard "shard" are formed due to sin-

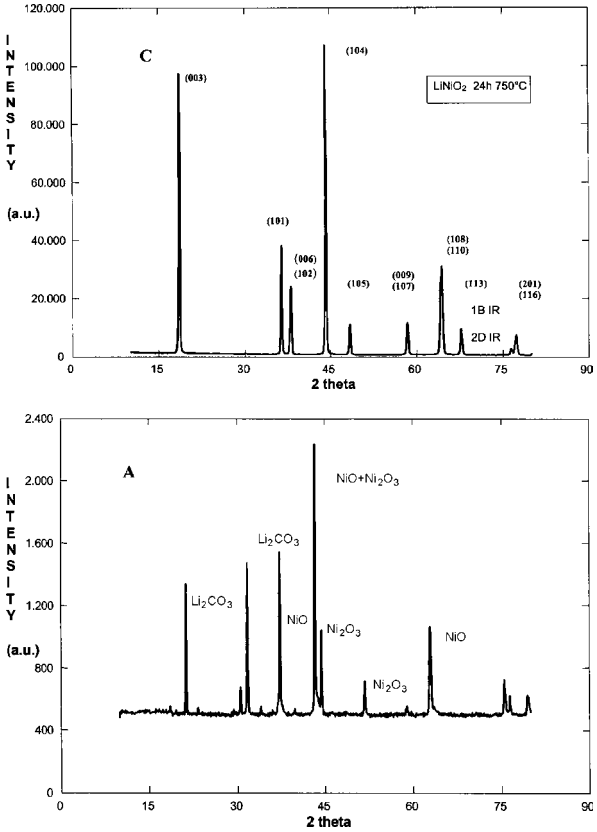

Fig.5. XRD patterns of $LiNiO_2$ samples before (A) and after (C) decarbonization.

tering, presumably with participation of the liquid phase of lithium carbonate. Pure $LiCoO_2$ sample in which lithium carbonate is not formed represents a free flowing powder.

For decarbonization we selected 2 first compositions indicated in that Table, with the highest carbon content. For attaining pH = 1 of the black slip, sufficient was the addition of approximately 1 ml of HNO_3/1 g of the sample. This value has been used, because evidently the carbonates are completely destroyed as can be observed in Fig.1, curve B. It has been observed that for lower acidity e.g. pH = 5, the decomposition of strong-bonded carbonates is incomplete.

The XRD of patterns of dried at 200°C gel $LiNiO_{0.75}Co_{0.25}O_2$ is shown in Fig.2.
From the presented data (IR and XRD) it can be noted that in gel significant quantities of nitrates are present.

Thermal decomposition of the dried gels (also $LiNiO_2$) is shown in Fig.3. The first endotherms correspond roughly to melting. During further heating intensive decompositions with evolution of gaseous bulbs in liquid was observed, followed by solidification at ~500°C. After final thermal treatment at 750°C, black soft cakes were formed. IR spectra (Fig.1, curve C) showed complete absence of carbonates. XRD patterns (Fig.4, curve C) indicated of the formation pure of perfect spinel phase. In Fig.4 (curve A) XRD pattern of "$LiNi_{0.75}Co_{0.25}O_2$" before processing indicates of the presence of many phases, e.g. Li_2CO_3, NiO, Ni_2O_3.

XRD patterns of $LiNiO_2$ sample as obtained by CSGP (curve A) and after processing (curve C) shown in Fig.5 evidently confirmed a high efficiency of the elaborated decarbonization process. It is necessary to underline that the pure nickel spinel is extremely difficult to be synthesized without using pure oxygen atmosphere. SEM micrographs of the above samples are shown in Fig.6. It is evident that before treatment the product is composed of large grains, despite long-term duration milling. After treatment fine powders are obtained.

Electrochemical properties, important for lithium-battery applications, were measured and detailed results will be presented elsewhere. It was found that for decarbonized samples their values are comparable with best those reported in the literature for layered oxides of similar compositions. In contrast, the samples before treatment exhibit very poor properties.

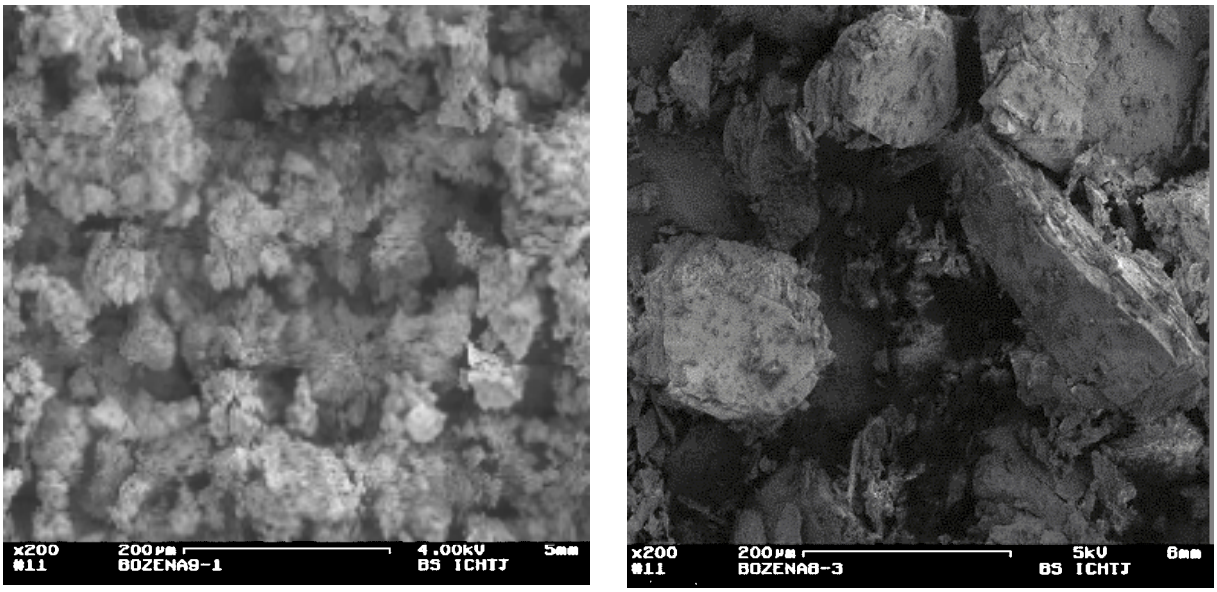

C A

Fig.6. SEM micrographs of $LiNiO_2$ samples before (A) and after (C) decarbonization.

References

[1]. Gover R., Kanno R., Mitchell B., Hirano A., Kawamoto Y.: J. Power Sources, 90, 82 (2000).
[2]. Tarascon J.M., McKinnon W.R., Coowar F., Bowmer T.N., Amatucci G., Guyomard D.: J. Electrochem. Soc., 141, 1421 (1994).
[3]. Barboux P., Tarascon J.M., Shokooh F.K.: J. Solid State Chem., 94, 185 (1991).
[4]. Deptuła A., Łada W., Olczak T., Croce F., Ronci F., Ciancia A., Giorgi L., Brignocchi A., Di Bartolomeo A.: Materials for Electrochemical Energy Storage and Conversion II – Batteries, Capacitors and Fuel Cells. Vol. 496. Eds. D.S. Ginley, D.H. Doughty, B. Scrosati. MRS Pittsburg 1998, p.237.
[5]. Kweon H.J., Kim G.B., Lim H.S., Nam S.S., Park D.G.: J. Power Sources, 83, 84 (1999).
[6]. Croce F., Deptuła A., Łada W., Marassi R., Olczak T., Ronci F.: Ionics, 3, 390 (1997).
[7]. Croce F., D'Epifanio A., Ronci F., Deptuła A., Łada W., Ciancia A., Di Bartolomeo A., Brignocchi A.: New Materials for Batteries and Fuel Cells. Vol. 575. Eds. D.H. Doughty, L.F. Nazar, M. Arakawa. MRS Pittsburgh 2000, p.97.
[8]. Deptuła A., Łada W., Olczak T., Croce F., D'Epifanio A., Di Bartolomeo A., Brignocchi A.: J. New Mater. Electrochem. Syst., 6, 39-44 (2003).
[9]. Deptuła A., Łada W., Croce F., Appetecchi G.B., Ciancia A., Giorgi L., Brignocchi A., Di Bartolomeo A.: New Materials for Fuel Cell and Modern Battery Systems. Eds. O. Savadogo, P.R. Roberge. Polytechnique de Montreal, Montreal 1997, p.732.
[10]. Deptuła A., Olczak T., Łada W., Goretta K.C., Di Bartolomeo A., Brignocchi A.: J. Mat. Res., 11, 1 (1996).

[11]. Deptuła A., Olczak T., Łada W.: Method for preparing of high temperature superconductors. Polish Patent No.168176.

[12]. Smith A.L.: Applied Infrared Spectrometry, Fundamentals, Techniques and Analytical Problem-Solving. John Wiley and Sons, New York 1979, p.251.

CRYSTAL CHEMISTRY OF COORDINATION COMPOUNDS WITH HETEROCYCLIC CARBOXYLATE LIGANDS. PART XLIV: THE CRYSTAL AND MOLECULAR STRUCTURE OF A CALCIUM(II) COMPLEX WITH PYRAZINE-2,6-DICARBOXYLATE AND WATER LIGANDS

Wojciech Starosta, Halina Ptasiewicz-Bąk, Janusz Leciejewicz

Dimeric units composed of two calcium(II) ions bridged by two carboxylate oxygen atoms each donated by a different ligand molecule have been recently discovered in a number of calcium complexes with pirydine and pyrazine dicarboxylate ligands. The dimers occur either as separate structural assemblies or, bridged by a pair of coordinated water oxygen atoms, form molecular ribbons. Recently, we came across single crystals of a novel calcium(II) complex with pyrazine-2,6-dicarboxylate and water ligands which, apart from solvation water molecules contains also free molecules of pyrazine-2,6-dicarboxylic acid molecules. The structure of {*catena*-[μ-aqua-O]bis[μ-pyrazine-2,6-dicarboxylato-O,N-O']}[diaqua-calcium(II)]}(pyrazine-2,6-dicarboxylic acid) dihydrate consists of dimeric units composed of two calcium(II) ions, two ligand molecules and six water molecules. The calcium ions are bridged by two bidentate oxygen atoms, each donated by one carboxylic group of the ligand. The calcium(II) ion is also coordinated by one oxygen atom of the second carboxylate group and the hetero-ring nitrogen atom belonging to the same ligand molecule. Both calcium ions in a dimer are bridged to the calcium(II) ions in adjacent dimers by a pair of water molecules forming infinite molecular ribbons. In addition, each calcium(II) ion is coordinated by three water molecules; one of them is used for bridging the adjacent dimer. The coordination polyhedron around the calcium(II) ion is a pentagonal bipyramid with two apices above and one apex below the equatorial plane. Six solvation water molecules and two molecules of pyrazine-2,6-dicarboxylic acid per unit cell interact *via* a system of hydrogen bonds with the molecular ribbons. A dimeric unit, three solvation water molecules and a molecule of the acid are shown in Fig.1. Figure 2 shows how they are oriented in respect to the unit cell.

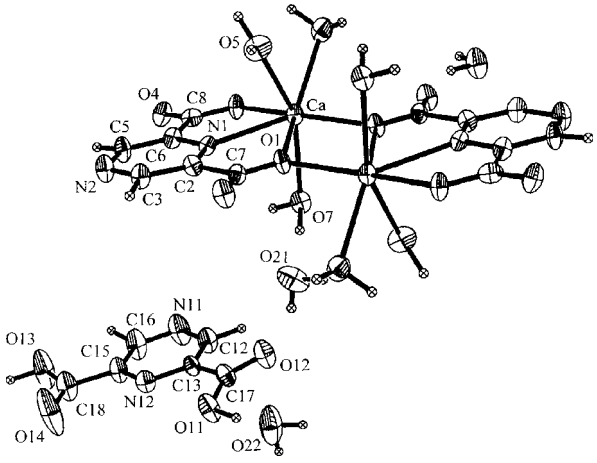

Fig.1. Dimeric structural unit, three solvation water molecules and a molecule of pyrazine-2,6-dicarboxylic acid with atom labelling scheme.

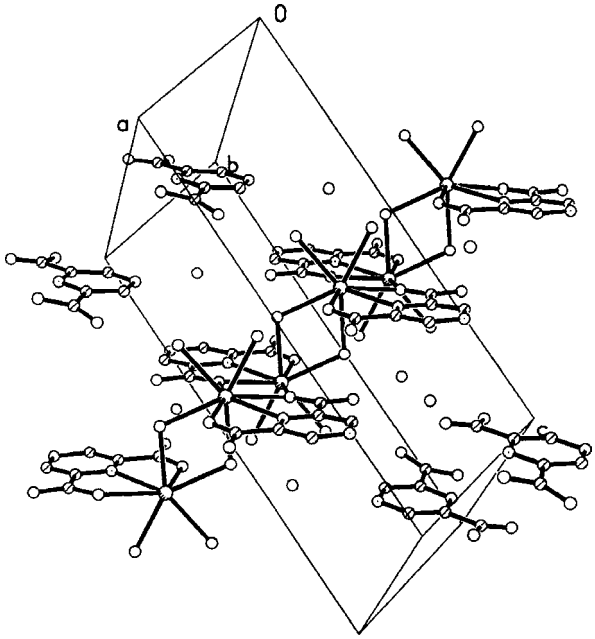

Fig.2. The alignment of molecules in respect to the unit cell.

X-ray diffraction measurements were carried out using the KUMA KM4 four circle diffractometer at this Institute. Structure solution and refinement was performed using SHELXL programme package.

References

[1]. Part XXXVII. Starosta W., Ptasiewicz-Bąk H., Leciejewicz J.: The crystal structure of an ionic calcium(II) complex with pyridine-3,5-dicarboxylate and water ligands. J. Coord. Chem., 56, 33 (2003).

[2]. Part XXXVIII. Ptasiewicz-Bąk H., Leciejewicz J.: The crystal structures of pyrazine-2,6-dicarboxylic acid dihydrate and hexaqua magnesium pyrazine-2,6-dicarboxylate. J. Coord. Chem., 56, 173 (2003).

[3]. Part XXXIX. Ptasiewicz-Bąk H., Leciejewicz J.: The crystal structure of a strontium(II) complex with pyrazine-2,6-dicarboxylate and water ligands. J. Coord. Chem., 56, 223 (2003).

[4]. Part XL. Starosta W., Ptasiewicz-Bąk H., Leciejewicz J.: The crystal structures of two calcium(II) complexes with pyrazine-2,6-dicarboxylate and water ligands. J. Coord. Chem., 56, 677 (2003).
[5]. Part XLI. Gryz M., Starosta W., Ptasiewicz-Bąk H., Leciejewicz J.: Crystal and molecular structure of pyridazine-3-carboxylic acid hydrochloride and zinc(II) pyridazine-3-carboxylate tetrahydrate. J. Coord. Chem., 55, 1505 (2003).
[6]. Part XLII. Gryz M., Starosta W., Ptasiewicz-Bąk H., Leciejewicz J.: Molecular chains in the structure of a zinc(II) complex with pyrazine-2,6-dicarboxylate and water ligands. J. Coord. Chem., 56, 1575 (2003).
[7]. Part XLIII. Ptasiewicz-Bąk H., Leciejewicz J., Premkumar T., Govindarajan S.: Crystal structure of a lanthanum(III) complex with pyrazine-2-carboxylate and water ligands. J. Coord. Chem., 57, 97 (2004).

CRYSTAL CHEMISTRY OF COORDINATION COMPOUNDS WITH HETEROCYCLIC CARBOXYLATE LIGANDS. PART XLV: THE CRYSTAL AND MOLECULAR STRUCTURE OF AN IONIC MAGNESIUM(II) COMPLEX WITH PYRIDAZINE-3,6-DICARBOXYLATE AND WATER LIGANDS

Michał Gryz[1/], **Wojciech Starosta, Janusz Leciejewicz**

[1/] Office for Medicinal Products, Medical Devices and Biocides, Warszawa, Poland

Two molecular patterns have up to now discovered in the structures of magnesium complexes with pyrazine dicarboxylate (PZDC) ligands: a polymeric structure observed in magnesium(II) complex with (2,3-PZDC) and water ligands and an ionic pattern detected in the complexes with (2,5-PZDC) and (2,6-PZDC) ligands. The structures of both latter compounds contain hexaqua magnesium cations $[Mg(H_2O)]_6^{2+}$ and $(2,5\text{-PZDC})^{2-}$ or $(2,6\text{-PZDC})^{2-}$ anions. A study of the magnesium complex with pyridazine-3,6-dicarboxylate ligand has been, therefore undertaken to find if the ionic structure is also characteristic of the above complex. Since the crystals obtained from aqueous (or methanol) solution of this complex turned out to be unsuitable for X-ray diffraction data collection, attempts have been made to improve their quality by adding to the solution small amounts of some other reagents such as urea or hydrazine. Well formed, colourless single crystals deposited after a couple of days from a solution to which few drops of hydrazine hydrate have been previously added.

The structure of the title compound is composed of $[Mg(PRDC)_2(H_2O)_2]^{2-}$ anions and $(H_3H{\cdot}NH_2)^{1+}$ cations. In addition, there are two solvation water molecules per unit cell. The magnesium(II) atom,

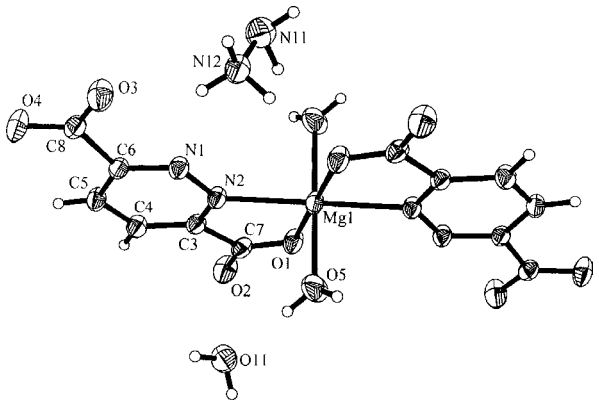

Fig.1. Atom labelling scheme in hydrogen hydrazine cation, zinc pyridazine-3,6-dicarboxylate anion and a solvation water molecule. Non-hydrogen atoms are shown as 50% elipsoids.

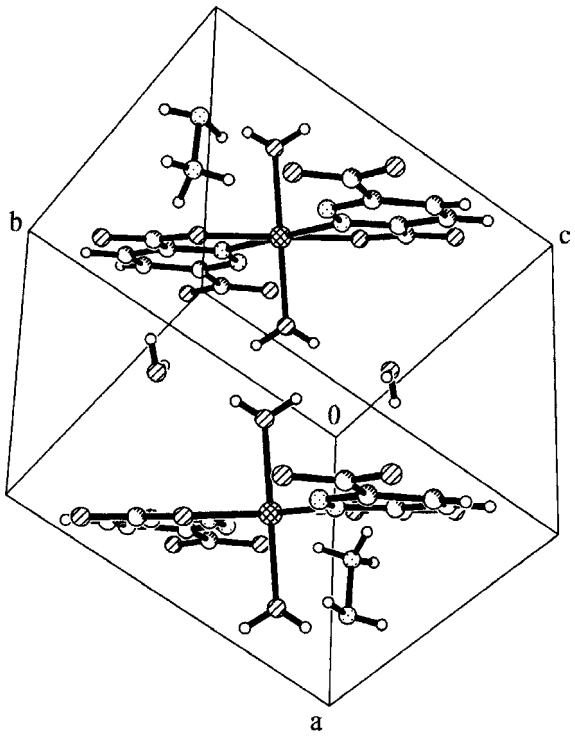

Fig.2. The packing diagram of di(hydrogen hydrazine) di(aqua-O)bis(pyridazine-3,6-dicarboxylato--N,O)zinc(II) dihydrate.

situated in the center of symmetry, coordinates two 3,6-PRDC ligands, each *via* the carboxylate oxygen atom and the nearest to it hetero-ring nitrogen atom. The second oxygen atoms of these carboxylate groups remain unengagged in coordination. The other carboxylate group of 3,6-PRDC ligands do not participate in any direct contact with the coordinated magnesium(II) atom. The atoms forming the pyrazine ring and both carboxylic groups are almost coplanar since the maximum shifts from the least squares plane range from +0.107 (the N2 atom) to -0.110 Å (the O2 atom). A carefull analysis of the Fourier maps did not indicate the presence of hydrogen atoms bonded to the carboxylate oxygen atoms. On the contrary, an additional

hydrogen atom attached to one of the hydrazine amino group was readily located. $(NH_3 \cdot NH_2)^{1+}$ cations were thus identified. Since there are two hydrazine molecules in a unit cell, the charge balance is mantained. Figure 1 shows an anion, a cation and a solvation water molecule with atom labelling scheme. Figure 2 shows the packing diagram of the title compound.

The hydrazine cation acts as a donor in the network of rather weak hydrogen bonds with the donor-acceptor distances around 3 Å. On the other hand, the hydrogen bonds in which solvation and coordination water molecules act as donors are stronger as indicated by the relevant bond distances falling in the range from 2.664(2) to 2.774(2) Å.

X-ray diffraction measurements were carried out using the KUMA KM4 four circle diffractometer at this Institute. Structure solution and refinement was performed using SHELXL programme package.

CRYSTAL CHEMISTRY OF COORDINATION COMPOUNDS WITH HETEROCYCLIC CARBOXYLATE LIGANDS. PART XLVI: THE CRYSTAL AND MOLECULAR STRUCTURE OF A ZINC(II) COMPLEX WITH PYRIDAZINE-3-CARBOXYLATE AND WATER LIGANDS

Michał Gryz[1/], **Wojciech Starosta, Janusz Leciejewicz**

[1/] Office for Medicinal Products, Medical Devices and Biocides, Warszawa, Poland

A novel zinc(II) complex with pyridazine-3-carboxylate and water ligands has been obtained accidently in the course of our studies on the structures of divalent metal compounds with diazine carboxylate ligands. In contrast to the triclinic structure of di(aqua-O)bis(pyridazine-3-carboxylato-N,O)zinc(II) dihydrate, the monoclinic crystals of the title compound do not contain solvation water molecules. The molecules of the title compound occur in the structure as monomeric units, each composed of a zinc(II) ion located in the centre of symmetry coordinated by two ligand molecules in trans planar position, both ligands chelating *via* the N,O bonding moieties. Two water oxygen atoms in the axial position complete a slightly distorted octahedron around the metal ion. This is illustrated in Fig.1 which shows also atom labelling scheme. The metal ion, and the pyridazine ring

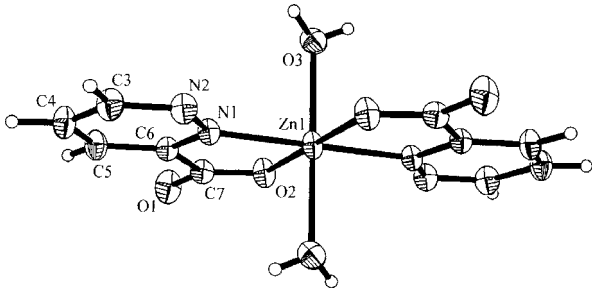

Fig.1. The molecule of $Zn(C_4N_2 \cdot COO)_2$ with atom labelling scheme.

carboxylate oxygen atoms in the adjacent monomers, as well as the coordinated water molecules and the hetero-ring nitrogen atoms.

X-ray diffraction measurements were carried out using the KUMA KM4 four circle diffractometer at this Institute. Structure solution and refinement was performed using SHELXL programme package.

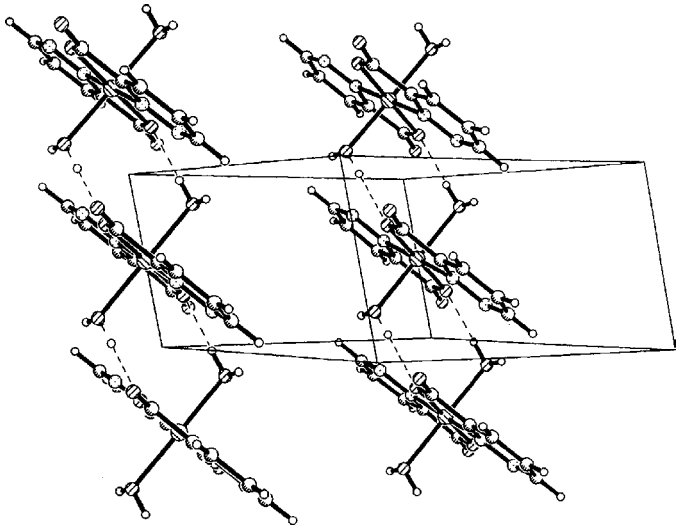

Fig.2. The packing of $Zn(C_4N_2 \cdot COO)_2$ molecules in the crystal.

and carboxylate atoms are almost planar. The packing diagram displayed in Fig.2 shows, how the monomers interact *via* hydrogen bonds which link the solvation water molecules with the uncoordinated

CRYSTAL CHEMISTRY OF COORDINATION COMPOUNDS WITH HETEROCYCLIC CARBOXYLATE LIGANDS. PART XLVII: THE CRYSTAL AND MOLECULAR STRUCTURE OF A THORIUM(IV) COMPLEX WITH PYRAZINE-2-CARBOXYLATE AND WATER LIGANDS

Thathan Premkumar[1/], Wojciech Starosta, Janusz Leciejewicz

[1/] Department of Chemistry, Bharathiar University, Coimbatore, Tamilnadu, India

In the course of our studies on the crystal chemistry of complexes with diazine carboxylate ligands (L) we have noticed that the compounds with the divalent 3d transition and alkaline earth metals (M) form always monomeric molecules $ML_2(H_2O)_n$ in which the coordination of the central ion proceeds *via* the N,O bonding moieties of two ligand molecules. Water oxygen atoms complete the characteristic for a particular ion coordination polyhedron. On the other hand, a polymeric molecular pattern has been discovered in the structure of lanthanum(III) complex with pyrazine-2-carboxylate and water ligands. Nothing has been known until now about the coordination modes occurring in the pyrazinates of tetravalent metals. Consequently, thorium pyrazinate has been synthetized, single crystals suitable for X-ray data collection grown and the structure of the complex determined.

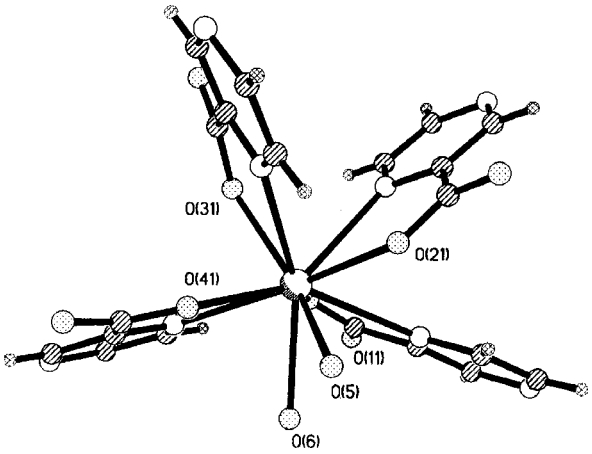

Fig.1. The molecule of thorium pyrazinate pentahydrate. Non-hydrogen atoms are dislpayed as 50% probability elipsoids.

The crystals of di(aqua-O)tetra(pyrazine-2-carboxylato-N,O)thorium(IV) trihydrate contain monomeric molecules composed of a thorium(IV) ion coordinated by N,O bonding moieties donated by four pyrazine-2-carboxylate ligands with mean Th-O bond distance of 2.390 Å and mean Th-N bond distance of 2.770 Å. Two water oxygen atoms with an average Th-O bond distance of 2.521 Å complete the number of coordinated atoms to ten. Figure 1 shows a monomer with non-hydrogen atoms displayed as 50% probability ellipsoids. Figure 2 shows the packing diagram of the structure. The coordination polyhedron around the thorium(IV) ion is a distorted hexadecahedron, shown in Fig.3. The monomers are held together by a network of moderately strong hydrogen bonds.

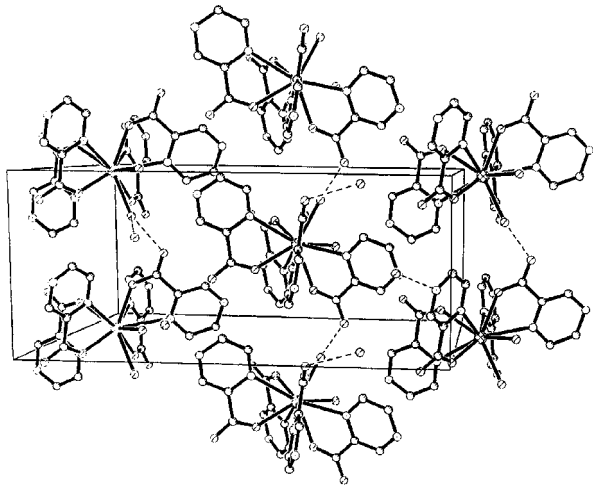

Fig.2. The packing diagram.

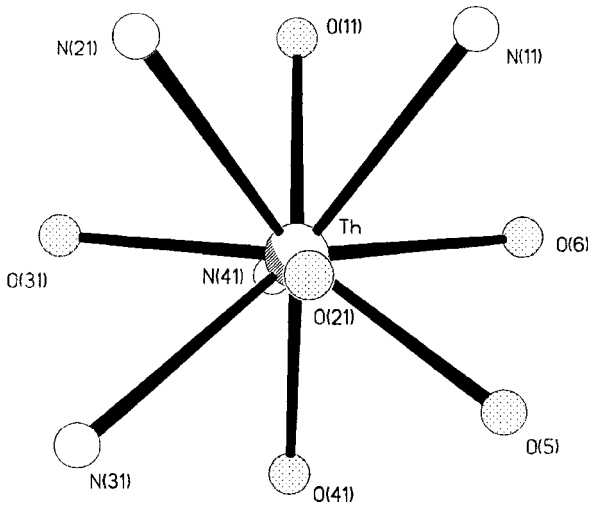

Fig.3. The coordination polyhedron of a thorium(IV) ion.

X-ray diffraction measurements were carried out using the KUMA KM4 four circle diffractometer at this Institute. Structure solution and refinement was performed using SHELXL programme package.

CRYSTAL CHEMISTRY OF COORDINATION COMPOUNDS WITH HETEROCYCLIC CARBOXYLATE LIGANDS. PART XLVIII: THE CRYSTAL AND MOLECULAR STRUCTURE OF AMMONIUM FUROATE

Beata Paluchowska[1/], **Jan K. Maurin**[1,2/], **Janusz Leciejewicz**

[1/] Institute of Atomic Energy, Świerk, Poland

[2/] National Institute of Public Health, Warszawa, Poland

Monoclinic crystals of ammonium furoate (furan-2-carboxylate) contain ammonium cations $(NH_4)^{1+}$ and furoate anions $(C_4H_2O{\cdot}COO)^{1-}$. The latter form molecular ribbons as displayed in Fig. The planes of furan rings of two adjacent anions are inclined by 40.5 deg each to other. Two anionic layers constitute a ribbon with the cations located between them. Each nitrogen atom of a cation interacts with four carboxylate oxygen atoms of the anions *via* rather weak hydrogen bonds directed towards the corners of a tetrahedron with N-H...O distances ranging from 2.77(5) to 2.88(5) Å. The ribbons are separated by a distance of 3.69 Å indicating weak van der Waals type interactions.

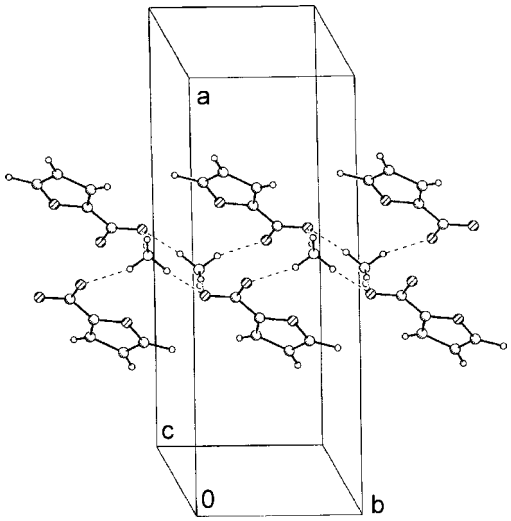

Fig. The structure of ammonium furoate – a fragment of the packing diagram. Broken lines indicate hydrogen bonds.

X-ray diffraction measurements were carried out using the KUMA KM4 four circle diffractometer at this Institute. Structure solution and refinement was performed using SHELXL programme package.

RADIOBIOLOGY

DIFFERENTIAL DNA DOUBLE STRAND BREAK FIXATION DEPENDENCE ON POLY(ADP-RIBOSYLATION) IN L5178Y AND CHO CELLS

Maria Wojewódzka, Barbara Sochanowicz, Irena Szumiel

L5178Y (LY) sublines, LY-R and LY-S, differ in response to combined treatment with poly(ADP-ribose) polymerase inhibitor, aminobenzamide (AB) and ionising radiation: 2 mM AB sensitises LY-S but not LY-R cells [1]. The high radiation sensitivity of LY-S cells is reasonably explained by deficiency in DNA double strand break (DSB) repair [2]. Since the rejoining of DNA breaks in LY-S cells is not sensitive to DNA-PK inhibitors [3], the high radiation sensitivity is likely due to the impaired function of nonhomologous end-joining (NHEJ).

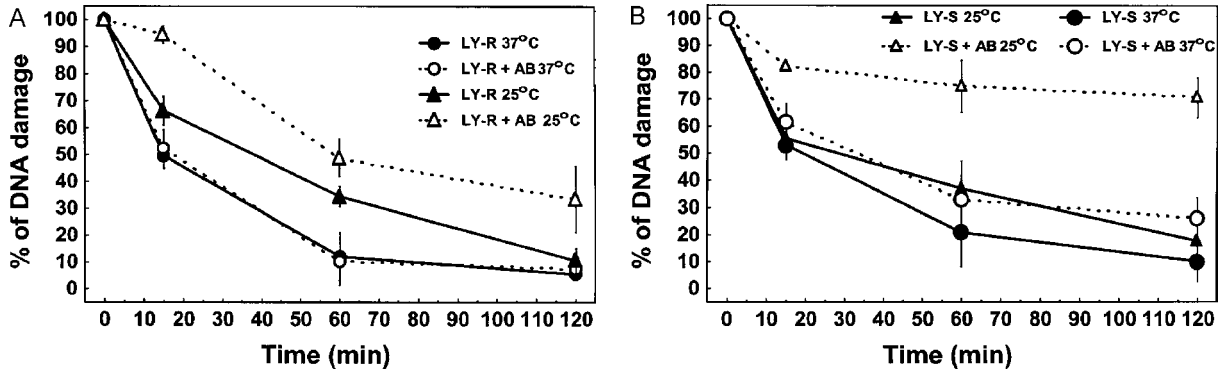

Fig.1. Temperature dependence of the course of DSB rejoining in the presence or absence of 2 mM AB in LY-R (A) and LY-S (B) cells. Irradiation at time 0 with 10 Gy X-rays. Post-irradiation incubation at 37 or 25°C. Mean results ± standard deviation from 3 experiments.

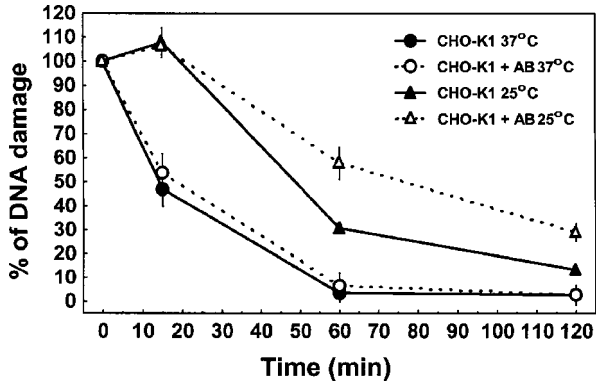

Fig.2. Temperature dependence of the course of DSB rejoining in the presence or absence of 2 mM AB in CHO cells. Irradiation at time 0 with 10 Gy X-rays. Post-irradiation incubation at 37 or 25°C. Mean results ± standard deviation from 3 experiments.

We investigated the role of poly(ADP-ribosylation) in DSB repair in L5178Y sublines, LY-R and LY-S, and a pair of CHO lines: wild type (WT) and mutant xrs6 cells. Cells (asynchronous, logarithmic phase) were incubated with 2 mM AB at 37°C for 2 h, X-irradiated with 10 Gy and allowed to repair DNA breaks for 15, 60 and 120 min at 37 or 25°C. The remaining DSB were estimated by the neutral comet assay.

At 37°C no effect of AB treatment on the repair kinetics was observed either in xrs6 or CHO (WT) cells. In contrast, AB inhibited the repair of DSB in LY-S line but not its parental LY-R line, in agreement with the previously observed sensitisation of LY-S cells to X-rays by poly(ADP-ribosylation) inhibition. However, DSB rejoining in the repair competent cell lines, CHO and LY-R, also was affected by AB when the post-irradiation incubation was carried out at 25°C (Figs.1A and 2). In LY-S cells the effect of AB is considerably enhanced in comparison to that at 37°C (Fig.1B).

Analysis of these results together with some earlier data on LY-S cells allowed to interpret these results in terms of Radford's [4] model of radiation damage fixation. The impaired repair of DNA breaks in LY-S results in a slow repair of a sector of DSBs (presumably in transcription factories). In the repair competent cell lines, slown down repair is achieved by incubation at 25°C. Then, fixation of DSB enhanced by poly(ADP-ribosylation) inhibition is revealed. The results indicate that poly(ADP-ribosylation) can be an important modulator of the conversion of DNA damage to lethal events.

References

[1]. Szumiel I., Wlodek D., Johanson K.J.: Acta Oncol., 27, 851-855 (1988).
[2]. Wlodek D., Hittelman W.N.: Radiat. Res., 112, 146-155 (1987).
[3]. Kruszewski M., Wojewodzka M., Iwanenko T., Szumiel I., Okuyama A.: Mutat. Res., 409, 31-36 (1998).
[4]. Radford I.R.: Int. J. Radiat. Biol., 78, 1081-1093 (2002).

CELL CYCLE PHASE DEPENDENT EFFECT OF 3-AMINOBENZAMIDE ON DNA DOUBLE STRAND BREAK REJOINING IN X-IRRADIATED CHO AND xrs6 CELLS

Maria Wojewódzka

Although the contribution of poly(ADP-ribose) polymerase-1 (PARP-1) (EC 2.4.2.30) to DNA repair was implicated, there were numerous discrepancies in the experimental data and the controversies remain in spite of a considerable progress in our understanding of the repair processes. PARP-null mice and cell lines were shown to be hypersensitive to X/γ-rays but experiments with *in vitro* DNA repair systems did not indicate a direct participation of the enzyme in the break rejoining (reviewed by Jeggo [1], Sanderson and Lindahl [2]). As concerns DNA double strand break (DSB) repair, the effect of poly(ADP-ribose) polymerase inhibitors on DSB repair usually is difficult to demonstrate and, at best, transient. For instance, Rudat *et al.* [3] showed that PARP inhibition induced a shift from rapid to slow DSB rejoining.

It was previously reported that 3-aminobenzamide (AB) does not affect DSB rejoining when measured with the use of neutral comet assay in CHO-K1 (wild type) and xrs6 (radiosensitive mutant) cells [4]. Here, to evaluate DNA damage repair in the examined cells in different phases of the cell cycle, the results obtained for single cells in each experiment were grouped according to the distribution in the cell cycle. Cell population was divided into subpopulations corresponding to cell cycle phases on the basis of DNA content assessed from the total comet fluorescence.

Figure shows that the repair rate in CHO-K1 cells in all cell cycle phases is comparable. In AB-treated and irradiated cells, some delay in rejoining at a 15 min interval is seen in subpopulations in S and G2 cell cycle phases. However, the levels of residual damage are close in all subpopulations. Predictably, the (nonhomologous end-joining) NHEJ-defective xrs6 cells in G1 phase rejoin DSB more slowly than in S and G2 phases. This is in agreement with the known cell cycle specificity of NHEJ. AB does not impair the rejoining in G1 phase, but a delay in rejoining at a 15 min interval is seen in subpopulations in S and G2 cell cycle phases. The effect is similar to that observed in CHO-K1 cells. This result is consistent with the observations of homologous recombination dependence on PARP [5].

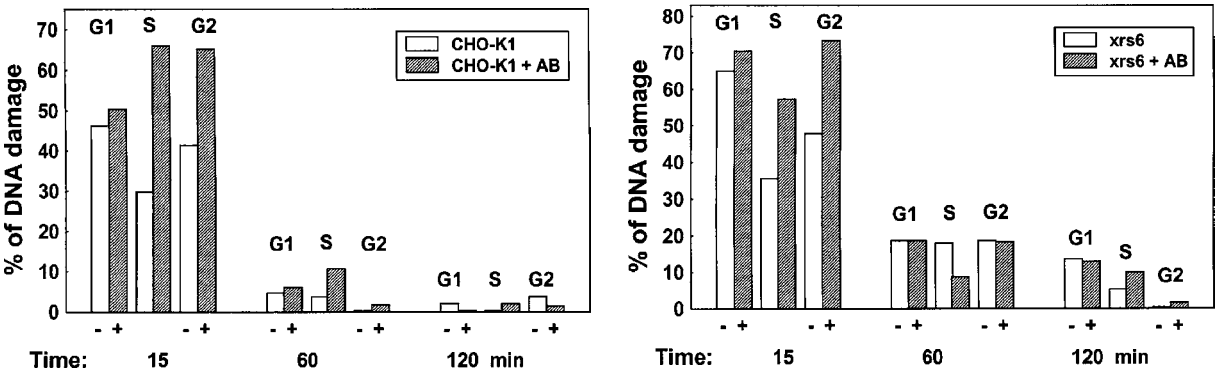

Fig. Cell cycle dependence of the course of DSB rejoining at 37°C in the presence or absence of 2 mM AB. Irradiation at time 0 with 10 Gy X-rays. Data for CHO and xrs6 cells from the neutral comet assay reported previously [4]. Cell populations were divided into subpopulations corresponding to cell cycle phases G1, S and G2, on the basis of DNA content assessed from the total comet fluorescence.

References

[1]. Jeggo P.A.: Curr. Biol., 8, R49-R51 (1998).
[2]. Lindahl T., Satoh M.S., Poirier G.G., Klungland A.: Trends Biochem. Sci., 20, 405-411 (1995).
[3]. Rudat V., Bachmann N., Kupper J.H., Weber K.J.: Int. J. Radiat. Biol., 77, 303-307 (2001).
[4]. Wojewódzka M.: In: INCT Annual Report 2002. Institute of Nuclear Chemistry and Technology, Warszawa 2003, p.110.
[5]. Chatterjee S., Berger S.J., Berger N.A.: Mol. Cell Biochem., 193, 23-30 (1999).

FREQUENCY OF HOMOLOGOUS RECOMBINATION IN TWO CELL LINES DIFFERING IN DNA DOUBLE STRAND BREAK REPAIR ABILITY

Maria Wojewódzka, Teresa Bartłomiejczyk, Marcin Kruszewski

There are two major pathways for DNA double strand break (DSB) repair in mammalian cells: homologous recombination (HR) and nonhomologous end-joining (NHEJ). In certain situations, repair of DSB is restricted to either NHEJ or HR. The restriction in type of DSB repair raises the

question as to how pathway choice is regulated. To better understand the factors that modulate the choice of DSB repair pathway in mammalian cells, we investigated the frequency of spontaneous and X-ray-induced homologous recombination in NHEJ-competent (CHO-K1) and NHEJ-defective (xrs6) cells lines. To study homologous recombination in mammalian cells, we used pLrec plasmid that carries two non-functional copies of a bacterial gene, *lacZ* (β-galactosidase) in a tandem array [1]. The *lacZ* genes are divided by a selective marker gene, which provides resistance to the geneticin antibiotic – G418 (gene *neo*). Generation of a functional copy of the gene takes place in result of HR. So, β-galactosidase activity in the transfected clones was the measure of HR either spontaneous or X-ray-induced.

The transfected clones were selected on a selective medium containing 500 μg/ml G418. The clones with a single plasmid copy and with two copies of *lacZ* were identified by Southern blotting and PCR. Single copy transfectants were irradiated with 2 Gy X-rays and cultured in the medium ± G418. β-Galactosidase activity in cell extracts was measured 48 h after irradiation according to [2]. We found that the frequency of spontaneous (not shown) and X-ray-induced (Table) homologous recombination is enhanced in NHEJ mutant cells. In NHEJ competent cells lines Ku binding to both ends of DSB inhibits access by the homologous recombination machinery, so that when Ku is absent, HR is enhanced [3].

Table. β-Galactosidase activity (units per mg protein in cell extracts) in transfected cells as a measure of frequency of homologous recombination in CHO and xrs6 cells.

Clones of CHO-K1 cells transfected with a single copy of pLrec plasmid			
TK15	- G418	Control	1.31 ± 0.65 U/mg protein
		2 Gy	1.35 ± 0.71 U/mg protein
	+ G418	Control	0.75 ± 0.13 U/mg protein
		2 Gy	0.67 ± 0.10 U/mg protein
N11	- G418	Control	1.51 ± 0.39 U/mg protein
		2 Gy	1.66 ± 0.66 U/mg protein
	+ G418	Control	1.40 ± 0.30 U/mg protein
		2 Gy	1.41 ± 0.43 U/mg protein
Clones of xrs6 cells transfected with a single copy of pLrec plasmid			
S9	- G418	Control	2.47 ± 0.69 U/mg protein
		2 Gy	2.65 ± 0.20 U/mg protein
	+ G418	Control	2.04 ± 0.46 U/mg protein
		2 Gy	2.14 ± 0.50 U/mg protein
S15	- G418	Control	4.79 ± 0.67 U/mg protein
		2 Gy	5.02 ± 0.71 U/mg protein
	+ G418	Control	4.02 ± 0.43 U/mg protein
		2 Gy	4.85 ± 0.14 U/mg protein

References

[1]. Herzing L.B., Meyn M.S.: Gene, 137, 163-169 (1993).
[2]. Sanbrook J., Fritsch E.F., Maniatis T.: Molecular Cloning: A Laboratory Manual. Second edition. Cold Spring Harbor Laboratory Press, Cold Spring Harbor 1989.
[3]. Pierce A.J., Hu P., Han M., Ellis N., Jasin M.: Genes Dev., 15, 3237-3242 (2001).

EFFECTS OF SIGNALLING INHIBITORS ON SURVIVAL OF X-IRRADIATED HUMAN GLIOMA CELLS

Iwona Grądzka, Iwona Buraczewska

Growth factor receptor pathways are often activated in tumor cells by ionizing radiation or active oxygen species. Specific inhibitors have been developed that block the function of these molecules, thereby slowing cell growth and promoting cell death responses after radiation exposure [1, 2]. The study aims at investigation of the cellular response to combined treatment with X-rays and signalling inhibitor, with the use of human glioma cells. These cells are known for their high resistance to radio- and chemotherapy due to the high expression of the receptors for the epidermal growth factor (EGF) and insulin-like growth factor (IGF). We have chosen two related cell lines: M059 K and M059 J;

the latter is considerably more sensitive to ionizing radiation than the first one, due to loss of the catalytic subunit of DNA-dependent protein kinase ($DNA\text{-}PK_{cs}$) [3, 4].

Inhibitors used in the study were: tyrphostine AG 1478 (T), specific for the receptor kinase EGFR and PD 098059 (P), specific for kinases MEK1/2.

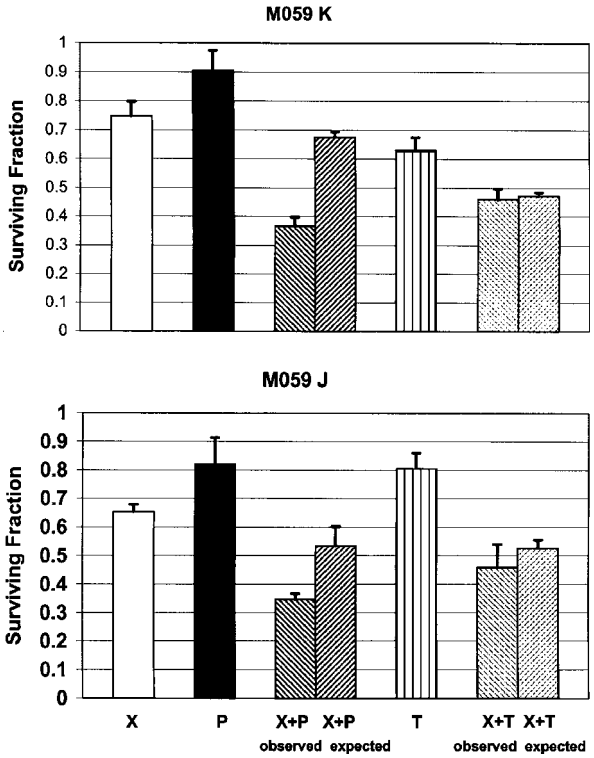

Fig. The effect of X-irradiation combined with P or T on colony-forming ability in M059 J (lower panel) and M059 K (upper panel) cells. Points represent mean values of 3 experiments ± SD.

Cellular sensitivity to X-radiation, bleomycin and the inhibitors was determined from the loss of colony forming ability. In brief, cells were seeded into 60-mm tissue culture dishes, at densities 300-10 000 cells per dish, treated with the inhibitors or/and X-radiation or bleomycin and then incubated for 10-14 days in a humidified atmosphere of 5% CO_2 at 37°C. After fixation with formaldehyde and staining with methylene blue, colonies of more than 50 cells were counted.

M059 J cells are much more sensitive to both X-radiation and bleomycin compared to M059 K cells, but inversely cross sensitive to T and P (not shown). Figure shows the effect of combined treatment with X-radiation and signalling inhibitors on colony forming ability in M059 J and M059 K cells. The concentrations of the inhibitors and the doses of X-rays were adjusted to exert nearly equitoxic effects in both cell lines, *i.e.*: M059 J cells were irradiated with 0.5 Gy of X-rays and treated with 20 μM of P and 5 μM of T. For M59 K cells 1 Gy dose was applied and 15 and 1.5 μM of P and T, respectively.

As shown in the Figure, P sensitizes both cell lines to X-radiation (more than additive effect of combined treatment with X-rays and P) while T exerts an additive effect. This difference may be related to the difference in the site of action: T inhibits the receptor tyrosine kinases, whereas P acts downstream, on the MAPK (ERK1/2) kinases. Hence, T can inhibit not only survival signals that are directed to the transcriptional machinery in the nucleus, but also the anti-apoptotic signalling.

References

[1]. Huang S.M., Harari P.: Clin. Cancer Res., 6, 2166-2174 (2000).
[2]. Huang S.M., Bock J.M., Harari P.: Cancer Res., 59, 1935-1940 (1999).
[3]. Allalunis-Turner M.J., Barron G.M., Day R.S. III, Dobler K.D., Mirzayans R.: Radiat. Res., 134, 349-354 (1993).
[4]. Anderson C.W., Dunn J.J., Freimuth P.I., Galloway A.M., Allalunis-Turner M.J.: Radiat. Res., 156, 2-9 (2001).

EFFECTS OF SIGNALLING INHIBITORS ON DNA DOUBLE STRAND BREAK REPAIR IN HUMAN GLIOMA CELLS

Iwona Grądzka, Barbara Sochanowicz, Irena Szumiel

A considerable radiosensitization by inhibitors of growth factor receptor pathways can be achieved with some types of cancer cells [1, 2], but the mechanism of this effect is not fully understood (review in [3]). The aim of this work is to examine the hypothesis that the radiosensitization is due to the effect on DNA repair systems.

The object of this study are human glioma cells – known for the high resistance to radio- and chemotherapy due to the high expression of growth factor receptors EGF (epidermal growth factor) and IGF (insulin-like growth factor). We used two related cell lines: M059 K (K) and M059 J (J); the J line is more sensitive to ionising radiation than the first one, due to loss of the catalytic subunit of the DNA-dependent protein kinase, $DNA\text{-}PK_{cs}$. This results in impaired DNA double strand break (DSB) rejoining. The preceding report [4] describes survival of these cell lines after X-irradiation alone and combined with inhibitors. The first inhibitor, PD 098059 (P), is specific for kinases MEK1/2; its use enables to assess the effect of signalling starting from both receptors, EGFR and IGFR. The second one, tyrphostine AG 1478 (T), is specific for the receptor kinase, EGFR.

A nonradioactive pulse field gel electrophoresis (PFGE) method [5] was used to estimate DNA DSBs in glioma cells. Inhibition of the signalling by P and T (30 min pre-treatment) affected the initial DNA fragmentation, as well as the level of

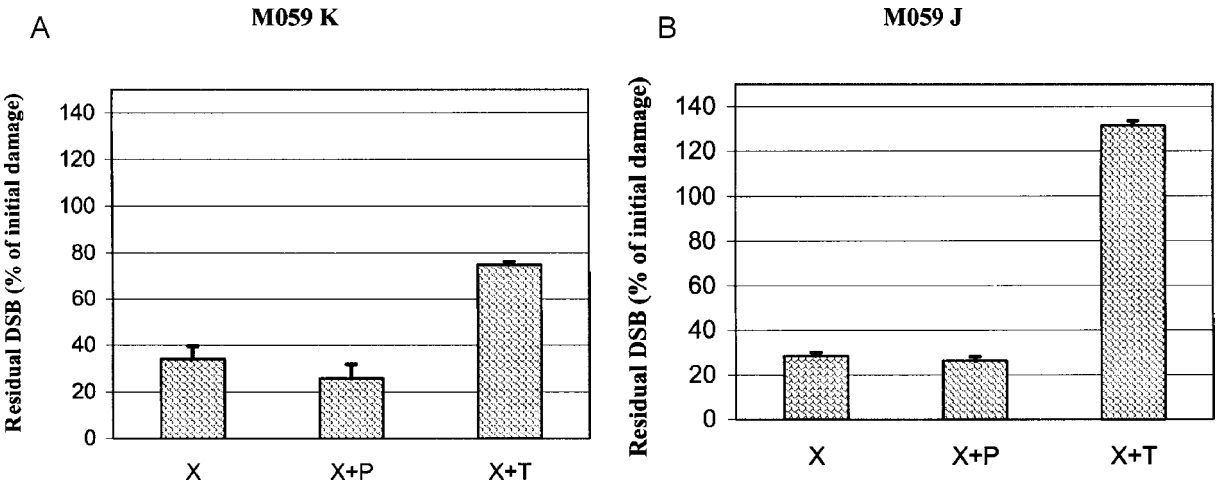

Fig.1. The effect of signalling inhibitors on DSB rejoining after X-irradiation of M059 K (A) and M059 J (B) cells. The cell cultures were treated with 5 μM of tyrphostine AG 1478 or 20 μM of PD 098059, 30 min before X-irradiation (10 Gy). DSB level was estimated by PFGE immediately after the treatment (0 min) and after 30 min (M059 K) or 60 min (M059 J) repair period. Here, DSB levels at 30 or 60 min are shown as percentages of the initial damage. Bars are mean values of 3 experiments ± SD.

DSB after 30 or 60 min repair period. In both cell lines, K (Fig.1A) and J (Fig.1B), the effect on the residual damage level was considerably stronger for T than for P. In K cells DSB are repaired by nonhomologous end-joining (NHEJ) involving DNA-dependent protein kinase (DNA-PK) and by homologous recombination (HR); in J cells only HR is functional. As shown in Fig.1, especially the effect of T was more pronounced on DSB repair in J cells than in K cells. The DNA-PK-dependent NHEJ system of DSB repair is non-functional in J cells. Therefore, these results may be taken as indication that the HR system (and possibly, the DNA-PK-independent NHEJ system) of DSB repair is affected by inhibition of signalling that starts at the plasma membrane.

References

[1]. Huang S.M., Harari P.: Clin. Cancer Res., 6, 2166-2174 (2000).
[2]. Huang S.M., Bock J.M., Harari P.: Cancer Res., 59, 1935-1940 (1999).
[3]. Dent P., Yacoub A., Contessa J., Caron R., Amorino G., Valerie K., Hagan M.P., Grant S., Schmidt-Ullrich R.: Radiat. Res., 159, 283-300 (2003).
[4]. Grądzka I., Buraczewska I.: In: INCT Annual Report 2003. Institute of Nuclear Chemistry and Technology, Warszawa 2004, pp.97-98.
[5]. Grądzka I., Buraczewska I., Kuduk-Jaworska J., Romaniewska A., Szumiel I.: Chem.-Biol. Interact., 146, 165-177 (2003).

EFFECT OF LABILE IRON POOL ON GENOTOXICITY INDUCED BY NITRIC OXIDE

Marcin Kruszewski, Rafał Starzyński[1/], Teresa Bartłomiejczyk, Teresa Iwaneńko, Paweł Lipiński[1/], Hanna Lewandowska

[1/] Institute of Genetics and Animal Breeding, Polish Academy of Sciences, Jastrzębiec, Poland

Nitric oxide (NO) is a physiological free radical important in signal transduction [1]. It is also produced as a powerful weapon that kills pathogenic bacteria and tumour cells in activated macrophages [2]. Excessive production of NO has also been implicated in causing human neurodegenerative diseases [3]. However, specific targets of NO cytotoxicity have not been well characterised.

NO is widely recognised as a molecule strongly altering intracellular iron metabolism. Numerous and complex interventions of NO in iron metabolism include regulation of expression of genes responsible for maintaining iron balance as well as inhibition of iron-containing enzymes participating in mitochondrial respiration, heme and DNA synthesis. All these changes lead to a massive loss of intracellular iron, which is a common feature observed in cells exposed to NO. On the other hand, NO is a potent inducer of cell death through the apoptosis pathway [4]. Here, we investigate the role of iron in the NO-induced genotoxicity focusing on the relationship between NO and labile iron pool (LIP), a cytosolic fraction of metabolically active and potentially toxic iron composed of low molecular-weight iron complexes. A pair of mouse lymphoma cell lines L5178Y-R (LY-R) and L5178Y-S (LY-S) differing in LIP level [5] has been used as an experimental model and SpermineNONOate (SperNO) as a NO donor.

The L5178Y lymphoblasts were incubated with SperNO at a density of 3-4x10^5 cells/ml medium in the presence or absence of iron chelator, salicyl-

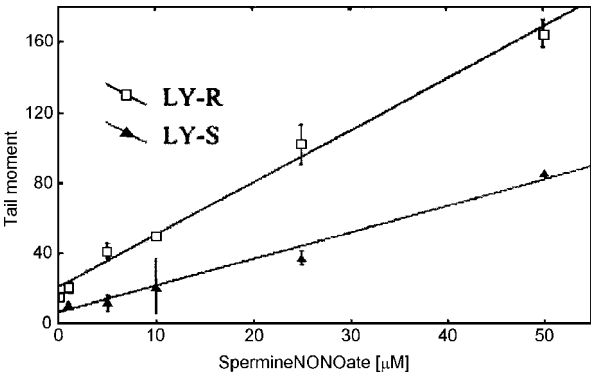

Fig.1. SperNO-induced DNA damage measured by the comet assay. LY cells were treated with different concentrations of SperNO for 2 h at 37°C.

aldehyde isonicotinoyl hydrazone (SIH). The initial DNA damage and its repair rate were determined by the alkaline version of the comet assay, performed as described by Singh *et al.* [6]. LIP was measured with the fluorescent metal sensor, calcein, as described by Epsztejn *et al.* [7]. Calcein

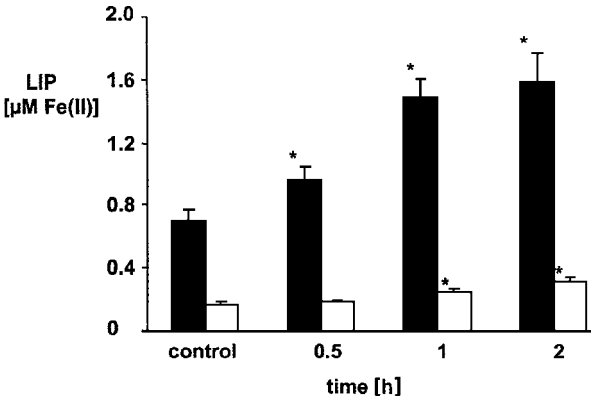

Fig.2. Changes in LIP levels in LY cells during exposure to SperNO. LIP levels as measured in 10^6 LY-R (solid bars) and LY-S (open bars) cells. Data shown are the means ± SD for 3 independent experiments; * denotes significant difference from the control, $P < 0.05$ (Student's *t*-test).

fluorescence (excitation – 488 nm, emission – 517 nm, slits – 10 nm) was measured on a Shimadzu RF 5000 spectrofluorimeter.

In both cell lines, NO induced DNA damage in a dose-dependent manner, as measured with the comet assay. However, in LIP-rich LY-R cells the yield of DNA damage was higher as compared with LIP-depleted LY-S cells (Fig.1). Induction of DNA damage corresponded to the rapid increase in LIP level in both cell lines as measured with calcein (Fig.2). Pre-treatment of cells with SIH, a highly permeant iron chelator and subsequent exposure

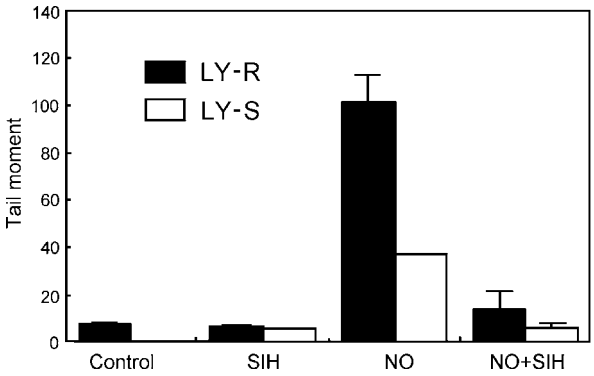

Fig.3. Permeable iron chelator SIH decreases SperNO-induced DNA damage, as measured by the comet assay. LY cells were treated with 25 μM SperNO for 2 h at 37°C in the presence or absence of SIH.

to SperNO resulted in a decrease in DNA damage (Fig.3). This demonstrates that SIH-chelatable iron may be involved in the generation of NO-induced DNA damage.

References

[1]. Ignarro L.J.: Biosci. Rep., 19, 2, 51-71 (1999).
[2]. Cifone M.G. *et al.*: Adv. Neuroimmunol., 5, 4, 443-461 (1995).
[3]. Liu B. *et al.*: Ann. NY Acad. Sci., 962, 318-331 (2002).
[4]. Kakhlon O. *et al.*: Free Rad. Biol. Med., 33, 8, 1037-4633 (2002).
[5]. Kruszewski M.: Podłoże odwrotnej krzyżowej oporności komórek L5178Y na promieniowanie jonizujące i nadtlenek wodoru. Instytut Chemii i Techniki Jądrowej, Warszawa 1999. Raporty IChTJ. Seria A No. 2/99.
[6]. Singh N.P. *et al.*: Exp. Cell. Res., 175, 1, 184-191 (1988).
[7]. Epsztejn S. *et al.*: Anal. Biochem., 248, 1, 31-40 (1997).

DINITROSYL IRON COMPLEXES INDUCED IN LIVING CELLS BY NITRIC OXIDE

Marcin Kruszewski, Rafał Starzyński[1/], Teresa Bartłomiejczyk, Teresa Iwaneńko, Paweł Lipiński[1/], Hanna Lewandowska

[1/] Institute of Genetics and Animal Breeding, Polish Academy of Sciences, Jastrzębiec, Poland

Nitric oxide (NO) is widely recognised as a molecule strongly altering intracellular iron metabolism. Numerous and complex interventions of NO in iron homeostasis include regulation of expression of genes responsible for maintaining iron balance as well as inhibition of iron-containing enzymes participating in mitochondrial respiration, heme and DNA synthesis. A primary target of NO action seems to be the iron-containing proteins, such as heme and non-heme iron proteins. NO and peroxynitrite lead to complete disruption of [4Fe-4S] cluster of recombinant human iron regulatory protein 1 (cytosolic aconitase) and release of iron ions [1]. Thus, the release of iron from heme and/or iron-sulphur clusters leads to an increase in redox active iron, likely in a form of labile iron pool (LIP), a low-molecular-weight pool of weakly chelated iron that rapidly passes through the cell.

It is assumed that dinitrosyl iron (I) complexes (DNIC) play a role in distribution of NO within the cell and are important factors in NO-dependent regulation pathways in the cell [2-5]. Following physiological induction of NO, DNIC is produced in the cell in considerable amounts. One of putative functions of DNIC is connected with regulation of labile iron pool [6]. Many thiol-containing compounds are shown to form DNIC in living cells [7, 8]. These findings point to large proteins as to the main targets of DNIC formation. Dinitrosyl complexes with these species are relatively stable and are suspected to have regulatory functions [2-5]. The question arises, which of the above mentioned pools of iron (coming from iron-sulphur proteins or labile iron pool) takes part in formation of NO complexes in living cells.

In this study, we used two mouse lymphoma L5178Y cell sublines differing in iron level [9]. In order to examine whether LIP is the source of DNIC, we used salicylaldehyde isonicotinoyl hydrazone (SIH), a chemical commonly used as Fe(II) chelator in fluorimetric determination of LIP with the use of calcein [10]. Cells were incubated with SperNO (nitric oxide donor) at a density of 3-4x10^5 cells/ml medium in the presence or absence of iron chelator. Approximately 2.5x10^7 LY-R cells were incubated for 30 min at 37°C in RPMI medium containing 100 μM of NO donor in the presence or absence of 100 μM SIH. After incubation, the cells were spun down and resuspended in phosphate buffered saline to the final volume of 200 μL. The samples obtained this way were put into 4 mm diameter quartz tubes, frozen and stored in liquid nitrogen. Electron paramagnetic resonance (EPR) spectra of all samples were measured on a Bruker 300e spectrometer. Spectra were obtained at 77 K. Microwave power was 1.002 mW, microwave frequency – 9.31 GHz, modulation amplitude – 3.027 G, time constant – 41 ms. For each sample the amount of protein was assayed by Coomassie Blue G method. Each spectrum was recounted for the amount of protein.

DNIC spectra can be observed in cells after treatment with NO donors. Spectra observed in LY cells had the same characteristic shape and did not evolve during incubation with NO. Signal is higher in LY-R cells than in LY-S cells and this can be explained by the differences in LIP levels (0.57 ± 0.1 and 0.18 ± 0.05 μM, respectively [9]). The pattern of the EPR signal suggests axial symmetry of the complex, but to definitely exclude the possibility of orthorombic symmetry measurements in W-band mode of spectrometer should be performed. Most possibly, spectra come from many miscellaneous thiol-Fe-NO complexes of a different symmetry and the observed spectrum is a result of these various signals. Spectra, shown in Fig., are characterised by g values of 2.039 and 2.013,

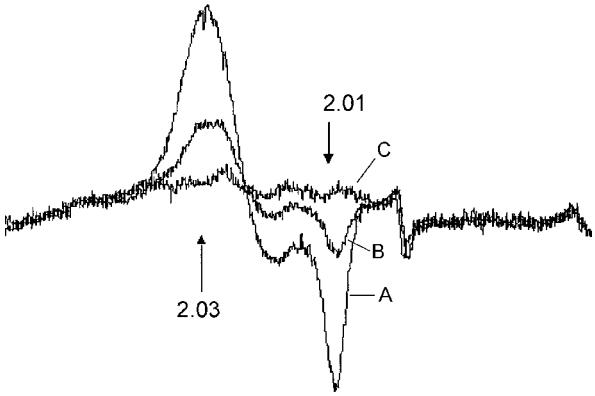

Fig. Formation of dinitrosyl-iron complex (DNIC) in LY cells treated with SpermineNONOate (SperNO) in the presence or absence of SIH. A typical EPR signal is shown of LY cells which were treated with 100 μM SperNO for 30 min at 37°C in the absence (A) or presence of SIH (B). In control cells (C) no signal could be detected.

consistent with findings of other researchers for different types of cells. In cells pre-treated with SIH the level of DNIC is substantially lower than in control cells, treated with NO alone. This demonstrates that LIP is involved in DNIC formation in living cells.

References

[1]. Soum E., Drapier J.C.: J. Biol. Inorg. Chem., 8, 1-2, 226-232 (2003).
[2]. Rogers P.A., Eide L., Klungland A., Ding H.: DNA Repair, 2, 7, 809-817 (2003).
[3]. Bouton C., Drapier J.C.: Sci. STKE, 182, pe17 (2003).
[4]. De Maria F., Pedersen J.Z., Caccuri A.M., Antonini G., Turella P., Stella L., Lo Bello M., Federici G., Ricci G.: J. Biol. Chem., 278, 43, 42283-42293 (2003).
[5]. Turella P., Pedersen J.Z., Caccuri A.M., De Maria F., Mastroberardino P., Lo Bello M., Federici G., Ricci G.: J. Biol. Chem., 278, 43, 42294-42299 (2003).
[6]. Lipinski P., Lewandowska H., Drapier J.C., Starzynski R., Bartomiejczyk T., Kruszewski M.: Increase in labile iron pool (LIP) level and generation of EPR-detectable dinitrosyl-non-heme iron complexes in L5178Y cells exposed to nitric oxide. In: Possible role of LIP as a source of iron for DNIC formation. Deregulations du metabolisme du fer : Chimie, biologie et therapeutiques, Gif-sur-Yvette, France, 3-5 September 2003.
[7]. Kennedy M.C., Antholine W.E., Beinert H.: J. Biol. Chem., 272, 20340-20347 (1997).
[8]. Rogers P.A., Ding H.: J. Biol. Chem., 276, 30980-30986 (2001).
[9]. Kruszewski M.: Podłoże odwrotnej krzyżowej oporności komórek L5178Y na promieniowanie jonizujące i nadtlenek wodoru. Instytut Chemii i Techniki Jądrowej, Warszawa 1999. Raporty IChTJ. Seria A No. 2/99.
[10]. Epsztejn S., Kakhlon O., Glickstein H., Breuer W., Cabantchik I.: Anal. Biochem., 248, 1, 31-40 (1997).

RADIATION-INDUCED MICRONUCLEI IN HUMAN PERIPHERAL BLOOD LYMPHOCYTES COLLECTED DURING DIFFERENT PHASES OF THE MENSTRUAL CYCLE

Marta Król, Sylwester Sommer, Iwona Buraczewska, Andrzej Wójcik

The health consequences of an overexposure to ionising radiation are proportional to the absorbed dose. Therefore, in order to predict the consequences of an accidental overexposure and to choose the right medical treatment, it is necessary to estimate the dose and patient's response [1]. When the circumstances of the exposure and the characteristics of the radiation source are well known, it is possible to calculate or measure the dose by physical methods. However, such a possibility often does not exist. In such situations the absorbed dose must be estimated on the basis of the biological effect induced by radiation [2]. Today, the most specific and most sensitive technique of biological dosimetry relies on estimating the frequency of chromosomal aberrations or micronuclei in peripheral blood lymphocytes of the exposed person [3, 4]. Numerous studies, performed both on animals and humans, have demonstrated a close correspondence between aberrations induced in peripheral blood lymphocytes under *in vitro* and *in vivo* conditions. This allows a radiation dose absorbed during an accident to be estimated by reference to an *in vitro* calibration curve.

The calibration curve is generated by irradiating lymphocytes of randomly chosen control donors. A precise dose estimation is thus only possible when the intrinsic radiosensitivity of the accident victim is similar to that of the control donors. There are data suggesting that the intrinsic radiosensitivity of female lymphocytes depends on the hormonal status of the donor [5]. From the point of view of biological dosimetry, it is important to estimate the impact of the hormonal status on the radiosensitivity of lymphocytes. The aim of the present investigation was to compare the sensitivity of female lymphocytes collected during the first and second halves of the menstrual cycle. The first half of the cycle is controlled by estrogen, the second one by progesterone. Lymphocytes collected from 12 pre-menopausal women not taking contraceptives, were exposed *in vitro* to 2 Gy X-rays, cultured and harvested. The frequencies of micronuclei were scored in 1000 binucleated cells.

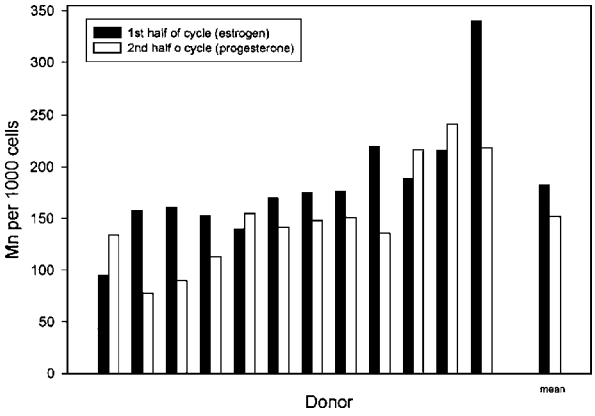

Fig. Frequencies of radiation-induced micronuclei in peripheral lymphocytes of female donors collected during the first and second half of the menstrual cycle.

The results are presented in Fig. A strong inter-individual variability in micronuclei was observed between the donors. On average, slightly more micronuclei were observed in lymphocytes collected during the first half of the menstrual cycle. However, the difference is not significant, mainly due to the strong inter-individual variability. Thus, although the hormonal status does have an impact on the radiation-induced frequencies of micronuclei, the influence is not consistent.

References

[1]. Ricks R.C., Berger M.E., O'Hara M., Jr.: The medical basis for radiation-accident preparedness. The Parthenon Publishing Group, Boca Raton 2002.
[2]. Müller W.-U., Streffer C.: Int. J. Radiat. Biol., 59, 863-873 (1991).
[3]. Cytogenetic analysis for radiation dose assessment. A manual. IAEA, Vienna 2001.
[4]. Voisin P., Barquinero J.F., Blakely B., Lindholm C., Lloyd D., Luccioni C., Miller S., Palitti F., Prasanna P.G., Stephan G., Thierens H., Turai I., Wilkonson D., Wojcik A.: Cell. Mol. Biol., 48, 501-504 (2002).
[5]. Ricoul M., Sabatier L., Dutrillaux B.: Mutat. Res., 374, 73-78 (1997).

KINETICS OF X-RAY INDUCED SCEs IN CHO CELLS PRELABELLED WITH BrdU

Elisabeth Bruckmann[1/], Andrzej Wójcik[2,3/], Günter Obe[1/]

[1/] Institute of Genetics, University of Duisburg-Essen, Essen, Germany
[2/] Institute of Nuclear Chemistry and Technology, Warszawa, Poland
[3/] Institute of Biology, Świętokrzyska Academy, Kielce, Poland

Sister chromatid exchangers (SCEs) are assumed to be a consequence of DNA replication on a damaged template and can arise only when a DNA lesion is not removed before the cell enters S phase [1-4]. Ionising radiation is a poor inducer of SCEs and it is only effective when applied to cells in G1

with chromosomes unifilarily substituted with BrdU [5, 6].

In order to investigate the relationship between the SCE frequency and the phase of the cell cycle in which DNA damage is induced, experiments

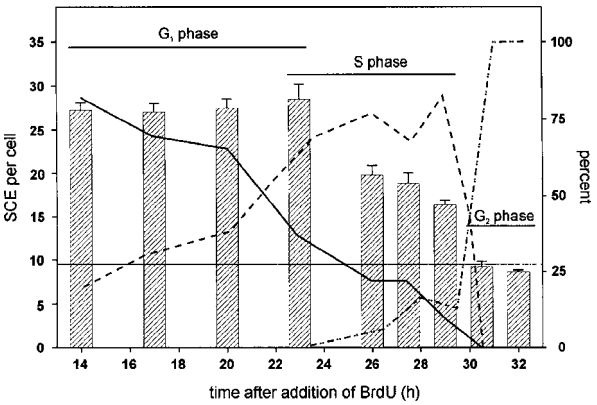

Fig. SCE frequencies and types of chromosomal aberrations in cells prelabelled with BrdU and irradiated with 4.8 Gy X-rays at various phases of the cell cycle. The horizontal line represents the control frequency of SCE. Columns show the induced SCEs. Curves show the percentages of cells with: chromosome-type aberrations (solid curve), mixed types of aberrations (dashed curve) and chromatid-type aberrations (dashed-dotted curve). Error bars represent standard deviations from 3 independent experiments.

were performed using cells pre-labelled with BrdU and exposed to 4.8 Gy of X-rays at various times before fixation. The results are presented in Fig. Scoring was restricted to cells with uniform differential labelling of sister chromatids. In addition to SCEs, per cent frequencies of cells showing chromosome-type aberrations, chromatid-type aberrations and both are plotted. The cell cycle phase in which the cells were irradiated was determined on the basis of the types of aberrations observed and the time between exposure and harvest. The highest frequency of SCEs was observed in cells treated in G1 phase, followed by S phase. Irradiation during G2 phase did not induce SCE above the control level. A striking observation was that during G1 the frequency of SCE remained at a similar level, irrespective of whether cells in early or late G1 phase were irradiated. In accordance with the data shown in Fig., a part of the SCEs are due to aberrations. Nevertheless, it appears that following X-ray irradiation the lesions responsible for SCE formation arise very quickly and their frequency does not decline during the G1 phase.

References

[1]. Shafer D.A.: Human Genet., 39, 177-190 (1977).
[2]. Painter R.B.: Mutat. Res., 70, 337-341 (1980).
[3]. Cleaver J.E.: Exp. Cell Res., 13, 27-30 (1981).
[4]. Schubert I.: Biol. Zentralbl., 109, 7-18 (1990).
[5]. Littlefield L.G., Colyer S.P., Joiner E.J., DuFrain R.J.: Radiat. Res., 78, 514-521 (1979).
[6]. Renault G., Gentil A., Chouroulinkov I.: Mutat. Res., 94, 359-368 (1982).

CYTOMETRIC ESTIMATION OF THE NUMBER OF TRANSFERRIN RECEPTORS ON THE OUTER PLASMA MEMBRANE OF L5178Y CELLS TREATED WITH NITRIC OXIDE

Marcin Kruszewski[1,2/], Agnieszka Gajkowska[2/], Tomasz Ołdak[2,3/], Eugeniusz K. Machaj[2,3/], Zygmunt Pojda[2,3/]

[1/] Institute of Nuclear Chemistry and Technology, Warszawa, Poland
[2/] Maria Skłodowska-Curie Memorial Cancer Center and Institute of Oncology, Warszawa, Poland
[3/] Military Institute of Hygiene and Epidemiology, Warszawa, Poland

Two murine leukaemic lymphoblast sublines L5178Y were studied differing in the intracellular iron level and activity of proteins participating in iron metabolism and maintaining iron homeostasis. These features are responsible for the differential sensitivity of these sublines to oxidants (reviewed in [1]) and the difference in response to treatment with nitric oxide (NO) donors. One effect of NO is an increase in the level of labile iron pool, which is the potential source of iron ions entering Fenton reaction and generating genotoxic hydroxyl radicals (reviewed in [2]). The study was undertaken to verify the recent claim that NO increases iron level by enhanced iron influx [3-5]. To this end, we determined transferrin receptors which are responsible for iron complexed transferrin (TfR) uptake in NO treated L5178Y cells.

L5178Y cells in suspension culture in RPMI1640 medium with 8% bovine serum were treated with the NO donor, SpermineNONOate (Sigma, USA), at a concentration of 25 μM for 2 h at 37°C. After treatment, the culture medium was changed, the cells incubated for 3 h and the relative number of TfR (CD71) molecules on L5178Y cells was estimated using phycoerithrin (PE) fluorescence quantification kit (QuantiBRITE™ PE*, Becton-Dickinson) and R-phycoerithrin (R-PE)-conjugated rat anti-mouse CD71 receptor antibody. In brief, $5x10^5$ cells were suspended in 100 μl ice-cold phosphate--buffered-saline (PBS). The non-specific binding of anti-CD71 antibody was blocked by adding 2 μl rat anti-mouse CD16/CD32 (Fcγ III/II receptor) monoclonal antibody (Pharmingen). The sample was incubated in dark for 5 min at 4°C and 5 μl of R-PE-conjugated rat anti-mouse CD71 monoclonal antibody (Pharmingen) was added. The sample was then incubated in the dark for 30 min at room temperature, spun down and washed with

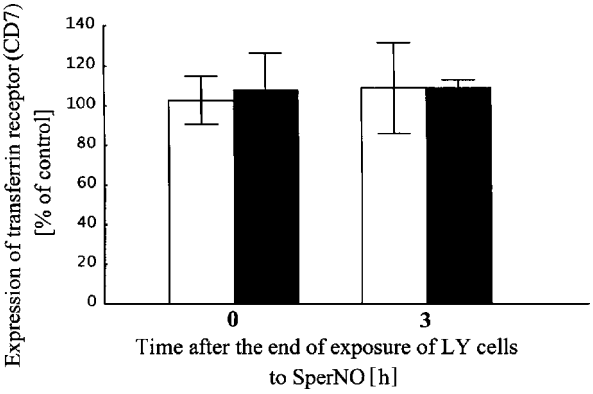

Fig. Cytometrically determined relative numbers of transferrin receptors in LY cells after 2 h incubation with SpermineNONOate, and a subsequent 3 h incubation in SpermineNONOate-free medium: open bars – LY-R cells, closed bars – LY-S cells.

PBS. Cells were than fixed in CellFix solution (Becton-Dickinson) and analysed in FaxCalibur cytometer (Becton-Dickinson) at the same settings as for the QuantiBRITE™ PE* kit. The number of CD71 molecules on LY cell was calculated from the calibration curve obtained with the QuantiBRITE™ PE* kit.

Figure shows that neither 2 h incubation with SpermineNONOate nor the subsequent 3 h incubation in SpermineNONOate-free medium altered the number of transferrin receptors. This result is in contrast with the views of other authors [3-5] who ascribe the increase in iron level in NO-treated mammalian cells to disturbed iron homeostasis and increased iron uptake. Our results indicate that the transient enhancement at the iron level after NO treatment most probably is due to release from the intracellular compartments.

References

[1]. Bożyk E., Grądzka I., Iwaneńko T., Kruszewski M., Sochanowicz B., Szumiel I.: Acta Biochim. Pol., 47, 881-888 (2000).
[2]. Kruszewski M.: Mutat. Res., 531, 81-92 (2003).
[3]. Kim S., Ponka P.: Biometals, 16, 125-135 (2003).
[4]. Kim S., Ponka P.: Blood Cells Mol. Dis., 29, 400-410 (2002).
[5]. Qian Z.M.: Biol. Rev. Camb. Philos. Soc., 77, 529-536 (2002).

IONIZING RADIATION-INDUCED DNA DAMAGE IN PROLIFERATING AND NON-PROLIFERATING HUMAN CD34$^+$ CELLS

Marcin Kruszewski[1,2/], Teresa Iwaneńko[1/], Tomasz Ołdak[2,3/], Agnieszka Gajkowska[2/], Eugeniusz K. Machaj[2,3/], Zygmunt Pojda[2,3/]

[1/] Institute of Nuclear Chemistry and Technology, Warszawa, Poland
[2/] Maria Skłodowska-Curie Memorial Cancer Center and Institute of Oncology, Warszawa, Poland
[3/] Military Institute of Hygiene and Epidemiology, Warszawa, Poland

We used proliferating and non-proliferating human CD34$^+$ cells in experiments aimed at:
- looking whether progression of cells through the cell cycle would affect the results obtained by the alkaline comet assay,
- whether is it possible to estimate the cell cycle dependence of DNA damage by a direct analysis of comet assay results.

Homogenous population of human CD34$^+$ cells were isolated from umbilical cord blood by magnetic cell sorting (CD34 Progenitor Cell Isolation Kit, Miltenyi) and purity of isolated cell population was checked with flow cytometry (FC). Pure populations (90%) were aliquoted and deep frozen. Thawed cells were divided into two portions. One was left in serum free growth medium Methocult (Stem Cell) (unstimulated cells), whereas the second was incubated in the same medium supplemented with growth factors (50 ng/ml TPO, 20 ng/ml SCF and 50 ng/ml Flt-3L) (stimulated cells). Two days later both populations were analysed by FC for cell cycle distribution (on the basis of DNA content). On the same day, DNA breakage in cells irradiated with 8 Gy of X-rays (180 kV, 1.1 Gy/min) was analysed by the alkaline comet assay (100 comets per experimental point). Olive tail mo-

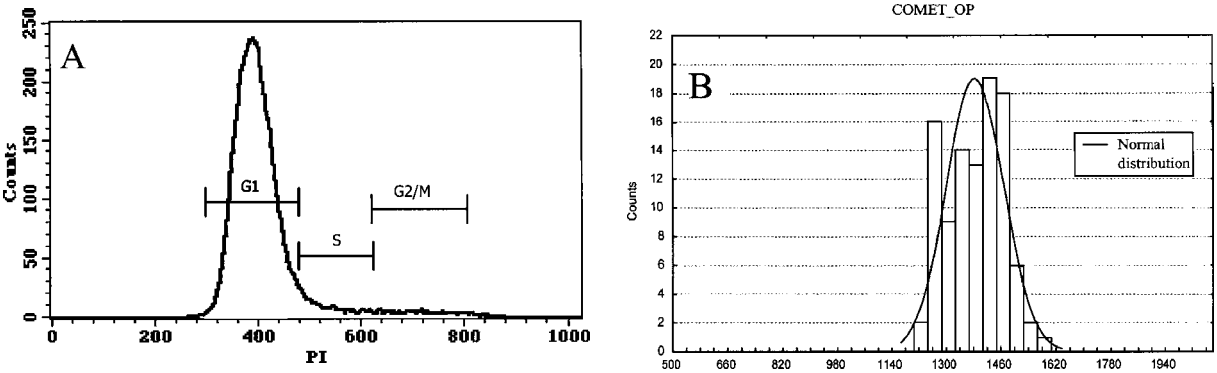

Fig.1. Cell cycle distribution of unstimulated CD34$^+$ cells estimated by flow cytometry (A) and by comet assay (B): PI – propidium iodide fluorescence, COMET_OP – total optical density.

ment (OTM) and head DNA (HDNA) were taken as DNA damage indicators, and comet optical density (COD) was taken as a measure of cell position in the cell cycle [1, 2].

Cell cycle distribution estimated from the COD values correlated well with that estimated with FC (cf Figs.1 and 2). In unirradiated, control cells, OTM values were 1.1 ± 0.8 and 3.2 ± 1.9 and HDNA values were 95.9 ± 3.0 and 94.4 ± 2.9 in unstimulated and stimulated cells, respectively. In irradiated cells, OTM values were 109.0 ± 11.6 and 92.5 ± 8.0 and HDNA values were 12 ± 4.9 and 17.7 ± 3.7 in unstimulated and stimulated cells, respectively. Interestingly, when we compared unirradiated and irradiated cells, we observed a substantial loss of COD in the latter ones. This could be due to the different binding of the applied fluorochrome (DAPI) to the damaged DNA or to the loss of DNA in the wake of electrophoresis. However, our preliminary data indicate that this is rather due to the different binding of DAPI to the damaged DNA, as use of a different fluorochrome, SYBR Green (Molecular Probes) increased the COD in damaged cells. Taken together, our results suggest that the comet assay can be a valuable tool to assess the cell cycle dependence of DNA damage and its repair.

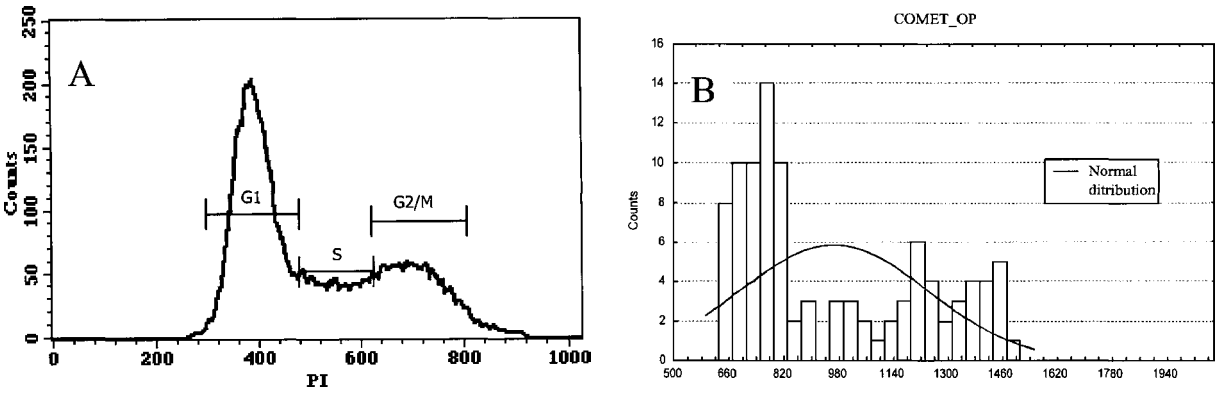

Fig.2. Cell cycle distribution of stimulated $CD34^+$ cells estimated by flow cytometry (A) and by comet assay (B): PI – propidium iodide fluorescence, COMET_OP – total optical density.

References

[1]. Wojewodzka M., Kruszewski M., Iwanenko T., Collins A.R., Szumiel I.: Mutat. Res., 416, 21-35 (1998).

[2]. Kruszewski M., Wojewodzka M., Iwanenko T., Szumiel I., Okuyama A.: Mutat. Res., 409, 31-36 (1998).

NUCLEAR TECHNOLOGIES
AND
METHODS

PROCESS ENGINEERING

TREATMENT OF CHLORINATED ORGANIC COMPOUNDS BY USING IONIZATION TECHNOLOGY

Andrzej G. Chmielewski , Yongxia Sun, Sylwester Bułka, Zbigniew Zimek

Chlorinated aliphatic and aromatic hydrocarbons, which are emitted from coal power stations and waste incinerators, are very harmful to the environment and human health. Recent studies show that chlorinated aliphatic and aromatic hydrocarbons are suspected to be precursors of dioxin formation. Dioxin emission into atmosphere will cause severe environmental problem by ecological contamination.

Volatile organic compounds treatment by using ionization technology has been studied many years ago. Chloroethylene degradation has been studied extensively in recent years by using different technologies, different products of chloroethylene degradation and by various authors under different experimental conditions. Electron beam (EB) treatment is a promising technology for removal of low concentration of chloroethylenes contained in air. One of the EB technological advantages is an energy saving process [1-4]. The aim of this work is to continue our investigation of chlorinated hydrocarbons, 1,4-dichlorobenzene degradation under EB irradiation in an air mixture. The G-value of 1,4-dichlorobenzene decomposition at 5 kGy was calculated and the results were compared with those of *cis*-dichloroethylene (*cis*-DCE).

The laboratory set up of gas preparation is described as follows: the modelling gas of 1,4-dichlorobenzene was prepared by passing synthetic air (O_2 – 21%, N_2 – 79%; from Praxair Co.) through solid 1,4-dichlorobenzene (purity – 99%; Aldrich Co.) at room temperature into 5 connected Pyrex glass reactors. The concentration of 1,4-dichlorobenzene in the model gas was adjusted by controlling the flow rates of the synthetic air by using a rotameter. When the gas mixtures was prepared, the 5 connected reactors were sealed off with stopcocks. The concentration of 1,4-dichlorobenzene was analyzed by gas chromatography before irradiation. The water concentrations in the model gas mixture were detected below 200 ppm.

An electron beam ILU-6 accelerator (2.0 MeV max, 20 kW max., HF resonance – pulsed type) was used for irradiation of the gas samples in Pyrex glass vessels. A dose distribution inside the reactor was measured by using CTA films (FTR-125, Fuji Photo Film Co.).

1,4-dichlorobenzene concentrations before and after irradiation were analyzed by gas chromatography (Perkin Elmer 8700) with a flame ionizing detector (FID) and a fused silicon column (length – 30 m, diameter – 0.32 mm, thickness – 0.25 μm film), analytical condition was as follows: oven – 70-94°C, 4°C/min; injector – 200°C; FID – 340°C; carry gas – helium, 18Psig.

G-values of decomposition of 1,4-dichlorobenzene under EB irradiation was calculated and the result are shown in Fig.1. It was found that G-values of 1,4-dichlorobenzene are small and show a linear

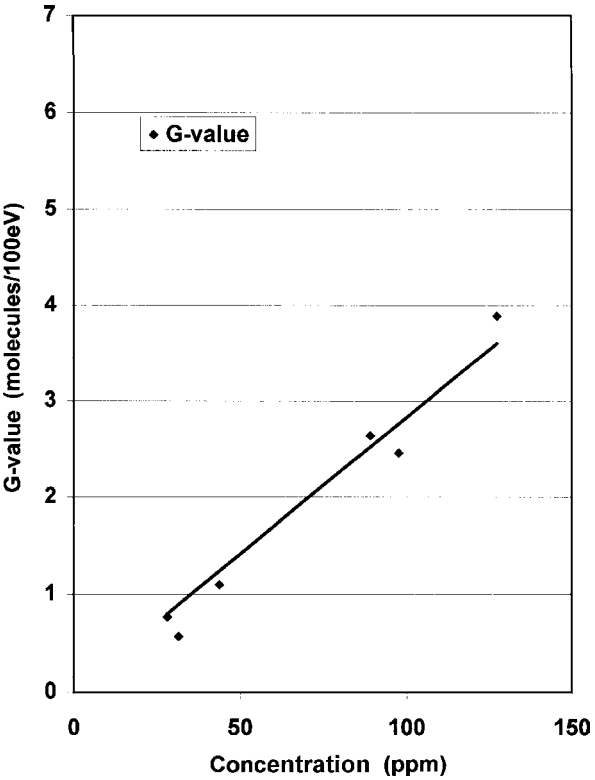

Fig.1. G-value *vs*. initial concentration of 1,4- dichlorobenzene/air at 5 kGy dose.

relationship *vs*. initial concentration of 1,4-dichlorobenzene. For example, G-values of 1,4-dichlorobenzene are 0.765 at 28 ppm and 3.89 at 127 ppm. The G-value *vs*. initial concentration of 1,4-dichlorobenzene under EB irradiation could be mathematically fitted by equation:

$$\text{G-value} = 0.0283 * C_0$$

where: G-value – molecules/100 eV; C_0 – initial concentration of 1,4-dichlorobenzene, 28 ppm$\leq C_0 \leq$130 ppm.

This phenomenon indicates that 1,4-dichlorobenzene decomposition proceeds by chain reactions.

G-values of decomposition of *cis*-DCE under EB irradiation are calculated and the result are shown in Fig.2. It was found that G-values of *cis*-DCE are bigger than those of 1,4-dichlorobenzene and markedly depend on the initial concentration. For

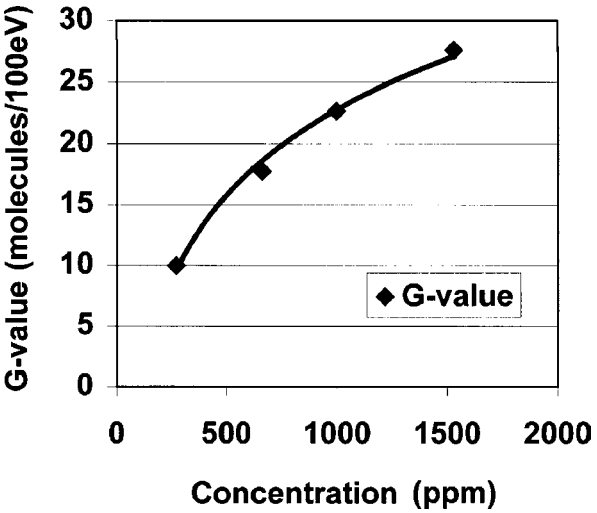

Fig.2. G-value *vs*. initial concentration of *cis*-DCE under EB irradiation.

example, G-values of *cis*-DCE are 10 at 270 ppm and 27.6 at 1530 ppm. The G-value *vs*. initial concentration of *cis*-DCE under EB irradiation could be mathematically fitted by equation:

$$\text{G-value} = 10.145 \ln(C_0) - 47.276$$

where: G-value – molecules/100 eV; C_0 – initial concentration of *cis*-DCE, 270 ppm ≤ C_0 ≤ 1530 ppm. This phenomenon indicates that *cis*-DCE decomposition partly proceeds by chain reactions.

Decomposition efficiency of *cis*-DCE is faster than that of 1,4-dichlorobenzene. The reason for this is that 1,4-dichlorobenzene has the benzene ring, which is much more stable and needs higher energy to be broken. The mechanism for 1,4-dichlorobenzene is a little different from that of *cis*-dichlorobenzene. For the former the positive ion charge transfer reaction plays a very important role for 1,4-dichlorobenzene decomposition; for the latter chlorinated secondary electron attachment play main roles, and peroxyl radicals reaction accelerated this process.

References

[1]. Prager L., Langguth H.L., Rummel S., Mennert R.: Radiat. Phys. Chem., 46, 1137-1142 (1995).
[2]. Penetrante B.M., Hsiao M.C., Bardsley J.N., Merritt B.T., Vogtlin G.E., Wallman P.H., Kuthi A., Burkhart C.P., Bayless J.R.: Pure & Appl. Chem., 68(5), 1083-1087 (1996).
[3]. Vitale S.A., Hadidi K., Cohn D.R., Bromberg L.: Phys. Lett. A, 232, 447-455 (1997).
[4]. Sun Y., Hakoda T., Chmielewski A.G., Hashimoto S., Zimek Z., Bulka S., Ostapczuk A., Nichipor H.: Radiat. Phys. Chem., 62, 353-360 (2001).

DETERMINATION OF SULFUR ISOTOPE RATIO IN COAL COMBUSTION PROCESS

Małgorzata Derda, Andrzej G. Chmielewski

On a global scale, combustion of fossil fuels accounts for 82% of the total sulfur dioxide emissions with 56% arising from coal [1]. Major environmental impact of atmospheric sulfur compounds is related to rain acidity, human health, climate, visibility and materials. Very important is the evaluation of economic responsibility for the emitted pollution. Therefore, scientists look for a suitable marker which could be used as an environmental tracer.

Literature review shows that there are a few data on sulfur isotope ratio in Polish coals and on fractionation of sulfur isotopes in the process of coal combustion. Results of a preliminary investigation concerning characteristics of the Polish coals were presented earlier [2]. The obtained results ($\delta^{34}S/^{32}S$ -6.62 to +15.88‰) suggest that the sulfur in coal originates from the sulfur being originally bounded by plants and depleted in the isotope ^{34}S. In some deposits isotopic composition is similar at different depths of the whole region, while in the others, this composition can change even at the depth of several meters [3]. There is a big differentiation in the obtained results not only in the concentration of the sulfur but also in its isotope ratio values.

This method was applied for the determination of changes of sulfur isotope ratio along the lignite combustion process at a big power complex: lignite mine-power station at Bełchatów. Solid samples (lignite, ashes and slag) were collected from the systems of the power station and samples of the flue gas, and the product (gypsum) from the desulfurization line were investigated [4]. Due to the fact that lignites are the one of the most important sources of energy in Poland, the characteristic of sulfur isotope ratio in lignites is of value.

Table 1. $\delta^{34}S$ in different forms of sulfur in lignite and the products of its combustion from the Turów Power Station.

	S_{org} [‰]	S_{pyrite} [‰]	$S_{sulfate}$ [‰]
Lignite	10.95 ± 0.03	-3.92 ± 0.06	-11.01 ± 0.03
Ash	6.07 ± 0.04	-	8.47 ± 0.04
Slug	10.92 ± 0.03	8.7 ± 0.02	3.02 ± 0.04

In Poland, three big power stations use lignite as an energy material: Bełchatów, Turów and Pątnów. The solid samples (coal, ashes and slag) were taken from the Turów and Pątnów Power Stations to determine sulfur isotope ratio ($^{34}S/^{32}S$) in the coal combustion process. Each form of sulfur has been prepared by extraction [5] of solid samples and transform into stable compounds, which can be subsequently converted to gas phase (SO_2) for mass spectrometric analysis [6] (Table 1 and 2).

Table 2. $\delta^{34}S$ in different forms of sulfur in lignite and the products of its combustion from the Pątnów Power Station.

	S_{org} [‰]	S_{pyrite} [‰]	$S_{sulfate}$ [‰]
Lignite	7.32 ± 0.03	22.6 ± 0.03	12.34 ± 0.06
Ash	6.69 ± 0.04	16.55 ± 0.01	9.2 ± 0.05
Slug	7.87 ± 0.04	14.84 ± 0.03	8.11 ± 0.04

The received results for the Turów Power Station (Table 1) ($\delta^{34}S$ range from -11.01 to 10.95‰) suggest that the sulfur isotope ratio, concerning organic sulfur in the lignite, is the same as in the primary plant material. Sulfur is an essential constituent of the living cell. The plant can take up SO_4^{2-} or SO_2 directly from the environment. The sulfur organic compounds, resulting from assimilatory of SO_4^{2-} reduction are depleted in ^{34}S.

In the case of the Pątnów Power Station, the sulfur is depleted in ^{34}S too ($\delta^{34}S$ range from 7.23 to 22.6‰). $\delta^{34}S$ values in the slag and ash from the Turów Power Station are enriched in the heavier isotope ^{34}S in the coal combustion process. The same effect was observed for the Bełchatów Power Station in earlier investigations [4]. The results $\delta^{34}S$ for the Pątnów Power Station are opposite. Sulfur in the ash and slag is depleted in the heavy isotope ^{34}S in the coal combustion process. This is not clear why this difference between these results occurs, but probably it arises due to the combustion process conditions.

The present and earlier data of sulfur isotope ratio in coal and lignite (including desulfurization process) indicate that it is possible to apply this method for further investigation of the migration of sulfur compounds in ground waters and atmosphere.

References

[1]. Harter P.: Sulphate in the atmosphere. IEA Coal Research Report ICTIS/TR30, London 1985, p.155.

[2]. Chmielewski A.G., Wierzchnicki R., Derda M., Mikołajczuk A.: Nukleonika, 47, 67 (2002).

[3]. Krouse H.R.: Stable isotope studies of sulfur flows and transformations in agricultural and forestry ecosystems. IAEA, 1991, IAEA-SM-313/108.

[4]. Chmielewski A.G., Derda M.: In: INCT Annual Report 2002. Institute of Nuclear Chemistry and Technology, Warszawa 2003, pp.122-123.

[5]. Westgate L.M., Anderson T.F.: Anal. Chem., 54, 2136 (1982).

[6]. Hałas S., Wolacewicz W.D.: Anal. Chem., 53, 686 (1981).

SULFUR SEPARATION FACTORS OBSERVED DURING ADSORPTION OF SO_2 ON DIFFERENT SILICA GELS

Agnieszka Mikołajczuk, Andrzej G. Chmielewski

During this experimental work the sulfur isotope ($^{34}S/^{32}S$) separation factors were determined. The kinetic and equilibrium isotope effects were observed during the adsorption of sulfur dioxide on different types of silica gel sorbents.

Adsorption is also used in separation and purification processes, including hazardous pollutant removal from flue gases. Sulfur dioxide is believed to be a major precursor of acid rains, therefore the control of sulfur dioxide emissions is a significant subject for research and development, as well as industrial implementation [1].

Many adsorbents were investigated for sulfur dioxide adsorption like carbonaceous adsorbents [2-4], metallic oxide sorbents of transition metals [5] or molecular sieves [6-7]. Process of sulfur dioxide adsorption has been studied extensively. The products of surface reactions were analyzed from the point of view of removal efficiency and the feasibility of regeneration. It was found that sulfur dioxide on the activated carbon is adsorbed with two adsorption energies [8].

The low energy, about 50 kJ/mol, corresponds to a weak physical adsorption and the second about 80 kJ/mol, to chemisorption [9]. The weak adsorption is related to interactions of sulfur dioxide and free sites on the surface, whereas a strong adsorp-

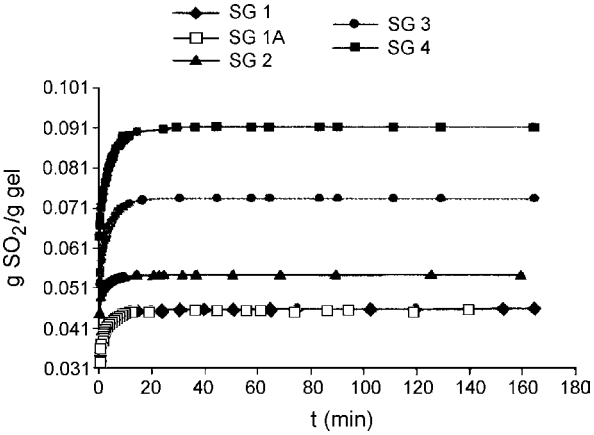

Fig. Experimental adsorption isotherms of sulfur dioxide on silica gels, T = 293 K, p_o = 870 hPa.

tion is connected with the presence of oxygen [8]. Raymundo-Pinero and co-workers suggested that oxidation of SO_2 to SO_3 occurs in the 7 Å pores.

The role of pore structure is not so well defined as the role of surface oxygenated groups [9]. Although it is believed that the developed porosity is important to "store" sulfuric acid as a product of oxidation, large pores decrease the conversion of SO_2 to SO_3, which is accompanied by a decrease in a total sorption capacity. On the other hand, when small pores are present sulfuric acid is strongly bonded to the surface [10].

In this work, the most important point was the sulfur separation factor. During the experimental work adsorption isotherms of sulfur dioxide on silica gels were determined (Fig.). According to the literature data [1], the adsorption isotherms are described by the Freundlich model or deactivation model which suggests a significant decrease of activity of the sorbent with time with respect to probable changes in pore structure, in the active surface area and active site distribution of the sorbent (silica gel). Properties of silica gels are shown in Table 1.

The adsorption of sulfur dioxide increases from silica gel SG 1A to SG 4. Silica gels SG 1 and SG 1A had similar physical properties because SG 1A additionally contained $CoCl_2$ incorporated in its structure as an indicator. Sulfur dioxide adsorption on SG 1A decreased by about $5x10^{-4}$ g SO_2/g gel compared with gel SG 1.

The sulfur separation factors were determined during sulfur dioxide adsorption on silica gel samples. At the beginning, in the experiments 4 g of silica gel was used, the pressure of sulfur dioxide in a vacuum line was 870 hPa. The experimental data are shown in Table 1.

The results presented in Table 2 demonstrate that the silica gel SG 1 has the best properties for the separation of sulfur isotope in such conditions; the silica gel mass, temperature and gaseous sulfur dioxide pressure over the adsorbent. The gas phase was enriched in the heavy sulfur isotope. Sulfur dioxide in a gas phase contained 4.49‰ isotope ^{34}S more when compared with sulfur dioxide adsorbed on the silica gel SG 1, while the time adsorption was 5 min. Sample SG 1A contained $CoCl_2$, it was the reason why the sulfur separation factor was smaller by *ca*. 1.33‰ than that obtained for SG 1. Sulfur dioxide adsorbed on silica gel was enriched in the ^{32}S. The separation factor was the smallest in the case when sulfur isotopes ^{34}S and ^{32}S were separated on SG 4.

During the experimental work, the time of adsorption of sulfur dioxide on silica gels was changed from 5 min to 600 h. After 1 month, the system attained the isotope equilibrium state. These separation data are shown in Table 3, which refer to the results completed last year [11].

Mass of silica gel SG 3 and 4 samples used was only 4 g due to the small volume of vacuum line.

Table 1. Properties of silica gels.

Silica gels number	SG 1	SG 1A	SG 2	SG 3	SG 4
Size granules [mm]	1-7	1-7	1-3	0.2-0.3	0.2-0.3
BET surface area [m^2/g]	432	496	500-800	600	400
Average pore radius [Å]	25	22	10	50	20

Table 2. Sulfur isotope fractionation factors between sulfur dioxide in gas phase and sulfur dioxide adsorbed on silica gel. Mass of silica gel samples was 4 g, p_o = 870 hPa, standard deviation of measurements – 0.02‰.

Adsorption time [min]	$(\alpha - 1)\,10^3 = \Delta^{34}S$ [‰]				
	SG 1	SG 1A	SG 2	SG 3	SG 4
5	4.49	3.16	2.95	2.99	1.76

Table 3. Sulfur isotope fractionation factors between sulfur dioxide in gas phase and sulfur dioxide adsorbed on silica gel. Weight of silica gels SG 1, SG 1A, SG 2 were 8 g; mass of silica gels SG 3 and SG 4 was 4 g; p_o = 870 hPa; standard deviation was 0.02‰.

Adsorption time [h]	$(\alpha - 1)\,10^3 = \Delta^{34}S$ [‰]				
	SG 1 [12]	SG 1A	SG 2	SG 3	SG 4
0.08	6.81	1149	11.32	2.99	1.76
~0.17	5.45	11.02	9.46	0.59	0.29
2	1.62	1.02	1.55	0.23	-0.46
~20	0.67	-1.87	0.63	-0.57	-0.57
~140	-1.01	-1.93	-0.29	-0.60	-0.45
~200	-1.21	-1.86	-1.88	-0.52	-0.47
~600	-1.17	-1.96	-1.85	-0.44	-0.45

Probably, the isotope separation factor will be higher if the mass of silica gel will be bigger. When the systems attained equilibrium state, the separation factor measured was almost the same for both gels. Sulfur dioxide in the gas phase was enriched in the isotope ^{32}S.

Sulfur separation factors were low in the equilibrium state (below 1). When the adsorption time was 5 min, the separation factor was higher for each sample of silica gels and the highest was for sample SG 2 (Table 3). Initially, on silica gel was adsorbed $^{32}SO_2$ and the gas phase was enriched in the heavy sulfur isotope. When the system has reached equilibrium state sulfur dioxide which contained isotope ^{34}S was predominantly adsorbed on silica gel.

The pressure/temperature kinetic process has much more advantages over equilibrium process in regard to possible applications. Silica gels SG 1, SG 1A and SG 2 may be used as adsorbents for the separation of sulfur isotopes. The experimental data have shown that the most important physical property of the sorbent affecting the process is pore radius. The pore radius size influences the separation factor, which is a result of sulfur dioxide oxidation.

This work was supported by the Polish State Committee for Scientific Research (KBN) – grant No. 4T09A 039 24.

References

[1]. Kopac T., Kocabas S.: Chem. Eng. Proc., 41, 223-230 (2002).
[2]. Bagreev A., Bashkova S., Bandosz T.J.: Langmuir, 18, 1257-1264 (2002).
[3]. Bashkova S., Bagreev A., Locke D.C., Bandosz T.J.: Environ. Sci. Technol., 35, 3263-3269 (2001).
[4]. Lee Y.-W., Park J.-W., Choung J.-H., Choi D.-K.: Environ. Sci. Technol., 36, 1086-1092 (2002).
[5]. Lin Y.S., Deng S.G.: Sep. Purif. Technol., 13, 65 (1998).
[6]. Kopac T., Kayamakci E., Kopac T.: Chem. Eng. Commun., 164, 99-110 (1998).
[7]. Kopac T.: Chem. Eng. Proc., 38, 45-53 (1999).
[8]. Davini P.: Carbon, 39 (9), 1387-1393 (2001).
[9]. Raymundo-Pinero E., Cazola-Amorós D., Salinas--Martinez de Lecea C., Linares-Solano A.: Carbon, 38 (3), 335-344 (2000).
[10]. Bagreev A., Rahman H., Bandosz T.J.: Environ. Sci. Technol., 34, 4587-4592 (2000).
[11]. Chmielewski A.G., Mikołajczuk A.: In: INCT Annual Report 2002. Institute of Nuclear Chemistry and Technology, Warszawa 2003, pp.123-124.
[12]. Chmielewski A.G., Miljević N., Mikołajczuk A.: Sposób rozdzielenia izotopów siarki ^{34}S i ^{32}S. Patent application P.354392.

DETERMINATION OF SURFACE WATER AND GROUNDWATER QUALITY IN STRIPMINE AREAS

Robert Zimnicki

To study the influence of engineering objects on the environment analysis of macro- and micro-ingredients was carried out. These analyses aim of comparing the content of suitable ions with the

Table. A list of chemical analyses of waters of drainage system.

Studied elements in surface waters														
Macro indicators	HCO_3^-	Cl	SO_4^{2-}	NH_4^+	Na	Ca	K	Fe						
Micro indicators	Ba	Cr	Zn	Cd	Cu	Ni	Pb	Hg	Ag	Sr	V	Al	I	Rb
Soluble substances														
Generally hardness	Hardness type													
COD(Mn)*	BOD5**	COD(Cr)*												
Oxygen dissolved														

Studied elements in waters of mine drainage system								
Macro indicators	Cl^-	SO_4^{2-}	HCO_3^-	Ca	Mg	Na		
Micro indicators	Sr	Ba	Br	Cr	Cd	Cu	Pb	Rb	Zn

Determination of isotopes						
Isotope	Rn-222	3H	O-18	S-34	D	O-18
Type of analysis	Structure of aquifer, radium activity	Ages of water	In SO_4^{2-} ion		In H_2O molecule	

* COD – chemical oxygen demand, ** BOD – biochemical oxygen demand.

norms and environmental regulations. Additionally, the determinations of isotope composition of elementary ions were carried out. The study is helpful for the formulation of hypotheses concerning the damaging influence of these objects on the natural environment. As a supplement of environmental analyses, a study of aquifer properties was performed, *i.e.* porosity, flow time, average velocity of the water. The experiments were carried out using flow tracers and the obtained data were elaborated by means of suitable mathematical models. The results of determinations are presented in Table.

In 2003, a full range of planned investigations on groundwater and the quality of surface water have been performed.

Determinations of micro- and macro-ingredients in groundwater on the quarry terrain and in surface water of drain network were carried out. The experiments were performed using a hydraulic contact in the area menaced to washing out a halite deposit.

In order to check the possibility of pollution infiltration from the ground surface, isotope composition of sulfates and water molecules has also been determined. Obtained data were presented in an industrial report in the form of appropriate correlations, diagrams and comparative dataset.

APPLICATION OF GS MEMBRANE METHODS FOR SEPARATION OF GAS MIXTURES IN THE SYSTEMS GENERATING ENERGY FROM BIOGAS

Marian Harasimowicz, Grażyna Zakrzewska-Trznadel, Andrzej G. Chmielewski

Biogas is produced during fermentation of bio-mass. It is composed of CH_4 (50-70%), CO_2 (30-40%) and a small amount of H_2 (< 5%), water vapour (< 0.3%) and the trace amount of H_2S (< 100 ppm). The raw biogas must be purified from water vapour and H_2S, and the concentration of CO_2, N_2 and H_2 must be decreased in order to obtain high-methane fuel gas of the composition and calorific value similar to the standard gas (methane concentration 90-95%). This can be reached by chemical methods or by separation on GS (gas separation) semi-permeable membranes characterized by a high value of retention factor for CH_4 and low for other compounds of biogas [1]. As a result of biogas transport through the GS membrane under pressure of 0.5-10.0 MPa, two gas streams are obtained: the retentate (CH_4 > 90%) and the permeate (CO_2 > 90%, CH_4 < 10%). To reduce the CO_2 concentration in the retentate and the CH_4 concentration in the permeate, multistage membrane systems with re-circulation of the permeate are applied. A higher purity of both gas streams, e.g. with concentration of CH_4 and CO_2 above 99%, can be obtained by application of supplementary treatment: sorption/desorption in amine solutions [2].

The aim of the project 4 T09C 041 24 is the investigation of biogas separation with various GS membrane modules and the possibility of application of the membrane method for processing of biogas into the standard fuel gas. In laboratory-scale experiments, the small A2 GS module (Fig.) for the separation of gas mixture CH_4+CO_2 was tested. The influence of the variation of the main operating parameters: pressure, temperature and gas flow on the separation process is investigated and the results should give a basis for elaboration a technology for biogas processing with selected GS modules, and for the preparation of a feasibility study for design and construction of a pilot plant of capacity ~130 Nm^3/h.

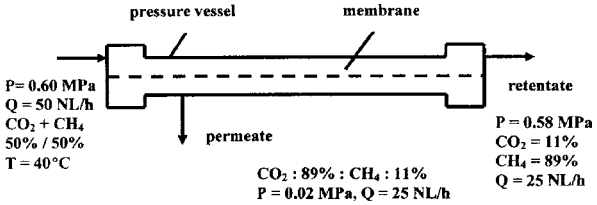

Fig. Separation of gas mixture CO_2 + CH_4 in the GS membrane module A2 (UBE, Japan).

References

[1]. Stookey D.J., Pope W.M.: Application of Membranes in Separation of Carbon Gases – Recovery of CO_2 from Man-Made Sources. Aragonne National Laboratory, 2000, pp.53-62, ANL CNSV-TM-166.

[2]. Puri S.: Proceedings of the Seminar "Ecological application of innovate membrane technology in chemical industry", Certaro, Italy, 12-15 May 1996.

THE USE OF CFD METHODS IN ELECTRON BEAM FLUE GAS TREATMENT INSTALLATION INVESTIGATION

Andrzej G. Chmielewski, Andrzej Pawelec, Bogdan Tymiński, Jacek Palige, Andrzej Dobrowolski

Although the electron beam flue gas treatment installation in the electric power station (EPS) "Pomorzany" (Szczecin) was put in operation in 2002, there is still work carried out in order to improve its effectiveness [1, 2]. As a result of lowering the electron energy from 800 to 700 keV, the

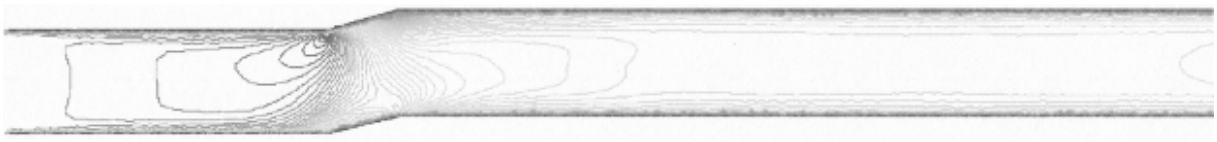

Fig.1. Contours of velocity magnitude for lifted bottom of reaction chamber.

bottom of the reaction chamber was to be lifted. This has changed the geometry of the reactor and caused different gas velocity profile. The gas flow dynamics under new conditions was investigated by means of computational fluid dynamics (CFD) methods. The FLUENT 5.0 program was used for simulations.

liminary research was concerned with the use of existing guide vanes for the lift of the gas under the first accelerator window. The Figs.2 and 3 show the gas flow profile with the guide vanes parallel to the reactor axis and inclined 20° to this axis. A strong effect is observed of the gas lift under the window that may caused up to 10% increase of the

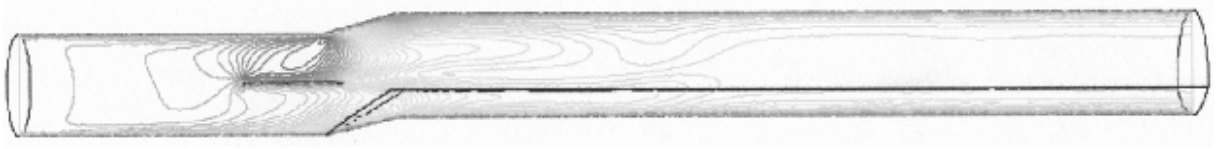

Fig.2. Contours of velocity magnitude for guide vanes parallel to the reactor axis.

Figure 1 shows the profile of gas velocity in the case of bottom lift. It is clearly visible that the gas is lifted in the entrance to the reaction chamber,

NO_x removal efficiency. The same effect may be obtained under the second window by installing an additional guide vane between the accelerators.

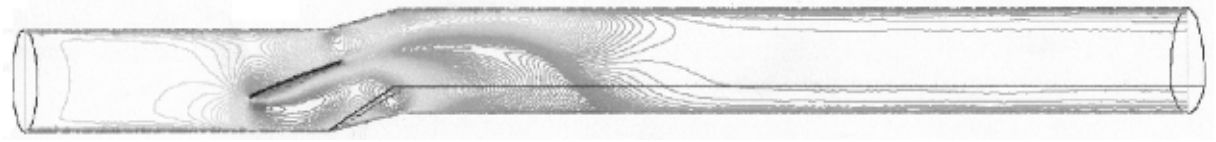

Fig.3. Contours of velocity magnitude for guide vanes inclined 20° to the reactor axis.

but the effect lasted for a short way and ended before the first accelerator was installed. For almost the whole length of the reactor the gas velocity was uniformed (in the sense of turbulent flow profile).

On the other hand, it is known that the dose distribution in the reaction chamber is not uniformed and differs very narrowly with distance from the accelerator widow. That is the reason that the non uniformed flow under the window would improve the effectiveness of the process. The pre-

The work described in this announcement is in progress and the results will be described in another paper.

References

[1]. Chmielewski A.G. *et al.*: Przem. Chem., 82, 8-9, 1013-1015 (2003), (in Polish).
[2]. Chmielewski A.G. *et al.*: Prace Naukowe Politechniki Warszawskiej, Konferencje, 23, 47-54 (2003), (in Polish).

APPLICATION OF TRACERS AND CFD METHODS FOR INVESTIGATIONS OF WASTEWATER TREATMENT INSTALLATION

Jacek Palige, Andrzej Owczarczyk, Andrzej Dobrowolski, Andrzej G. Chmielewski, Sylwia Ptaszek

Waste water treatment process is realized in different apparatus such as equalizers, aeration tanks (with surface aeration or with bubbling system), settlers (circle or rectangular) and final sedimentation basins. Each of these installations represents a complicated system where the processes of clarification, flow rate and chemical composition equalization, biochemical reactions, sedimentation and others are occurring. The efficiencies of all apparatus strongly depend on both the liquid and solid phase flow structure.

An ample research concerning identification and optimization of flow structure in such apparatus were carried out. Using the tracer technique

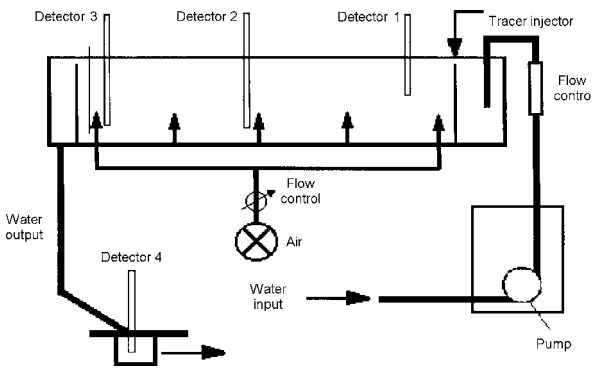

Fig.1. Scheme of aeration laboratory tank.

the experimental residence time distribution (RTD) functions can be determined. For these purpose the radiotracers (Br-82, Tc-99, La-140) and colored tracers (fluorescein, rodamine *etc*.) are used. The method of pulse-response type is practically applied for RTD function measuring the output of apparatus. This, so called "black box method" enable to derive an overall model of flow hydrodynamics by comparison of experimental and theoretical (for appropriate proposed model of flow) RTD functions. Model parameters are usually obtained by a multiparameter optimization procedure. Unfortunately, the same experimental RTD function can be described by various models with comparable accuracy.

For validation of flow model are necessary some additional data describing, irrespectively of tracer experiment, the flow structure of phases (liquid or solid) inside the apparatus. One of the techniques which are used for this purpose is the computational fluid dynamics (CFD) method. The application of tracer technique and validation of these results by the CFD method during the investigations of preliminary rectangular settlers for sedimentation of sludge after aeration process are presented in papers [1, 2]. Experimental RTD curves obtained for different tracers were compared with numerical RTD function calculated using a DRW (discreet random walk) procedure in the FLUENT software. The structure of flow is obtained by solving appropriate Navier-Stokes equations, continuity equation, boundary conditions and relations describing turbulence of flow. The sufficient agreement between experimental and numerical data was observed.

As a more complicated apparatus, the aeration tank with bubbling system installed was investigated. The scheme of tank is presented in Fig.1. Dimensions of tank are: length – 4.95 m, width – 1.3 m and height – 0.45 m. All the tracer experiments and numerical calculations were carried out for the constant water flow Q_w = 2.7 m^3/h and air flow rate at interval 0-18 m^3/h. Numerical simulations of flow structure for 2D case were carried out using the Euler-Euler model of water and air bubble flow and standard k-ε model of flow turbulence. Numerical RTD function was obtained by the Lagrangian method (trajectory of liquid particles). The calculated flow structure and velocity field for air flow Q_a = 3 m^3/h is presented in Fig.2.

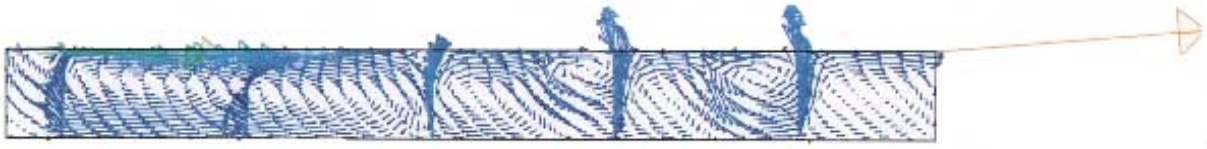

Fig.2. Flow structure and velocity field for water flow rate Q_w = 2.7 m^3/h, Q_a = 3 m^3/h.

A comparison of experimental and numerical RTD functions is presented in Fig.3. The observed agreement between both curves is very good. More detailed information concerning this kind of research is presented in [3].

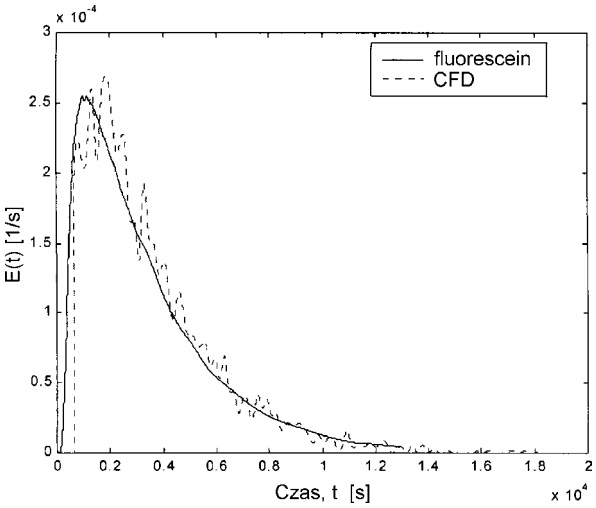

Fig.3. Comparison of experimental and numerical RTD function for liquid phase (Q_w = 2.7 m^3/h, Q_a = 3 m^3/h).

Data obtained in tracer experiments can be quantified by CFD results making the proposed model of flow more realistic and physically reasonable.

The work was supported by the Polish State Committee for Scientific Research (KBN) – grant No. 7T09C 02221.

References

[1]. Palige J., Owczarczyk A., Dobrowolski A., Chmielewski A.G., Ptaszek S.: In: INCT Annual Report 2002. Institute of Nuclear Chemistry and Technology, Warszawa 2003, pp.129-130.

[2]. Palige J., Owczarczyk A., Dobrowolski A., Chmielewski A.G., Ptaszek S.: Inż. i Ap. Chem., 4s, 72-75 (2003), (in Polish).

[3]. Palige J., Owczarczyk A., Dobrowolski A., Chmielewski A.G., Ptaszek S.: Inż. i Ap. Chem., 5s, 151-152 (2003), (in Polish).

MATERIAL ENGINEERING, STRUCTURAL STUDIES, DIAGNOSTICS

ION IMPLANTATION OF OXYGEN, TITANIUM AND IRON INTO AIN CERAMICS FOR DIRECT BONDING TO COPPER

Jerzy Piekoszewski[1,2/], Wiesława Olesińska[3/], Jacek Jagielski[3/], Dariusz Kaliński[3/], Marcin Chmielewski[3/], Zbigniew Werner[2/], Marek Barlak[2/]

[1/] Institute of Nuclear Chemistry and Technology, Warszawa, Poland
[2/] The Andrzej Sołtan Institute for Nuclear Studies, Świerk, Poland
[3/] Institute of Electronic Materials Technology, Warszawa, Poland

Aluminum nitride (AlN) is gaining an increasing interest as an attractive substrate material for electronic applications in high power density packing owing to such features as: high thermal conductivity, good electrical insulation, thermal expansion similar to silicon and non-toxicity e.g. [1-6]. The requirement of heat dissipation imposes the need of forming low thermal resistance (thin) joint with a high thermal conductivity metal, preferably copper. According to the recent literature, the direct bonding (DB) of the substrate to the conductor is considered as the most promising technique. The direct bonding was originally developed for joining alumina to copper. In DB technique the metal is joined immediately to the ceramic with only very thin transition layer between metal-ceramics components. One of the important advantage of AlN over Al_2O_3 as an substrate in high power density packing is that AlN has ten times higher heat conductivity than alumina in a wide range of temperature, so it is not surprising that a lot of effort is aimed at application of DB for joining the Cu-AlN system. In one of pioneering works [1], Entezarian and Drew demonstrated satisfactory result of AlN-Cu bonding by addition of 1-1.5 at % of oxygen as an active element to AlN-Cu system without intentional modification of the substrate surface. The bonding process was conducted at 1065-1075°C in flowing commercial nitrogen containing 500 ppm of oxygen. In our approach, it is expected that the formation of nano-thickness layer with enhanced content of favorable additives introduced by ion implantation into AlN and pre-oxidation of copper should result in even better wettability between the bonded elements.

For ion implantation into commercially available AlN substrates oxygen, titanium and iron ions have been chosen. Implantation of oxygen offers the possibility of formation of an extremely thin (few nanometer) graded transition layer between the copper and ceramics. Oxygen implantation is also considered as a low temperature alternative to thermal oxidation of AlN surface – known to improve adhesion of copper layer [7]. The choice of titanium was dictated by a commonly known beneficial effect of this element on metal-ceramic joints quality [8].

The obtained results show that in all investigated experimental variants implantation gives better results than oxidation procedure. It seems that in order to obtain good-quality direct bond joint, two conditions must be satisfied:

- The concentration of the active element at the surface must be sufficiently high.
- Transition in ceramic material between the unmodified substrate and its surface layer cannot have the form of an abrupt junction but should be of graded type.

Ion implantation seems to be ideally suited for such purposes. We expect that after optimization of the implantation process, it will be generally adopted for bond technique. The advantages of ion implantation include fast processing time, accuracy in creating the appropriate oxygen content, flexibility in tailoring the desired distribution of the introduced atoms and ability to form non-equilibrium compounds.

References

[1]. Entezarian E., Drew R.A.: Mat. Sci. Eng., A212, 206-212 (1996).
[2]. Exel K.P., Haberl P., Maier P.H.: PCIM Europe (previously Powerconversion & Intelligent Motion for Power Electronics, Drives and Motion; PCIM Power Electronic Systems Europe), 11, 28 (1999).
[3]. Joyeux T., Jarrige J., Labbe J.C., Lecompte J.P.: Key Eng. Mater., 206-213, 555-558 (2001).
[4]. Olesińska W., Librant Z.M., Rak Z.: Key Eng. Mater., 206-213, 503-506 (2001).
[5]. Joyeux T., Jarrige J., Labbe J.C., Lecompte J.P., Alexandre T.: Key Eng. Mater., 206-213, 535-538 (2001).
[6]. Zanghi D., Traverse A., Gautro S., Kaïtasov O.: J. Mater. Res., 16, 512-516 (2000).
[7]. Lee J.W., Radu I., Alexe M.: J. Mater. Sci.: Mater. Electron., 13, 131-137 (2002).
[8]. Nicholas M.G.: Joining of Ceramic. Chapman and Hall, London 1990.

SUPERCONDUCTIVITY IN MgB_2 THIN FILMS PREPARED BY ION IMPLANTATION AND PULSE PLASMA TREATMENT

Jerzy Piekoszewski[1,2/], Wojciech Kempiński[3/], Jan Stankowski[3/], Edgar Richter[4/], Jacek Stanisławski[2/], Zbigniew Werner[2/]

[1/] Institute of Nuclear Chemistry and Technology, Warszawa, Poland

[2/] The Andrzej Sołtan Institute for Nuclear Studies, Świerk, Poland

[3/] Institute of Molecular Physics, Polish Academy of Sciences, Poznań, Poland

[4/] Forschungszentrum Rossendorf e.V., Institut für Ionenstrahlphysik und Materialforschung, Dresden, Germany

In 2001, superconductivity at a temperature as high as T_c = 39 K was discovered in MgB_2 inter-metallic compound by Nagamatsu *et al*. [1]. This discovery stirred the research community and attracted a great deal of interest. Exploration of the new material started in two directions: (i) development of new methods of fabricating and improving quality of solid MgB_2 and (ii) the same as above, in the area of thin MgB_2 films formed on various substrates. The present studies belong to (ii). Encouraging results obtained in this field were reported in the literature e.g. [2, 3]. Common feature of approaches presented thus far is that superconducting MgB_2 films are formed from the solid phase in the Mg-B system.

Goal of the present studies is to synthesize superconducting MgB_2 film from liquid phase without annealing in Mg vapor. In order to reach superconducting layer of MgB_2, ion implantation and the transient melting processes (TMP) method was used. Substrates of Mg were implanted with B^+ ions at energy of 100 keV and a dose of $5x10^{18}$ B/cm^2. Subsequent irradiations with 2 short (μs range) high-intensity pulsed hydrogen plasma beams melt the surface layer of the substrate. Energy density and number of pulses were 1.9 J/cm^2 (sample "44") and 3.0 J/cm^2 (sample "49"). According to computer simulation, melt depth of substrate reaches up to 5 μm, liquid phase lasts 2-3 μs and cooling rate after solidification of the near-surface region is of the order of 10^7 K/s.

For the first time the synthesis of superconducting MgB_2 layers by means of B^+ ion implantation into Mg substrate and TMP was achieved. Superconductivity is confirmed by the MMMA (magnetically modulated microwave absorption) method. Below 20 K for hydrogen plasma pulses with energy density of 1.9 J/cm^2 weak superconducting MMMA signals *vs*. temperature or the magnetic field appear. Increase in the energy density of melting pulses to 3.0 J/cm^2 shifts T_c to 31 K. Results are compared to those of MgB_2 powder obtained by the standard powder/powder annealing method [1]. Encouraging is the observation of the islands of superconductive material. However, further study is needed aimed at formation of macroscopic percolation chains.

References

[1]. Nagamatsu J., Nakagawa N., Muranaka T., Zenitani T.Y., Akimitsu J.: Nature, 410, 63-64 (2001).

[2]. Bumel B.D., Kang J., Lee H.N., Moon S.H., Oh B.: Appl. Phys. Lett., 79, 3464-3466 (2001).

[3]. Schiesel S., Carosella C.A., Horowitz J.S., Osofsky M., Kendziora C., Qadri S.B., Knies D.L.: Surf. Coat. Technol., 158-159, 568-602 (2002).

NOVEL PROPERTIES OF META-ARAMID FIBRES MODIFIED BY IMMERSING FOR A SHORT TIME IN BOILING WATER-BENZYLALCOHOL SOLUTION (BY "SHOCK" CRYSTALLIZATION)

Andrzej Łukasiewicz, Dagmara Chmielewska, Lech Waliś, Jacek Michalik, Luzja Rowińska, Janusz Turek

Aromatic polyamide (aramid) fibres have many and growing applications. Meta-aramid fibres (Nomex® – Du Pont registered trademark) are used, among other things, in flame-resistant fabrics [1].

Our research on Nomex fabrics was initiated by some problems of dying process. These problems were solved by modification of Nomex properties. Crude Nomex III® (uncrystallized) used for commercial dying was immersed for a short time in a boiling water-benzylalcohol (BA) solution containing 8-8.5% BA. After washing with water modified ("shock" crystallized) Nomex was dyed by heating in an n-butanol-water solution of a cationic dye [2]. This dying method appeared very effective. We supposed some structural changes in "shock" crystallized Nomex, which can affect other properties of the meta-aramid fibres. Indeed, it appeared that the shock-crystallized Nomex acquired a high affinity for silver. In this communiqué, metallization of meta-aramid fibres with silver is preliminarily described.

A wet sample of uncrystallized Nomex of size 6x6 cm was immersed quickly in boiling water (21.5 cm^3) + BA (2 cm^3) solution, was kept a boiling for 2-5 min, washed with water and dried or used immediately for metallization.

Fig.1. Proposal of the structure of Nomex modified by "shock" crystallization.

Metallization of Nomex was carried out as follows: "Shock" crystallized sample (3x3 cm) was kept in 0.2% $AgNO_3$ for 3 or 20 h settled in the darkness. Was washed well with water and irradiated with UV light (Philips UVA Mini Studio HB 171) for 1 h (0.5 h for each side of the sample). A control sample (Nomex unmodified by "shock" crystallization, treated with $AgNO_3$) was irradiated simultaneously. "Shock" crystallized sample became intensively coloured in red-brown or brown colour, whereas the control sample remained almost unchanged.

It appeared further that the metallized sample Nomex-Ag can be metallized additionally with silver: Nomex-Ag saturated e.g. with 0.2% $AgNO_3$ and irradiated with UV becomes very intense coloured and Ag^+ disappears from the solution (~0.3-0.5% Ag incorporates into the Nomex-Ag fibres to Nomex-AgAg during this second stage). Crystallized conventionally Nomex T-450® modified by "shock" re-crystallization shows a similar affinity to silver and ability to reduce silver photochemically like Nomex III though to a smaller extent. Intense colours were obtained for double metallized Nomex T-450-AgAg fabric.

Silver incorporated into meta-aramid fibres can be oxidized again by treating with $HgCl_2$ solution (discolouring of the sample).

Silver-gold Nomex (Nomex-AgAu) is obtained by irradiating Nomex-Ag saturated with a gold salt or complex e.g. NH_4AuCl_4.

Main observations only are noted in this communiqué. Further work is being developed extensively.

We propose a working model for possible structural changes of Nomex modified by "shock" crystallization (or re-crystallization), (Fig.1).
We suppose that as a result of a "shock" (violent) crystallization or re-crystallization, reorientation of CONH groups in polyamide chains takes place, enabling mutual interactions of these groups. Silver should occupy these regions.

We carried out preliminary investigations of electron paramagnetic resonance (EPR) signals of

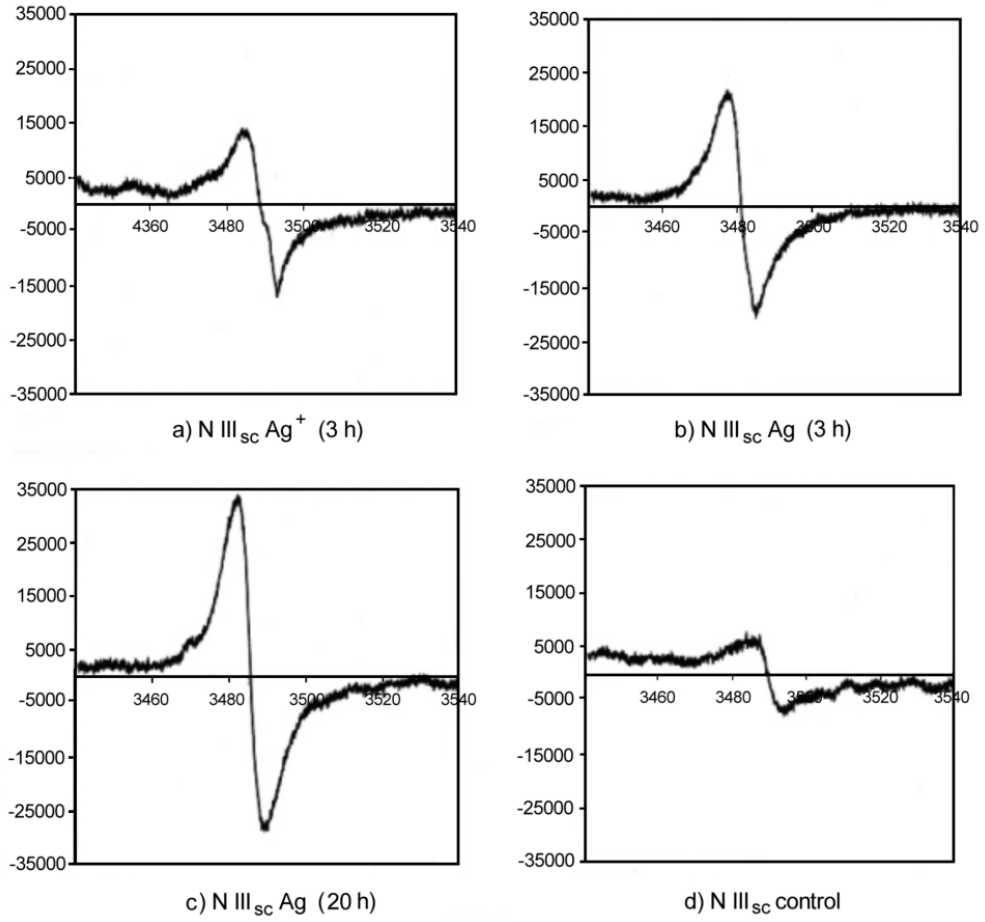

Fig.2. EPR signals of Nomex modified by "shock" crystallization and metallized with silver.

Nomex-Ag and Nomex-AgAg samples as well as of control samples. For comparison Nylon 6/6-Ag samples were prepared [3]. Some results are shown in Figs.2 and 3.

Nomex-Ag and Nomex-AgAg show EPR signal more intense for Nomex-AgAg than Nomex-Ag (and more intense for Nomex T-450 than Nomex III). It is surprising, however, that Nomex-Ag^+ as well Nomex T-450 show a similar signal. It is too early to discuss these data. We suppose only, that exchange of electrons between the aromatic system of Nomex and silver takes place. Absence of EPR signal in Nylon-Ag seems to support this conclusion.

This communiqué is first of the series concerning novel properties of "shock" crystallized aramid fibres as well as nylons.

It is rather impossible to indicate how important consequences of "shock" crystallization of aramid fibres and nylon are.

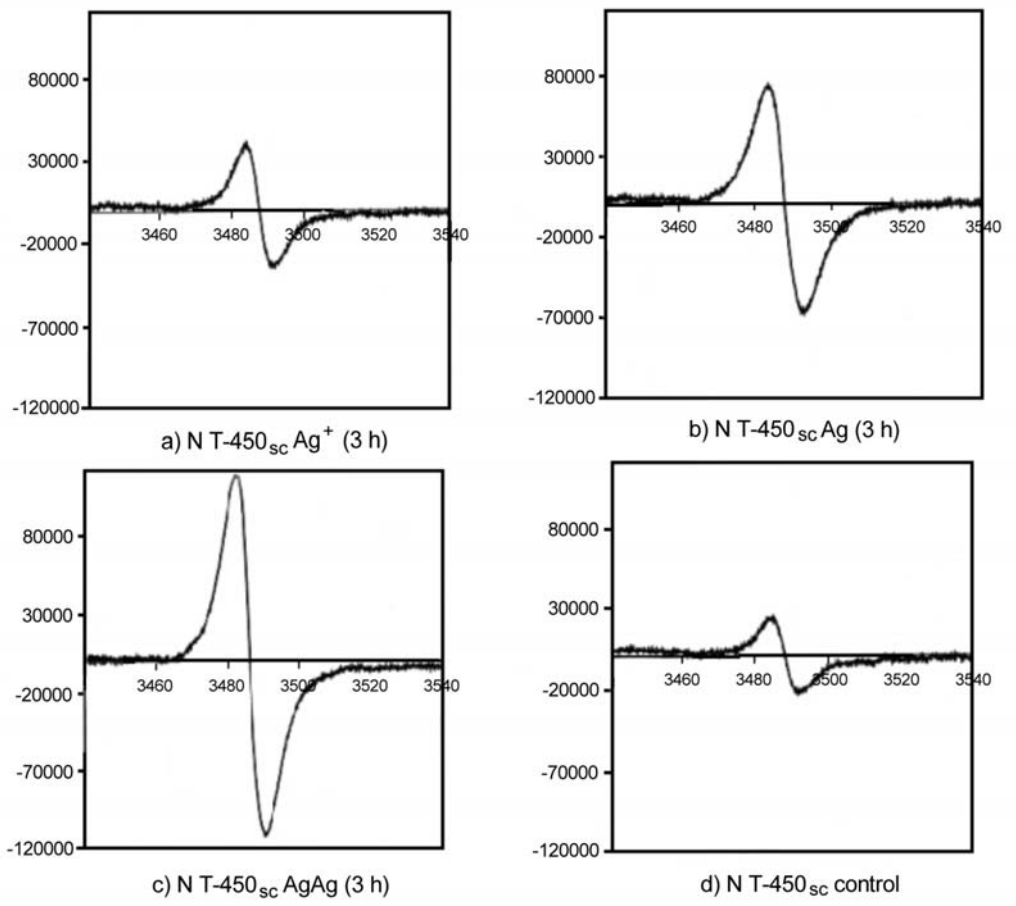

Fig.3. EPR signals of Nomex modified by "shock" crystallization and metallized with silver.

We thank Du Pont de Nemours Company for inspiration to our investigations on Nomex fibres.

References

[1]. Du Pont Engineering fibres, Nomex, H-53646 (2/94) BTL 402012.
[2]. Patent Application P. 352620.
[3]. Patent Application P. 357660.

APPLICATION OF INAA FOR ANALYZING TRACE ELEMENTS IN LEAD WHITE ORIGINATED FROM THE HANS MEMLING'S TRIPTYCH *THE LAST JUDGMENT*

Ewa Pańczyk, Justyna Olszewska-Świetlik[1/]

[1/] Institute of Monuments and Cultural Science, Nicolaus Copernicus University, Toruń, Poland

Beside identification of the type of lead white, determination of trace elements in this pigment is also helpful in the determination of age of painting and in identification of any repainting and conservatory treatment.

Samples for the analysis have been taken from the Hans Memling's triptych *The Last Judgment* (1465/67-1471). At present, the retable belongs to the collection of National Museum in Gdańsk. It has been founded by Angelo di Jacopo Tani, a

banker of the Medici family with the aim to be placed in the Badia Fiesolana church near Florence. In 1473, the triptych, along with other goods has been shipped from the Netherlands to Italy on the *Santa Mateo* galley leased by the Medici's bank representative at Bruges, Thomas Portinari. Near the coast of Gdańsk the galley has been attacked and robbed by the ship *Peter von Danzing* commanded by captain Paul Brenecke.

The triptych had been assigned to Saint Mary's Basilica at Gdańsk, which has become its owner till 1939.

Memling's *The Last Judgment* is one of the most precious works of art in Polish collections. During the past ages it was subjected to numerous conservatory procedures. Literature references list three conservations that are most important due to the scope of intervention concerning paint layers.

First of the conservations has been performed in 1718 by Christopher Krey a painter from Gdańsk. As the first step, at the left wing's obverse the painter has made the following inscription: "Renovirt Anno 1718 den 29 Julius Christoph Krey".

The second conservation has been performed by professor Bock in Berlin in 1815. It has involved cleaning the painting and partial removal of repaintings.

In 1851, the painting required thorough conservatory treatment that has been performed by professor Ch. Xeller from Berlin in co-operation with a painter named Stilbe. During the conservatory work aimed at removing repaintings, the head of the Redempted Man on a scale pan has been partially washed through, exposing a tin foil placed in this place. The author has performed reconstruction of the damage using a painting technique.

Investigations of the lead white should allow *inter alia* to find out if the distribution of trace elements concentration resembles that from other samples taken from the triptych or if it indicated later repaintings.

Aim of the tests of the lead white by neutron activation analysis was to determine the type of this pigment used in the workshop of Hans Memling and to find out if the distribution of trace elements concentration resembles that of other samples taken from the triptych or if it comes from later repaintings.

Four samples have been selected for the tests. Places, where the samples were taken from are indicated in Table 1.

The analysis of lead white samples has been performed by an instrumental neutron activation analysis (INAA) without any chemical treatment but using standards of the analyzed elements. Assuming that isotopes of the elements undergo nuclear reactions with thermal neutrons, the method allows for a quick, non-destructive, concurrent analysis of tens of elements. The biggest advantage of INAA is its high sensitivity that allows to detect numerous elements. An additional advantage results from the fact that the matrix – lead white ($2PbCO_3Pb(OH)_2$) does not contain any elements that would give a gamma radiation emitting isotopes as a result of the nuclear reaction (n, γ).

After recording their weights, all samples were placed in sealed quartz ampoules and packed in batches along with standards of 42 elements being determined. Standards of scandium and gold were added to each batch of samples as monitors of thermal neutron flux.

Irradiation of the samples has been performed in the MARIA reactor at Świerk (Poland) in a channel of a density of thermal neutron flux equal to 8×10^{13} n/cm^{2}s. The samples were irradiated for 24 h and cooled down for 12 h. Radioactivity measurements of the irradiated samples have been performed using an HP-class germanium detector, manufactured by ORTEC, coupled to a spectrometric system CANBERRA – System S100 controlled by an IBM computer. The analysis of spectra of gamma radiation emitted by the samples has been performed using a micro-SAMPO and Genie-2000 software provided by CANBERRA. Six series of the measurements have been performed within 2 months since irradiating the samples in the reactor. Time of the measurement has varied from 1000 to 10 000 s.

Forty elements have been identified and determined in the examined samples. Concentrations of the determined elements are shown in Table 2.

A multi-dimensional statistical analysis methods – analysis of agglomeration and analysis of major components – have been used for processing of the obtained data, using a STATISTICA 5.5 software manufactured by Statsoft. Analysis of agglomeration was performed for all determined elements. The results, obtained for 4 examined samples and 40 determined elements are presented in Fig.1 in the form of a dendrogram.

Concentration of trace elements in the lead white that was used for painting the triptych is char-

Table 1. Description of samples.

Sample No.	Place	Sample No. on the drawing
1	Lead white, impasto, cloud, left side of the painting, central table	m-1
2	Lead white, impasto, eye of the Redempted Man (Tomas Portinari) on the scale pan of Archangel Gabriel, central table	m-2
3	Lead white, impasto, white trimming of the dress of Caterina Tanagli, reverse, right wing	m-3
4	Lead white, impasto, first step next to the signature of Ch. Krey, *The Paradise*, obverse, wing	m-4

Table 2. Concentration of determined elements in the lead white samples taken from the H. Memling's painting *The Last Judgment*.

Sample No. / Element	1	2	3	4
Na	52 900	199 000	17 600	133 000
K	5 680	22 000	8 060	65 300
Sc	11 000	49 900	19.3	77.1
Cr	53.50	179	1 460	4 960
Mn	72.80	340		9 140
Fe	701	3 370	505	1 860
Co	11.40	52.20	6.19	33.60
Cu	17	168	22.40	76.20
Ni	103	401	24.70	
Zn	0.275	2.21	0.18	1.64
Ga		249		
As	9.46	7.18	1.72	6.47
Br	1 620	24 900	7 200	23 400
Se	58.5	365		437
Rb	308	3 810		
Sr	5 280			
Mo	161	84.6	66.4	107
Ag	3.21	14.8	5	11.9
Cd	643	558		
Sn	11 300	13 300	80.6	1 440
Sb	74.3	228	97.7	84.9
Cs	350	1 090	64.4	266
Ba	13 900	40 400	22 700	155 000
La	1.32	4.56	0.46	1.54
Ce	7.87	31.40	0.413	1.41
Sm	0.358	2.82	0.086	0.338
Nd	479	1 530		
Eu	0.115	0.652	0.0143	0.0713
Pr				3.17
Ho			0.76	
Yb	0.582		1.29	4.07
Lu			8.3	9.61
Hf	3.95			
Ta	0.11	0.47		
W	37.1	55.6	46.8	203
Ir	1.08	5.51	0.89	0.84
Au	2.92	7.75	7.98	2.8
Hg	109.0	529.0	74.7	40.9
Th	0.99	38.30	0.31	1.22
^{238}U	0.2	2.67	0.248	0.14

acteristic of the so-called transalpine white that has been used in Northern Europe.

Transalpine white differs from the so-called cisalpine white by lower concentrations of copper and manganese and higher concentrations of silver and antimony.

Samples from the central part of the triptych (sample No. 1) and from the obverse (sample No. 3) have been considered as the original white paint.

Sample No. 2, taken from the face of the Redempted Man differs both from the original samples (No. 1 and No. 3) as well as from that cor-

responding to the conservation performed in 1718 (sample No. 4). Both those samples (No. 2 and No. 4) show higher concentrations of copper, manga-

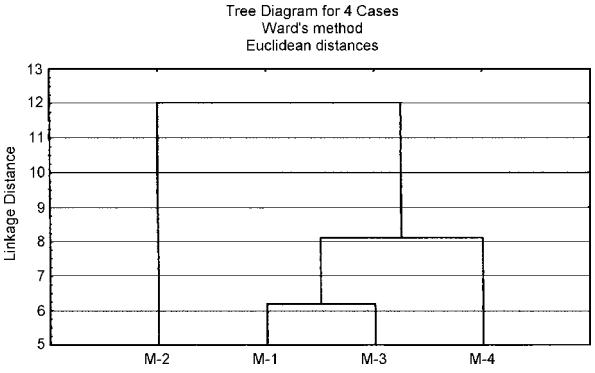

Fig.1. Cluster analysis of 4 samples taken from *The Last Judgment* by H. Memling described by 40 features.

nese, silver and cobalt, also concentration of zinc is higher compared to that in the remaining samples. Furthermore, concentrations of antimony and thorium in the sample No. 2 are higher than those in the remaining samples. Analysis of the content of lanthanium, cerium, samarium, europium and ytterbium with respect to chondrite (Fig.2) shows also that the sample No. 2 differs significantly from

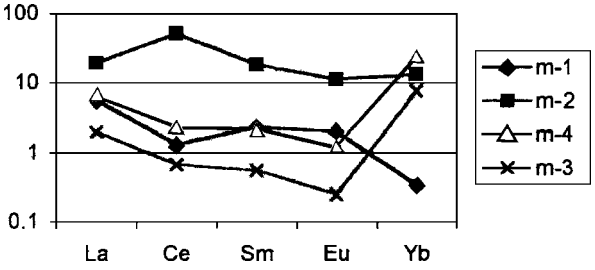

Fig.2. Trace element pattern in 4 lead white samples taken from *The Last Judgment* by H. Memling.

the other samples. Some authors [1] are suggesting that identification of lead white should be based upon the ratio of copper and lead (Cu/Ag) concentrations. The ratio (sample No. 1 – 5.3, sample No. 2 – 11.35, sample No. 3 – 4.48 and sample No. 4 – 6.4, respectively), determined for the examined samples confirms also that the sample No. 2 differs significantly from the remaining samples (Fig.3).

Performed examinations have proven that for painting the triptych Hans Memling had used a white paint characteristic by a high purity. Different type of lead white from the face of the Re-

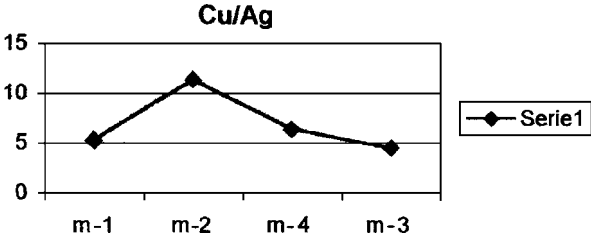

Fig.3. The ratio Cu/Ag determined for 4 samples of lead white taken from *The Last Judgment* by H. Memling.

dempted Man confirms subsequent repainting done by Xeller, described in the literature. Distribution of trace elements concentration is close to that of the 19th century lead white.

This observation confirms the washing of the face of the Redempted Man by Xeller and its subsequent reconstruction. Determination of the scope of this reconstruction would require examining a larger number of samples. Most certainly, the upper layers, such as the highest lights and impastos have been repainted. This circumstance has precluded the possibility to compare the lead white to the original and thus to dispel all doubts concerning repainting the Redempted Man's head.

The examinations, performed by neutron activation analysis have indicated what type of the lead white has been used by Hans Memling to paint the triptych. They have allowed to differentiate two, distant in time, layers of repainting.

References

[1]. Kuhn H.: Trace elements in white lead and their determination by emission spectrum and neutron activation analysis. Stud. Conserv., 2, 4 (1966).

SEM INVESTIGATIONS OF PARTICLE TRACK MEMBRANES WITH DIFFERENT SHAPES OF PORES

Bożena Sartowska, Oleg Orelovitch[1/]

[1/] Flerov Laboratory of Nuclear Reaction, Joint Institute for Nuclear Research, Dubna, Russia

The production process of particle track membranes is well documented in the literature [1, 2]. During the last years some kinds of membranes with new parameters were produced. To understand details of the production process, we need to investigate membrane parameters and determine their characteristic features. We investigated membrane surfaces and fractures and characterized their pores using a scanning electron microscopy (SEM).

Track membranes made with special technology from PC (polycarbonate) and PET (polyethylene terephthalate) were investigated. We expected to obtain non-cylindrical channels through the membrane and very small pores on the surface. This type of asymmetrical membranes were produced in the Center of Applied Physics of Joint Institute for Nuclear Research (Dubna, Russia). To investigate these kinds of small objects we need to use special technique of sample preparation. The surface of the membrane was observed to determine the diameter of pores. Fractures were investigated to determine the shape of pores and to measure detailed data on the membrane structure.

The brittle fracture of the membrane was made using the destruction of samples by UV irradiation [3, 4]. The samples were fixed using the con-

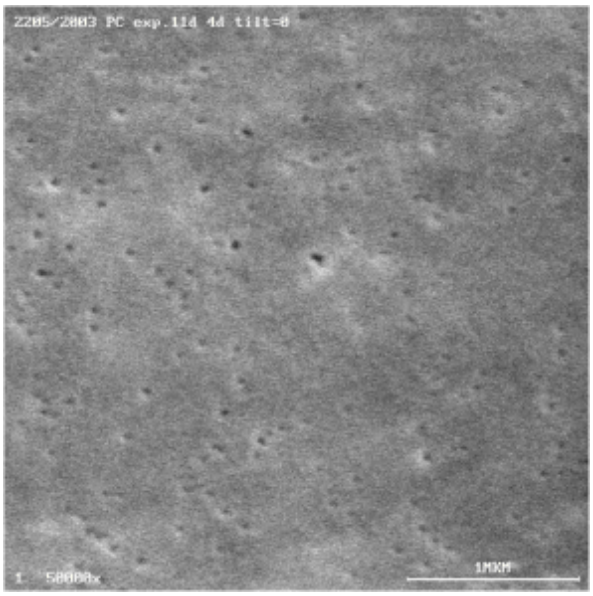

Fig.1. View of the surface of the PC particle track membrane.

ductive glue (Quick Drying Silver Paint, Agar Scientific Ltd.). The samples were coated with a thin layer of metal to reduce the charging which takes place during SEM observations [5]. Then, they were covered with a layer (about 10 nm) of gold using a vacuum evaporator JEE-4X (JEOL, Japan) with high vacuum 2.5×10^{-4} Pa. A special facility inside the bell was used to diminish the influence of overheating of the membrane surface. The distance between the Au source and sample level was 24 cm. This condition allow us to protect the sample from heat destruction and to keep real parameters of objects [6]. Observations were carried out using

Fig.2. Fracture through the PC particle track membrane.

SEM JSM 840 (JEOL, Japan) and SEM LEO 1530 GEMINI (Leo, Germany) with low accelerating voltage – 1.35 kV. This SEM has enough resolution to measure small morphological objects, not only register the presence of them.

Figure 1 presents surface morphology of investigated PC membrane. The pore diameter on the surface measured by SEM was on average 52.31 nm with standard deviation $\sigma = 12.42$ nm. Multiple pores can be seen. Counted pore density was 1.7×10^9 cm^{-2}.

Figure 2 shows the fracture through the PC membrane. Non-cylindrical pores can be clearly seen. Pores were in the shape like spindle with increasing diameter from the membrane surfaces to the core. The diameter of the inner part of pores is bigger than the pore diameter on the surface and it was estimated as 90.0 nm with standard deviation $\sigma = 16.46$ nm. Pores were randomly oriented – not parallel to each other and their directions are not perpendicular to the surface.

Figure 3 shows the fracture through the PET membrane. Non-cylindrical pores can be observed. Pores were in the bottle like shape with increasing

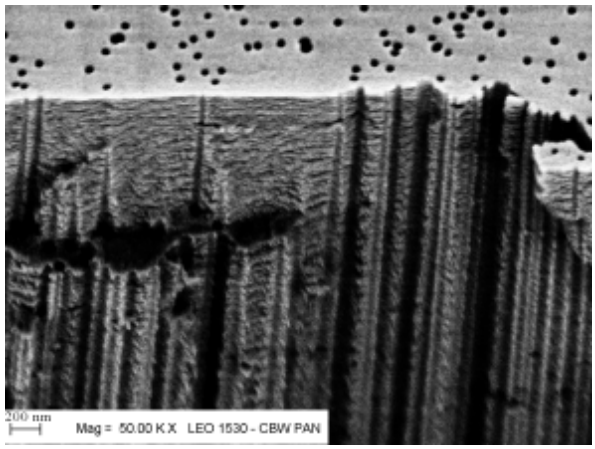

Fig.3. Fracture through the PET particle track membrane.

diameter from the surfaces to the core. The diameter of the inner part of pores is bigger than the pores diameter on the surface and it was estimated as 92.31 nm with standard deviation $\sigma = 15.34$ nm. The length of the upper part of the bottle like pores were estimated in the range 600-800 nm. Pores are parallel to each other, their directions are perpendicular to the surface.

Scanning electron microscope is an useful tool for investigations of very small objects like non-cylindrical pores in non-symmetrical membranes.

Investigations of non-symmetrical membranes using a special preparation procedure and SEM observations will be continued.

Thanks to Dr. Adam Presz (Unipress, Warszawa, Poland) for help in SEM observation.

References

[1]. Kuznietsov V.I., Didyk A.Yu., Apel P.Yu.: Radiat. Meas., 19, 1-4, 919-924 (1991).
[2]. Spohr R.: Ion Tracks and Microtechnology. Principles and Applications. Vieweg, Braunschweig 1990, 272 p.
[3]. Orelovitch O.L., Apel P.Yu.: Instrum. Exp. Tech., 44, 1, 111-114 (2001).
[4]. Orelovitch O.L., Apel P.Yu., Sartowska B.: Mater. Chem. Phys., 81, 2-3, 349-351 (2003).

[5]. Goldstein I.J.: Electron Microscopy and X-Ray Microanalysis. Text for Biologist, Material Scientists and Geologists. Plenum Press, New York 1992, 820 p.
[6]. Orelovitch O., Sartowska B.: Methods of Scanning Electron Microscopy in Particle Track Membrane Investigations. X Conference on Electron Microscopy of Solids, Warszawa-Serock, Poland, 20-23 September 1999, pp. 397-400.

INVESTIGATIONS OF PHASE TRANSFORMATIONS IN THE NEAR SURFACE LAYER OF CARBON STEELS MODIFIED WITH SHORT INTENSE NITROGEN AND ARGON PLASMA PULSES

Bożena Sartowska[1/], Jerzy Piekoszewski[1,2/], Lech Waliś[1/], Zbigniew Werner[2/], Jacek Stanisławski[2/], Władysław Szymczyk[2/], Michał Kopcewicz[3/]

[1/] Institute of Nuclear Chemistry and Technology, Warszawa, Poland
[2/] The Andrzej Sołtan Institute for Nuclear Studies, Świerk, Poland
[3/] Institute of Electronic Materials Technology, Warszawa, Poland

It is well documented in the literature that when stainless steel is exposed to nitrogen at elevated temperature incorporation by such techniques as ion implantation, plasma immersion ion implantation (PI^3) and rf plasma nitriding, then several nitrides are formed depending on the processing conditions. Among all phases formed in this way an expanded austenite, denoted by γ_N or S phase, attracts a special interest of many authors, e.g. [1-6]. The expanded austenite is an interstitial solution of N – γN or (C – denoted by γ_C) in FCC lattice of iron. Figure 1 presents position of iron atoms and octahedral interstitial sites in FCC lattice. As for Fe-C austenite it is generally accepted that carbon atoms are separately distributed among the octahedral sites in the FCC lattice and, therefore, that there exists a repulsive interaction between the carbon atoms. As for the Fe-N austenite, it has been presumed that nitrogen atoms are randomly distributed. The interaction is strongly repulsive between the first nearest-neighbouring atoms and weakly attractive between the second nearest [3]. Figure 2 presents the possibilities of iron and nitrogen (carbon) atoms configurations [4]. Authors' interest is generated by the fact that due to the presence of γ_N phase in stainless steel, good corrosion resistance is maintained while the wear resistance is increased. As stated in [5] the γ_N phase can only be formed if iron, chromium and nickel elements are available in the system. The situation becomes quite different when the process applied leads to melting of the near-surface region of the steel substrate.

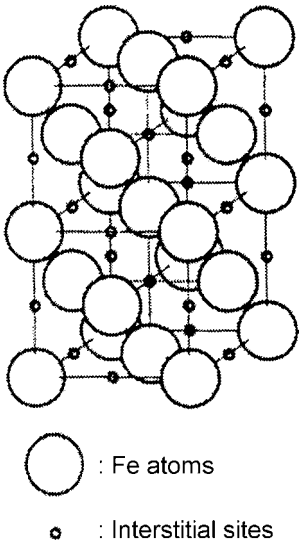

Fig.1. Position of iron atoms and octahedral interstitial sites in FCC lattice.

The aim of this work was to investigate the phase transformations in the near surface layer of various types of carbon steels irradiated with short (μs range), intense (5-6 J/cm^2) nitrogen and argon plasma pulses.

Five carbon steels with different concentration of carbon in the range of 0.01 to 0.93% wt. were used. Samples were heat treated according to standard procedures predicted for these steels (PN-93/H-8409 and PN-84/H-8500) and polished to $R_a < 0.35$ μm.

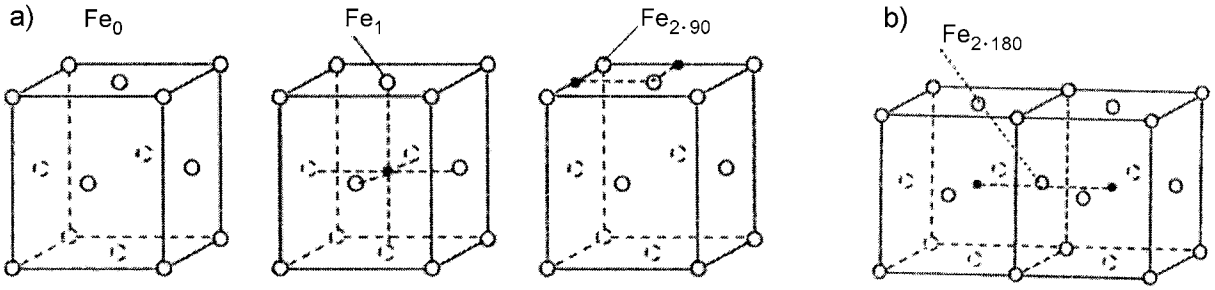

Fig.2. a) A single carbon (nitrogen) atom and carbon (nitrogen) atom pair in the first coordination sphere (90° pair), b) nitrogen atoms in 180° configurations.

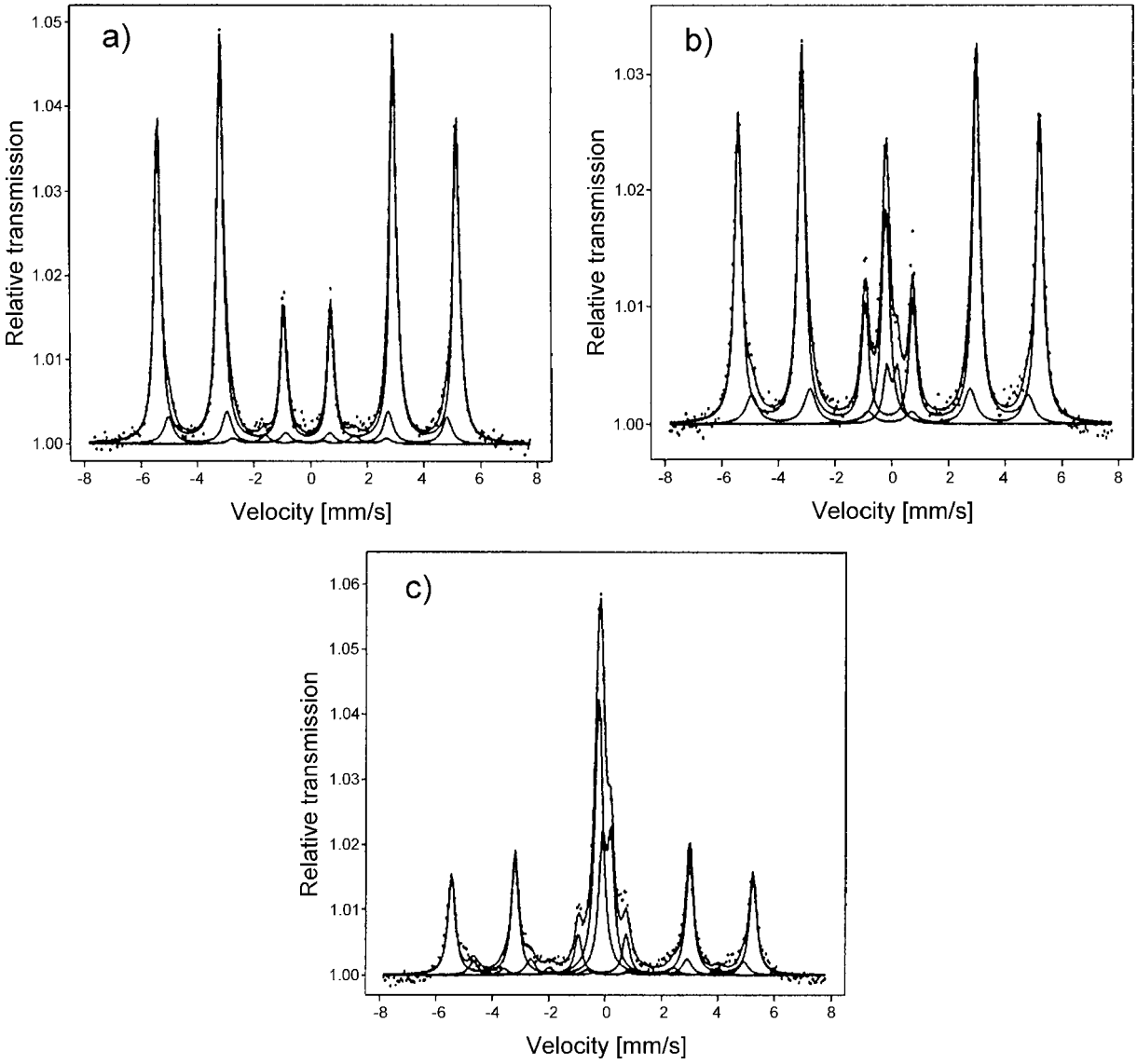

Fig.3. CEMS data for steel 45: a) initial, b) modified with argon intense pulsed plasma beam, c) modified with nitrogen intense pulsed plasma beam.

The plasma pulses were generated in a rod plasma injector (RPI) type of plasma generator described in [7]. The device is used at the Andrzej Sołtan Institute for Nuclear Studies for material modifi-

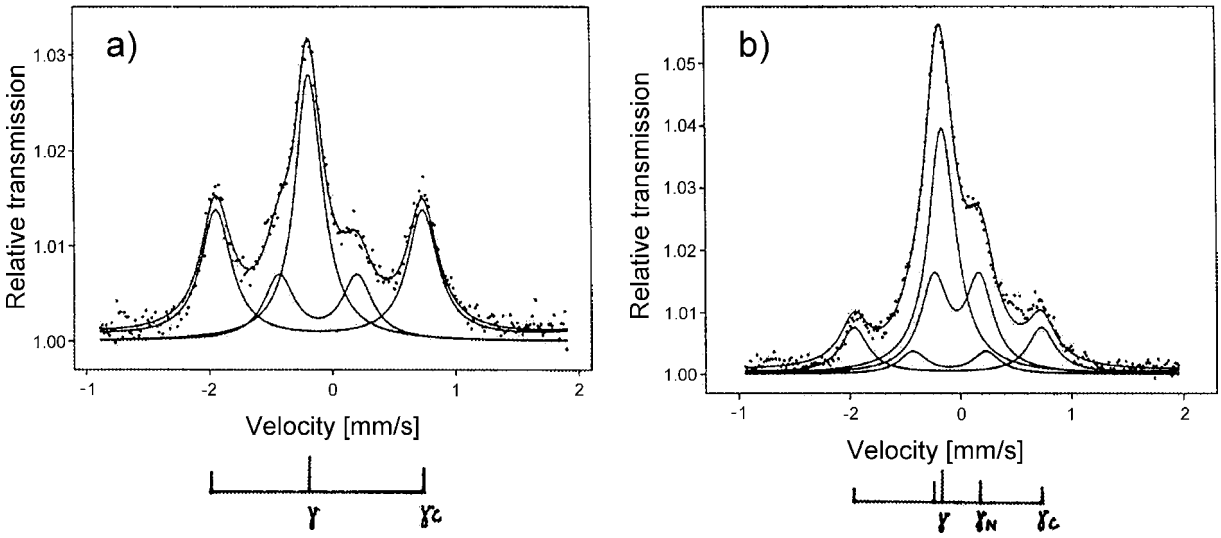

Fig.4. CEMS data with fitted identified phases for steel 45: a) modified with argon intense pulsed plasma beam, b) modified with nitrogen intense pulsed plasma beam.

cations. In the experiment, two types of plasma pulses were used to compare effects of thermal processes and supplied reactive gas. The samples were irradiated with five plasma – argon or nitrogen short (μs range) pulses at an energy density of about 5 J/cm^2. The cooling rate was in the range of 10^7-10^8 K/s.

In our nitrogen phase investigations, samples were characterised by the following methods: nuclear reaction analysis (NRA) $^{14}N(d,\alpha)^{12}C$ for determination of retained nitrogen dose, conversion electron Mössbauer spectroscopy (CEMS) for phase identification and quantitative analysis of phase presence, X-ray diffraction analysis (GXRD) with grazing incidence angle Θ between 0.5 and 2° for phase identification.

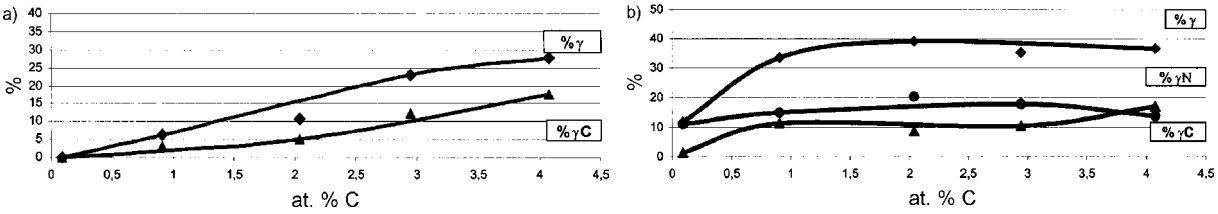

Fig.5. Fraction of paramagnetic phases after the intense pulsed plasma: a) argon, b) nitrogen intense pulsed plasma beam modification.

CEMS measurements, phase identification and determination of phase value were carried out using a procedure described in [8]. CEMS spectra obtained for all states of investigated materials (initial and modified with argon or nitrogen plasma) show the difference between these sets of samples. It means that the phase composition was transformed as a result of irradiation processes and it was different for argon and nitrogen treatment. Figure 3 presents CEMS spectra for steel 45. Changes in the central part of them can be seen.

Following the literature data [3-6, 8] we could predict that the nitrogen austenite – γ_N phase will be part of the observed paramagnetic phase. Obtained graph analyse (fitting procedure) confirmed our prediction (Fig.4). In steels irradiated with argon the γ and γ_C – carbon austenite were found. In all steels irradiated with nitrogen plasma the γ, γ_N – nitrogen austenite, γ_C – carbon austenite and ε – Fe_3N phases were found.

Figure 5 shows the presence of paramagnetic phase in modified layer of samples. It can be clearly seen that fraction of paramagnetic phases (γ, γ_C and γ, γ_C, γ_N for argon and nitrogen, respectively) in a modified layer is on the higher level after nitrogen plasma modification. These results show big differences in austenitization efficiency between argon and nitrogen modification processes.

To make our point stronger, X-ray diffraction investigations were carried out. GXRD measurements confirmed the fact of presence γ_N phase in samples modified with nitrogen. This fact was determined in order to peaks shifting as a result of change the austenite lattice parameter amounts to 0.83%.

In conclusion: thin modified layers were created in the near-surface region of carbon steels (without presence of nickel and chromium) treated with short intense pulsed argon or nitrogen plasma beams. The paramagnetic phases were detected in the modified layers. The nitrogen expanded austenite – γ_N phase was created using nitrogen intense pulsed plasma beam. For now the full explanation of the observed differences in austenitization efficiency between argon and nitrogen plasma modification is not ready.

Further studies in this direction are in progress in our laboratories. Especially we plan to determine the nitrogen and carbon distribution in a modified layer.

References

[1]. Williamson D.L., Oztruk O., Glick S., Wei R., Wilbur P.J.: Nucl. Instrum. Meth. Phys. Res. B., 59/60, 737-741 (1991).

[2]. Collins G.A., Hutchings R., Short K.T., Tendys J., Li X., Samandi M.: Surf. Coat. Technol., 74-75, 417-424 (1995).

[3]. Oda K., Umezu K., Ino H.: J. Phys.: Condens. Matter., 10147-10158 (1990).

[4]. Gavriljuk V.G., Berns H.: High nitrogen steels. Structure, Properties, Manufactures, Applications. Springer-Verlag, Berlin Heidelberg 1999, 384 p.

[5]. Menthe E., Rie K.-T., Schultze J.W., Simon S.: Surf. Coat. Technol., 74-75, 412-416 (1995).

[6]. Jirásková Y., Blawert C., Schneeweiss O.: Phys. Status Solidi A, 175, 537-548 (1999).

[7]. Werner Z., Piekoszewski J., Szymczyk W.: Vacuum, 63, 701-708 (2001).

[8]. Piekoszewski J., Langner J., Białoskórski J., Kozłowska B., Pochrybniak C., Werner Z., Kopcewicz M., Waliś L., Ciurapiński A.: Nucl. Instrum. Meth. Phys. Res. B., 80/81, 344-347 (1993).

NUCLEONIC CONTROL SYSTEMS AND ACCELERATORS

A NEW XRF ANALYSER AF-30

Ewa Kowalska, Edward Świstowski, Piotr Urbański, Jan Mirowicz

A new analyser was designed and manufactured (Fig.1). As compared with the previous models of the XRF analysers produced in the Institute of Nuclear Chemistry and Technology [1], the AF-30 has a better performance and user-friendly operation.

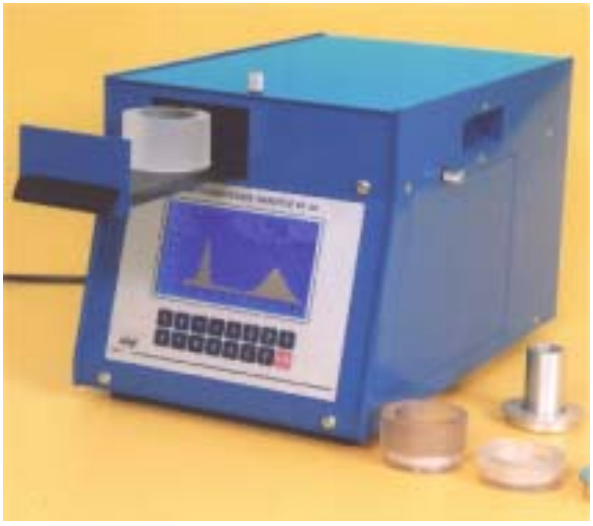

Fig.1. General view of fluorescent analyser AF-30.

It is a laboratory device intended for the analysis of elements having atomic numbers higher than 16 in solid, liquid and powdered samples. The principle of operation is based on the low resolution of X-ray fluorescence and its block diagram is shown in Fig.2. Four different types of the radioactive sources can be used: Fe-55, Pu-238, Cd-109 and Am-241, as well as proportional counters filled with various gases (Ar, Xe, Kr). The instrument was designed in such a way that the distances between the sample and detector as well as between the source and detector could be controlled separately with high precision. It allows to optimise the signal to background ratio and to improve accuracy of measurements. The secondary radiation excited in a sample is registered by a proportional counter and after amplification and preliminary discrimination is fed to the multichannel analyser. A microprocessor unit performs further processing of the signal. The developed software allows operating the analyser AF-30 in the dialogue system using numerical keyboard and display. The instrument can operate as the 256-channel pulse high analyser (PHA) and as a dedicated device for the elemental analysis of a sample. The X-ray spectra collected by the PHA can be displayed, smoothed and stored in the internal memory (up to 8 spectra). Three different windows can be chosen using cursors, and the count number registered within the windows can be displayed and stored.

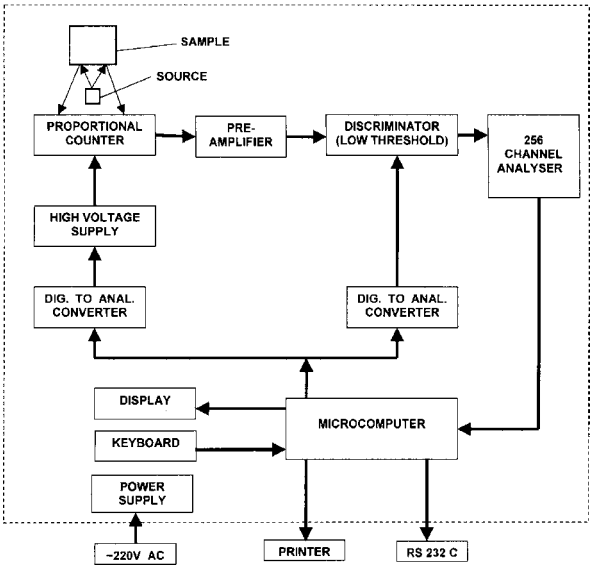

Fig.2. Functional diagram of analyser AF-30.

Qualitative analysis of samples of unknown chemical composition as well as preliminary setting of measuring parameters can be performed in the mode ANALYSER. Operation of the instrument in the mode MEASUREMENTS is possible after a calibration model for the chosen measurement is introduced and stored in the memory. Such procedure can be accomplished by the manufacturer or by the end user.

The modern software used for operation of the instrument allows introducing even very sophisticated calibration procedures [2-5]. The results of the measurements are displayed, printed or transmitted to a computer and stored in the memory (up to 99 results).

The developed analyser is a versatile instrument and can find numerous applications. Three analysers were applied for routine measurements of the ash content in lignite in a power station in Mongolia.

References

[1]. Urbański P.: Application, manufacturing and trends in development of nucleonic gauges in Poland. Institute of Nuclear Chemistry and Technology, Warszawa 1998. Raporty IChTJ. Seria A No. 2/98.

[2]. Urbański P., Kowalska E.: X-Ray Spectrom., 24, 70-75 (1995).

[3]. Urbański P., Kowalska E.: Nukleonika 42, 3, 719-726 (1997).
[4]. Urbański P., Kowalska E.: Wielowymiarowe metody kalibracji przyrządów pomiarowych. IV Konferencja „Metrologia wspomagana komputerowo", Rynia near Warszawa, Poland, 7-10 June 1999, pp.251-258.
[5]. Kowalska E., Jakowiuk A.: Opracowanie procedur transferu modeli kalibracyjnych do analizatora fluorescencyjnego AF-20. Instytut Chemii i Techniki Jądrowej, Warszawa 2001. Raporty IChTJ. Seria B No. 8/2001.

MEASUREMENTS OF ASH CONTENT IN LIGNITE FROM MONGOLIAN MINES

Ewa Kowalska, Piotr Urbański

Composition of the Mongolian lignite is different compared with the Polish one, generally because of lower content of calcium and a higher range of ash contents. The ash content in the Mongolian lignite depends strongly on the pit from which it was mined.

The AF-30 analyser with an Ar proportional counter and a Cd-109 X-ray source was used for laboratory analysis of the air-dry powdered lignite samples. Diameter of the powdered lignite was below 0.2 mm. The samples were poured into a measuring cell whose bottom is made of a mylar foil of 6 μm thick. Spectra of the three samples of various ash contents are presented in Fig.1. The main information about the ash content (average atomic number $Z \approx 11$) in coal ($Z = 6$) is contained by the intensity of scattered radiation (I_R) represented by peak 3 in Fig.1. Intensity of the scattered radiation increases with a decrease of the ash content [1]. Since the atomic numbers of calcium and iron (20 and 26, respectively) are much higher than the average atomic number of ash, their variability in the measured samples should be taken into account by the calibration model. Thus, the intensity of the K Fe X-rays (I_{Fe} – peak 2) as well as K Ca X-rays (I_{Ca} – peak 1) should be included in the calibration model.

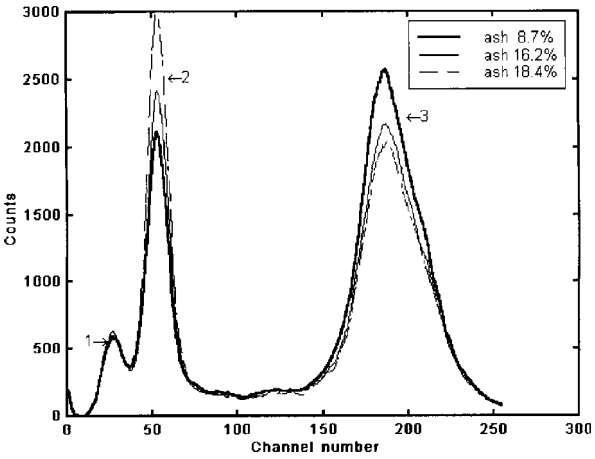

Fig.1. Spectra of the secondary X-rays from the lignite samples irradiated with Cd-109 source.

The set of calibration samples contained two subset of samples from two different pits: subset 1 – 23 samples of ash content from 8.7 to 21.4%, subset 2 – 16 samples of ash content from 11.5 to 26.46%.

The X-ray spectra of the calibration samples were measured and five different calibration models were investigated: I – full spectrum partial least square (PLS) regression [2, 3]; II – multi-linear regression (MLR) for three variables I_{Ca}, I_{Fe}, I_R; III – MLR for three variables I_{Ca}, I_{Fe}, $1/I_R$; IV – MLR for two variables I_{Fe}, I_R; V – MLR for two variables I_{Fe}, $1/I_R$.

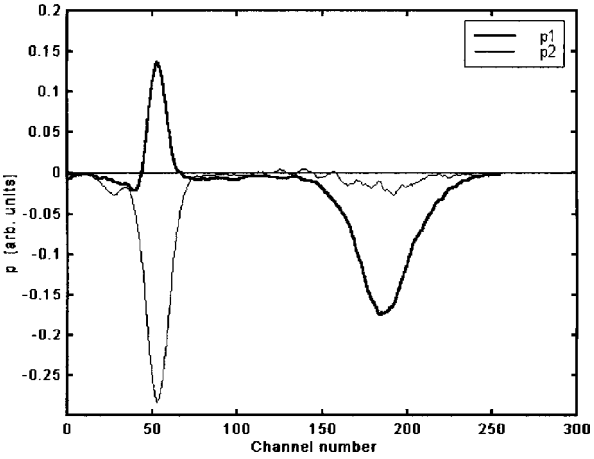

Fig.2. Spectra of two loadings of the PLS model.

For assessment of the considered models two parameters were chosen: RMSEE (root mean square error of estimation) and RMSECv (root

Table. Performance of the calibration models.

Samples	Parameter	PLS $a=2$	MLR 3 variables I_{Ca}, I_{Fe}, I_R	MLR 3 variables $I_{Ca}, I_{Fe}, 1/I_R$	MLR 2 variables I_{Fe}, I_R	MLR 2 variables $I_{Fe}, 1/I_R$
Subset 1	RMSEE	0.777	0.75	0.784	0.78	0.824
	RMSECv	**0.976**	**0.962**	**1.04**	**0.938**	**1.006**
Subset 2	RMSEE	1.8	1.92	1.76	1.937	1.808
	RMSECv	**2.05**	**2.22**	**2.00**	**2.16**	**2.016**

mean square error of cross-validation) [4, 5], and the obtained results are summarised in Table.

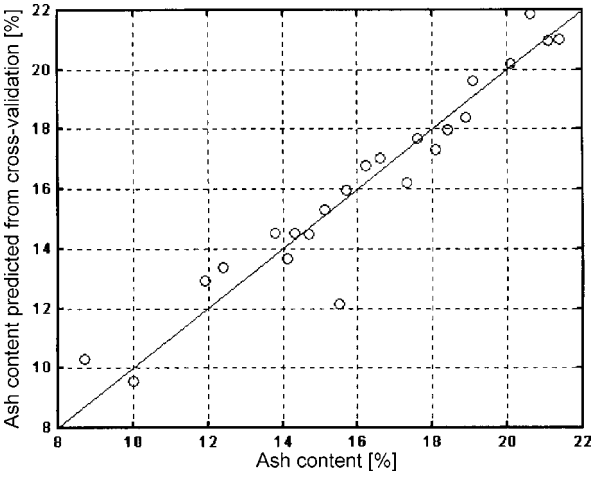

Fig.3. Cross-validated *vs*. reference ash content for the three variable MLR model.

It is seen that there are no significant differences between the considered calibration models. For the PLS with two factors ($a = 2$) about 94.6% variability of ash content is explained by the model. Third factor ($a = 3$) included into the model improves slightly RMSEE, however gives a higher value of the RMSECv. The spectra of the two loadings p1 and p2 of the PLS model are shown in Fig.2. It can be seen that the intensities of the I_{Fe} and I_R are much more important for determination of the ash content than intensity of the I_{Ca}. If so, one can expect to obtain similar results applying simpler models. Instead of the full-spectrum model, the MLR models with three (I_{Ca}, I_{Fe}, I_R) or two variables (I_{Fe}, I_R) were considered.

Results of cross-validation of the three variables MLR model:

$$C = a_0 + a_1 I_{Ca} + a_2 I_{Fe} + a_3 I_R \qquad (1)$$

where: C – ash content; a_0, a_1, a_2, a_3 – regression coefficients, are presented in Fig.3.

In the AF-30 analyser designed for application of ash content in lignite for a Mongolian power station both the three variables and two variables MLR models were programmed.

To compensate decay of the Cd-109 X-ray source, all measured count rates are related to the count rates obtained from the standard sample delivered with every AF-30 analyser.

References

[1]. Sikora T., Czerw B.: Nukleonika, 44, 4, 669-674 (1999).
[2]. Urbański P., Kowalska E.: X-Ray Spectrom., 24, 70-75 (1995).
[3]. Urbański P., Kowalska E.: Nukleonika, 42, 4, 879-885 (1997).
[4]. Kowalska E., Urbański P.: Wielowymiarowa kalibracja w radiometrycznych pomiarach popiołowości węgla. Instytut Chemii i Techniki Jądrowej, Warszawa 2000. Raporty IChTJ. Seria B No. 10/2000.
[5]. Urbanski P., Kowalska E., Jakowiuk A.: Multivariate techniques in processing data from radiometric experiments. Conference "Isotope and Nuclear Analytical Techniques for Health and Environmental", Vienna, Austria, 10-13 June 2003.

MEASUREMENT OF RADON CONCENTRATION IN WATER

Bronisław Machaj, Jakub Bartak

The method of measurement of radon concentration in water described in [1] based on flushing large radon laden water sample in a closed loop with small air volume and measurement of radon concentration in air with the Lucas cell [2-6] was improved in further investigations. The improvement consists in applying a porous membrane filter that splits flushing air into tiny streams and a longer (5 min) flushing time (Fig.1) ensuring that equilibrium between the radon dissolved in water and radon flushed out into air is achieved. For such a case the relations can be written:

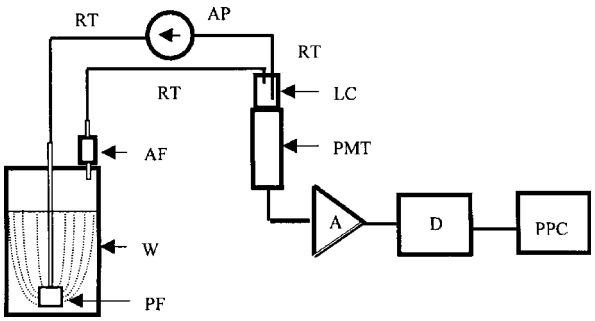

Fig.1. Measuring arrangement for measurement of radon concentration in water: WC – water container; AP – air pump; AF – air filter, cylinder ϕ15x55 mm filled with cotton; LC – Lucas cell 0.17 l; PMT – photomultiplier tube; A – pulse amplifier; D – pulse discriminator; PPC – programmable pulse counter; RT – rubber tubes (black) ϕ5 mm; PF – porous membrane filter.

$$Q = q\,kV_w + qV_p \qquad (1)$$

$$q = \frac{Q}{kV_w + V_p}\ \text{(Bq/l)} \qquad (2)$$

where: q – radon concentration in air, Q – radon concentration in water before flushing, k – coefficient of radon solubility in water [7-11], V_w – volume of water sample, V_p – volume of air. High radon concentration in air is achieved when the volume of air is smaller than the volume of water sample. This is illustrated in Fig.2 showing the radon concentration changes with variation of air volume at constant water volume. It can be shown that radon concentration in water is given by the relation:

$$Q = \frac{n}{180\ \nu\ k_t \varepsilon}\ (k + \frac{V_p}{V_w})\ \text{(Bq/l)} \qquad (3)$$

where: n – pulse count rate, ν – volume of Lucas cell, ε – detection efficiency of alpha radiation, k_t –

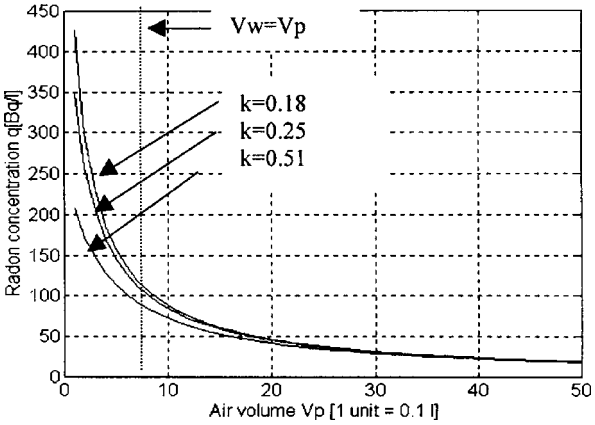

Fig.2. Radon concentration per air unit volume $q_p = 100/(V_p + k \cdot V_w)$ flushed out from water. Diagram is made for water sample V_w = 0.75 l, variable air volume, and for water temperature 0÷30°C (different k), radon concentration in water before flushing is 100 Bq/0.75 l.

coefficient taking into account no equilibrium between radon and radon daughters at the time of pulse counting as illustrated in Fig.3. For counting time equal to 10 min the k_t coefficient is defined as the ratio of mean count rate in the period 0-10 min to the mean count rate in the period 181-200 min.

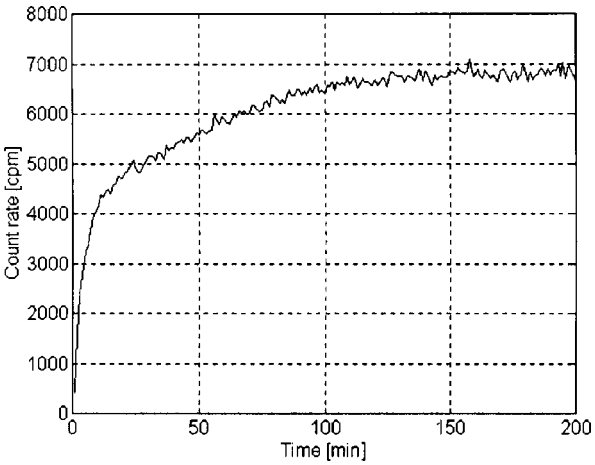

Fig.3. Count rate registered by Lucas cell against time since the moment flushing started for radon concentration in water 300 Bq/l.

Measurements of gauge model shown in Fig.1 indicate that sensitivity of the gauge is 9 cpm/(Bq/l) for counting time 10 min, Lucas cell volume v=0.17 l, detection efficiency ε = 0.66, water sample volume – 0.75 l, air volume – approximately 0.5 l. Minimum detectable radon concentration is Q_{mi} = 0.11 Bq/l. Relative random error of radon concentration in water due to fluctuations of count rate, decreases with an increase of radon concentration and at radon concentration: 1, 10, 100, 1000, 10 000 Bq/l is equal to: 11, 3.6, 1.1, 0.4, 0.1%, correspondingly.

References

[1]. Machaj B.: In: INCT Annual Report 2001. Institute of Nuclear Chemistry and Technology. Warszawa 2002, pp.135-136.
[2]. Lucas H.F.: Rev. Sci. Instrum., 28, 680-683 (1957).
[3]. Machaj B., Urbański P.: Nukleonika, 44, 579-594 (1999).
[4]. Machaj B. Urbański P.: Nukleonika, 47, 39-42 (2002).
[5]. Wardaszko T., Grzybowska D.: Nukleonika, 38, 103-108 (1993).
[6]. Surbeck H.: A radon in water monitor based on fast gas transfer membranes. International Conference on Technologically Enhanced Natural Radioactivity by Non-uranium Mining, Szczyrk, Poland, 16-19 October 1996.
[7]. Boyle R.W.: Phil. Mag., 22, 840 (1911).
[8]. Radon property and solubility. www.ed.gifu-u.ac.jp/~tasaka/html/property.html.
[9]. Weigel F.: Chemiker Zeitung, 102, 287 (1978).
[10]. Clever H.L.: In: Krypton-, Xenon-, Radon Gas Solubilities. Vol.2. Pergamon Press, Oxford 1985, pp.227-237. Solubility Data Series.
[11]. Karangelos D.J., Petropoulus N.P., Hinis E.P., Sinopoulus S.E.: Radon in water secondary standard preparation. www.nuclear.ntua.gr/public/rp_files/erricca_water.pdf.

ACTIVITY MEASUREMENT OF Tc-99m IN A LIQUID SOURCE

Edward Świstowski, Jan Mirowicz, Bronisław Machaj

A laboratory gauge designed for measurement of Tc-99m radioisotope in liquid form, flowing through a steel coil, was elaborated. The gauge is intended for use in the Department of Radiochemistry of the Institute of Nuclear Chemistry and Technology and was developed as part of a grant from the Polish State Committee for Scientific Research (KBN). Block diagram of the gauge is shown in Fig.1. A well NaI(Tl) scintillator is used as radiation detector. Output pulses from the photomultiplier tube (PMT) after amplification are fed to a single channel analyzer (SCA) and then are periodically counted by a programmable pulse counter under the control of microprocessor system. The measured count rate is simultaneously displayed on the gauge screen in the form of a diagram against elapsed time and is stored into the gauge memory. The SCA window covering energy range from 60-180 keV ensures a high detection efficiency and low sensitivity to gain variation. Differential spectrum of Tc-99m and position of the SCA window in respect to the spectrum is shown in Fig.2. Analysis of the spectrum in Fig.2 shows that variation of count rate due to PMT gain variation 5-7% that occurs within a short period of operation (some weeks) is not higher than 0.4%. To compensate variation of PMT gain in a longer period of time (some months) a semi-automatic gain control is foreseen. To carry out semi-automatic PMT gain control, the scintillator of the gauge is irradiated with an external low activity Cs-137 gamma source. The amplitude of the Cs-137

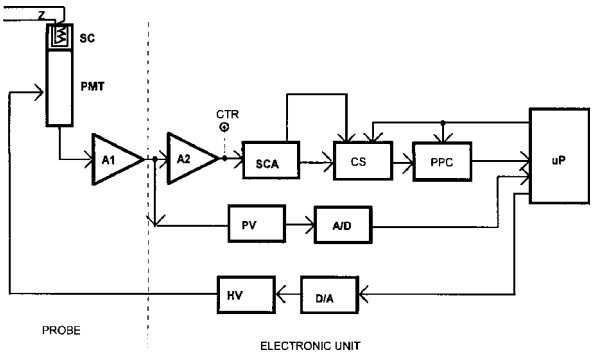

Fig.1. Block diagram of Tc-99m activity gauge: Z – liquid Tc-99m source; SC – well scintillator NaI(Tl); PMT – photomultiplier tube; A1, A2 – pulse amplifiers; CTR – control socket; SCA – single channel analyzer; CS – channel switch; PPC – programmable pulse counter; uP – microprocessor; PV – pulse amplitude; A/D – analog-to-digit converter; HV – high voltage power supply; D/A – digit-to-analog converter.

pulses measured by a peak voltmeter and by an analog-to-digit converter, is sensed by a microprocessor, and is compared with a reference voltage stored in the gauge memory. PMT high voltage is controlled by the microprocessor in such a manner as to get the Cs-137 pulse amplitude equal to the reference voltage.

Dead time of the measuring channel is 1 μs. Programmed counting time is 0.5-6 s. The gauge memory can store 20 series, each containing 1024 periodic count rate readings. Measuring results stored in the memory can be displayed on the gauge display. Any selected range of periodic measurements can be marked with a visible marker and the total sum of counts can be computed in a selected range. Serial port RS232 enables transmission of measuring results to an external computer.

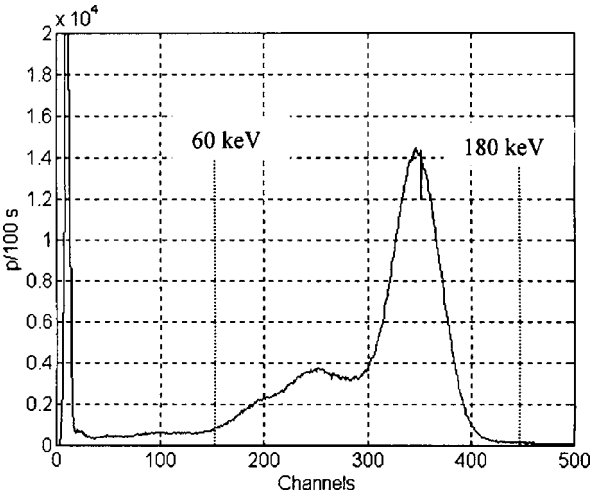

Fig.2. Differential spectrum of Tc-99m measured with a NaI(Tl) scintillator.

A RADIOMETER FOR MEASUREMENT OF LOW ACTIVITY ENVIRONMENTAL SAMPLES

Edward Świstowski, Jan P. Pieńkos

A radiometer RMA-1 for measurement of radioactive samples was developed in the Department of Radioisotope Instruments and Methods of the Institute of Nuclear Chemistry and Technology (INCT).

The gauge employs up to day technology and large scale integration electronics. Thanks to a microprocessor system used in the gauge, a high level of automatization of measuring process is ensured. The radiometer is equipped with three measuring channels for connection of scintillation probes type SSU-70 for measurement of α-, β- and γ-radiation. Additionally, the monitor is equipped with an interface for spectrometric measurement with a TUKAN multichannel analyzer. Block diagram of the monitor is shown in Fig.1.

The main component of the radiometer is a control and processing unit using the 8 bit microprocessor Z84C000, controlling operation of the monitor, collecting measuring results, processing measured signal and storing the data in the gauge RAM memory. The investigated processes can be watched on the screen at graphic display with 240x128 pixels resolution. The monitor is equipped with a 3.6 V battery (back-up battery) thanks to which the memory and real time clock of the monitor are backed up and the parameters are not lost.

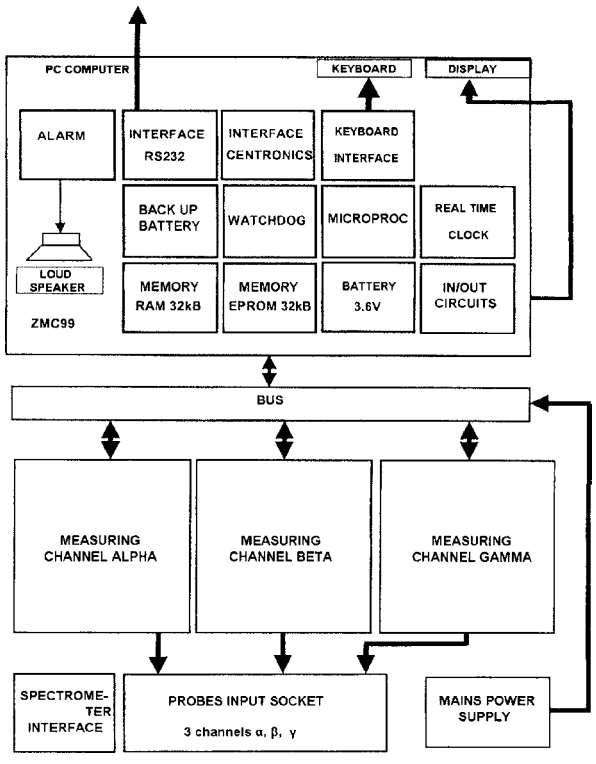

Fig.1. Block diagram of RMA-1 radiometer.

CMOS (complementary metal oxide silicon) technique used secures that current consumption is minimal and is approximately 1.5 A. Communication of the monitor with an external PC computer is ensured by serial port RS232. Operation of the monitor: setting parameters of measurements, communication, selection of measured data to be reviewed or displayed is ensured by reliable, long lasting, foil keyboard.

Each measuring channel is programmed individually. Counting time is set in the range 1-3600 s, number of measurements automatically repeated – 1-1024, pulse discrimination level – 0-4.096 V, photomultiplier tube high voltage – 600-1500 V. Up to 20 series of measurements, each 1024 reading long, for each measuring channel can be stored in the memory. The measuring results are displayed at the monitor display. An example of measuring results is shown in Fig.2.

The radiometer is designed for the needs of Radiation Protection Department of the INCT to carry out measurement of radioactive samples of low activity taken from different places of the environment (sewage, water, containers, environmental wastes), to make diagrams and reports from check up measurements.

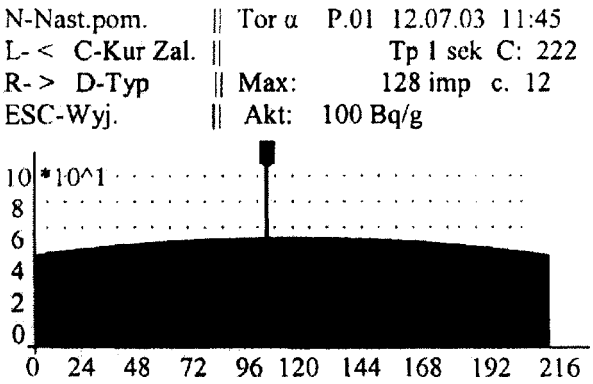

Fig.2. Example of measuring results shown at monitor display: N – display next measurements from the memory; C – switch on/off cursor movement; L, R – move cursor left/right; ESC – exit; D – type of diagram; Tor – measuring channel; P01 – measurements from the memory No. 1; Tp 1 sek – counting time 1 s; Max 128 imp c:12 – maximum count number 128 in channel 12; Akt – activity.

MODERNIZATION OF AMIZ-2000 – AN AIR DUST CONCENTRATION MONITOR

Adrian Jakowiuk, Edward Świstowski, François Kha[1/]

[1/] École des Mines de Nantes, France

Taking into consideration increasing requirements concerning ease of collection, better visualization and processing of measured data, as well as archival needs, special software for the air dust monitor AMIZ-2000 became a necessity. Such software should present measured data in the form of diagrams and tables. To develop such software, the LabVIEW development program of National Instrument was employed [1].

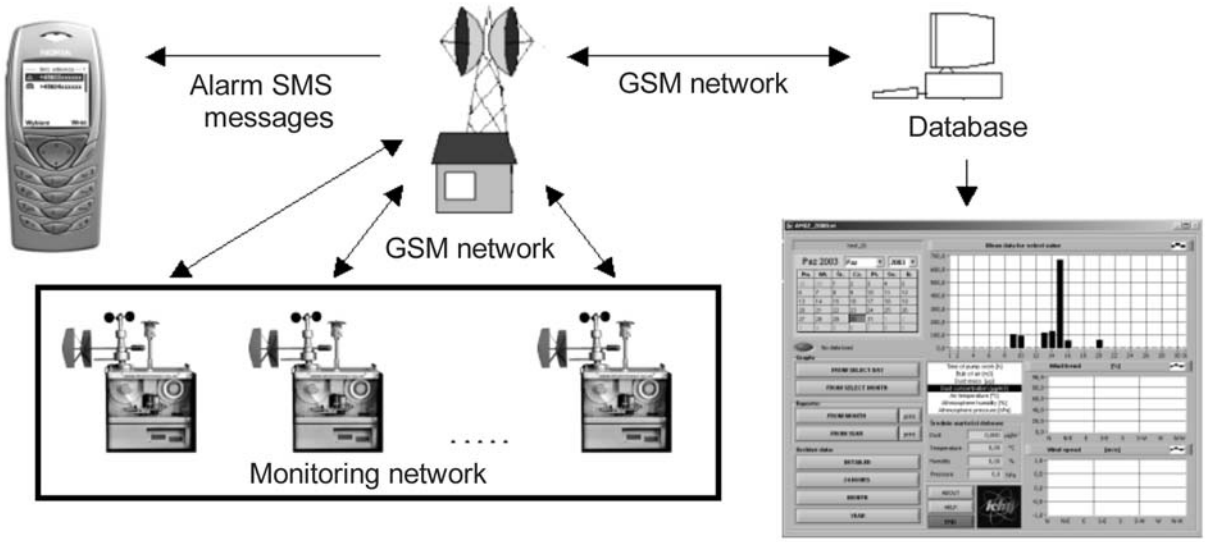

Fig.1. Functional diagram of a monitoring network employing AMIZ-2000 air dust concentration monitors.

The air dust monitor AMIZ-2000 is installed usually in places, where not always wire connection can be ensured, which creates a serious problem and makes the collecting of measured results difficult. Equipping the monitor with a GSM modem, remote communication with AMIZ-2000 is ensured, exists also the possibility of creation of a monitoring network including a number of dust concentration monitors on the basis of specialist software. This means that measured results from all the monitors in the network can be collected in one central computer equipped with modem and appropriate software.

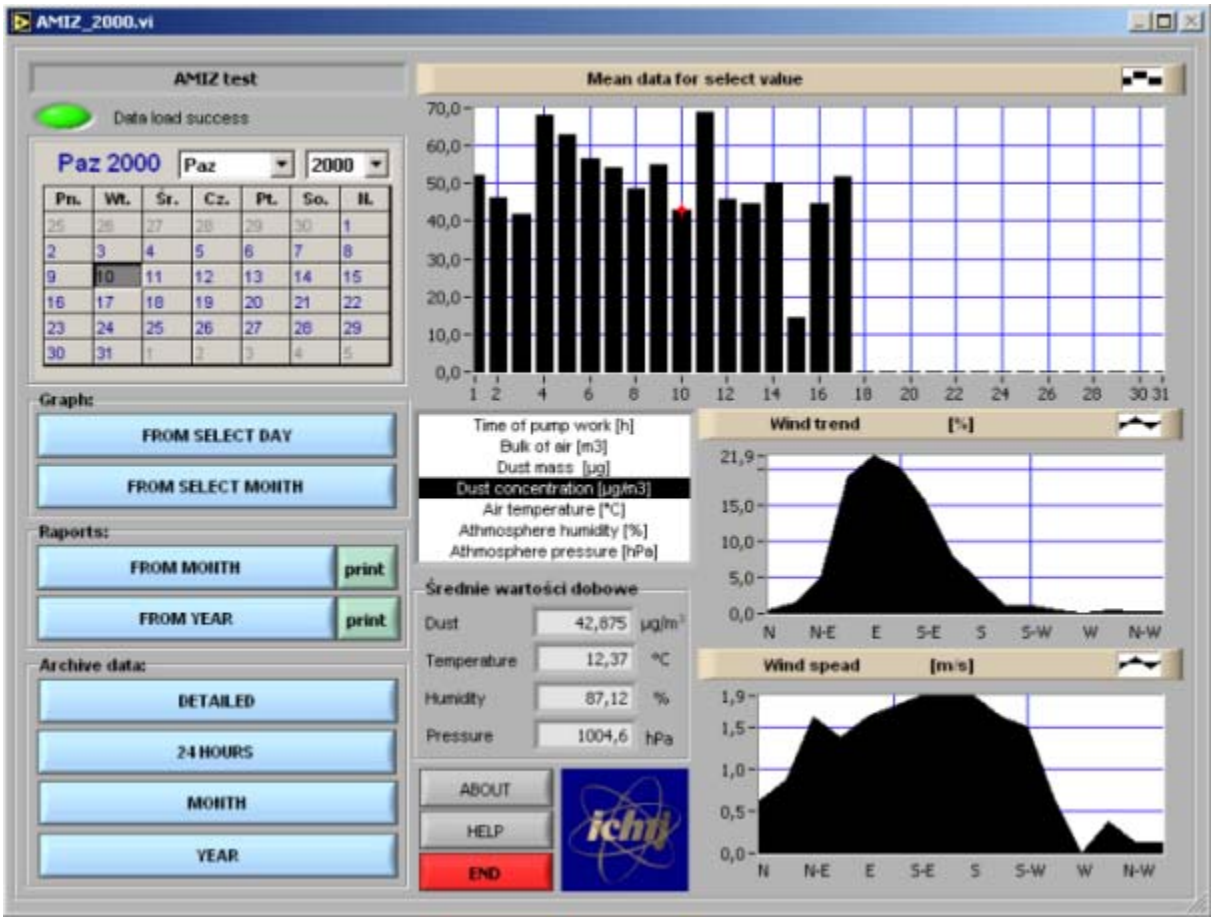

Fig.2. View of the main window of measuring results database showing daily dust concentration in consecutive days, wind direction and corresponding wind speed. By clicking appropriate option other measuring parameters can be selected.

Contemporary transmission of data makes it possible to create an information channel which enables transmission of results from measuring devices to places where these data are collected and processed, and to build second channel permitting for control of measuring system. Present typical solutions of wireless transmission are based on the use of existing infrastructure and services of mobile telephone networks. The data between the measuring devices and the central computer are transmitted with the help of GSM modems [2], as shown in Fig.1.

Developed program AMIZ-2000 is used for collection and presentation of measured data from air dust monitor AMIZ-2000 [3]. The monitor ensures measurements of such environmental parameters as: dust concentration, air temperature, relative humidity, atmospheric pressure, wind direction and wind speed. In the main window of the program (Fig.2) daily mean values are presented for the current month. Detailed values of measured data concerning a selected day can be chosen by clicking “Graph from selected day”. In a similar way, clicking “Graph from selected month” data concerning any selected month are chosen. Apart from detailed data from selected day or month, the program ensures print out of recapitulating reports of measurements carried out in the selected month or year and also in any selected period of time.

Thanks to the use of LabVIEW development program specialized software was developed for collecting, presentation and archival storage of the measured results. The developed program for AMIZ-2000 widens considerably its possibilities. Until now, the user was forced to collect the measured data and to process them by himself, now he obtains a program that makes the job for him. Program AMIZ-2000 can easily generate monthly or yearly reports, also for other selected periods of time. The wind direction can easily be determined, e.g. corresponding to the highest dust concentration measured within a day, or to check what were the mean meteorological parameters for a selected period of time and compare them with the parameters of other period. The developed system ensures the user the following possibilities:

- collection of measured data from any monitor in the monitoring network;
- check up of operating parameters of any monitor – their review and setting new values;
- receiving warnings messages (in the form of SMS text) on any mobile phone number;
- review of database of measurements carried out by each measuring station;
- creation of wide range of recapitulation reports of the measurements (daily, monthly, yearly reports and other periodic reports).

References

[1]. User Manual LabVIEW 6.0. National Instruments 2000.
[2]. Jakowiuk A., Kha F.: Elaboration and implementation wireless communication between airborne dust con-

centration gauge AMIZ-2000 and personal computer. Institute of Nuclear Chemistry and Technology, Warszawa 2003, unpublished information.
[3]. Jakowiuk A.: Wizualizacja danych pomiarowych miernika zapylenia powietrza AMIZ-2000 przy użyciu programu LabVIEW. In: Technika jądrowa w przemyśle, medycynie, rolnictwie i ochronie środowiska. T.2. Instytut Chemii i Techniki Jądrowej, Warszawa 2002. Raporty IChTJ. Seria A No. 2/2002, pp. 525-532.

USE OF MULTIVARIATE ANALYSIS TO IMAGE PROCESSING

Adrian Jakowiuk

When making a photo of some elements or a surface it is necessary to adjust light so that the whole object is equally illuminated. In many cases it is difficult to satisfy this requirement. To solve that problem one of the methods of statistical analysis was used – the principal component analysis (PCA). The method was verified by processing images of steel 45 achieved with an electron microscope (100 times enlargement) and images of metal inclusions in engine oil (500 times enlargement).

Principal component analysis [1] is the decomposition of a matrix **X** (*NxK*) into simpler matrices $\mathbf{M_a}$:

$$\mathbf{X} = \sum_{a=1}^{A} \mathbf{M_a} \tag{1}$$

The smallest value of *A* for which this equation still works is called the "rank" of **X**. The $\mathbf{M_a}$ are all matrices of size *NxK*. The $\mathbf{M_a}$ have a special property of all having rank=1. They can, therefore, be represented as the outer product of two vectors, **t** and **p**:

$$\mathbf{M_a} = \mathbf{t_a p_a'} \tag{2}$$

The $\mathbf{t_a}$ are vectors of size *Nx1* and the $\mathbf{p_a}$ are vectors of size *Kx1*.
The total PCA equation becomes:

$$\mathbf{X} = \sum_{a=1}^{A} \mathbf{M_a} = \sum_{a=1}^{A} \mathbf{t_a p_a'} = \mathbf{TP'} \tag{3}$$

The vectors $\mathbf{t_a}$ are called "scores" (or score vectors) and the vectors $\mathbf{p_a}$ are called "loadings" (or loading vectors). The loading vectors have the property of orthonormality, just like the eigenvectors introduced earlier:

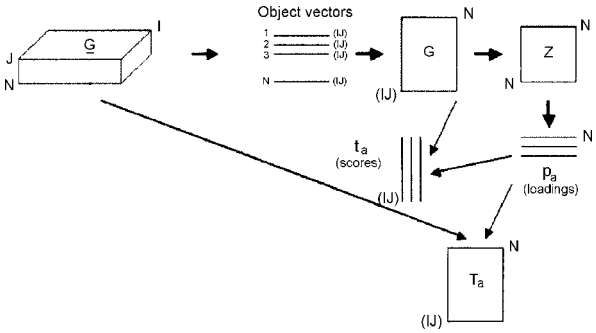

Fig.1. General overview of the elements used in a data analysis by PCA.

$$\mathbf{p_i' p_j} = \delta_{ij} \tag{4}$$

As a matter of fact, the loading vectors of a matrix **X** are exactly the eigenvectors of **X'X**. The scores have the property of orthogonality:

$$\mathbf{t_i' t_j} = \delta_{ij}\lambda_i \tag{5}$$

where λ_i is an eigenvalue of **X'X**. This defines the relationship between principal component analysis and eigenvector – eigenvalue equation. It is easily shown that scores can be calculated from loadings and *vice versa*:

$$\lambda_a \mathbf{p_a'} = \mathbf{t_a' X}; \quad \mathbf{t_a} = \mathbf{X p_a} \tag{6}$$

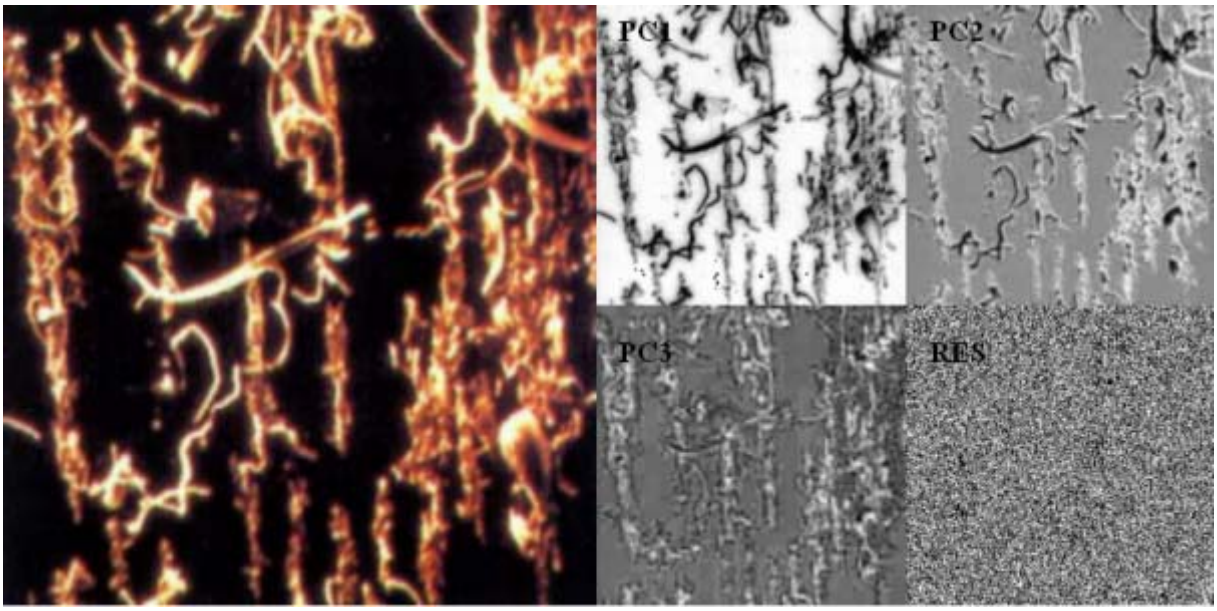

Fig.2. Image of metal inclusions in engine oil (500 times enlargement): PC1 to PC3 – main components of the image achieved when PCA analysis is used, RES – noise contained in the image.

or in general:

$$\mathbf{D^2P' = T'X; \quad T = XP} \qquad (7)$$

with $\mathbf{D}^2$ as a diagonal matrix with the eigenvalues λ_a on the diagonal. A general overview of this analysis is given in Fig.1.

of the same object taken at different conditions (e.g. different directions, or different intensity of light), or using components from which different images are composed instead of series of images. After the PCA is performed, images are achieved composed of particular components of the image.

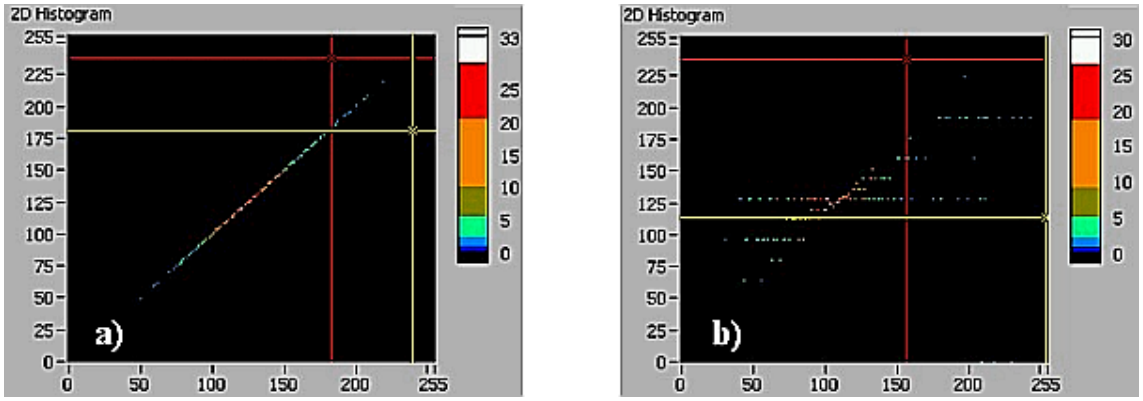

Fig.3. Two dimensional histogram for steel images 45a (a) and 45 n (b) with marked area of ROI.

Multivariate image analysis enables to extract from the image features that are invisible to other methods. It is done by analyzing series of images

Example images containing main components are shown in Fig.2. It is clearly seen how the PCA method split the image into main components. The

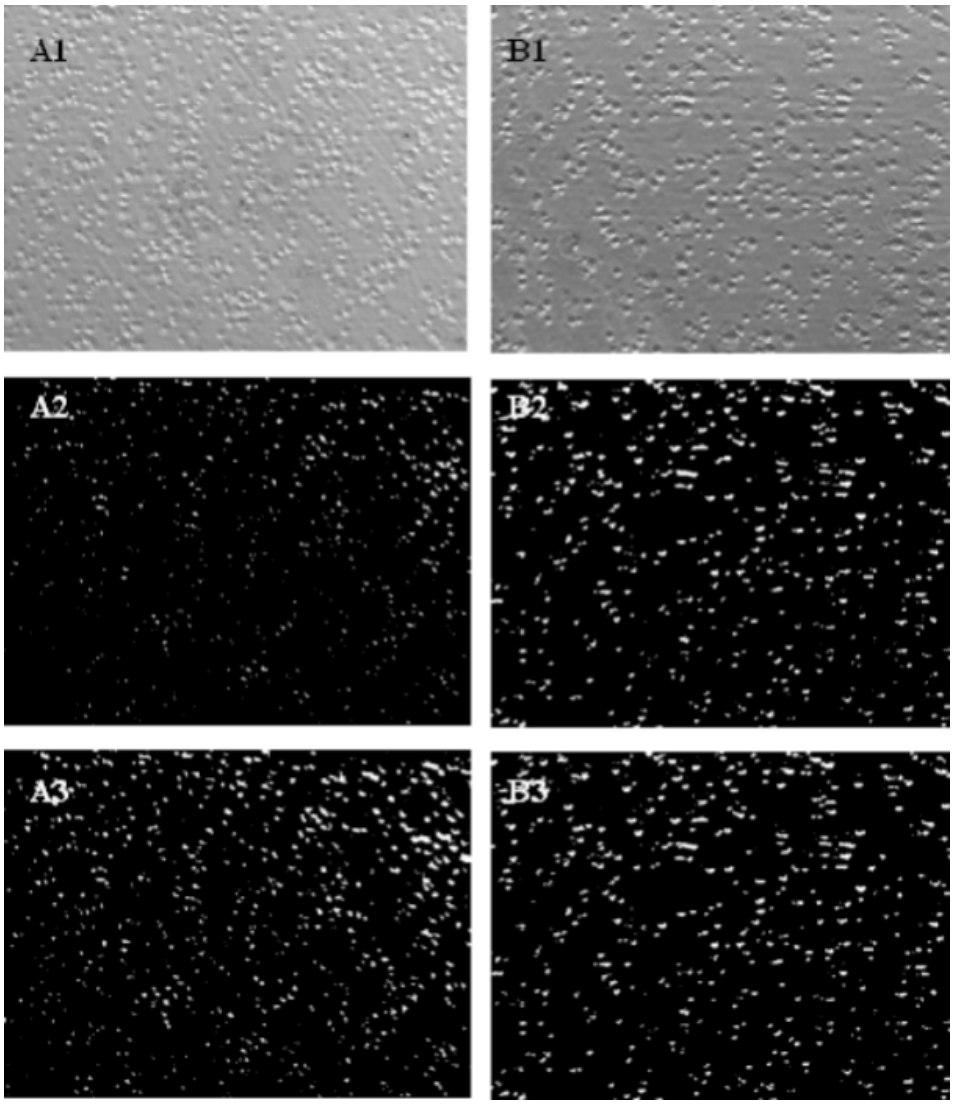

Fig.4. Images of steel A1 – 45a, B1 – 45n; A2, B2 – 1 bit images obtained by the use of threshold values method; A3, B3 – 1 bit images obtained by the use of PCA.

PC1 component contains information about the basic elements of the image. The PC2 component shows the surface of the best illuminated elements, and the PC3 component presents information about surroundings of the elements. The last component (RES) shows the noise removed from the image.

The consecutive step in the multivariate analysis of an image is separation from the image a region of interest (ROI) that is to be further analyzed. This is made by creating a two dimensional histogram from the PC images (examples of histograms for steel 45a (a) and 45n (b) are shown in Fig.3) and marking a ROI in the histogram diagram.

A separated areas ROI for steel 45a and 45n are shown in Fig.4.

These images were used to check if PCA is able to decrease errors when the Minkowski's functional method is applied (the errors result mostly from unequal illumination of investigated surface) [2]. After analysis of these images was made, considerably lower errors were observed. The error decreased from 22 to 7% for steel 45a (the image was unequally illuminated) and from approximately 6 to 4.5% for 45n steel. Such errors were achieved by splitting 1 bit image into 9 equal sub-images for which Minkowski's functionals were computed, and then computed standard deviation was treated as error [3].

Thanks to the use of the multivariate PCA for preparatory image processing, and then thanks to its segmentation (separation of range of interest ROI) and further analysis, it was possible to remove, in a considerable degree, the effect of unequal illumination of the investigated images. This error constitutes a considerable part of the total error of image analysis. Its minimization permits to get better result of further image analysis (with the use of other methods).

In the case of steel images 45a it was possible to decrease the error from approximately 22 to approximately 7%. Thanks to that the result of analysis by the Minkowski's functional method is more exact.

References

[1]. Geladi P., Grahn H.: Multivariete image analysis. Physics Reports. WILEY, England 1996.
[2]. Michielsen K., De Raedt H.: Comput. Phys. Commun., 132, 94-103 (2000).
[3]. Jakowiuk A.: Application of the morphological image analysis for identification of the steel surfaces irradiation with plasma pulses. In: INCT Annual Report 2002. Institute of Nuclear Chemistry and Technology, Warszawa 2003, pp.147-148.

DOSE DETECTOR OF THE PULSE RADIOLYSIS EXPERIMENTAL SET

Sylwester Bułka, Zygmunt Dźwigalski, Zbigniew Zimek

LAE 10 accelerator is used in nanosecond pulse radiolysis experiments as a source of high energy electron beams [1]. The main point of interest for the researchers is dose of electrons absorbed by the medium placed in a thick-wall cubic glass cell, but the other parameters such as pulse duration time, pulse pedestal, pulse time dispersion, electron energy are important also. The measurements of the over mentioned parameters have already been carried out and the results will be presented, but the main aim of this work is as follows: presentation the results of electron dose detector measurements.

The results of electron dose detector measurements are especially interesting. However, the value of the absorbed dose can be precisely determined by using well known chemical dosimeter – aqueous solution of KSCN (potassium thiocyanate) placed in the cell. It is impossible to do it during experiment because this cell must be used for substances under test. In this case there are several other (indirect) methods for dose measurements [2-4]. One of them [5] was applied in our experiments after essential improvements. We obtained sensitivity sufficient for dose range commonly used by radiolysis researchers and satisfying fidelity of electron beam pulse shape visualization.

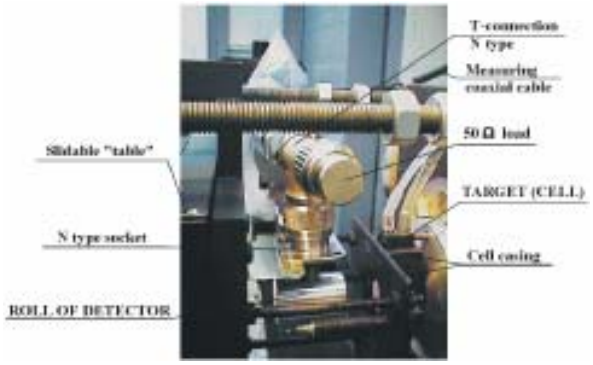

Fig.1. View of the electron beam detector.

Figure 1 is a view of the electron beam detector (simplified Faraday's cup) and Fig.2 shows the target (cell) with the detector placed behind it and connected to the described measurement system.

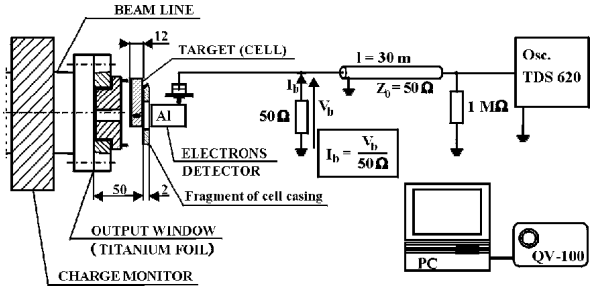

Fig.2. Target (cell) and detector with diagram of measurement circuit.

The typical experimental cell contains small (several mm^3) volume of the tested liquid substance in the cavity in the cubic glass block with the window for analyzing light beam passing through.

Such as thick glass object causes strong electron beam absorption and dissipation, so it is only a part (less than 25%) of initial electron beam that can reach the detector, even when placed only 2 mm from the cell's rear wall.

As it was concluded from [10] electron beam detector can be used for the measurements of dose absorbed in the tested object. It was taken [5], that the value of the dose is proportional to the area between the curve of the pulse recorded from detector and time axis.

Figure 3 shows electron beam current pulse shapes for three different doses. The pulse amplitude for the maximum dose (around 10 Gy in this case), obtained as a result of accelerator parameters optimization, reaches 12 V.

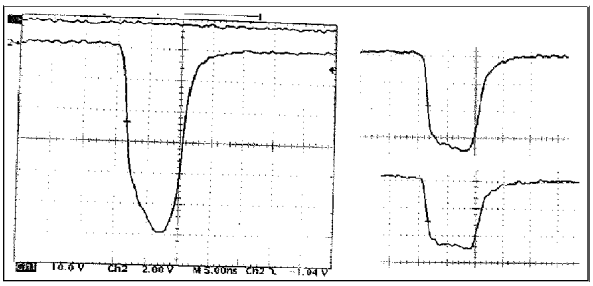

Fig.3. Shapes of electrons beam pulses for various dose.

Smaller doses can be obtained by changing certain accelerator's parameters. The one way of dose control, preferred by the researchers is decreasing the accelerating section focusing coil current, this causes some changes of the recorded pulse shape (Fig.3).

It appears as if the original optimized pulse was clamped at the various level, it's undoubtedly related with the non-uniform energetic spectra of the electron beam.

Another kind of pulse distortions can be observed (Fig.4a,b) in case when the detector's collecting surface was set not precisely perpendicularly to the electron beam direction. An inclination of 2-3° results in the visible pulse form changes.

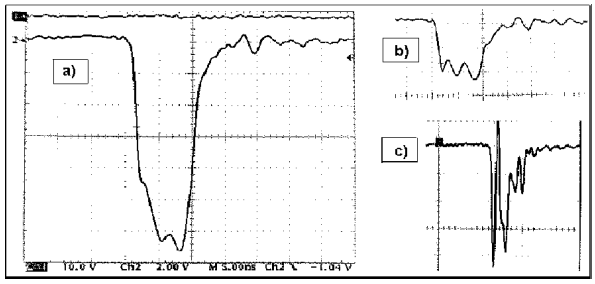

Fig.4. Inappropriate pulse shapes recorded from the detector.

It is necessary for the researchers to pay attention when dealing with the cell, otherwise the dose readings would be erroneous.

Knowing that the precision of the detector positioning is so important, we equipped the Faraday's cup with flexible connection (25 mm long, 1.5 mm^2 thick copper cord) to the coaxial socket of N type. Unfortunately the oscillating character of the pulse, as seen in Fig.4c, was obtained due to excess inductivity introduced and we had to return to the version with rigid, shortest possible connection.

References

[1]. Mirkowski J., Wiśniowski P., Bobrowski K.: In: INCT Annual Report 2000. Institute of Nuclear Chemistry and Technology, Warszawa 2001, pp.31-33.
[2]. Dźwigalski Z., Zimek Z.: Elektronika, 2, 11-13 (2002), (in Polish).
[3]. Hug G.L.: Private communications.
[4]. Dźwigalski Z., Zimek Z.: Proceedings of EPAC 2002 (Eight European Particle Accelerator Conference), Paris, France, 3-7 June 2002, pp.2786-2788.
[5]. Dźwigalski Z., Zimek Z.: Prace Naukowe Politechniki Warszawskiej. Seria Elektronika, 143, 119-122 (2002), (in Polish).

THE INCT PUBLICATIONS IN 2003

ARTICLES

1. **Ambroż H., Przybytniak G.K.**
   EPR studies on radiation-damaged DNA – the contribution of Martyn Symons.
   Progress in Reaction Kinetics and Mechanism, 28, 35-55 (2003).

2. **Balcerczyk A., Rychlik B., Kruszewski M., Burchell B., Bartosz G.**
   MRP1-transfected cells do not show increased resistance against oxidative stress.
   Free Radical Research, 37, 189-195 (2003).

3. **Bik J., Głuszewski W., Rzymski W.M., Zagórski Z.P.**
   EB radiation crosslinking of elastomers.
   Radiation Physics and Chemistry, 67, 421-423 (2003).

4. **Bik J., Zagórski Z.P., Rzymski W.M., Głuszewski W.**
   Radiacyjne sieciowanie elastomeru butadienowo-akrylonitrylowego (Radiation crosslinking of butadiene-nitrile elastomer).
   Prace Naukowe Instytutu Technologii Organicznej i Tworzyw Sztucznych Politechniki Wrocławskiej. Nr 52. Seria: Konferencje, 25, 147-150 (2003).

5. **Bilewicz A., Łyczko K.**
   Adsorption of ^{220}Rn on dioxygenyl hexafluoroantimonate surface. A model experiment for studies of the chemistry of element 112.
   Nukleonika, 48, 137-139 (2003).

6. **Bonilla F.A., Ong T.S., Skeldon P., Thompson G.E., Piekoszewski J., Chmielewski A.G., Sartowska B., Stanisławski J.**
   Enhanced corrosion resistance of titanium foil from nickel, nickel-molybdenum and palladium surface alloying by high intensity pulsed plasmas.
   Corrosion Science, 45, 403-412 (2003).

7. **Chmielewski A.G.**
   Radiation technologies in Middle/East Europe.
   Radiation and Industries, 100, 50-56 (2003).

8. **Chmielewski A.G., Ostapczuk A., Licki J., Kubica K.**
   Emisja lotnych związków organicznych z kotła energetycznego opalanego pyłem węglowym (Emission of volatile organic compounds (VOCs) from a coal-fired power station boiler).
   Ochrona Powietrza i Problemy Odpadów, 37, 142-147 (2003).

9. **Chmielewski A.G., Sun Y., Licki J., Bułka S., Kubica K., Zimek Z.**
   NO_x and PAHs removal from industrial flue gas by using electron beam technology with alcohol addition.
   Radiation Physics and Chemistry, 67, 555-560 (2003).

10. **Chmielewski A.G., Tymiński B., Pawelec A., Dobrowolski A., Zimek Z.**
    Reaktor do oczyszczania spalin metodą radiacyjną (A reactor for radiation purification of flue gases).
    Przemysł Chemiczny, 82, 1013-1015 (2003).

11. **Chmielewski A.G., Tymiński B., Pawelec A., Palige J., Dobrowolski A.**
    Radiacyjna metoda oczyszczania spalin i jej zastosowanie w energetyce (The radiation method of flue gas treatment and its use in power engineering).
    Prace Politechniki Warszawskiej. Seria: Konferencje, 23, 47-54 (2003).

12. Ciesielski B., Schultka K., Kobierska A., Nowak R., Peimel-Stuglik Z.
In vivo alanine/EPR dosimetry in daily clinical practice: a feasibility study.
International Journal of Radiation Oncology, Biology, Physics, 56, 899-905 (2003).

13. Cieśla K.
Gamma irradiation influence on wheat flour gelatinisation.
Journal of Thermal Analysis and Calorimetry, 74, 259-274 (2003).

14. Cieśla K., Eliasson A.-C.
DSC studies of gamma irradiation influence on gelatinisation and amylose-lipid complex transition occurring in wheat starch.
Radiation Physics and Chemistry, 68, 933-940 (2003).

15. Deptuła A., Łada W., Olczak T., Sartowska B., Giorgi L., Moreno A., Di Bartolomeo A.
Preparation of Pt/WO_3 powders and thin films on porous carbon black and metal supports by the complex sol-gel process.
Journal of New Materials for Electrochemical Systems, 6, 71-74 (2003).

16. Deptuła A., Olczak T., Łada W., D'Epifanio A., Di Bartolomeo A., Brignocchi A.
Some comments on the synthesis of $LiNi_xCo_{1-x}O_2$ powders by thermal decomposition of organic precursors.
Journal of New Materials for Electrochemical Systems, 6, 39-44 (2003).

17. Drzewicz P., Bojanowska-Czajka M., Trojanowicz M., Nałęcz-Jawecki G., Sawicki J., Wołkowicz S.
Application of ionizing radiation for degradation of organic pollutants in waters and wastes.
Polish Journal of Applied Chemistry, 47, 127-136 (2003).

18. Dybczyński R.
Materiały odniesienia w nieorganicznej analizie śladowej (Reference materials in inorganic trace analysis).
Analityka, Nauka i Praktyka, 1, 10, 12, 14-16 (2003).

19. Dybczyński R., Danko B., Kulisa K., Maleszewska E., Polkowska-Motrenko H., Samczyński Z., Szopa Z.
Performance and frequency of use of NAA and other techniques during the certification of two new Polish CRMs prepared by INCT.
Czechoslovak Journal of Physics, 53, Supplement A, A171-A179 (2003).

20. Dybczyński R., Kulisa K.
Observations on the effect of temperature on performance and stability of anion exchange columns in ion chromatography.
Chromatographia, 57, 475-484 (2003).

21. Dziembowska T., Szafran M., Jagodzińska E., Natkaniec I., Pawlukojć A., Kwiatkowski J.S., Baran J.
DFT studies of the structure and vibrational spectra of 8-hydroxyquinoline *N*-oxide.
Spectrochimica Acta Part A, 59, 2175-2189 (2003).

22. Farooq M., Khan I.H., Ghiyas-ud-Din, Gul S., Palige J., Dobrowolski A.
Radiotracer investigations of municipal sewage treatment stations.
Nukleonika, 48, 57-61 (2003).

23. Fuks L., Samochocka K., Anulewicz-Ostrowska R., Kruszewski M., Priebe W., Lewandowski W.
Structure and biological activity of cationic $[PtLCl(DMSO)]NO_3 \cdot DMSO$ complex containing a chelated diaminosugar: methyl-3,4-diamino-2,3,4,6-tetradeoxy-α-L-lyxopyranoside.
European Journal of Medicinal Chemistry, 38, 775-780 (2003).

24. Głuszewski W., Zagórski Z.P.
Sterylizacja radiacyjna wyrobów medycznych (Radiation sterilization of health care products).
Współczesna Onkologia, 7, 787-790 (2003).

25. Gniazdowska E., Dobrowolski P., Narbutt J.
Proton nuclear magnetic resonanse studies on hydration of oxaalkanes in benzene solutions.
Journal of Molecular Liquids, 107, 99-107 (2003).

26. Grądzka I., Buraczewska I., Kuduk-Jaworska J., Romaniewska A., Szumiel I.
Radiosensitizing properties of novel hydroxydicarboxylatoplatinum(II) complexes with high or low reactivity with thiols: two modes of action.
Chemico-Biological Interactions, 146, 165-177 (2003).

27. Grądzka I., Sochanowicz B., Buraczewska I., Szumiel I.
Effect of signalling inhibition on DNA double strand break rejoining in X-irradiated human glioma cell lines.
Acta Biochimica Polonica, 50 (suppl.), 139-140 (2003).

28. Grodkowski J., Neta P., Wishart J.F.
Pulse radiolysis study of the reactions of hydrogen atoms in the ionic liquid methyltributylammonium bis[(trifluoromethyl)sulfonyl]imide.
Journal of Physical Chemistry A, 107, 9794-9799 (2003).

29. Gryz M., Starosta W., Ptasiewicz-Bąk H., Leciejewicz J.
Crystal and molecular structure of pyridazine-3-carboxylic acid hydrochloride and zinc(II) pyradizine-3-carboxylate tetrahydrate.
Journal of Coordination Chemistry, 56, 1505-1511 (2003).

30. Gryz M., Starosta W., Ptasiewicz-Bąk H., Leciejewicz J.
Molecular chains in the structure of a zinc(II) complex with pyrazine-2,6-dicarboxylate and water ligands.
Journal of Coordination Chemistry, 56, 1575-1579 (2003).

31. Hilczer B., Smogór H., Goslar J., Warchoł S.
Radiation-induced changes in the dielectric response of poly(vinylidene fluoride) type polymers.
Radiation Effects & Defects in Solids, 158, 349-355 (2003).

32. Kaczmarek S.M., Berkowski M., Tsuboi T., Wabia M., Włodarski M., Olesińska W., Wrońska T.
Blue fluorescence of Ti^{3+} ions in Ti^{3+}-doped, γ-irradiated $SrAl_{0.5}Ta_{0.5}O_3$:$LaAlO_3$ crystals.
Nukleonika, 48, 35-40 (2003).

33. Końca K., Lankoff A., Banasik A., Lisowska H., Kuszewski T., Góźdź S., Koza Z., Wójcik A.
A cross-platform public domain PC image-analysis program for the comet assay.
Mutation Research, Genetic Toxicology and Environmental Mutagenesis, 534, 15-20 (2003).

34. Kornacka E., Przybytniak G.K.
Reactions of thiols with DNA radicals in model system studied by EPR.
Molecular Physics Reports, 37, 29-34 (2003).

35. Krajewski A., Stachowicz W.
Zwalczanie promieniami gamma owadów niszczących drewno zabytków (Elimination of insects destroying the wooden relicts of art by gamma rays).
Postępy Techniki Jądrowej, 46, 2, 26-35 (2003).

36. Krajewski A., Stachowicz W.
Zwalczanie promieniami gamma owadów niszczących zabytkowe tkaniny, materiały wełnopochodne, futra i muzealne zbiory zoologiczne (Elimination of insects destroying the relicts of art made of woven fabrics, wool, furs and zoological collections by gamma rays).
Postępy Techniki Jądrowej, 46, 4, 36-44 (2003).

37. Krejzler J., Narbutt J.
Adsorption of strontium, europium and americium(III) ions on a novel adsorbent Apatite II.
Nukleonika, 48, 171-175 (2003).

38. Kruszewski M.
Free radicals, DNA damage and cardiovascular diseases.
Annals of Diagnostic Paediatric Pathology, 7, 25-33 (2003).

39. Kruszewski M.
Labile iron pool: the main determinant of cellular response to oxidative stress.
Mutation Research, Fundamental and Molecular Mechanisms of Mutagenesis, 531, 81-92 (2003).

40. Kruszewski M., Boużyk E., Oldak T., Samochocka K., Fuks L., Lewandowski W., Fokt I., Priebe W.
Differential toxic effect of *cis*-platinum(II) and palladium(II) chlorides complexed with methyl 3,4-diamine-2,3,4,6-tetradeoxy-α-L-lyxo-hexopyranoside in mouse lymphoma cell lines differing in DSB and NER repair ability.
Teratogenesis, Carcinogenesis, and Mutagenesis, Supplement 1, 1-11 (2003).

41. Kruszewski M., Iwaneńko T.
Labile iron pool correlates with iron content in the nucleus and the formation of oxidative DNA damage in mouse lymphoma L5178Y cell lines.
Acta Biochimica Polonica, 50, 211-215 (2003).

42. Kruszewski M., Lewandowska H., Starzyński R., Bartłomiejczyk T., Iwaneńko T., Lipiński P.
Iron chelation reduces nitric oxide-induced genotoxicity.
Acta Biochimica Polonica, 50 (suppl.), 25 (2003).

43. Lankoff A., Banasik A., Obe G., Deperas M., Kuzminski K., Tarczynska M., Jurczak T., Wójcik A.
Effect of microcystin-LR and cyanobacterial extract from Polish reservoir of drinking water on cell cycle progression, mitotic spindle, and apoptosis in CHO-K1 cells.
Toxicology and Applied Pharmacology, 189, 204-213 (2003).

44. Legocka I., Mirkowski K., Nowicki A., Zimek Z.
Działanie ochronne wybranych dodatków do polipropylenu przy stosowaniu dawek sterylizacyjnych (Destruction of polypropylene inhibition by use of some additives at sterilization dose).
Prace Naukowe Instytutu Technologii Organicznej i Tworzyw Sztucznych Politechniki Wrocławskiej. Nr 52. Seria: Konferencje, 25, 620-624 (2003).

45. Lewandowski W., Fuks L., Kalinowska M., Koczoń P.
The influence of selected metals on the electronic system of biologically important ligands.
Spectrochimica Acta Part A, 59, 3411-3420 (2003).

46. Licki J., Chmielewski A.G., Iller E., Zimek Z., Mazurek J., Sobolewski L.
Electron-beam flue-gas treatment for multicomponent air-pollution control.
Applied Energy, 75, 145-154 (2003).

47. Lipiński P., Starzyński R., Drapier J.-C., Bouton C., Bartłomiejczyk T., Sochanowicz B., Smuda E., Gajkowska A., Kruszewski M.
Nitric oxide regulates cytosolic labile iron pool by different mechanisms.
Acta Biochimica Polonica, 50 (suppl.), 13-14 (2003).

48. Liu W., Lund A., Shiotani M., Michalik J., Biglino D., Bonora M.
Structure and dynamics of radicals in zeolite matrices: ESR and theoretical studies.
Applied Magnetic Resonance, 24, 285-302 (2003).

49. Łada W., Deptuła A., Sartowska B., Olczak T., Chmielewski A.G., Carewska M., Scaccia S., Simonetti E., Giorgi L., Moreno A.
Synthesis of $LiCoO_2$ and $LiMg_{0.05}O_2$ thin films on porous Ni/NiO cathodes for MCPC by complex sol-gel process (CSGP).
Journal of New Materials for Electrochemical Systems, 6, 33-37 (2003).

50. Majdan M., Pikus S., Kowalska-Ternes M., Gładysz-Płaska A., Staszczuk P., Fuks L., Skrzypek H.
Equilibrium study divalent *d*-electron metals adsorption on A-type zeolite.
Journal of Colloid and Interface Science, 262, 321-330 (2003).

51. Malec-Czechowska K., Stachowicz W.
Detection of irradiated components in flavour blends composed of non-irradiated spices, herbs and vegetable seasonings by thermoluminescence method.
Nukleonika, 48, 127-132 (2003).

52. Malec-Czechowska K., Strzelczak G., Dancewicz A.M., Stachowicz W., Delincee H.
Detection of irradiation treatment in dried mushrooms by photostimulated luminescence, EPR spectroscopy and thermoluminescence measurements.
European Food Research and Technology, 216, 157-165 (2003).

53. Michalik J., Sadło J., Danilczuk M.
Paramagnetic silver clusters in molecular sieves: zeolite rho.
Solid State Phenomena, 94, 197-200 (2003).

54. Nichipor H., Dashouk E., Yacko S., Chmielewski A.G., Zimek Z., Sun Y., Vitale S.A.
The kinetics of 1,1-dichloroethene ($CCl_2=CH_2$) and trichloroethene ($HClC=CCl_2$) decomposition in dry and humid air under the influence of electron beam.
Nukleonika, 48, 45-50 (2003).

55. Orska-Gawryś J., Surowiec I., Kehl J., Rejniak H., Urbaniak-Walczak K., Trojanowicz M.
Identification of natural dyes in archeological Coptic textiles by liquid chromatography with diode array detection.
Journal of Chromatography A, 989, 239-248 (2003).

56. Palige J., Dobrowolski A., Owczarczyk A., Chmielewski A.G., Ptaszek S.
Zastosowania obliczeniowej mechaniki płynów (CFD) do modelowania struktury przepływu w osadnikach prostokątnych (Application of CFD methods for flow structure modeling in rectangular settlers).
Inżynieria i Aparatura Chemiczna, 34, 72-75 (2003).

57. Palige J., Dobrowolski A., Owczarczyk A., Ptaszek S., Chmielewski A.G.
Badania metodami znacznikowymi i CFD komory pęcherzykowego napowietrzania ścieków (Investigations of bubbling airation tank for wastewater treatment by tracers and CFD methods).
Inżynieria i Aparatura Chemiczna, 34, 151-152 (2003).

58. Parus J., Kierzek J., Raab W., Donohue D.
A dual purpose Compton suppression spectrometer.
Journal of Radioanalytical and Nuclear Chemistry, 258, 123-132 (2003).

59. Pawlukojć A., Bator G., Sobczyk L., Grech E., Nowicka-Scheibe J.
Inelastic neutron scattering, Raman, infrared and DFT theoretical studies on chloranilic acid.
Journal of Physical Organic Chemistry, 16, 709-714 (2003).

60. Pawlukojć A., Leciejewicz J., Natkaniec I., Nowicka-Scheibe J.
Neutron spectroscopy, IR, raman and *ab initio* study of L-proline.
Polish Journal of Chemistry, 77, 75-85 (2003).

61. Pawlukojć A., Natkaniec I., Bator G., Sobczyk L., Grech E.
Inelastic neutron scattering (INS) spectrum of tetracyanoquinodimethane (TCNQ).
Chemical Physics Letters, 378, 665-672 (2003).

62. Pawlukojć A., Natkaniec I., Nowicka-Scheibe J., Grech E., Sobczyk L.
Inelastic neutron scattering (INS) studies on 2,5-dihydroxy-1,4-benzoquinone (DHBQ).
Spectrochimica Acta Part A, 59, 537-542 (2003).

63. Piekoszewski J., Krajewski A., Prokert F., Senkara J., Stanisławski J., Waliś L., Werner Z., Włosiński W.
Brazing of alumina ceramics modified by pulsed plasma beams combined with arc PVD treatment.
Vacuum, 70, 307-312 (2003).

64. Poboży E., Halko R., Krasowski M., Wierzbicki T., Trojanowicz M.
Flow-injection sample preconcentration for ion-pair chromatography of trace metals in waters.
Water Research, 37, 2019-2026 (2003).

65. Pogocki D.
Alzheimer's β-amyloid peptide as a source of neurotoxic free radicals: the role of structural effects.
Acta Neurobiologiae Experimentalis, 63, 131-145 (2003).

66. Pogocki D., Schöneich Ch., Kanski J., Aksenova M., Butterfield A.
Alzheimer's β-amyloid peptide as a source of neurotoxic free radicals. Mechanism and proof of concept.
Acta Neurobiologiae Experimentalis, 63, 159 (2003).

67. Pogocki D., Serdiuk K.

Neurotoksyczność amyloidalnego β-peptydu Alzheimera, rola Met^{35} i miedzi kompleksowanej przez peptyd (Neurotoxicity of the Alzheimer amyloid β-peptide, function of Met^{35} and copper complexed by the peptide).

Wiadomości Chemiczne, 57, 461-475 (2003).

68. Pogocki D., Serdiuk K., Schöneich Ch.

Computational characterization of sulfur-oxygen three-electron-bonded radicals in methionine and methionine-containing peptides: important intermediates in one-electron oxidation processes.

Journal of Physical Chemistry A, 107, 7032-7042 (2003).

69. Polkowska-Motrenko H.

Neutronowa analiza aktywacyjna w badaniach składu meteorytów (Neutron activation analysis in the study of the meteorites composition).

Postępy Techniki Jądrowej, 46, 2, 22-25 (2003).

70. Pruszyński M., Bilewicz A.

Izotopy astatu w medycynie (Astatine isotopes in medicine).

Postępy Techniki Jądrowej, 46, 4, 22-26 (2003).

71. Ptasiewicz-Bąk H., Leciejewicz J.

The crystal structure of a strontium(II) complex with pyrazine-2,6-dicarboxylate and water ligands.

Journal of Coordination Chemistry, 56, 223-229 (2003).

72. Ptasiewicz-Bąk H., Leciejewicz J.

The crystal structures of pyrazine-2,6-dicarboxylic acid dihydrate and hexaaquamagnesium(II) pyrazine-2,6-dicarboxylate.

Journal of Coordination Chemistry, 56, 173-180 (2003).

73. Samochocka K., Fokt I., Anulewicz-Ostrowska R., Przewłoka T., Mazurek A.P., Fuks L., Lewandowski W., Kozerski L., Bocian W., Bednarek E., Lewandowska H., Sitkowski J., Priebe W.

Platinum(II) and palladium(II) complexes with methyl 3,4-diamino-2,3,4,6-tetradeoxy-α-L-*lyxo*-hexopyranoside.

Dalton Transactions, 11, 2177-2183 (2003).

74. Sartowska B., Buczkowski M., Starosta W.

SEM observations of particle track membrane surfaces modificated using plasma treatment.

Materials Chemistry and Physics, 81, 352-355 (2003).

75. Schöneich Ch., Pogocki D., Hug G.L., Bobrowski K.

Free radical reactions of methionine in peptides: mechanisms relevant to β-amyloid oxidation and Alzheimer's disease.

Journal of American Chemical Society, 125, 13700-13713 (2003).

76. Smogór H., Goslar J., Hilczer B., Warchoł S.

Radiation damage to P(VDF/TrFE) (50/50) ferroelectric copolymer studied by ESR, Raman and IR spectroscopy.

Molecular Physics Reports, 37, 95-99 (2003).

77. Smogór H., Hilczer B., Pawlaczyk Cz., Goslar J., Warchoł S.

Dielectric relaxation and conformational disorder in P(VDF/TrFE)(50/50) copolymer films irradiated with fast electrons.

Ferroelectrics, 294, 191-201 (2003).

78. Stachowicz W.

Czy wszystkie metody sterylizacji spełniają wymagania współczesnej medycyny (Are all methods of sterilisation meeting the requirements of the temporary medicine).

Postępy Techniki Jądrowej, 46, 4, 27-35 (2003).

79. Starosta W., Ptasiewicz-Bąk H., Leciejewicz J.

The crystal structure of an ionic calcium complex with pyridine-3,5-dicarboxylate and water ligands.

Journal of Coordination Chemistry, 56, 33-39 (2003).

80. Starosta W., Ptasiewicz-Bąk H., Leciejewicz J.
The crystal structures of two calcium(II) complexes with pyrazine-2,6-dicarboxylate and water ligands.
Journal of Coordination Chemistry, 56, 677-682 (2003).

81. Sun Y., Hakoda T., Chmielewski A.G., Hashimoto S.
Destruction of 1,1-dichloroethylene/air mixture under gamma-ray irradiation.
Radiochimica Acta, 91, 295-298 (2003).

82. Sun Y., Hakoda T., Chmielewski A.G., Hashimoto S.
Trans-1,2-dichloroethylene decomposition in low-humidity air under electron beam irradiation.
Radiation Physics and Chemistry, 68, 843-850 (2003).

83. Surowiec I., Orska-Gawryś J., Biesaga M., Trojanowicz M., Hutta M., Halko R., Urbaniak-Walczak K.
Identification of natural dyestuff in archeological Coptic textiles by HPLC with fluorescence detection.
Analytical Letters, 36, 1211-1229 (2003).

84. Szopa Z.
Obróbka i interpretacja danych pochodzących z porównań międzylaboratoryjnych i testów biegłości za pomocą pakietu AQCS-PC (Evaluation and interpretation of the data from interlaboratory comparison and proficiency tests with the aid of the AQCS-PC package).
Analityka, 4, 11-16 (2003).

85. Szostek B., Orska-Gawryś J., Surowiec I., Trojanowicz M.
Investigation of natural dyes occuring in historical Coptic textiles by high-performance liquid chromatography with UV-Vis and mass spectrometric detection.
Journal of Chromatography A, 1012, 179-192 (2003).

86. Szumiel I.
The bystander effect: is reactive oxygen species the driver?
Nukleonika, 48, 113-120 (2003).

87. Szumiel I.
Układ nadzorujący genom (Genome surveillance system).
Postępy Biologii Komórki, 30, 359-374 (2003).

88. Szumiel I., Wójcik A.
Apoptoza komórek naczyń krwionośnych. Nowa nadzieja radioterapii? (Apoptosis of vascular epithelial cells. A new hope for radiotherapy?)
Postępy Techniki Jądrowej, 46, 3, 2-5 (2003).

89. Szydłowski A., Banaszak A., Fijał I., Jaskóła M., Korman A., Sadowski M., Zimek Z.
Influence of intensive γ and electron radiation on tracks formation in the PM-355 detectors.
Radiation Measurement, 36, 111-113 (2003).

90. Trojanowicz M.
Application of conducting polymers in chemical analysis.
Microchimica Acta, 143, 75-91 (2003).

91. Trojanowicz M., Poboży E., Gübitz G.
Speciation of oxidation states of elements by capillary electrophoresis.
Journal of Separation Science, 26, 983-995 (2003).

92. Trojanowicz M., Surowiec I., Orska-Gawryś J., Szostek B., Urbaniak-Walczak K.
Chromatographic investigation of dyes extracted from Coptic textiles from collection on National Museum in Warsaw.
Egyptian Journal of Analytical Chemistry, 12, 1-8 (2003).

93. Trojanowicz M., Szewczyńska M., Wcisło M.
Electroanalytical flow measurements. Recent advances.
Electroanalysis, 15, 5-6, 1-19 (2003).

94. Trojanowicz M., Wójcik L., Urbaniak-Walczak K.
Identification of natural dyes in historical Coptic textiles by capillary electrophoresis with diode array detection.
Chemia Analityczna, 48, 607-620 (2003).

95. Tudek B., Cieśla Z., Janion C., Boiteux S., Bębenek K., Shinagawa H., Bartsch H., Laval J., Zeeland A.A. van, Mullenders L.F.H., Szyfter K., Collons A., Kruszewski M.
Meeting report. (32nd Annual Meeting of European Environmental Mutagen Society: DNA damage and repair fundamental aspects and contribution to human disorders).
DNA Repair, 2, 765-781 (2003).

96. Urbanik W., Kukołowicz P., Kuszewski T., Góźdź S., Wójcik A.
Modelling the frequencies of chromosomal aberrations in peripheral lymphocytes of patients undergoing radiotherapy.
Nukleonika, 48, 3-8 (2003).

97. Wawrzyńska E., Baran S., Leciejewicz J., Sikora W., Stüsser N., Szytuła A.
Magnetic structures of $R_3Mn_4Sn_4$ (R = La, Pr and Nd).
Journal of Physics: Condensed Matter, 15, 803-814 (2003).

98. Werner Z., Piekoszewski J., Grötzschel R., Richter E., Szymczyk W.
Resistance to high-temperature oxidation in B + Si implanted TiN coatings on steel.
Vacuum, 70, 93-96 (2003).

99. Werner Z., Stanisławski J., Piekoszewski J., Levashov E.A., Szymczyk W.
New types of multi-component hard coatings deposited by ARC PVD on steel pre-treated by pulsed plasma beams.
Vacuum, 70, 263-267 (2003).

100. Włodzimirska B., Bartoś B., Bilewicz A.
Preparation of ^{225}Ac and ^{228}Ac generators using a cryptomelane manganese dioxide sorbent.
Radiochimica Acta, 91, 553-556 (2003).

101. Wojewódzka M., Bartłomiejczyk T., Kruszewski M.
Does the defect in NHEJ-mediated DSB repair pathway result in elevated frequency of homologous recombination?
Acta Biochimica Polonica, 50 (suppl.), 339-340 (2003).

102. Woźniak A.
Badanie jakości złącza rur preizolowanych (Quality test of the interconnection between pre-isolated tubes).
Instal: teoria i praktyka w instalacjach, 12, 32-33 (2003).

103. Wójcik A.
Rad, radon i zdrowie. Historia bez końca (Radium, radon and health. A neverending story).
Postępy Techniki Jądrowej, 46, 4, 7-21 (2003).

104. Wójcik A., Cosset J.-M., Clough K., Gourmelon P., Bottolier J.-F., Stephan G., Sommer S., Wieczorek A., Słuszniak J., Kułakowski A., Góźdź S., Michalik J., Stachowicz W., Sadło J., Bulski W., Izewska J.
The radiological accident at the Bialystok Oncology Center: cause, dose estimation and patient treatment.
Strahlentherapie und Onkologie, 179, 77 (2003).

105. Wójcik A., Günter S., Sommer S., Buraczewska I., Kuszewski T., Wieczorek A., Góźdź S.
Chromosomal aberrations and micronuclei in lymphocytes of breast cancer patients after an accident during radiotherapy with 8 MeV electrons.
Radiation Research, 160, 677-683 (2003).

106. Wójcik A., Sonntag C. von, Obe G.
Application of the biotin-dUTP chromosome labelling technique to study the role of 5-bromo-2'-deoxyuridine in the formation of UV-induced sister chromatid exchanges in CHO cells.
Journal of Photochemistry and Photobiology B: Biology, 69, 139-144 (2003).

107. Wójcik A., Stachowicz W., Sadło J., Michalik J., Sommer S., Bulski W., Cosset J.-M., Clough K., Gourmelon P., Bottolier J.-F., Wieczorek A., Słuszniak J., Kułakowski J., Góźdź S., Izewska J.

EPR analysis of dose to ribbone samples breast cancer patients following an accident during radiotherapy with 8 MeV electrons.

Radiotherapy & Oncology, 68, Supplement 1, S25 (2003).

108. Wójcik A., Szumiel I., Liniecki J.

Niskie dawki promieniowania i długość życia (Low doses of radiation and life span).

Postępy Techniki Jądrowej, 46, 1, 27-32 (2003).

109. Zagórski Z.P.

Diffuse reflection spectrophotometry (DRS) for recognition of products of radiolysis in polymers.

International Journal of Polymeric Materials, 52, 323-333 (2003).

110. Zagórski Z.P.

Kauczuki i chemia radiacyjna (Cautchuck and radiation chemistry).

Tworzywa Sztuczne i Chemia (dodatek do nr-u 4/2003), 26-27 (2003).

111. Zagórski Z.P.

Panspermia czyli: czyżby życie przybyło z kosmosu? (Panspermia, it means: did life come to Earth from the Cosmos?)

Postępy Techniki Jądrowej, 46, 2, 42-52 (2003).

112. Zagórski Z.P.

Pół wieku sieciowania radiacyjnego polietylenu czyli pochwała nauki pozauczelnianej (Half of the century of radiation crosslinking of polyethylene: a tribute to the science developed outside Academia).

Postępy Techniki Jądrowej, 46, 4, 10-16 (2003).

113. Zagórski Z.P.

Radiation chemistry and origins of life on earth.

Radiation Physics and Chemistry, 66, 329-354 (2003).

114. Zagórski Z.

Trzecia Międzynarodowa Konferencja "Plutonium Futures 2003" czyli o starzeniu się plutonu (The third International Conference "Plutonium Futures 2003", that means the ageing of plutonium).

Postępy Techniki Jądrowej, 46, 3, 34-38 (2003).

115. Zagórski Z.P., Rajkiewicz M.

Chemia radiacyjna a elastomery (Radiation chemistry and elastomers).

Elastomery, 7, 9-17 (2003).

116. Zakrzewska-Trznadel G.

Radioactive solutions treatment by hybrid complexation-UF/NF process.

Journal of Membrane Science, 225, 25-39 (2003).

117. Zimek Z.

5-te Międzynarodowe Sympozjum IRaP 2002 na temat promieniowania jonizującego w zastosowaniu do polimerów (5th International Symposium on Ionizing Radiation and Polymers IRaP 2002).

Postępy Techniki Jądrowej, 46, 2, 14-20 (2003).

118. Zimek Z.

Wykorzystanie promieniowania hamowania do sterylizacji radiacyjnej sprzętu medycznego jednorazowego użytku (Bremsstrahlung application for radiation sterilization of medical disposables).

Postępy Techniki Jądrowej, 46, 3, 21-28 (2003).

119. Żuchowska D., Zagórski Z.P., Przybytniak G.K., Rafalski A.

Influence of butadiene/styrene copolymers on the modification of polypropylene in electron beam irradiation.

International Journal of Polymeric Materials, 52, 335-344 (2003).

CHAPTERS IN BOOKS

1. Chmielewski A.G.

Iść w stronę słońca (To go towards the Sun).

In: Z dziejów polskich badań nad oddziaływaniem promieniowania z materią. Wspomnienia. Pod red. J. Kroh. Łódź 2003, pp. 383-412.

2. Chmielewski A.G., Ostapczuk A., Licki J., Kubica K.

VOCs emission from coal – fired power station boiler.

In: Environmental engineering studies: Polish research on the way to the EU. New York 2003, pp. 33-42.

3. Dancewicz A.M., Szumiel I.

Od tajnej uchwały do badań nad DNA (From a secret resolution to DNA research).

In: Z dziejów polskich badań nad oddziaływaniem promieniowania z materią. Wspomnienia. Pod red. J. Kroh. Łódź 2003, pp. 203-233.

4. Ostyk-Narbutt J.

Bez ostatniego rozdziału (Department of Radiochemistry at the Institute of Nuclear Research, later the Institute of Nuclear Chemistry and Technology in Warsaw).

In: Z dziejów polskich badań nad oddziaływaniem promieniowania z materią. Wspomnienia. Pod red. J. Kroh. Łódź 2003, pp. 129-155.

5. Stachowicz W., Żegota H., Bachman S., Fiszer W.

O napromieniowaniu żywności (About food irradiation).

In: Z dziejów polskich badań nad oddziaływaniem promieniowania z materią. Wspomnienia. Pod red. J. Kroh. Łódź 2003, pp. 447-462.

6. Szumiel I.

O radiobiologii w Instytucie Chemii i Techniki Jądrowej w Warszawie. Ostatnie dziesięciolecie (About radiobiology at the Institute of Nuclear Chemistry and Technology. The ten last years).

In: Z dziejów polskich badań nad oddziaływaniem promieniowania z materią. Wspomnienia. Pod red. J. Kroh. Łódź 2003, pp. 203-233.

7. Zagórski Z.P.

Chemik w stuleciu totalizmów (The chemist during the age of totalitarian systems).

In: Z dziejów polskich badań nad oddziaływaniem promieniowania z materią. Wspomnienia. Pod red. J. Kroh. Łódź 2003, pp. 265-300.

THE INCT REPORTS

1. INCT Annual Report 2002.

Institute of Nuclear Chemistry and Technology, Warszawa 2003, 206 p.

2. Machaj B., Pieńkos J.P.

Pomiar stężenia radonu w wodzie za pomocą komory Lucasa (Measurement of radon concentration in water with a Lucas cell detector).

Instytut Chemii i Techniki Jądrowej, Warszawa 2003. Raporty IChTJ. Seria B nr 1/2003, 18 p.

3. Peimel-Stuglik Z., Fabisiak S.

Walidacja źródła kobaltowego "Issledovatel" po remoncie w czerwcu 2003 roku (The validation of the gamma source "Issledovatel" after its repair in June 2003).

Instytut Chemii i Techniki Jądrowej, Warszawa 2003. Raporty IChTJ. Seria B nr 2/2003, 14 p.

4. Peimel-Stuglik Z., Fabisiak S.

Cukry jako dwu-sygnalne dozymetry do pomiaru dużych dawek promieniowania jonizującego. Badania wstępne (Sugars as double-signal high dose dosimeters of ionizing radiation. Preliminary results).

Instytut Chemii i Techniki Jądrowej, Warszawa 2003. Raporty IChTJ. Seria B nr 3/2003, 22 p.

5. Lehner K., Stachowicz W.

Badanie metodą EPR trwałości rodników celulozowych powstających w napromieniowanych przyprawach (Stability of cellulose radicals produced by radiation in spices as studied by the EPR spectroscopy).

Instytut Chemii i Techniki Jądrowej, Warszawa 2003. Raporty IChTJ. Seria B nr 4/2003, 14 p.

CONFERENCE PROCEEDINGS

1. **Bik J., Głuszewski W., Rzymski W.M., Zagórski Z.P.**
   Radiation crosslinking of hydrogenated butadiene-nitrile rubber.
   TECHNOMER 2003, 13-15.11.2003, pp. 1-9, 61.

2. **Chmielewski A.G., Iller E., Tymiński B., Zimek Z., Ostapczuk A., Licki J.**
   Industrial plant for electron beam flue gas treatment.
   Radiation technology in emerging industrial applications. Proceedings of a symposium held in Beijing, China, 6-10.11.2000. Conference & Symposium Papers 18/P, pp. 185-189 (2003 – CD edition).

3. **Chmielewski A.G., Pawelec A., Tymiński B., Zimek Z., Licki J.**
   Industrial applications of electron beam flue gas treatment.
   Emerging applications of radiation processing for the 21st century. Report from a technical meeting held in Vienna, Austria on 28-30.04.2003, pp. 172-180.

4. **Chmielewski A.G., Pawelec A., Tymiński B., Zimek Z., Licki J.**
   Industrial applications of electron beam flue gas treatment.
   The 15th Symposium on Environmental Protection and Safety – Environmental Protection with Ionizing Radiation. Seoul, Korea, 17.10.2003, pp. 43-52 (2003).

5. **Chmielewski A.G., Tymiński B., Zimek Z., Pawelec A., Licki J.**
   Industrial plant for flue gas treatment with high power electron accelerators.
   Application of accelerators in research and industry. 17th International Conference on the application of accelerators in research and industry. Denton, Texas, USA, 12-16 11.2002. Melville 2003, pp. 873-876.

6. **Chmielewski A.G., Zimek Z., Iller E.,Tymiński B., Licki J.**
   Preliminary exploitation of industrial facility for flue gas treatment.
   Radiation technology in emerging industrial applications. Proceedings of a symposium held in Beijing, China, 6-10.11.2000. Conference & Symposium Papers 16/P, pp. 1-4 (2003 – CD edition).

7. **Deptuła A., Olczak T., Łada W., Sartowska B., Chmielewski A.G., Alvani C., Casadio S., Di Bartolomeo A., Croce F., Goretta K.C.**
   Fabrication of spherical and irregularly shaped powders of Li and Ba titanates from titanium tetrachloride by inorganic sol-gel process.
   CIMTEC 2002 – 1st International Ceramics Congress and 3rd Forum on New Materials. 10th International Ceramics Congress – Part A, pp. 441-452 (2003).

8. **Deptuła A., Olczak T., Łada W., Sartowska B., Chmielewski A.G., Hassoun J.**
   Preparation of $LiFePo_4$/metallic (Ni, Cu, and Ag) nanocomposites for electrochemical applications by complex sol-gel process.
   CIMTEC 2002 – 1st International Ceramics Congress and 3rd Forum on New Materials. 10th International Ceramics Congress – Part D, pp. 119-126 (2003).

9. **Głuszewski W., Panta P.P.**
   Kontrola dozymetryczna przemysłowej sterylizacji radiacyjnej (Dosimetric inspection in industrial radiation sterilization process).
   VII Szkoła Sterylizacji i Higienizacji Radiacyjnej. Warszawa, Poland, 16-17.10.2003, pp. VIII-1-6.

10. **Harasimowicz M., Zakrzewska-Trznadel G., Chmielewski A.G.**
    Application of gas separation membranes for processing of biogas.
    Proceedings of the XVIIIth International Symposium on Physico-Chemical Methods of the Mixtures Separation "Ars Separatoria 2003". Złoty Potok n. Częstochowa, Poland, 2-5.06.2003, pp. 125-127.

11. **Harasimowicz M., Zakrzewska-Trznadel G., Chmielewski A.G.**
    Wykorzystanie metod membranowych do wzbogacania w metan gazu z wysypisk i reaktorów biologicznych (Application of membrane methods for enrichment in methane of the gas from waste dumps and biological reactors).
    Dla miasta i środowiska. Konferencja "Problemy unieszkodliwiania odpadów": materiały konferencyjne. Warszawa, Poland, 1.12.2003, pp. 84-87.

12. **Kałuska I.**
    Określanie dawki sterylizacyjnej (Sterilization dose determination).
    VII Szkoła Sterylizacji i Higienizacji Radiacyjnej. Warszawa, Poland, 16-17.10.2003, pp. IV-1-6.

13. Kałuska I.

Walidacja procesu sterylizacji radiacyjnej (Validation of radiation sterilization process).

VII Szkoła Sterylizacji i Higienizacji Radiacyjnej. Warszawa, Poland, 16-17.10.2003, pp. VII-1-2.

14. Kunicki-Goldfinger J.

Preventive conservation strategy for glass collections. Identification of glass objects susceptible to crizzling.

Proceedings of the 5th EC Conference "Cultural Heritage Research: a Pan-European Challenge". Kraków, Poland, 16-18.05.2003, pp. 301-304.

15. Kunicki-Goldfinger J., Kierzek J., Kasprzak A.J., Dzierżanowski P., Małożewska-Bućko B.

Lead in Central European 18th century colourless vessel glass.

Archäometrie und Denkmalpflege. Kurzberichte 2003. Berlin, Germany, 12-14.03.2003, pp. 56-58.

16. Legocka I., Zimek Z., Mirkowski K., Zielonka M.

Polyethylene blends for heat shrinkable product fabrication.

Radiation technology in emerging industrial applications. Proceedings of a symposium held in Beijing, China, 6-10.11.2000. Conference & Symposium Papers 18/P, pp. 8-17 (2003 – CD edition).

17. Michalik J., Sadło J., Danilczuk M.

Paramagnetic silver clusters in molecular sieves: zeolite rho.

Interfacial effects and novel properties of nanomaterials: proceedings of the Symposium on Interfacial Effects in Nanostructured Materials. Warsaw, Poland, 14-18.09.2002, pp. 197-200 (2003).

18. Migdał W.

Napromieniowanie żywności w Unii Europejskiej i w Polsce (Food irradiation in European Union and Poland).

VII Szkoła Sterylizacji i Higienizacji Radiacyjnej. Warszawa, Poland, 16-17.10.2003, pp. IX-1-4.

19. Obrębska M., Chmielewski A.G., Mamełka D.

Czy warszawskie śmieci należy spalać, czy lepiej nadal wywozić na składowiska? (Should be Warsaw wastes burned or better transported to a storage area?)

Dla miasta i środowiska. Konferencja "Problemy unieszkodliwiania odpadów": materiały konferencyjne. Warszawa, Poland, 1.12.2003, pp. 164-168.

20. Ostapczuk A., Chmielewski A.G., Licki J.

Możliwość zastosowania wiązki elektronów do usuwania SO_2, NO_x i WWA oraz dioksyn z gazów spalinowych spalarni śmieci (The possibility of applying electron beam for SO_2, NO_x, PAH and dioxin removal from incineration plant flue gas).

Dla miasta i środowiska. Konferencja "Problemy unieszkodliwiania odpadów": materiały konferencyjne. Warszawa, Poland, 1.12.2003, pp.137-141.

21. Panta P.P.

Podstawy oddziaływania promieniowania jonizującego z materią (Fundamentals of interaction of ionizing radiation with matter).

VII Szkoła Sterylizacji i Higienizacji Radiacyjnej. Warszawa, Poland, 16-17.10.2003, pp. II-1-7.

22. Pańczyk E., Waliś L., Kalicki A., Rowińska L.

Techniki jądrowe w badaniach obrazów (Nuclear techniques in painting research).

Zachodnioukraińska sztuka cerkiewna: dzieła – twórcy – ośrodki techniki. Materiały z międzynarodowej konferencji naukowej. Łańcut, Poland, 10-11.05.2003, pp. 432-448.

23. Przybytniak G.

Obróbka radiacyjna produktów farmaceutycznych (Radiation sterilization of pharmaceutical products).

VII Szkoła Sterylizacji i Higienizacji Radiacyjnej. Warszawa, Poland, 16-17.10.2003, pp. XIII-1-7.

24. Sartowska B., Piekoszewski J., Waliś L., Kopcewicz M., Werner Z., Stanisławski J., Szymczyk W., Prokert F.

Phase transformations in the near surface layer of carbon steels modified with short intense nitrogen and argon plasma pulses.

Nitriding technology: theory & practice. Proceedings of the 9th International Seminar. Warszawa, Poland. Ed. by A. Nakonieczny. Warszawa 2003, pp. 227-235.

25. Stachowicz W.

Samodzielne Laboratorium Napromieniowania Żywności (Laboratory for Detection of Irradiated Foods).

VII Szkoła Sterylizacji i Higienizacji Radiacyjnej. Warszawa, Poland, 16-17.10.2003, pp. X-1-6.

26. Stachowicz W.

Sterylizacja radiacyjna na tle innych metod wyjaławiania (Radiation sterilization as compared with other sterilization methods).

VII Szkoła Sterylizacji i Higienizacji Radiacyjnej. Warszawa, Poland, 16-17.10.2003, pp. I-1-11.

27. Tymiński B., Chmielewski A.G., Zwoliński K.

Paliwa ciekłe z odpadów polietylenu (Liquid fuels from polyethylene wastes).

Dla miasta i środowiska. Konferencja "Problemy unieszkodliwiania odpadów": materiały konferencyjne. Warszawa, Poland, 1.12.2003, pp. 153-159.

28. Wójcik A., Szumiel I.

Biologiczne działanie i ryzyko promieniowania jonizującego (Biological effects and risk of ionising radiation).

VII Szkoła Sterylizacji i Higienizacji Radiacyjnej. Warszawa, Poland, 16-17.10.2003, pp. XXII-1-6.

29. Zagórski Z.P.

Sterylizacja radiacyjna sprzętu medycznego w świetle konferencji w latach 2002 i 2003 (Medical disposable sterilization review basing on 2002 and 2003 conferences).

VII Szkoła Sterylizacji i Higienizacji Radiacyjnej. Warszawa, Poland, 16-17.10.2003, pp. XIX-1-5.

30. Zagórski Z.P., Dziewinski J., Conca J.

Radiolytic effects of plutonium.

Plutonium futures – the science: Third Topical Conference on Plutonium and Actinides. Albuquerque, New Mexico, USA, 6-10.07.2003, pp. 336-338.

31. Zagórski Z.P., Głuszewski W.

Sterylizacja radiacyjna wyrobów z tworzyw sztucznych dla medycyny (Radiation sterilization of plastic products for the medicine).

X Seminarium "Tworzywa sztuczne w budowie maszyn". Referaty. Kraków, Poland, 29.09-1.10.2003, pp. 431-436.

32. Zakrzewska-Trznadel G., Harasimowicz M.

Removal of radioactive compounds with ceramic membranes.

Ars Separatoria 2003. Proceedings of the XVIIIth International Symposium on Physico-Chemical Methods of the Mixtures Separation. Złoty Potok near Częstochowa, Poland, 2-5.06.2003, pp. 112-115.

33. Zimek Z.

Accelerator technology for radiation processing: recent development.

Emerging applications of radiation processing for the 21st century. Report from a technical meeting held in Vienna, Austria on 28-30.04.2003, pp. 67-78.

34. Zimek Z.

Electron accelerators for radiation processing: criteria of selection and exploitation.

Radiation technology in emerging industrial applications. Proceedings of a symposium held in Beijing, China, 6-10.11.2000, Conference & Symposium Papers 16/P, pp. 1-8 (2003 – CD edition).

35. Zimek Z.

Electron beam technology and applications in Poland.

Recent developments in electron accelerator technology and applications. Consultants' Meeting. Quebec, Canada, 18-20.09.2002, [11] p.

36. Zimek Z.

Przegląd rozwiązań konstrukcyjnych akceleratorów stosowanych w technice i technologii radiacyjnej (Review of the technical solutions of accelerators applied in radiation technology).

VII Szkoła Sterylizacji i Higienizacji Radiacyjnej. Warszawa, Poland, 16-17.10.2003, pp. V-1-7.

37. Zimek Z.

Restrictions and limits of accelerator technology applied in industry and environment protection.

Emerging applications of radiation processing for the 21st century. Report from a technical meeting held in Vienna, Austria on 28-30.04.2003, pp. 93-99.

38. Zimek Z.

Wykorzystanie promieniowania hamowania do sterylizacji radiacyjnej sprzętu medycznego jednorazowego użytku (Bremsstrahlung application for radiation sterilization process).

VII Szkoła Sterylizacji i Higienizacji Radiacyjnej. Warszawa, Poland, 16-17.10.2003, pp. XXI-1-11.

39. Zimek Z., Bułka S., Mirkowski J., Roman K.

Secondary electrons monitor for continuous electron energy measurements in UHF linac.

Radiation technology in emerging industrial applications. Proceedings of a symposium held in Beijing, China, 6-10.11.2000. Conference & Symposium Papers 16/P, pp. 1-4 (2003 – CD edition).

40. Zimek Z., Kałuska I.

Implementation of EB radiation sterilization process in Poland.

Radiation technology in emerging industrial applications. Proceedings of a symposium held in Beijing, China, 6-10.11.2000. Conference & Symposium Papers 18/P, pp. 248-252 (2003 – CD edition).

CONFERENCE ABSTRACTS

1. Banasik A., Lankoff A., Lisowska H., Piskulak A., Kuszewski T., Góźdź S., Wójcik A.

Micronuclei frequencies in peripherial blood lymphocytes following aluminium treatment.

VI International Symposium on Chromosomal Aberrations. Essen, Germany, 10-13.09.2003, p. 74.

2. Bik J., Głuszewski W., Rzymski W.M., Zagórski Z.P.

Sieciowanie radiacyjne uwodnionego kauczuku nitrylowego (Radiation crosslinking of hydrogenated nitrile rubber).

Międzynarodowa konferencja naukowo-techniczna z okazji jubileuszu 50-lecia Instytutu Przemysłu Gumowego "Stomil": Elastomery 2003. Nauka dla przemysłu. Pułtusk, Poland, 12-13.06.2003, pp. 35-36.

3. Bobrowski K., Pogocki D., Hug G.L., Schöneich Ch.

Stabilization of sulfur radical cations in methionine-containing peptides: complementary conductometric and spectrophotometric pulse radiolysis studies.

23rd Miller Conference on Radiation Chemistry. Białowieża, Poland, 6-12.09.2003, p. L-08.

4. Bobrowski K., Pogocki D., Marciniak B., Hug G.L., Schöneich Ch.

Oxidation of methionine-containing peptides: spectral and conductomeric pulse radiolysis studies.

1st International Meeting on Applied Physics APHYS-2003. Book of abstracts. Badajoz, Spain, 13-18.10.2003, p. 297.

5. Chmielewski A.G., Ostapczuk A., Licki J.

Electron beam process for destruction of polycyclic aromatic hydrocarbons emitted from coal-fired boiler.

Abstracts: 1st International Symposium on Incomplete Combustion. Kuopio, Finland, 9-11.11.2003, [4] p.

6. Chmielewski A.G., Pawelec A., Tymiński B., Zimek Z.

Operational; experience of the industrial plant for electron beam flue gas treatment.

2003 International Meeting on Radiation Processing. Conference program and abstracts. Chicago, USA, 7-12.09.2003, p. 170.

7. Chmielewski A.G., Sun Y., Bułka S., Zimek Z., Hakoda T., Hashimoto S.

Chlorinated aliphatic and aromatic VOC decomposition in air mixture by using electron beam irradiation.

2003 International Meeting on Radiation Processing. Conference program and abstracts. Chicago, USA, 7-12.09.2003, p. 160.

8. Chmielewski A.G., Wierzchnicki R., Derda M., Mikołajczuk A., Zakrzewska-Trznadel G.

Application od stable isotopes in environmental studies and in food authentication.

Third Conference: Isotopic and Molecular Processes. Cluj-Napoca, Romania, 25-27.09.2003, p. 30.

9. Chwastowska J., Skwara W., Sterlińska E., Pszonicki L.

Analiza specjacyjna chromu (III) i (VI) metodą GF-AAS po ich wstępnym rozdzieleniu (Speciation of chromium (III) and (VI) after their separation).

Nowoczesne metody przygotowania próbek i oznaczania śladowych ilości pierwiastków. Materiały XII Poznańskiego Konwersatorium Analitycznego, Poznań, Poland, 8-9.05.2003, p. 128.

10. Chwastowska J., Skwara W., Sterlińska E., Pszonicki L.

Zachowanie się palladu i platyny jako zanieczyszczeń gleby i ich ługowanie dla celów analitycznych (Behaviour of palladium and platinum pollutants in soil and their leaching for analytical purposes).

Nowoczesne metody przygotowania próbek i oznaczania śladowych ilości pierwiastków. Materiały XII Poznańskiego Konwersatorium Analitycznego, Poznań, Poland, 8-9.05.2003, p. 127.

11. Cieśla K., Rahier H., Zakrzewska-Trznadel G.

The cellulose membrane – water interaction studied by differential scanning calorimetry.

CCTA 9. 9th Conference on Calorimetry and Thermal Analysis. Abstracts. Zakopane, Poland, 31.08.-5.09.2003, p. 156.

12. Cieśla K., Salmieri S., Lacroix M., Le Tien C.

Gamma irradiation influence on physical properties of milk proteins.

2003 International Meeting on Radiation Processing. Chicago, USA, 7-12.09.2003, p. 64.

13. Danko B.

High-accuracy method of molybdenum determination in biological materials by RNAA.

International Conference on Isotopic and Nuclear Analytical Techniques for Health and Environment, Vienna, Austria, 10-13.06.2003. Book of abstracts. IAEA-CN-103/021P, p. 81.

14. Dybczyński R.

Materiały odniesienia i ich znaczenie we współczesnej analizie chemicznej (Reference materials and their significance in contemporary analytical chemistry).

XLVI Zjazd Naukowy PTChem i SITPCh, Lublin, Poland, 15-18.09.2003. Materiały zjazdowe. Tom 2, Sekcje S6-S12, p. 449.

15. Dybczyński R.S.

Very accurate (definitive) methods by radiochemical NAA and their significance for quality assurance in trace analysis.

NEMEA: Neutron measurements and evaluations for applications, Budapest, Hungary, 5-8.11.2003. Book of abstracts, [1] p.

16. Dybczyński R., Bobrowski K., Kruszewski M.

Nuclear and radiation techniques in the life sciences research at the Institute of Nuclear Chemistry and Technology (Warsaw).

Perspectives of life sciences research at nuclear centres. First coordination meeting, Riviera, Zlatny Piasatsi, Bulgaria, 21-27.11.2003. Abstracts, pp. 30-31.

17. Dybczyński R., Danko B., Kulisa K., Chajduk-Maleszewska E., Polkowska-Motrenko H., Samczyński Z., Szopa Z.

Dwa nowe materiały odniesienia dla nieorganicznej analizy śladowej (Two new CRMs for inorganic trace analysis).

Nowoczesne metody przygotowania próbek i oznaczania śladowych ilości pierwiastków. Materiały XII Poznańskiego Konwersatorium Analitycznego, Poznań, Poland, 8-9.05.2003, p. 49.

18. Dybczyński R., Danko B., Kulisa K., Maleszewska E., Polkowska-Motrenko H., Samczyński Z., Szopa Z.

Two new reference materials for inorganic trace analysis.

BERM9: Ninth international symposium on biological and environmental reference materials, Berlin, Germany, 15-19.06.2003. Book of abstracts, p. S 7-8.

19. Dybczyński R., Danko B., Samczyński Z., Kulisa K.

Oznaczanie lantanowców w materiałach biologicznych za pomocą neutronowej analizy aktywacyjnej chromatografii jonów (Determination of lanthanides in biomaterials by NAA and IC).

Nowoczesne metody przygotowania próbek i oznaczania śladowych ilości pierwiastków. Materiały XII Poznańskiego Konwersatorium Analitycznego, Poznań, Poland, 8-9.05.2003, p. 129.

20. Dźwigalski Z., Zimek Z.

Akcelerator LAE 10 jako część stanowiska radiolizy impulsowej (The LAE 10 accelerator as a part of pulse radiolysis experimental set).

III Kongres Polskiego Towarzystwa Próżniowego. Polanica Zdrój, Poland, 2003, p. 53.

21. Głuszewski W., Zagórski Z.P.

Zdolności przerobowe akceleratorów IChTJ do obróbki radiacyjnej (Processing capabilities of INCT accelerators for irradiation treatment).

Międzynarodowa konferencja naukowo-techniczna z okazji jubileuszu 50-lecia Instytutu Przemysłu Gumowego "Stomil": Elastomery 2003. Nauka dla przemysłu. Pułtusk, Poland, 12-13.06.2003, pp. 100-101.

22. Głuszewski W., Zimek Z., Zagórski Z.P.

Radiacyjna modyfikacja polimerów (Radiation modification of polymers).

Szóste Spotkanie Inspektorów Ochrony Radiologicznej. Streszczenia referatów oraz materiały konferencyjne. Dymczewo Nowe, Poland, 3–6.06.2003, p. 37.

23. Grądzka I., Buraczewska I., Szumiel I.

DNA double strand break rejoining in M059J and K human glioma cells X-irradiated and treated with signaling pathways inhibitors.

Gliwice Scientific Meetings 2003. Materiały z konferencji. Gliwice, Poland, 21-22.11.2003, p. 48.

24. Grodkowski J., Neta P.

Formation and reaction of Br_2 radicals in the ionic liquid methyltributylammonium bis(trifluoromethylsulfonyl)imide and in other solvents.

23rd Miller Conference on Radiation Chemistry. Białowieża, Poland, 6-12.09.2003, p. P-20.

25. Harasimowicz M., Zakrzewska-Trznadel G., Chmielewski A.G.

Enrichment of biogas to 90-95% of CH_4 using GS membranes.

PERMEA 2003. Proceedings of the conference. Tatranské Matliare, Slovakia, 7-11.09.2003, p. 171.

26. Kałuska I., Lazurik V.T., Lazurik V.M., Popov G.F., Rogov Y.V., Zimek Z.

Boundary effects in the heterogeneous materials irradiated by electron beams.

2003 International Meeting on Radiation Processing. Conference program and abstracts. Chicago, USA, 7-12.09.2003, p. 167.

27. Kałuska I., Zimek Z.

Dozymetria procesu sterylizacji radiacyjnej – pomiar dawki pochłoniętej (Radiation sterilization dosimetry – the absorbed dose measurements).

Przeszczep w walce z kalectwem. 40 lat bankowania tkanek i sterylizacji radiacyjnej w Polsce. Konferencja jubileuszowa. Warszawa, Poland, 22-23.05.2003, p. 61.

28. Kałuska I., Zimek Z.

Walidacja procesu sterylizacji radiacyjnej (Validation of radiation sterilization process).

Przeszczep w walce z kalectwem. 40 lat bankowania tkanek i sterylizacji radiacyjnej w Polsce. Konferencja jubileuszowa. Warszawa, Poland, 22-23.05.2003, p. 62.

29. Kciuk G., Sicard-Roselli C., Houée-Levin Ch., Mirkowski J., Bobrowski K.

Radiation – induced oxidation of enkephalins and their dipeptide fragments.

23rd Miller Conference on Radiation Chemistry. Białowieża, Poland, 6-12.09.2003, p. P-30.

30. Kierzek J., Kunicki-Goldfinger J., Kasprzak A.J.

An application of the X-ray fluorescence and multivariate analysis for the study of the 18th century vessels from Lubaczow glasshouse.

International Conference on Isotopic and Nuclear Analytical Techniques for Health and Environment, Vienna, Austria, 10-13.06.2003. Book of abstracts. IAEA-CN-103/080P, p. 108.

31. Kornacka E., Przybytniak G.K.

Reactions of thiols with DNA radicals in model system.

XX Seminar on Radio- and Microwave Spectroscopy. RAM 2003. Poznań, Poland, 24-26.04.2003, p. P-30.

32. Korzeniowska-Sobczuk A., Hug G.L., Mirkowski J., Bobrowski K.

Radical cations, radicals, and final products derived from aromatic carboxylic acids containing thioether group: pulse and γ-radiolysis studies.

23rd Miller Conference on Radiation Chemistry. Białowieża, Poland, 6-12.09.2003, p. P-32.

33. Kozakiewicz J., Legocka I., Sadło J., Brzozowska M., Celuch M., Przybylski J.

Effect of polysiloxaneurethaneurea elastomer structure on free radical formation in sterillisation by E-beam/gamma irradiation.

E-MRS 2003 Fall Meeting. Warszawa, Poland, 15-19.09.2003, pp. 177-178.

34. Kruszewski M.

Labile iron pool, oxidative DNA damage and cancerogenesis.

Gliwice Scientific Meetings 2003. Materiały z konferencji. Gliwice, Poland, 21-22.11.2003, p. 14.

35. Kruszewski M.

Technical aspects of the comet assay.

Comet Assay Workshop No 5. Aberdeen, Scotland, 29-30.08.2003, p. 3.

36. Kruszewski M., Iwaneńko T., Oldak T., Gajkowska A., Machaj E.K., Pojda Z.

Ionizing radiation-induced DNA damage in proliferating and non-proliferating human $CD34^+$ cells.

Comet Assay Workshop No 5. Aberdeen, Scotland, 29-30.08.2003, p. 62.

37. Kruszewski M., Lewandowska H., Starzyński R.R., Bartłomiejczyk T., Iwaneńko T., Lipiński P.

Role of labile iron pool in nitric oxide-induced genotoxicity.

From Hazard to Risk. European Environmental Mutagen Society 33rd Meeting. Aberdeen, Scotland, 24-28.08.2003, p. 65.

38. Kunicki-Goldfinger J., Kierzek J., Kasprzak A.J., Małożewska-Bućko B., Dzierżanowski P.

A provenance study of Baroque glass.

Cultural Heritage Research: a Pan-European Challenge. Proceedings of the 5th EC Conference. Kraków, Poland, 16-18.05.2003, p. 376.

39. Legocka I., Celuch M., Sadło J., Kozakiewicz J.

Type of radicals formed in select siloxanurethane polymers under irradiation method of sterilization.

E-MRS 2003 Fall Meeting. Warszawa, Poland, 15-19.09.2003, p. 171.

40. Legocka I., Kostrzewa M., Sadło J., Kozakiewicz J.

Radiation sterilization aspects of poly(siloxaneurethanes) used as medical scaffolds for tissue engineering.

International Conference "Polymers in XXI Century". Kiev, Ukraine, 27-30.10.2003, p. 51.

41. Lipinski P., Lewandowska H., Drapier J.-C., Starzynski R., Bartłomiejczyk T., Kruszewski M.

Increase in labile iron pool (LIP) level and generation of EPR-detectable dinitrosyl-non-heme iron complexes in L5178Y cells exposed to nitric oxide. Possible role of LIP as a source of iron for DNIC formation.

Deregulations du metabolisme du FER: chimie, biologie et therapeutiques. Gif-sur-Yvette, France, 3-5.09.2003, [1] p.

42. Lisowska H., Lankoff A., Banasik A., Wieczorek A., Kuszewski T., Góźdź S., Wójcik A.

Chromosome aberrations frequencies in peripheral blood lymphocytes from patients with larynx cancer.

VI International Symposium on Chromosomal Aberrations. Essen, Germany, 10-13.09.2003, p. 76.

43. Lucchini J.-F., Rafalski A., Riggs M., Conca J.

Influence of radiolysis by products on the actinide chemistry in brines from geological saline repository.

Plutonium futures – the science: Third Topical Conference on Plutonium and Actinides. Albuquerque, New Mexico, USA, 6-10.07.2003, pp. 305-306.

44. Machaj B., Urbański P.

Influence of aerosol concentration and multivariate data processing on indication of radon progeny concentration in air.

International Conference on Isotopic and Nuclear Analytical Techniques for Health and Environment, Vienna, Austria, 10-13.06.2003. Book of abstracts. IAEA-CN-103/030P, p. 86.

45. Malec-Czechowska K., Stachowicz W.

Wykrywanie napromieniowania przypraw zawartych w wybranych produktach spożywczych (Detection of irradiated spices in some foodstuffs).

Ogólnopolskie Sympozjum "Wartość zdrowotna i zanieczyszczenia żywności". Gdańsk, Poland, 18-19.09.2003, p. 123.

46. Malec-Czechowska K., Stachowicz W.

Wykrywanie napromieniowania ziół i przypraw w wybranych produktach spożywczych metodą termoluminescencji (Detection of irradiation in herbs and spices in some foodstuffs by TL method).

XXXIV Sesja Naukowa Komitetu Nauk o Żywności PAN "Jakość polskiej żywności w przededniu integracji polski z Unią Europejską". Wrocław, Poland, 10-11.09.2003, p. 368.

47. Michalik J., Liu W., Lund A., Shiotani M., Komaguchi K., Danilczuk M.

Structure and dynamics of amine radical-cations generated radiolytically in molecular sieves.

5th Meeting of the European Federation of EPR Groups. Book of Abstracts. Lisbon, Portugal, 7-11.09.2003, p. P-50.

48. Michalik J., Migdał W., Polkowska-Motrenko H., Stachowicz W., Starosta W.

Działalność Instytutu Chemii i Techniki Jądrowej na rzecz bezpieczeństwa żywności (Activity of the Institute of Nuclear Chemistry and Technology for food safety).

Bezpieczeństwo żywności i żywienie jako problem zdrowia publicznego w Polsce w przededniu integracji z Unią Europejską. Konferencja Naukowa. Streszczenia, Warszawa, Poland, 29-31.10.2003, pp. 92-93.

49. Michalik J., Sadło J., Danilczuk M.

ESR and ESEEM study of silver clusters in ZK-4 zeolites.

45th Rocky Mountain Conference on Analytical Chemistry. Final Program and Abstracts. Rocky Mountain, USA, 27-31.07.2003, p. 70.

50. Narbutt J.

Trikarbonylkowe kompleksy technetu(I) i renu(I) – nowy kierunek rozwoju chemii radiofarmaceutycznej (Tricarbonyl complexes of technetium(I) and rhenium(I) – a new direction of radiopharmaceutical chemistry).

XLVI Zjazd Naukowy PTChem i SITPChem, Lublin, Poland, 15-18.09.2003. Materiały zjazdowe. Tom 1, Sekcje S1-S5, p. 272.

51. Neta P., Behar D., Grodkowski J.

Pulse radiolysis studies of reaction kinetics in ionic liquids.

23rd Miller Conference on Radiation Chemistry. Białowieża, Poland, 6-12.09.2003, p. L-19.

52. Nieminuszczy J., Grzesiuk E., Kruszewski M., Płazińska M.T., Grzesiuk W.

Damage to DNA and its repair assessed by the "comet" assay in patients with autonomous thyroid modules receiving 131-Iodine therapy.

Gliwice Scientific Meetings 2003. Materiały z konferencji. Gliwice, Poland, 21-22.11.2003, p. 63.

53. Palige J., Dobrowolski A., Owczarczyk A., Chmielewski A.G.

Radiotracers and CFD methods for wastewater treatment apparatus investigation.

International Conference on Isotopic and Nuclear Analytical Techniques for Health and Environment, Vienna, Austria, 10-13.06.2003. Book of abstracts. IAEA-CN-103/174P, p. 139.

54. Panta P.P.

Początki sterylizacji radiacyjnej przeszczepów kostnych w Polsce (History of radiation sterilization of bone allografts in Poland).

Przeszczep w walce z kalectwem. 40 lat bankowania tkanek i sterylizacji radiacyjnej w Polsce. Konferencja jubileuszowa. Warszawa, Poland, 22-23.05.2003, p. 44.

55. Peimel-Stuglik Z., Bryl-Sandelewska T.

Alanpol – cheap, water resistant alanine-polymer routine dosimeter.

8th International Workshop "Electron Magnetic Resonance of Disordered Systems". Abstracts. Sofia-Boyana, Bulgaria, 7-16.06.2003, [1] p.

56. Peimel-Stuglik Z., Skuratov V.A.

Dosimetric response of alanine-polymer foils for 10^9-10^{11} fluences of heavy ions.

8th International Workshop "Electron Magnetic Resonance of Disordered Systems". Abstracts. Sofia-Boyana, Bulgaria, 7-16.06.2003, [1] p.

57. Polkowska-Motrenko H.

Implementation of quality system, production of reference materials and performing proficiency tests – status report of Poland.

1st Project co-ordinators meeting report on the preparation of reference materials and organization of proficiency test rounds, Manila, Philippines, 10-14.03.2003. IAEA Project INT/1/054, [12] p. (CD edition).

58. Polkowska-Motrenko H., Danko B., Dybczyński R.

Metrological assessment of the high-accuracy RNAA method of Co determination in biological materials.

International Conference on Isotopic and Nuclear Analytical Techniques for Health and Environment, Vienna, Austria, 10-13.06.2003. Book of abstracts. IAEA-CN-103/037, p. 11.

59. Przybytniak G., Kornacka E.

DNA radicals as seen by EPR spectroscopy.

XX Seminar on Radio- and Microwave Spectroscopy. RAM 2003. Poznań, Poland, 24-26.04.2003, p. L-19.

60. Sadło J., Michalik J., Yamada H., Michiue Y.

New type of paramagnetic silver clusters in sodalite: Ag_8^{n+}.

E-MRS 2003 Fall Meeting. Warszawa, Poland, 15-19.09.2003, p. 200.

61. Sadło J., Stachowicz W., Michalik J., Dziedzic-Gocławska A.

Ocena rozkładu dawki pochłoniętej w masywnym przeszczepie kostnym sterylizowanym wiązką elektronów 10 MeV (Evaluation of dose ditribution in a massive bone graft sterilized with a beam of 10 MeV electrons).

Przeszczep w walce z kalectwem. 40 lat bankowania tkanek i sterylizacji radiacyjnej w Polsce. Konferencja jubileuszowa. Warszawa, Poland, 22-23.05.2003, p. 59.

62. Serdiuk K., Pogocki D.

A computational estimation of the reduction potential of Met^{35} in Alzheimer's β-peptide.

23rd Miller Conference on Radiation Chemistry. Białowieża, Poland, 6-12.09.2003, p. P-40.

63. Serdiuk K., Pogocki D.

Słabe oddziaływania siarka-tlen w białkach (Weak interactions of sulfur-oxygen type in proteins).

Metody fizykochemiczne badania oddziaływań międzycząsteczkowych w układach biologicznych. Szkoła Fizykochemii Organicznej. Przesieka, Poland, 9-14.06.2003, p. 27.

64. Serdiuk K., Sadło J., Płusa M., Pogocki D.

Some substituted thioethers are able to spontaneously reduce Cu(II) imidazole complexes. A possible implication for the copper-related neurotoxic properties of Alzheimer's amyloid β-peptide.

23rd Miller Conference on Radiation Chemistry. Białowieża, Poland, 6-12.09.2003, p. P-39.

65. Serdiuk K., Sadło J., Pogocki D.

Podstawione tioetery mogą spontanicznie redukować Cu(II). Procesy o potencjalnym znaczeniu dla związanej z Cu neurotoksyczności β-amyloidowego peptydu Alzheimera (Some substituted thioethers are able to spontaneously reduce Cu(II) imidazole complexes. A possible implication for neurotoxic properties of Alzheimer's amyloid β-peptide).

Metody fizykochemiczne badania oddziaływań międzycząsteczkowych w układach biologicznych. Szkoła Fizykochemii Organicznej. Przesieka, Poland, 9-14.06.2003. Suppl.1, [1] p.

66. Skwara W., Chwastowska J., Sterlińska E., Dudek J., Pszonicki L.

Zastosowanie GF-AAS do badania zachowania się platyny i palladu występujących jako zanieczyszczenia środowiska (Behaviour of palladium and platinum in soil and their determination by GF-AAS).

VIII Konferencja: Zastosowanie metod AAS, ICP-AES i ICP-MS w analizie środowiskowej, Warszawa, Poland, 17-18.11.2003, p. 8.

67. Sommer S., Buraczewska I., Wojewódzka M., Bożyk E., Szumiel I., Wójcik A.

Analysis of the frequencies of exchange type aberration in chromosomes 2, 8 and 14 in lymphocytes of four donors by chromosome paintings.

VI International Symposium on Chromosomal Aberrations. Essen, Germany, 10-13.09.2003, pp. 80-81.

68. Stachowicz W.

Zagadnienia techniczne sterylizacji przeszczepów tkankowych za pomocą promieniowania gamma i szybkich elektronów (Technical aspects of radiation sterilisation of tissue grafts with gamma rays and fast electrons).

Przeszczep w walce z kalectwem. 40 lat bankowania tkanek i sterylizacji radiacyjnej w Polsce. Konferencja jubileuszowa. Warszawa, Poland, 22-23.05.2003, p. 46.

69. Stachowicz W., Michalik J., Dziedzic-Gocławska A., Ostrowski K.

Badanie metodą spektrometrii elektronowego rezonansu paramagnetycznego (EPR) rodników oraz centrów paramagnetycznych powstających w tkankach szkieletowych pod wpływem promieniowania jonizującego (EPR studies on radicals and paramagnetic centres evoked in skeletal tissues under the action of ionising radiation).

Przeszczep w walce z kalectwem. 40 lat bankowania tkanek i sterylizacji radiacyjnej w Polsce. Konferencja jubileuszowa. Warszawa, Poland, 22-23.05.2003, p. 45.

70. Strzelczak G., Sadło J., Stachowicz W., Michalik J., Callens F., Goovaerts E.
Multifrequency EPR study of some natural dosimetric materials.
23rd Miller Conference on Radiation Chemistry. Białowieża, Poland, 6-12.09.2003, p. P-46.

71. Trojanowicz M., Drzewicz P., Bojanowska-Czajka A.
Chemical monitoring of the effectiveness of radiolytic degradation of organic pollutants in wasters and wastes.
3rd SENSPOL Workshop "Monitoring in polluted environments for investigated water-soil management", Kraków, Poland, 3-6.06.2003. Extended abstracts, pp. 1-6.

72. Urbański P., Kowalska E.
Multivariate techniques in processing data from radiometric experiments.
International Conference on Isotopic and Nuclear Analytical Techniques for Health and Environment, Vienna, Austria, 10-13.06.2003. Book of abstracts. IAEA-CN-103/031P, p. 87.

73. Wierzchnicki R., Derda M., Mikołajczuk A.
Stable isotope composition of food from different regions of Poland.
International Conference on Isotopic and Nuclear Analytical Techniques for Health and Environment, Vienna, Austria, 10-13.06.2003. Book of abstracts. IAEA-CN-103/169P, p. 135.

74. Wiśniowski P.B., Bobrowski K., Carmichael I., Hug G.L.
UV-VIS and ESR time-resolved pulse radiolysis study: β-scission of α-(methylthio)acetamide derived radical.
23rd Miller Conference on Radiation Chemistry. Białowieża, Poland, 6-12.09.2003, p. P-55.

75. Wiśniowski P., Carmichael I., Fessenden R.W., Hug G.L.
What time-resolved ESR tells us about the radiolytic oxidation of amino acids.
23rd Miller Conference on Radiation Chemistry. Białowieża, Poland, 6-12.09.2003, p. L-09.

76. Wojewódzka M., Bartłomiejczyk T., Kruszewski M.
Frequency of homologous recombination in two cell lines differing in DSB repair ability.
From Hazard to Risk. European Environmental Mutagen Society 33rd Annual Meeting. Aberdeen, Scotland, 24-28.08.2003, p. 65.

77. Wojewódzka M., Kruszewski M.
Comet assay study of the role of poly(ADP-ribosylation) in DNA-PK-mediated pathway of DNA repair in L5178Y and CHO cells.
Comet Assay Workshop No 5. Aberdeen, Scotland, 29-30.08.2003, p. 31.

78. Wojewódzka M., Kruszewski M.
DNA double strand break repair dependence on poly(ADP-ribosylation) in L5178Y and CHO cells.
12th International Congress of Radiation Research. Brisbane, Queensland, Australia, 17-22.08.2003, p. 305.

79. Wojewódzka M., Sochanowicz B., Szumiel I.
Differential DNA double strand break fixation dependence on poly(ADP-ribosylization) in L5178Y and CHO cells.
Gliwice Scientific Meetings 2003. Materiały z konferencji. Gliwice, Poland, 21-22.11.2003, p. 78.

80. Woźniak A.
Badanie jakości złącza rur preizolowanych (Quality test of the interconnection between pre-isolated tubes).
VII Forum Ciepłowników Polskich. Międzyzdroje, Poland, 15-17.09.2003, pp. 276-277.

81. Wójcik A., Bruckmann E., Stoilov L., Sonntag C. von, Goedecke W., Zdzienicka M., Obe G.
Insights into the mechanisms of SCE formation.
VI International Symposium on Chromosomal Aberrations. Essen, Germany, 10-13.09.2003, p. 68.

82. Zagórski Z.P.
EB – crosslinking of elastomers, how does it compare with a radiation crosslinking of other polymers?
2003 International Meeting on Radiation Processing. Conference program and abstracts. Chicago, USA, 7-12.09.2003, p. 279.

83. Zagórski Z.P., Głuszewski W.
Modyfikacja własności polimerów w procesie sterylizacji radiacyjnej (Modification of properties of polymers in the process of radiation sterilization).

Przeszczep w walce z kalectwem. 40 lat bankowania tkanek i sterylizacji radiacyjnej w Polsce. Konferencja jubileuszowa. Warszawa, Poland, 22-23.05.2003, p. 63.

84. Zagórski Z.P., Rajkiewicz M.

Chemia radiacyjna a elastomery (Radiation chemistry and elastomers).

Międzynarodowa konferencja naukowo-techniczna z okazji jubileuszu 50-lecia Instytutu Przemysłu Gumowego "Stomil". Elastomery 2003. Nauka dla przemysłu. Pułtusk, Poland, 12-13.06.2003, p. 34.

85. Zakrzewska-Trznadel G., Chmielewski A.G., Miljević N., Van Hook A.

Separation of hydrogen and oxygen isotopes by membrane method.

Third Conference: Isotopic and Molecular Processes. Cluj-Napoca, Romania, 25-27.09.2003, p. 15.

86. Zakrzewska-Trznadel G., Harasimowicz M.

Application of ceramic membranes for hazardous wastes processing: pilot plant experiments with radioactive solutions.

PERMEA 2003. Proceedings of the conference. Tatranské Matliare, Slovakia, 7-11.09.2003, p. 48.

87. Zimek Z.

Akceleratory elektronów dla potrzeb bankowania tkanek (Electron accelerators for tissue banking).

Przeszczep w walce z kalectwem. 40 lat bankowania tkanek i sterylizacji radiacyjnej w Polsce. Konferencja jubileuszowa. Warszawa, Poland, 22-23.05.2003, p. 60.

SUPPLEMENT LIST OF THE INCT PUBLICATIONS IN 2002

ARTICLES

1. Chmielewski A.G.

Wiek pary – wiek atomu. Polsko-chilijskie badania w dziedzinie chemii i techniki jądrowej (Century of the steam – century of the atom. Polish-Chilean investigation in the domain of nuclear chemistry and technology).

Ameryka Łacińska, 10, 69-79 (2002).

2. Chmielewski A.G., Sun Y., Bułka S., Zimek Z., Licki J., Kubica K.

NO_x reduction by using EB irradiation under influence of alcohol.

Acta Agrophysica, 80, 343-348 (2002).

3. Ciurapiński A., Parus J., Donohue D.

Particle analysis for a strengthened safeguards system: Use of a scanning electron microscope equipped with EDXRF and WDXRF spectrometers.

Journal of Radioanalytical and Nuclear Chemistry, 251, 1, 345-352 (2002).

4. Dancewicz A.M., Malec-Czechowska K., Szot Z.

Natural and induced thermoluminescence of soils.

Polish Journal of Soil Science, 35, 2, 1-10 (2002).

5. Grigoriew H., Wolińska-Grabczyk A., Bernstorff S., Jankowski A.

Temperature effected structural transitions in polyurethanes saturated with solvents studied by SAXS synchrotron method.

Journal of Macromolecular Science–Pure and Applied Chemistry A, 39, 7, 629-642 (2002).

6. Hołderna-Natkaniec K., Szyczewski A., Natkaniec I., Khavryutchenko V.D., Pawlukojć A.

Progesterone and testosterone studies by neutron-scattering methods and quantum chemistry calculations.

Applied Physics A, 74 (Suppl.), S1274-S1276 (2002).

7. Łyczko K.

Chemia gazów szlachetnych (Chemistry of the noble gases).

Wiadomości Chemiczne, 56, 9-10, 771-792 (2002).

8. Majdan M., Pikus S., Gładysz-Płaska A., Fuks L., Zięba E.

Adsorption of light lanthanides on the zeolite A surface.

Colloids and Surfaces A, 209, 27-35 (2002).

9. Samochocka K., Lewandowski W., Priebe W., Fuks L.
Vibrational studies of Pt(II) and Pd(II) complexation by 3,4-diamino lyxo-hexopyranoside.
Journal of Molecular Structure, 614, 203-209 (2002).

BOOKS

1. Chmielewski A.G., Dembiński W., Zakrzewska-Trznadel G., Miljević N., Van Hook A.
Stable isotopes – some new fields of application.
Red. R. Zarzycki. Polska Akademia Nauk, Łódź 2002, 85 p.

CHAPTERS IN BOOKS

1. Chmielewski A.G.
Environmental effects of fossil fuel combustion.
In: Encyclopedia of life support systems (EOLSS). Eolss Publishers, Oxford, UK 2002.

2. Chmielewski A.G.
Environmental effects of suspended and toxic materials from coal and peat combustion.
In: Encyclopedia of life support systems (EOLSS). Eolss Publishers, Oxford, UK 2002.

3. Chmielewski A.G.
Environmental significance of fuel-derived organic compounds.
In: Encyclopedia of life support systems (EOLSS). Eolss Publishers, Oxford, UK 2002.

CONFERENCE ABSTRACTS

1. Derda M., Wierzchnicki R., Chmielewski A.G.
Determination of $^{34}S/^{32}S$ sulfur isotope ratio in the products of coal combustion process.
VI Isotope Workshop. Abstracts. Tallinn, Estonia, 29.06.-4.07.2002, p. 23.

2. Mikołajczuk A., Wierzchnicki R., Chmielewski A.G.
Investigation of $^{34}S/^{32}S$ isotope for the system gaseous SO_2 – nitrobenzene SO_2 solution.
VI Isotope Workshop. Abstracts. Tallinn, Estonia, 29.06.-4.07.2002, p. 73.

3. Wierzchnicki R., Miljević N., Chmielewski A.G.
Oxygen and hydrogen isotopic measurements for food authentication.
VI Isotope Workshop. Abstracts. Tallinn, Estonia, 29.06.-04.07.2002, p. 127.

NUKLEONIKA
THE INTERNATIONAL JOURNAL OF NUCLEAR RESEARCH

CONTENTS OF No. 1/2003

CONTENTS OF No. 2/2003

Proceedings of the 2nd International Symposium on Low Energy Electron-Molecule Interactions, 29th August – 2nd September 2003, Chlewiska/Siedlce, Poland

CONTENTS OF No. 3/2003

CONTENTS OF No. 4/2003

SUPPLEMENT No. 1/2003

Proceedings of the All-Polish Seminar on Mössbauer Spectroscopy OSSM'2002, 9-12 June 2002, Goniądz, Poland

SUPPLEMENT No. 2/2003

Proceedings of the XXXIII European Cyclotron Progress Meeting, 17-21 September 2002, Warsaw and Kraków, Poland

Information

INSTITUTE OF NUCLEAR CHEMISTRY AND TECHNOLOGY
NUKLEONIKA
Dorodna 16, 03-195 Warszawa, Poland
phone: (+4822) 811-30-21 or 811-00-81 int. 14-91; fax: (+4822) 811-15-32;
e-mail: nukleon@orange.ichtj.waw.pl
Abstracts are available on-line at http://www.ichtj.waw.pl/ichtj/general/nukleon.htm

PRESS PUBLICATIONS AND INTERVIEWS IN 2003

PRESS PUBLICATIONS

1. **Wójcik Andrzej**
   Serca Hiroszimy – skutki wojny atomowej (The hearts of Hiroshima – effects of nuclear war). Gazeta Wyborcza, 03.03.2003, p.18.

INTERVIEWS

1. **Michalik Jacek**
   Jazurkiewicz Z.: Trudne lata chemii jądrowej (Difficult years of nuclear chemistry). Przegląd Techniczny, 22, 6-7 (2003).
2. **Kruszewski Marcin**
   Sitkiewicz M.: Bis misja (The Radio BIS mission). Radio BIS, 24.09.2003.
3. **Kruszewski Marcin**
   Las uśpił geny (The forest has drowsed genes). Gazeta Wyborcza, 24.09.2003, p.12.
4. **Kruszewski Marcin**
   Mar K.: Bis misja (The Radio BIS mission). Radio BIS, 25.09.2003.
5. **Kruszewski Marcin**
   Sitkiewicz M.: Bis misja (The Radio BIS mission). Radio BIS, 16.10.2003.
6. **Waliś Lech, Michalik Jacek**
   Karwowski M.: Nieszkodliwe promieniowanie (Harmless radiation). Forum Akademickie, 6, 49-51 (2003).
7. **Wojewódzka Maria**
   Rzeczpospolita, 13.06.2003, p.A10.
8. **Wójcik Andrzej**
   Bobrowska K.: Bis misja (The Radio BIS mission). Radio BIS, 23.02.2003.
9. **Wójcik Andrzej**
   Mar K.: Bis misja (The Radio BIS mission). Radio BIS, 10.06.2003.

THE INCT PATENTS AND PATENT APPLICATIONS IN 2003

PATENTS

1. Urządzenie do mieszania gazów reagujących chemicznie (A device for mixing gases reacting chemically)
   B. Tymiński, A. Chmielewski
   Polish patent No. 185420

PATENT APPLICATIONS

1. Urządzenie do równomiernego rozdziału strumienia gazu na wlocie do aparatu (A device for uniform separation of gas stream at the inlet to an apparatus)
   A.G. Chmielewski, A. Pawelec, B. Tymiński
   P.359352
2. Sposób otrzymywania termotopliwej wkładki grzejnej (Method for obtaining a thermofucible heating insert)
   I. Legocka, A. Woźniak, K. Mirkowski, Z. Zimek, A. Nowicki
   P.360169
3. Sposób przygotowania przemysłowych gazów odlotowych do oczyszczania z SO_2 i NO_x metodą radiacyjną (Method for preparing industrial flue gases to be purified from SO_2 and NO_x by radiation technique)
   A. Pawelec, B. Tymiński, P.D. Dimitrova, D.Z. Naydenov, L.T. Radkov
   P.362266
4. Sposób otrzymywania bioceramicznego materiału (Method for obtaining a bioceramic material)
   W. Łada, A. Ignaciuk, A. Deptuła, M. Kozłowski, T. Olczak
   P.362370
5. Sposób oczyszczania beznośnikowego kwasu ortofosforowego $H_3{}^{32}PO_4$ od siarczanów (Method for purification of carrier-free orthophosphoric acid, $H_3{}^{32}PO_4$ from sulphates)
   R. Dybczyński, H. Polkowska-Motrenko, E. Chajduk-Maleszewska, K. Kulisa, B. Danko, K. Chrustowski, M. Domaradzki
   P.362637

M. Fedorowicz (The Children's Memorial Health Institute, Warszawa, Poland), M. Birbach (The Children's Memorial Health Institute, Warszawa, Poland), B. Maruszewski (The Children's Memorial Health Institute, Warszawa, Poland)

- Działalność Banku Tkanek Oka w Warszawie w latach 1995-2002 (The activity of Warsaw Eye Bank in 1995-2002)
  J. Szaflik (Warsaw Eye Bank, Poland), I. Grabska-Liberek (Warsaw Eye Bank, Poland), M. Brix-Warzecha (Warsaw Eye Bank, Poland)
- Powstanie i działalność Banku Tkanek Oka w Lublinie (Establishment and activity of Lublin Eye Bank)
  B. Rymgayłło-Jankowska (Lublin University School of Medicine, Poland), D. Durakiewicz (Lublin University School of Medicine, Poland), Z. Zagórski (Lublin University School of Medicine, Poland)
- Pozyskiwanie tkanki kostnej po pobraniach wielonarządowych w Pomorskiej Akademii Medycznej w Szczecinie (Harvesting of bone tissue following multi-organ procurement in Pomeranian Medical School in Szczecin)
  A. Bohatyrewicz (Pomeranian Academy of Medicine, Szczecin, Poland), R. Bohatyrewicz (Pomeranian Academy of Medicine, Szczecin, Poland), R. Mazur (Regional Blood Center Tissue Bank, Morawica, Poland), P. Białecki (Pomeranian Academy of Medicine, Szczecin, Poland), D. Larysz (Pomeranian Academy of Medicine, Szczecin, Poland), M. Kędzierski (Pomeranian Academy of Medicine, Szczecin, Poland), A. Dziedzic-Gocławska (Medical University of Warsaw, Poland)
- Zasady współpracy z zagranicznymi bankami tkanek (International co-operation with tissue banks)
  E. Biernat-Kałuża (Carolina Medical Center, Warszawa, Poland)

Session III. ZASTOSOWANIA KLINICZNE ALLOGENICZNYCH PRZESZCZEPÓW KOSTNYCH W REWIZYJNYCH OPERACJACH STAWÓW (CLINICAL APPLICATION OF ALLOGENIC BONE GRAFTS IN HIP REVISION SURGERY)

Chairman: T. Gaździk (Medical University of Silesia, Sosnowiec, Poland), P. Małdyk (Institute of Rheumatology, Warszawa, Poland)

- Allogeniczne, mrożone, sterylizowane radiacyjnie przeszczepy kostne w zabiegach rewizyjnych po protezoplastyce stawu biodrowego i kolanowego (Allogenic bone grafts in reconstructive hip and knee revision surgery)
  A. Górecki (Medical University of Warsaw, Poland), T. Jabłoński (Medical University of Warsaw, Poland), M. Kowalski (Medical University of Warsaw, Poland), K. Purski (Medical University of Warsaw, Poland)
- Zastosowanie allogenicznych przeszczepów kostnych zamrożonych i radiacyjnie wyjałowionych w uzupełnianiu ubytków panewki w protezoplastyce rewizyjnej stawu biodrowego (Application of frozen radiation-sterilised bone allografts for various acetabulum defect reconstructions)
  K. Kwiatkowski (Clinical Military Hospital, Warszawa, Poland), J. Płomiński (Clinical Military Hospital, Warszawa, Poland)
- Ocena przebudowy allogenicznych przeszczepów kostnych zamrożonych i radiacyjnie wyjałowionych po protezoplastyce rewizyjnej panewki stawu biodrowego (Incorporation of frozen, radiation-sterilized bone allografts after cement acetabular revison)
  K. Kwiatkowski (Clinical Military Hospital, Warszawa, Poland), J. Płomiński (Clinical Military Hospital, Warszawa, Poland), M. Żabicka (Clinical Military Hospital, Warszawa, Poland)
- Zastosowanie mrożonych, sterylizowanych radiacyjnie, allogenicznych przeszczepów kostnych w plastykach dachu panewek stawów biodrowych i osteotomiach miednicy (Application and evaluation of bone allografts in shelf-type acetabuloplasty and pelvic osteotomies)
  W. Przybysz (Medical University of Warsaw, Poland), S. Chaberek (Medical University of Warsaw, Poland), A. Sionek (Medical University of Warsaw, Poland), A. Czop (Medical University of Warsaw, Poland), W. Zasacki (Medical University of Warsaw, Poland), A. Kraus (Medical University of Warsaw, Poland)

Session IV. ZASTOSOWANIA KLINICZNE ALLOGENICZNYCH PRZESZCZEPÓW TKANKOWYCH W ORTOPEDII I CHIRURGII URAZOWEJ (CLINICAL APPLICATION OF ALLOGENIC GRAFTS IN ORTHOPAEDICS AND TRAUMA SURGERY)

Chairman: A. Górecki (Medical University of Warsaw, Poland), W. Marczyński (Clinical Military Hospital, Warszawa, Poland)

- Ocena kliniczna zastosowania mrożonych, sterylizowanych radiacyjnie, allogenicznych przeszczepów kostnych w ortopedii i chirurgii urazowej (Clinical evaluation of application of allogenic, radiation sterilized bone grafts in orthopaedics and trauma surgery)
  W. Marczyński (Clinical Military Hospital, Warszawa, Poland)
- Przeszczep allogeniczny więzadła rzepki w rekonstrukcji rewizyjnej aparatu wyprostnego kolana – opis przypadku (Allograft of knee-cup ligament in the reconstructive revision surgery of knee – description of a case)
  R. Śmigielski (Carolina Medical Center, Warszawa, Poland), P. Chomicki-Bindas (Carolina Medical Center, Warszawa, Poland), Z. Czyrny (Carolina Medical Center, Warszawa, Poland), M. Drwięga (Carolina Medical Center, Warszawa, Poland)

- Wykorzystanie alloprzeszczepów łąkotek w kolanach po meniscektomii (Use of allografts of meniscuses in knees after meniscectomy)
  R. Śmigielski (Carolina Medical Center, Warszawa, Poland), Z. Czyrny (Carolina Medical Center, Warszawa, Poland), A. Mioduszewski (Carolina Medical Center, Warszawa, Poland), M. Drwięga (Carolina Medical Center, Warszawa, Poland)
- Allogeniczne mrożone przeszczepy ze ścięgna Achillesa w rekonstrukcji więzadeł krzyżowych (Frozen allografts from the Achilles tendon in the reconstruction of sacral ligaments)
  A. Mioduszewski (Carolina Medical Center, Warszawa, Poland), R. Śmigielski (Carolina Medical Center, Warszawa, Poland), Z. Czyrny (Carolina Medical Center, Warszawa, Poland), E. Biernat-Kałuża (Carolina Medical Center, Warszawa, Poland)
- Rozległa martwica kłykcia przyśrodkowego kości udowej leczona świeżym przeszczepem chrzęstno-kostnym – opis przypadku (Vast necrosis of the paracentral condyle of thigh bone treated with a fresh cartilage-bony graft – description of a case)
  R. Śmigielski (Carolina Medical Center, Warszawa, Poland), P. Chomicki-Bindas (Carolina Medical Center, Warszawa, Poland), Z. Czyrny (Carolina Medical Center, Warszawa, Poland), M. Drwięga (Carolina Medical Center, Warszawa, Poland)
- Zastosowanie i ocena allogennych przeszczepów kostnych w operacjach wad stóp u dzieci (Application of preserved, radiation-sterilised bone allografts in paediatric orthopaedic surgery)
  A. Sionek (Medical University of Warsaw, Poland), W. Przybysz (Medical University of Warsaw, Poland), A. Czop (Medical University of Warsaw, Poland), W. Zasacki (Medical University of Warsaw, Poland), A. Kraus (Medical University of Warsaw, Poland)

Session V. ZASTOSOWANIA KLINICZNE ALLOGENICZNYCH PRZESZCZEPÓW TKANKOWYCH W KARDIOCHIRURGII (CLINICAL APPLICATION OF ALLOGENIC GRAFTS IN CARDIOSURGERY)

Chairman: Z. Religa (Institute of Cardiology, Warszawa, Poland), J. Sadowski (Collegium Medicum, Jagiellonian University, Kraków, Poland), B. Maruszewski (The Children's Memorial Health Institute, Warszawa, Poland)

- Wczesne wyniki przeszczepiania homograftów mitralnych (Clinical application of mitral valve homografts)
  Z. Religa (Institute of Cardiology, Warszawa, Poland), G. Religa (Institute of Cardiology, Warszawa, Poland)
- Allogenne zastawki aortalne i płucne w leczeniu wad lewego ujścia tętniczego i tętniaków aorty wstępującej (Allogenic aortal and pulmonary valves in the treatment of left arterial ostium defects and ascending aorta aneurysms)
  G. Marek (Collegium Medicum, Jagiellonian University, Kraków, Poland), J. Sadowski (Collegium Medicum, Jagiellonian University, Kraków, Poland), B. Kapelak (Collegium Medicum, Jagiellonian University, Kraków, Poland), R. Pfitzner (Collegium Medicum, Jagiellonian University, Kraków, Poland), A. Dziatkowiak (Collegium Medicum, Jagiellonian University, Kraków, Poland)
- Dwadzieścia lat doświadczeń klinicznych w implantacji zastawek allogennych u dzieci z wrodzonymi wadami serca operowanych w Klinice Kardiochirurgii Instytutu „Pomnik Centrum Zdrowia Dziecka" (20 years of clinical experience in allograft heart valve implantation in children with congenital heart diseases in the Department of Cardiothoracic Surgery, the Children's Memorial Health Institute)
  B. Maruszewski (The Children's Memorial Health Institute, Warszawa, Poland), A. Pastuszko (The Children's Memorial Health Institute, Warszawa, Poland), A. Kansy (The Children's Memorial Health Institute, Warszawa, Poland), P. Burczyński (The Children's Memorial Health Institute, Warszawa, Poland), M. Birbach (The Children's Memorial Health Institute, Warszawa, Poland), W. Lipiński (The Children's Memorial Health Institute, Warszawa, Poland), K. Mozol (The Children's Memorial Health Institute, Warszawa, Poland), F. Orchowski (The Children's Memorial Health Institute, Warszawa, Poland), M. Mirkowicz-Małek (The Children's Memorial Health Institute, Warszawa, Poland), M. Fedorowicz (The Children's Memorial Health Institute, Warszawa, Poland)

Session VI. ZASTOSOWANIA KLINICZNE ALLOGENICZNYCH PRZESZCZEPÓW TKANKOWYCH W OKULISTYCE (CLINICAL APPLICATION OF ALLOGRAFTS IN OPHTHALMOLOGY)

Chairman: J. Szaflik (Medical University of Warsaw, Poland), Z. Zagórski (Lublin University School of Medicine, Poland)

- Zastosowanie owodni ludzkiej w okulistyce (Amniotic membrane application in ocular surface diseases)
  I. Grabska-Liberek (Medical University of Warsaw, Poland), M. Rowiński (Medical University of Warsaw, Poland), J. Szaflik (Medical University of Warsaw, Poland), A. Dziedzic-Gocławska (Medical University of Warsaw, Poland)
- Kliniczne zastosowanie tkanek pozyskiwanych w Lubelskim Banku Tkanek Oka (Clinical application of tissue harvested in the Lublin Eye Bank)
  Z. Zagórski (Lublin University School of Medicine, Poland), E. Rakowska (Lublin University School of Medicine, Poland), B. Rymgayłło-Jankowska (Lublin University School of Medicine, Poland), A. Kudasiewicz-Kardaszewska (Lublin University School of Medicine, Poland)

- Ocena morfologiczna śródbłonka rogówki u pacjentów po przeszczepie (Indication for corneal graft and morphological evaluation of cornea endothelium after keratoplasty)
  I. Grabska-Liberek (Medical University of Warsaw, Poland), J. Izdebska (Medical University of Warsaw, Poland), J. Szaflik (Medical University of Warsaw, Poland)

Session VII. BADANIA DOŚWIADCZALNE W BANKOWANIU TKANEK (RESEARCH IN TISSUE BANKING)

Chairman: J. Michalik (Institute of Nuclear Chemistry and Technology, Warszawa, Poland), A. Dziedzic-Gocławska (Medical University of Warsaw, Poland)

- Początki sterylizacji radiacyjnej przeszczepów kostnych w Polsce (History of radiation sterilization of bone allografts in Poland)
  P.P. Panta (Institute of Nuclear Chemistry and Technology, Warszawa, Poland)
- Badanie metodą spektrometrii elektronowego rezonansu paramagnetycznego (EPR) rodników oraz centrów paramagnetycznych powstających w tkankach szkieletowych pod wpływem promieniowania jonizującego (EPR studies on radicals and paramagnetic centres evoked in skeletal tissues under the action of ionising radiation)
  W. Stachowicz (Institute of Nuclear Chemistry and Technology, Warszawa, Poland), J. Michalik (Institute of Nuclear Chemistry and Technology, Warszawa, Poland), A. Dziedzic-Gocławska (Medical University of Warsaw, Poland), K. Ostrowski (Medical University of Warsaw, Poland)
- Zagadnienia techniczne sterylizacji przeszczepów tkankowych za pomocą promieniowania gamma i szybkich elektronów (Technical aspects of sterilization of tissue grafts with gamma rays and fast electrons)
  W. Stachowicz (Institute of Nuclear Chemistry and Technology, Warszawa, Poland)
- Zastosowanie modelu heterotopowej indukcji osteogenezy dla oceny jakości konserwowanych, sterylizowanych radiacyjnie przeszczepów kostnych (The effect of various methods of preservation with subsequent radiation sterilisation on osteoinductive properties of bone grafts (a model of heterotopically induced osteogenesis as a quality test for bone allografts))
  A. Dziedzic-Gocławska (Medical University of Warsaw, Poland), A. Kamiński (Medical University of Warsaw, Poland)
- Wpływ metod konserwacji i warunków sterylizacji radiacyjnej na degradację kolagenu – podstawowego składnika przeszczepów tkankowych (Solubility *in vitro* of collagen as a quality test of connective tissue grafts preserved in different manners)
  A. Dziedzic-Gocławska (Medical University of Warsaw, Poland), A. Kamiński (Medical University of Warsaw, Poland)
- Wpływ procesów konserwacji i warunków sterylizacji radiacyjnej na wytrzymałość mechaniczną kości (The effect of preservation procedures (fresh, lyophilised, deep-frozen bone samples) and radiation-sterilisation conditions (doses, temperatures) on mechanical properties of bone)
  A. Kamiński (Medical University of Warsaw, Poland), A. Komender (Medical University of Warsaw, Poland), A. Dziedzic-Gocławska (Medical University of Warsaw, Poland)
- Ocena cytotoksyczności polimerów używanych do pakowania sterylizowanych radiacyjnie przeszczepów tkankowych (Cytotoxicity tests for polymers used in tissue banking practice)
  I. Uhrynowska-Tyszkiewicz (Medical University of Warsaw, Poland), E. Olender (Medical University of Warsaw, Poland), A. Kamiński (Medical University of Warsaw, Poland), A. Dziedzic-Gocławska (Medical University of Warsaw, Poland)

Session VIII. BADANIA DOŚWIADCZALNE W BANKOWANIU TKANEK c.d. (RESEARCH IN TISSUE BANKING contd.)

Chairman: M. Lewandowska-Szumieł (Medical University of Warsaw, Poland), A. Kamiński (Medical University of Warsaw, Poland)

- Operacje rekonstrukcyjne długich zwężeń moczowodów z użyciem kolagenu ksenogenicznego (Reconstructive surgery in urethra stenosis with xenogenic collagen)
  A. Koziak (Regional Hospital in Siedlce, Poland), T. Dmowski (Regional Hospital in Siedlce, Poland), A. Marcheluk (Regional Hospital in Siedlce, Poland), A. Dorobe (Regional Hospital in Siedlce, Poland)
- Odtworzenie skóry ludzkiej *in vitro* na bazie kompozytu kolagenowego (Reconstruction of human skin on the basis of collagen composite)
  D. Śladowski (Medical University of Warsaw, Poland), A. Kinsner (Medical University of Warsaw, Poland), G. Gut (Medical University of Warsaw, Poland), K. Lipski (Medical University of Warsaw, Poland)
- Przykład zastosowania hodowli komórkowych do wstępnej oceny modyfikacji biomateriałów (The use of human cell culture in early analysis of biomaterial modifications)
  M. Lewandowska-Szumieł (Medical University of Warsaw, Poland), D. Krupa (Warsaw University of Technology, Poland), J. Błaszkiewicz (Warsaw University of Technology, Poland)

- Hamowanie procesu resorpcji kości przez osteoprotegerynę (OPG) (Inhibition of bone resorption by osteoprotegerin (OPG))
  K. Ostrowski (Medical University of Warsaw, Poland)
- Bankowanie komórek i tkanek do celów badawczych (Banking of human cells and tissues for research purposes)
  D. Śladowski (Medical University of Warsaw, Poland)

Session IX. STERYLIZACJA RADIACYJNA (RADIATION STERILIZATION)

Chairman: J.M. Rosiak (Technical University of Łódź, Poland), W. Stachowicz (Institute of Nuclear Chemistry and Technology, Warszawa, Poland)

- Ocena rozkładu dawki pochłoniętej w masywnym przeszczepie kostnym sterylizowanym wiązką elektronów 10 MeV (Evaluation of dose distribution in a massive bone grafts sterilized with a beam of 10 MeV electrons)
  J. Sadło (Institute of Nuclear Chemistry and Technology, Warszawa, Poland), W. Stachowicz (Institute of Nuclear Chemistry and Technology, Warszawa, Poland), J. Michalik (Institute of Nuclear Chemistry and Technology, Warszawa, Poland), A. Dziedzic-Gocławska (Medical University of Warsaw, Poland)
- Akceleratory elektronów dla potrzeb bankowania tkanek (Electron accelerators for tissue banking)
  Z. Zimek (Institute of Nuclear Chemistry and Technology, Warszawa, Poland)
- Dozymetria procesu sterylizacji radiacyjnej – pomiar dawki pochłoniętej (Radiation sterilization dosimetry – the absorbed dose measurements)
  I. Kałuska (Institute of Nuclear Chemistry and Technology, Warszawa, Poland), Z. Zimek (Institute of Nuclear Chemistry and Technology, Warszawa, Poland)
- Walidacja procesu sterylizacji radiacyjnej (Validation of radiation sterilization process)
  I. Kałuska (Institute of Nuclear Chemistry and Technology, Warszawa, Poland), Z. Zimek (Institute of Nuclear Chemistry and Technology, Warszawa, Poland)
- Modyfikacja własności polimerów w procesie sterylizacji radiacyjnej (Modifications of properties of polymers in the process of radiation sterilization)
  Z.P. Zagórski (Institute of Nuclear Chemistry and Technology, Warszawa, Poland), W. Głuszewski (Institute of Nuclear Chemistry and Technology, Warszawa, Poland)
- Radiacyjne tworzenie hydrożeli i ich medyczne zastosowania (Radiation formation of hydrogels for biomedical applications)
  J.M. Rosiak (Technical University of Łódź, Poland), I. Janik (Technical University of Łódź, Poland), S. Kadłubowski (Technical University of Łódź, Poland), M. Kozicki (Technical University of Łódź, Poland), P. Kujawa (Technical University of Łódź, Poland), P. Stasica (Technical University of Łódź, Poland), P. Ulański (Technical University of Łódź, Poland)

2. VII SZKOŁA STERYLIZACJI I HIGIENIZACJI RADIACYJNEJ (7th TRAINING COURSE ON RADIATION STERILIZATION AND HYGIENIZATION), 16-17 OCTOBER 2003, WARSZAWA, POLAND

Organized by the Institute of Nuclear Chemistry and Technology, Polish Nuclear Society

Organizing Committee: Z. Zimek, Ph.D., I. Kałuska, M.Sc., W. Głuszewski, M.Sc.

LECTURES

- Sterylizacja radiacyjna na tle innych metod wyjaławiania (Radiation sterilization as compared with other sterilization methods)
  W. Stachowicz (Institute of Nuclear Chemistry and Technology, Warszawa, Poland)
- Podstawy oddziaływania promieniowania jonizującego z materią (Fundamentals of interaction of ionizing radiation with matter)
  P.P. Panta (Institute of Nuclear Chemistry and Technology, Warszawa, Poland)
- Mikrobiologiczne aspekty sterylizacji radiacyjnej (Microbiological aspects of radiation sterilization)
  D. Lachiewicz (Balton Ltd., Warszawa, Poland), M. Jaśkowska (Balton Ltd., Warszawa, Poland)
- Określanie dawki sterylizacyjnej (Sterilization dose determination)
  I. Kałuska (Institute of Nuclear Chemistry and Technology, Warszawa, Poland)
- Przegląd rozwiązań konstrukcyjnych akceleratorów stosowanych w technice i technologii radiacyjnej (Review of the technical solutions of accelerators applied in radiation technology)
  Z. Zimek (Institute of Nuclear Chemistry and Technology, Warszawa, Poland)
- Izotopowe źródła promieniowania w sterylizacji radiacyjnej (Isotopic sources of radiation used for radiation sterilization)
  W. Bogus (Technical University of Łódź, Poland)

- Walidacja procesu sterylizacji radiacyjnej (Validation of radiation sterilization process)
  I. Kałuska (Institute of Nuclear Chemistry and Technology, Warszawa, Poland)
- Kontrola dozymetryczna przemysłowej sterylizacji radiacyjnej (Dosimetric inspection in industrial radiation sterilization process)
  W. Głuszewski (Institute of Nuclear Chemistry and Technology, Warszawa, Poland), P.P. Panta (Institute of Nuclear Chemistry and Technology, Warszawa, Poland)
- Napromieniowanie żywności w Unii Europejskiej i w Polsce (Food irradiation in European Union and Poland)
  W. Migdał (Institute of Nuclear Chemistry and Technology, Warszawa, Poland)
- Samodzielne Laboratorium Identyfikacji Napromieniowania Żywności (Laboratory for Detection of Irradiated Foods)
  W. Stachowicz (Institute of Nuclear Chemistry and Technology, Warszawa, Poland)
- 40 lat bankowania tkanek i sterylizacji radiacyjnej w Polsce (Forty years of tissue banking and radiation sterilization in Poland)
  A. Dziedzic-Gocławska (Medical University of Warsaw, Poland), A. Kamiński (Medical University of Warsaw, Poland)
- Wpływ warunków sterylizacji radiacyjnej I stopnia uwodnienia próbek na inaktywację patogenów oraz na radiacyjnie indukowane zmiany w przeszczepach tkankowych i ich składnikach (The influence of radiation sterilization conditions and sample hydration on pathogenes inactivation and changes initiated by radiation in tissue grafts and their components)
  A. Dziedzic-Gocławska (Medical University of Warsaw, Poland), A. Kamiński (Medical University of Warsaw, Poland)
- Sztuczne materiały implatacyjne – rola biomateriałów w inżynierii tkanowej (Artificial implant materials – role of biomaterials in tissue engineering)
  M. Lewandowska-Szumieł (Medical University of Warsaw, Poland)
- Obróbka radiacyjna produktów farmaceutycznych (Radiation sterilization of pharmaceutical products)
  G. Przybytniak (Institute of Nuclear Chemistry and Technology, Warszawa, Poland)
- Metodyka badań produktów farmaceutycznych sterylizowanych radiacyjnie (Investigation methods for medical devices radiation sterilizated)
  B. Marciniec (Poznań University of Medical Sciences, Poland)
- Prawo farmaceutyczne (Pharmaceuticals law)
  D. Prokopczyk (POLFA S.A., Warszawa, Poland)
- Polimery stosowane w wyrobach sterylizowanych radiacyjnie (Polymers used in radiation sterilized devices)
  T. Achmatowicz (National Institute of Public Health, Warszawa, Poland)
- Zasady rejestracji, klasyfikacja i ocena zgodności wyrobów medycznych (Registration, rules, classification and evaluation of consistence of medical articles)
  I. Lasocka (Office for Medicinal Products, Medical Devices and Biocides, Warszawa, Poland)
- Radiacyjna inżynieria biomedyczna (Radiation biomedical engineering)
  J.M. Rosiak (Technical University of Łódź, Poland)
- Sterylizacja radiacyjna sprzętu medycznego w świetle konferencji w latach 2002 i 2003 (Medical disposable sterilization review basing on 2002 and 2003 conferences)
  Z.P. Zagórski (Institute of Nuclear Chemistry and Technology, Warszawa, Poland)
- Wykorzystanie promieniowania hamowania do sterylizacji radiacyjnej sprzętu medycznego jednorazowego użytku (Bremsstrahlung application for radiation sterilization process)
  Z. Zimek (Institute of Nuclear Chemistry and Technology, Warszawa, Poland)
- Biologiczne działanie i ryzyko promieniowania jonizującego (Biological effects and risk of ionising radiation)
  A. Wójcik (Institute of Nuclear Chemistry and Technology, Warszawa, Poland), I. Szumiel (Institute of Nuclear Chemistry and Technology, Warszawa, Poland)

3. KONFERENCJA „PROBLEMY UNIESZKODLIWIANIA ODPADÓW" (CONFERENCE ON PROBLEMS OF WASTE DISPOSAL), 1 DECEMBER 2003, WARSZAWA, POLAND

Organized by the Warsaw University of Technology, Plant for Utilization of Solid Municipal Wastes (Warszawa), Technical University of Łódź, Institute of Nuclear Chemistry and Technology

Organizing Committee: M. Obrębska, Ph.D., A. Ostapczuk, M.Sc.

Session I. GOSPODARKA ODPADAMI – REFERATY (WASTE MANAGEMENT – PAPERS)

Chairman: Prof. A.G. Chmielewski, Ph.D., D.Sc. (Warsaw University of Technology; Institute of Nuclear Chemistry and Technology, Warszawa, Poland)

- Termiczne przekształcanie odpadów komunalnych w systemach gospodarki odpadami – podstawowe uwarunkowania (Thermal transformation of municipal wastes in the systems of waste disposal – conditioned principles)
  T. Pająk (Academy of Mining and Metallurgy, Kraków, Poland)
- Warszawski ZUSOK – polskie realia gospodarcze funkcjonowania spalarni odpadów komunalnych w aspekcie krajowego planu gospodarki odpadami (ZUSOK Warszawa – Polish economic realities of the functioning of incinerating plants of municipal wastes in the aspect of national plans of waste management)
  J. Kaznowski (Plant for Utilization of Solid Municipal Wastes, Warszawa, Poland)
- Termiczne zagospodarowanie balastu z kompostowni systemu DANO (Thermal management of the ballast from compost heaps of the DANO system)
  K. Wolska (Warsaw University of Technology, Poland), K. Skalmowski (Warsaw University of Technology, Poland)
- Właściwości kompozytów otrzymywanych z pozyskiwanych na wysypiskach komunalnych butelek PET (Properties of the composites obtained from PET bottles recovered from waste dumps)
  J. Polaczek (Cracow University of Technology, Poland), P. Przybek (Poznań University of Economics, Poland)
- Zagospodarowanie odpadów poli(tereftalanu etylenu) (PET) pochodzących z butelek po napojach w procesie wytwarzania farb i lakierów (Management of ethylene polyterphthalate (PET) wastes originating from bottles after beverages in the process of production of paints and lacquers)
  G. Rokicki (Warsaw University of Technology, Poland), L. Łukasik (Warsaw University of Technology, Poland)

Session II. PRZYGOTOWANIE I REALIZACJA PRJEKTÓW ORAZ UWARUNKOWANIA PRAWNO-EKONOMICZNE, OSADY ŚCIEKOWE – REFERATY (PREPARATION AND REALIZATION OF PROJECTS IN ACCORDANCE WITH LAW AND ECONOMY; SEWAGE PRECIPITATIONS – PAPERS)

Chairman: J. Kaznowski, M.Sc. (Plant for Utilization of Solid Municipal Wastes, Warszawa, Poland)

- Jak sporządzić dobry biznesplan? (How to prepare a good business plan?)
  A. Zielińska (Prochem, Warszawa, Poland)
- Najlepsza dostępna technika w spalarniach odpadów (The best available technique in waste incinerating plants)
  G. Wielgosiński (Technical University of Łódź, Poland), T. Pająk (Academy of Mining and Metallurgy, Kraków, Poland)
- Termiczne unieszkodliwianie komunalnych osadów ściekowych drogą pirolizy w bateriach koksowniczych (Thermal disposal of liquid municipal wastes by pyrolisis in coke oven batteries)
  A. Sobolewski (Institute for Chemical Processing of Coal, Zabrze, Poland), R. Wasielewski (Institute for Chemical Processing of Coal, Zabrze, Poland)

Session III. ZAPROSZENIE DO DYSKUSJI PRZY PLAKACIE (INVITATION TO DISCUSSION AT POSTERS)

- Zastosowanie dynamicznej wersji modelu optymalizacyjnego systemu wywozu i unieszkodliwiania odpadów w procesie tworzenia planów gospodarki odpadami (Application of dynamic version of optimal model for the system of garbage disposal in the process of formation of waste management plans)
  S. Biedugnis (Warsaw University of Technology, Poland), M. Smolarkiewicz (Warsaw University of Technology, Poland), P. Podwójci (Warsaw University of Technology, Poland)
- Zakład pośredni zbierania zwłok zwierzęcych (Intermediate plant for the collection of carcasses)
  J. Dowgiałło (Ministry of Agriculture and Rural Development, Warszawa, Poland), J. Nunberg (Polish Union of Feed Producers, Poland), K. Rudnik (Institute for Building, Mechanisation and Electrification of Agriculture, Poland), K. Wierzbicki (Institute for Building, Mechanisation and Electrification of Agriculture, Poland)
- Eksploatacja instalacji segregacji odpadów, doświadczenia i znaczenie technologiczne dla ZUSOK (Exploitation of an installation of waste segregation; experience and technological significance for ZUSOK)
  P. Kośla (Plant for Utilization of Solid Municipal Wastes, Warszawa, Poland)
- Kompostowanie frakcji organicznej odpadów komunalnych w ZUSOK systemem „siloda" z uwzględnieniem optymalizacji i dostosowywania technologii do warunków klimatycznych Polski (Composting of organic fraction of municipal wastes for ZUSOK by the "siloda" system considering optimization and accomodation of technology suitable for Polish climatic conditions)
  T. Wadas (Plant for Utilization of Solid Municipal Wastes, Warszawa, Poland)

- Jakość kompostów polskich w świetle kryteriów Unii Europejskiej oraz innych krajów (Quality of Polish composts in the light of criteria of European Union and other countries)
  G. Wasiak, M. Madej (School of Ecology and Administration, Warszawa, Poland)

Session IV. ZAPROSZENIE DO DYSKUSJI PRZY PLAKACIE (INVITATION TO DISCUSSION AT POSTERS)

- Beztlenowa fermentacja odpadów komunalnych jako źródło metanu (Oxygen-free fermentation of municipal wastes as a source of methane)
  J. Cebula (Silesian University of Technology, Gliwice, Poland)
- Wykorzystanie metod membranowych do wzbogacania w metan gazu z wysypisk i reaktorów biologicznych (Application of membrane methods for enrichment in methane of the gas from waste dumps and biological reactors)
  M. Harasimowicz (Institute of Nuclear Chemistry and Technology, Warszawa, Poland), G. Zakrzewska-Trznadel (Institute of Nuclear Chemistry and Technology, Warszawa, Poland), A.G. Chmielewski (Institute of Nuclear Chemistry and Technology, Warszawa, Poland)
- Biodegradacja substancji organicznych w obecności bakterii unieruchomionych w warstwie fluidalnej (Biodegradation of organic substances in the presence of bacteria immobilized in the fluidal layer)
  B. Kawalec-Pietrenko (Gdańsk University of Technology, Poland), M. Łazarczyk (Gdańsk University of Technology, Poland)
- Bioutylizacja odpadów stałych z gospodarstw domowych (Bioutilization of solid wastes from households)
  L. Krzystek (Technical University of Łódź, Poland), S. Ledakowicz (Technical University of Łódź, Poland), H.-J. Kahle (Lausitzer Naturkundliche Akademie LANAKA e.V., Cottbus, Germany)
- Metodyka sporządzania i weryfikacji linii bazowych emisji gazu wysypiskowego (Methodics of preparation and verification of base lines of gas emission from waste dumps)
  J. Rachwalski (Oil and Gas Institute, Poland), K. Steczko (Oil and Gas Institute, Poland)
- Kierunki działań Centrum KOMAG dla racjonalnej gospodarki odpadami komunalnymi (Trends of action of the KOMAG Centre for the rational management of municipal wastes)
  Z. Szkudlarek (Mining Mechanization Centre KOMAG, Gliwice, Poland)

Session V. ZAPROSZENIE DO DYSKUSJI PRZY PLAKACIE (INVITATION TO DISCUSSION AT POSTERS)

- Usuwanie cząstek PM 2.5 w procesach spalania odpadów (Removal of 2.5 PM particles in the processes of incinerating of wastes)
  J. Dąbrowska (Warsaw University of Technology, Poland), J. Warych (Warsaw University of Technology, Poland)
- Zawartość metali w popiołach ze spalarni odpadów medycznych w Polsce (Content of metals in ashes from an incinerating plant of medical wastes in Poland)
  A. Zawadzka (Technical University of Łódź, Poland), E. Gromadzińska (Institute of Textile Materials Engineering, Łódź, Poland), G. Wielgosiński (Technical University of Łódź, Poland)
- System recyklingu chromu (Recycling system of chromium)
  A. Mróz (INWATEC Sp. z o.o., Warszawa, Poland)
- Sorbenty z biomasy w oczyszczaniu wody (Sorbents from the biomass in purification of water)
  K. Bratek (Wrocław University of Technology, Poland), W. Bratek (Wrocław University of Technology, Poland), M. Kułażyński (Wrocław University of Technology, Poland)
- Ocena sposobów zagospodarowania odpadowych środków smarowych (Assessment of the management methods of lubrication wastes)
  J. Molenda, M. Grądkowski, M. Makowska (Institute of Technology of Exploitation, Radom, Poland)
- Ogniotrwałe wyłożenie monolityczne kotła do spalania biomasy (Monolithic refractory lining of a furnace for combustion of biomass)
  I. Majchrowicz (Institute of Refractory Materials, Gliwice, Poland), J. Witek (Institute of Refractory Materials, Gliwice, Poland), J. Wojsa (Institute of Refractory Materials, Gliwice, Poland)
- Możliwość zastosowania wiązki elektronów do usuwania SO_2, NO_x i WWA oraz dioksyn z gazów spalinowych spalarni śmieci (The possibility of applying electron beam for SO_2, NO_x, PAH and dioxin removal from incineration plant flue gas)
  A. Ostapczuk (Institute of Nuclear Chemistry and Technology, Warszawa, Poland), A.G. Chmielewski (Institute of Nuclear Chemistry and Technology, Warszawa, Poland), J, Licki (Institute of Atomic Energy, Świerk, Poland)

CONFERENCES ORGANIZED AND CO-ORGANIZED BY THE INCT IN 2003

1. KONFERENCJA JUBILEUSZOWA „PRZESZCZEP W WALCE Z KALECTWEM – 40 LAT BANKOWANIA TKANEK I STERYLIZACJI RADIACYJNEJ W POLSCE" (JUBILEE CONFERENCE "TISSUE GRAFTS IN THE FIGHT AGAINST CRIPPLEHOOD – 40 YEARS OF RADIATION STERILISATION AND TISSUE BANKING IN POLAND"), 22-23 MAY 2003, WARSZAWA, POLAND

Organized by the Department of Transplantology and Central Tissue Bank, Medical University of Warsaw and Institute of Nuclear Chemistry and Technology

Organizing Committee: D. Śladowski, M.D., Ph.D. (Chairman), M. Brix-Warzecha, M.Sc., H. Bursig, M.Sc., S. Dyląg, M.Sc., M. Fedorowicz, M.Sc., W. Głuszewski, M.Sc., G. Gut, M.D., I. Kałuska, M.Sc., A. Komender, M.D., Ph.D., P. Krajewski, M.D., Ph.D., E. Lesiak-Cyganowska, M.D., Ph.D., R. Mazur, M.Sc., J. Stalmasiński, M.Sc., I. Uhrynowska-Tyszkiewicz, M.D., J. Truchanowicz, M.Sc., J. Wszołek, M.Sc.

Session I. OTWARCIE (OPENING)

Chairman: A. Dziedzic-Gocławska (Medical University of Warsaw, Poland), J. Michalik (Institute of Nuclear Chemistry and Technology, Warszawa, Poland)

- Powitanie (Address)
  A. Dziedzic-Gocławska (Medical University of Warsaw, Poland)
- Początki bankowania tkanek w Polsce (Introduction of tissue banking in Poland)
  K. Ostrowski (Medical University of Warsaw, Poland)
- Rozwój bankowania tkanek w Polsce (Development of tissue banking in Poland)
  J. Komender (Medical University of Warsaw, Poland)

Session II. BANKOWANIE TKANEK W POLSCE (TISSUE BANKING IN POLAND)

Chairman: K. Ostrowski (Medical University of Warsaw, Poland), J. Komender (Medical University of Warsaw, Poland)

- 40 lat działalności Centralnego Banku Tkanek (Forty years of activity of Central Tissue Bank)
  A. Dziedzic-Gocławska (Medical University of Warsaw, Poland)
- Bank Tkanek Regionalnego Centrum Krwiodawstwa i Krwiolecznictwa w Katowicach (Regional Blood Center Tissue Bank in Katowice)
  H. Bursig (Regional Blood Center Tissue Bank, Katowice, Poland), S. Dyląg (Regional Blood Center Tissue Bank, Katowice, Poland)
- Historia i osiągnięcia Regionalnego Centrum Krwiodawstwa i Krwiolecznictwa w Kielcach (History and activity of the Regional Blood Center Tissue Bank in Kielce)
  R. Mazur (Regional Blood Center Tissue Bank, Morawica, Poland), J. Stalmasiński (Regional Blood Center Tissue Bank, Morawica, Poland)
- Działalność Pracowni Biologicznej Zastawki Serca utworzonej przez Fundację Rozwoju Kardiochirurgii w Zabrzu (Activity of Biological Heart Valve Laboratory established by Foundation of Cardiac Surgery Development in Zabrze)
  J. Wszołek (Foundation of Cardiac Surgery Development, Zabrze, Poland), G. Religa (Foundation of Cardiac Surgery Development, Zabrze, Poland), Z. Religa (Foundation of Cardiac Surgery Development, Zabrze, Poland), L. Pawlus-Łachecka (Foundation of Cardiac Surgery Development, Zabrze, Poland)
- Bank allogennych zastawek serca w Krakowie – 23 lata doświadczeń (Bank of Allogenic Heart Valves in Kraków – 23 years of experience)
  G. Marek (Collegium Medicum, Jagiellonian University, Kraków, Poland), Z. Marcinkowska (Collegium Medicum, Jagiellonian University, Kraków, Poland), D. Barecka (Collegium Medicum, Jagiellonian University, Kraków, Poland), M. Jaskier (Collegium Medicum, Jagiellonian University, Kraków, Poland), J. Sadowski (Collegium Medicum, Jagiellonian University, Kraków, Poland), A. Dziatkowiak (Collegium Medicum, Jagiellonian University, Kraków, Poland)
- 22 lata doświadczeń w bankowaniu allogennych zastawek serca Kliniki Kardiochirurgii Instytutu „Pomnik Centrum Zdrowia Dziecka" (Twenty two years of experience in allograft heart banking in the Department of Cardiothoracic Surgery, the Children's Memorial Health Institute)

Session VI. ZAPROSZENIE DO DYSKUSJI PRZY PLAKACIE (INVITATION TO DISCUSSION AT POSTERS)

- Eksploatacja pieca rusztowego do spalania odpadów komunalnych na przykładzie warszawskiego ZUSOK (Exploitation of an grate oven for combustion of municipal wastes; ZUSOK Warszawa as an example)
  J. Naumienko (Plant for Utilization of Solid Municipal Wastes, Warszawa, Poland)
- Model termicznej degradacji polimerów (Model of thermal degradation of polymers)
  P. Grzybowski (Warsaw University of Technology, Poland)
- Paliwa ciekłe z odpadów polietylenu (Liquid fuels from polyethylene wastes)
  B. Tymiński (Institute of Nuclear Chemistry and Technology, Warszawa, Poland), A.G. Chmielewski (Institute of Nuclear Chemistry and Technology, Warszawa, Poland), K. Zwoliński (Institute of Nuclear Chemistry and Technology, Warszawa, Poland)
- Problemy dekontaminacji złóż ziarnistych (Decontamination problems of granular deposits)
  A. Adach (Warsaw University of Technology, Poland), S. Wroński (Warsaw University of Technology, Poland)
- Czy warszawskie śmieci należy spalać, czy lepiej nadal wywozić na składowiska? (Should be Warsaw wastes burned or better transported to a storage area?)
  M. Obrębska (Warsaw University of Technology, Poland), A.G. Chmielewski (Warsaw University of Technology, Poland), D. Mamełka (Miejskie Laboratorium Chemiczne Przy Urzędzie Miasta Stołecznego Warszawy, Poland)
- Ekoinżynieryjny kompromis potrzeb człowieka i przyrody (Eco-engineering compromise between human needs and nature)
  K. Lewandowski

4. EXPERT MEETING ON THE FOLLOW UP OF THE PATIENTS INVOLVED IN THE BIAŁYSTOK RADIATION ACCIDENT", 3 DECEMBER 2003, WARSZAWA, POLAND

Organized by the Institute of Nuclear Chemistry and Technology, Świętokrzyskie Oncology Center

Participants: J.-M. Cosset (Institute Curie, Paris, France), A. Kułakowski (Świętokrzyskie Oncology Center, Kielce, Poland), J. Słuszniak (Świętokrzyskie Oncology Center, Kielce, Poland), A. Wieczorek (Świętokrzyskie Oncology Center, Kielce, Poland), A. Wójcik (Institute of Nuclear Chemistry and Technology, Warszawa, Poland)

The aim of the meeting was to discuss the results of surgical treatment of the patients overexposed to radiation due to an accident during radiotherapy in the Białystok Oncology Center in February 2001.

EDUCATION

Ph.D. PROGRAMME IN CHEMISTRY

The Institute of Nuclear Chemistry and Technology holds a four-year Ph.D. degree programme for graduates of chemical, physical and biological departments of universities, for graduates of medical universities and to engineers in chemical technology and material science.

The main areas of the programme are:

- radiation chemistry and biochemistry,
- chemistry of radioelements,
- isotopic effects,
- radiopharmaceutical chemistry,
- analytical methods,
- chemistry of radicals,
- application of nuclear methods in chemical and environmental research, material science and protection of historical heritage.

The candidates accepted for the aforementioned programme can be employed in the Institute. The candidates can apply for a doctorial scholarship. The INCT offers accommodation in 10 rooms in the guesthouse for Ph.D. students not living in Warsaw.

During the four-year Ph.D. programme the students participate in lectures given by senior staff from the INCT, Warsaw University and the Polish Academy of Sciences. In the second year, the Ph.D. students have teaching practice in the Chemistry Department of Warsaw University. Each year the Ph.D. students are obliged to deliver a lecture on topic of his/her dissertation at a seminar. The final requirements for the Ph.D. programme graduates, consistent with the regulation of the Ministry of National Education, are:

- submission of a formal dissertation, summarizing original research contributions suitable for publication;
- final examination and public defense of the dissertation thesis.

In 2003, the following lecture series were organized:

- "Chemistry of elements" – Prof. Sławomir Siekierski, Ph.D. (Institute of Nuclear Chemistry and Technology);
- "Fundamentals of spectroscopy" – Prof. Joanna Sadlej, Ph.D., D.Sc. (Department of Chemistry, Warsaw University);
- "Selected problems of biochemistry" – Assoc. Prof. Marcin Kruszewski, Ph.D., D.Sc. (Institute of Nuclear Chemistry and Technology);
- "From soup bubbles to periodic structures (periodic surfaces). Periodic structures in the mesoscale – X-ray spectra. Possible applications – photonic crystals made from periodic structures" – Prof. Robert Hołyst, Ph.D., D.Sc. (Institute of Physical Chemistry, Polish Academy of Sciences).

Most of the students expand their knowledge during a short or long training in numerous renowned European research centres, e.g. European Institute of Transuranium Elements (Karlsruhe, Germany), Philips Cyclotron in Paul Scherrer Institute (Switzerland), Gent University (Belgium), Orsay University (France), Mainz University (Germany), etc.

The qualification interview for the Ph.D. programme takes place in the mid of October. Detailed information can be obtained from:

- Head: Assoc. Prof. Aleksander Bilewicz, Ph.D., D.Sc.
  (phone: (+4822) 811-30-21 ext. 15-98, e-mail: abilewic@orange.ichtj.waw.pl);
- Secretary: Dr. Ewa Gniazdowska
  (phone: (+4822) 811-30-21 ext. 15-96, e-mail: studium@orange.ichtj.waw.pl).

TRAINING OF STUDENTS

Institution	Country	Number of participants	Period
Academy of Mining and Metallurgy	Poland	6	2 weeks

Institution	Country	Number of participants	Period
École des Mines de Nantes	France	1	3 months
International Atomic Energy Agency	Bulgaria	3	1 month
International Atomic Energy Agency	Mongolia	3	3 months
International Atomic Energy Agency	Pakistan	1	3 months
International Atomic Energy Agency	Syria	2	1 month
International Atomic Energy Agency	Syria	1	3 months
Warsaw University of Technology, Faculty of Physics	Poland	30	one-day practice
Technical School of Chemistry	Poland (Warszawa)	4	1 month

RESEARCH PROJECTS AND CONTRACTS

RESEARCH PROJECTS GRANTED BY THE POLISH STATE COMMITTEE FOR SCIENTIFIC RESEARCH IN 2003 AND IN CONTINUATION

1. **Radiation and photochemically induced radical processes in aromatic carboxylic acids containing thioether group.**
   supervisor: Prof. Krzysztof Bobrowski, Ph.D., D.Sc.
2. **Detection of irradiated additives (spices) in foodstuffs.**
   supervisor: Kazimiera Malec-Czechowska, M.Sc.
3. **Multiphase flow dynamics determination by radiotracer and computational fluid dynamics (CFD) methods.**
   supervisor: Jacek Palige, Ph.D.
4. **Estimation of post-irradiation chromosomal translocations in human blood lymphocytes for biological dosimetry purposes with the use of chromosome painting and PCC.**
   supervisor: Prof. Irena Szumiel, Ph.D., D.Sc.
5. **Influence of relativistic effect on hydrolytic properties, stabilization of lower oxidation states and $6s^2$ and $6p_{1/2}^2$ lone pair character of the heaviest elements.**
   supervisor: Assoc. Prof. Aleksander Bilewicz, Ph.D., D.Sc.
6. **Catalytic tubular reactor for olefine polymers cracking with distillation products of decomposition.**
   supervisor: Bogdan Tymiński, Ph.D.
7. **Investigations in the range of functionalization technology of particle track-etched membranes and their application.**
   supervisor: Assoc. Prof. Tadeusz Żółtowski, Ph.D., D.Sc.
8. **Tricarbonyl technetium(I) and rhenium(I) complexes with chelating ligands as radiopharmaceutical precursors.**
   supervisor: Prof. Jerzy Narbutt, Ph.D., D.Sc.
9. **Investigation of the mechanism of human glioma MO59 cells radiosensitisation by inhibitors of signal transduction pathways which are growth factors dependent: influence on DNA double-strand break rejoning and apoptosis.**
   supervisor: Iwona Grądzka, Ph.D.
10. **Neutron activation analysis and ion chromatography as a tool for reliable lanthanides determination in the biological and environmental samples.**
    supervisor: Bożena Danko, Ph.D.
11. **The chemical isotope effects of gallium, indium and thallium in ligand exchange and red-ox reactions.**
    supervisor: Wojciech Dembiński, Ph.D.
12. **Comparative analysis of telomere length, chromosomal aberration frequency and DNA repair kinetics in peripheral blood lymphocytes of healthy donors and cancer patients.**
    supervisor: Assoc. Prof. Andrzej Wójcik, Ph.D., D.Sc.
13. **Baroque glass in Polish collections (provenance verification).**
    supervisor: Jerzy Kunicki-Goldfinger, Ph.D.
14. **Application of membrane methods for separation of gas mixtures in the systems generating energy from biogas.**
    supervisor: Marian Harasimowicz, Ph.D.
15. **The role of PARP-1 in DNA double strand breaks repair.**
    supervisor: Maria Wojewódzka, Ph.D.
16. **Crystal chemistry of calcium complexes with azinedicarboxylate ligands.**
    supervisor: Prof. Janusz Leciejewicz, Ph.D., D.Sc.

17. **Hydrolysis of heavy element cations.**
supervisor: Assoc. Prof. Aleksander Bilewicz, Ph.D., D.Sc.
18. **Sodium and silver clusters in gamma irradiated sodalites.**
supervisor: Prof. Jacek Michalik, Ph.D., D.Sc.
19. **Paramagnetic products of radiolysis stabilized in molecular sieves: small radicals and metallic nanoparticles.**
supervisor: Prof. Jacek Michalik, Ph.D., D.Sc.
20. **Equilibrium sulfur isotope effects ($^{34}S/^{32}S$) in selected SO_2 containing systems.**
supervisor: Prof. Andrzej G. Chmielewski, Ph.D., D.Sc.
21. **Radiation induced decomposition of selected chlorinated hydrocarbons in gaseous phase.**
supervisor: Prof. Andrzej G. Chmielewski, Ph.D., D.Sc.

IMPLEMENTATION PROJECTS GRANTED BY THE POLISH STATE COMMITTEE FOR SCIENTIFIC RESEARCH IN 2003 AND IN CONTINUATION

1. **Polish certified reference materials: maize meal and soia flour for the quality control of laboratories analyzing food.**
06 PO6 2002C/05899
supervisor: Halina Polkowska-Motrenko, Ph.D.

RESEARCH PROJECTS ORDERED BY THE POLISH STATE COMMITTEE FOR SCIENTIFIC RESEARCH IN 2003

1. **Radiation processing application to modify and sterilize polymer scaffolds.**
PBZ-KBN-082/T08/2002
supervisor: Assoc. Prof. Izabella Legocka, Ph.D., D.Sc.
2. **Radiation processing application to form nanofillers with different structure including hybrid and functionalized.**
PBZ-KBN-095/T08/2003
supervisor: Zbigniew Zimek, Ph.D.
3. **Mutual interactions between nutritional components in steering of development of the intestinal immunological system.**
PBZ-KBN-093/P06/2003
supervisor: Assoc. Prof. Marcin Kruszewski, Ph.D., D.Sc.

IAEA RESEARCH CONTRACTS IN 2003

1. **Electron beam treatment of gaseous organic compounds emitted from fossil fuel combustion.**
11093/RO
principal investigator: Prof. Andrzej G. Chmielewski, Ph.D., D.Sc.
2. **Application of ionizing radiation for removal of pesticides from ground waters and wastes.**
12016/RO
principal investigator: Prof. Marek Trojanowicz, Ph.D., D.Sc.
3. **Radiation resistant polypropylene for medical applications and as component of structural engineering materials.**
12703/RO
principal investigator: Zbigniew Zimek, Ph.D.

IAEA TECHNICAL CONTRACTS IN 2003

1. **Industrial scale demonstration plant for electron beam purification of flue gases.**
POL/8/014

2. **Accredited laboratory for the use of nuclear and nuclear-related analytical techniques.**
   POL/2/014
3. **Feasibility Study for a Sewage Irradiation Plant in Egypt.**
   RAF0014-91650L
4. **Complete three XRF analysers, model AF-30, for determination of ash in lignite in coal plant laboratory conditions through sample measurement.**
   MON 8005-84723G

EUROPEAN COMMISSION RESEARCH PROJECTS IN 2003

1. **Electron beam for processing of flue gases, emitted in metallurgical processes, for volatile organic compounds removal.**
   supervisor: Prof. Andrzej G. Chmielewski, Ph.D., D.Sc.
   ICA2-CT-2000-10005 under FP.5, programme coordinated by the INCT
2. **Research Training Network: Sulfur radical chemistry of biological significance: the protective and damaging roles of thiol and thioether radicals.**
   principal investigator: Prof. Krzysztof Bobrowski, Ph.D., D.Sc.
   RTN-2001-00096 under FP.5
3. **European Cooperation in the Field of Scientific and Technical Research. COST D27 – Prebiotic chemistry and early evolution. Role of radiation chemistry in the origin of life on Earth.**
   supervisor: Prof. Zbigniew Zagórski, Ph.D., D.Sc.

LIST OF VISITORS TO THE INCT IN 2003

1. **Al-Khateeb Shatha**, Atomic Energy Commission of Syria, Damascus, Syria, *16.10-31.12*.
2. **Armstrong David**, University of Calgary, Canada, *03-06.09*, *12-13.09*.
3. **Asmus Klaus-Dieter**, University of Notre Dame, USA, *02-06.09*.
4. **Baev Alexei K.**, Belarusian Technological Institute, Belarus, *08-09.08*.
5. **Bernard Olivier**, France, *15.09-31.12*.
6. **Cardoso Alain**, International Atomic Energy Agency, United Nations, *06.02*.
7. **Chigrinov Sergey**, National Academy of Sciences of Belarus, Scientific and Technical Center "Sosny", Belarus, *30.03-02.04*.
8. **Cosset Jean-Marc**, Institute Curie, Paris, France, *03.12*.
9. **Damdinsuren Zuzaan**, Nuclear Research Center, Mongolia, *04.05-03.08*.
10. **Dimitrova Petya**, "Maritsa Iztok" Power Station, Bulgaria, *03.08-04.09*.
11. **Doutzkinov Nikolay**, National Electric Co., Bulgaria, *17-23.08*.
12. **Du Zhiwen**, University of Science and Technology, Hefei, China, *10.10-10.11*.
13. **Fainchtein Aleksander**, Research and Design Institute ENERGOSTAL, Ukraine, *13-29.08*.
14. **Gryzlov Anatolij**, State Research and Production Corporation TORIJ, Russia, *13.05-02.06*.
15. **Haseek Nazih**, Atomic Energy Commission of Syria, Damascus, Syria, *02.11-03.12*.
16. **Hayata Isamu**, National Institute of Radiobiological Sciences, Chiba, Japan, *24-31.05*.
17. **Houée-Levin Chantal**, Université Paris-Sud, France, *05-06.09*, *12.09*.
18. **Hug Gordon**, University of Notre Dame, USA, *05.09*.
19. **Kasztovszky Zsolt**, Institute of Isotope and Surface Chemistry, Hungary, *22.09-04.10*.
20. **Kha Françis**, École des Mines de Nantes, France, *05.05-31.07*.
21. **Kim Jaevoo**, Korea Atomic Energy Research Institute, Taejon, Korea, *13-17.01*.
22. **Lazurik Vladymir**, Kharkiv National University, Ukraine, *03-07.03*.
23. **Lodoysamba Sereeter**, Nuclear Energy Commission, Mongolia, *02-14.03*.
24. **Mahlous Mohamed**, Nuclear Research Center, Algeria, *17-26.10*.
25. **Mundwiller Stefan**, University of Zurich, Switzerland, *08-13.04*.
26. **Narantsetseg Dashdendev**, Thermal Electric Power Station No.4, Ulaanbaatar, Mongolia, *04.05-03.08*.
27. **Neta Pedatsur**, National Institute of Standards and Technology, USA, *01-06.09*, *12-16.09*.
28. **Nichipor Henrieta**, Institute of Radiation Physical and Chemical Problems, Academy of Sciences of Belarus, Belarus, *27-31.03*, *14-18.07*, *23-25.07*, *03-07.12*.
29. **Noda Eddie Orestes Sanches**, International Scientific Orthopaedics Complex "Frank Pais", Havana, Cuba, *01.10*.
30. **Olovsson Ivar**, University of Uppsala, Sweden, *10.12*.
31. **Panavas Romanas**, Vilniaus Ventos Puslaidinikiai Joint Stock Co., Ltd., Lithuania, *27-30.10*.
32. **Pieszekhonov Vladimir**, State Research and Production Corporation TORIJ, Russia, *13.05-02.06*.
33. **Popov Genadij**, Kharikiv National University, Ukraine, *03-07.03*.
34. **Radkov Lyulin**, "Maritsa Iztok" Power Station, Bulgaria, *03.08-04.09*.
35. **Robouch Piotr**, Institute for Reference Materials and Measurements, Joint Research Centre, Geel, Belgium, *08.10*.
36. **Roduner Emil**, University of Stuttgart, Germany, *07.05*.
37. **Salah Uddin Ahmed Salahuddin**, Bangladesh Atomic Energy Commission, Bangladesh, *19.10-01.11*.
38. **Saranhuu Bayartaivan**, National University of Mongolia, Mongolia, *04.05-03.08*.
39. **Shadyra Aleh**, Belarusian State University in Minsk, Belarus, *05-06.05*.

40. **Shiotani Masaru**, Hiroshima University, Japan, *14-15.09*.
41. **Streffer Christian**, International Commission on Radiation Protection, Essen, Germany, *23.05.*
42. **Suliman Omran**, Atomic Energy Commission of Syria, Damascus, Syria, *29.09-01.11*.
43. **Syed Mohsin Reza**, Applied Chemistry Division PINSTECH, Islamabad, Pakistan, *01.04-27.06*.
44. **Tamura Kenji**, National Institute of Material Science, Japan, *17-20.06.*
45. **Thyn Jiri**, Technical University of Prague, Czech Republic, *15-19.12*.
46. **Wishart James**, Brookhaven National Laboratory, Upton, USA, *12-15.09*.
47. **Yamada Hirohisa**, National Institute of Material Science, Japan, *17-20.06*.
48. **Zhelev Dimitar**, "Maritsa Iztok" Power Station, Bulgaria, *03.08-04.09*.
49. **Zuzaan Purew**, Nuclear Research Center, National University of Mongolia, Mongolia, *02-14.03*.

THE INCT SEMINARS IN 2003

1. Prof. Wojciech Cellary, Ph.D., D.Sc. (Poznań University of Economics, Poland)
   Wyzwania edukacyjne w drodze do globalnego społeczeństwa informacyjnego (An educational challenge on the way to global information society)
2. Prof. Jean-Marc Cosset, Ph.D. (Institute Curie, Paris, France)
   Radiation accidents: a medical perspective
3. Przemysław Drzewicz, M.Sc. (Institute of Nuclear Chemistry and Technology, Warszawa, Poland)
   Analityczne badania produktów degradacji wybranych chlorofenoli i pestycydów chloroorganicznych pod wpływem promieniowania jonizującego (Analytical investigation of radiolytic degradation products of selected chlorophenols and chloroorganic pesticides)
4. Assoc. Prof. Stanisław Filipek, Ph.D., D.Sc. (Institute of Physical Chemistry, Polish Academy of Sciences, Warszawa, Poland)
   Badanie układów metal-wodór w warunkach ekstremalnych (Studies on the metal-hydrogen systems in extreme conditions)
5. Michał Gryz, M.Sc. (Office for Medicinal Products, Medical Devices and Biocides, Warszawa, Poland)
   Badania koordynacji jonów magnezu i cynku w ich kompleksach z podstawnikami dwuazynokarboskylowymi (Study of coordination of magnesium and zinc ions in their complexes with diazinecarboxylic ligands)
6. Prof. Isamu Hayata (National Institute of Radiobiological Sciences, Chiba, Japan)
   Biological dose estimation in the Tokai-Mura criticality accident
7. Dr. Stefan Mundwiler (University of Zurich, Switzerland)
   Selective release of technetium complexes from the solid phase due to C-N bond cleavage upon metal coordination
8. Prof. Ivar Olovsson (Angstrom Laboratory, University of Uppsala, Sweden)
   Forbidden symmetry and quasicrystals
9. Prof. Adam Proń, Ph.D., D.Sc. (Comissariat a l'Energie Atomique, Grenoble, France; Warsaw University of Technology, Poland)
   26 lat polimerów przewodzących: od domieszkowania poliacetylenu do elektroniki molekularnej (Twenty six years of conducting polymers: from additives to polyacetylene, to molecular electronics)
10. Prof. Emil Roduner (University of Stuttgart, Germany)
    Paramagnetic centres and transients in zeolite catalysts
11. Prof. Aleh Shadyra (Belarusian State University in Minsk, Belarus)
    Application of radiation chemistry methods in the search for free-radical reaction inhibitory with properties useful for medicine and industry
12. Assoc. Prof. Zbigniew Sojka, Ph.D., D.Sc. (Jagiellonian University, Kraków, Poland)
    Spektroskopia EPR układów heterogenicznych – małe vademecum (EPR spectroscopy of heterogeneous systems – a short vademecum)
13. Prof. Christian Streffer (International Commission on Radiation Protection, Essen, Germany)
    Effects after prenatal irradiation and implications for radioprotection
14. Prof. Ludomir Ślusarski, Ph.D., D.Sc. (Technical University of Łódź, Poland)
    Kierunki rozwoju materiałów polimerowych (Development trends in polymer materials)
15. Dr. Małgorzata Świderska (National Contact Point of the Sixth EU Framework Programme - Specific Programme Euratom, Warszawa, Poland), Anna Ostapczuk, M.Sc. (Institute of Nuclear Chemistry and Technology, Warszawa, Poland)
    I Konkurs 6. Programu Ramowego Unii Europejskiej (I Competition of the Sixth EU Framework Programme)
16. Prof. Zbigniew Zagórski, Ph.D., D.Sc. (Institute of Nuclear Chemistry and Technology, Warszawa, Poland), Prof. Jerzy Ostyk-Narbutt, Ph.D., D.Sc. (Institute of Nuclear Chemistry and Technology, Warszawa, Poland)

Chemia radiacyjna i radiochemia: krewniacy czy powinowaci? (Radiation chemistry and radiochemistry: next to kin or remote?)

17. Prof. Maria Ziółek, Ph.D., D.Sc. (Adam Mickiewicz University in Poznań, Poland)
    Mikro- i mezoporowate katalizatory zawierające niob (Micro- and mesoporous catalysts containing niobium)

LECTURES AND SEMINARS DELIVERED OUT OF THE INCT IN 2003

LECTURES

1. **Chmielewski A.G.**
   Technika radiacyjna (Radiation techniques).
   Sympozjum „100 rocznica nagrody Nobla Marii Skłodowskiej-Curie (1903-2003)", Łódź, Poland, 02.12.2003.

2. **Dembiński W., Krejzler J., Vogl J., Pritzkow W., Bulska E., Wysocka A.**
   Chemical isotope effects of Ga, In and Ge a challenge for mass spectrometry and isotope chemistry.
   International Workshop on Problems in the Use of Gases and Isotopic Substances in Metrology and for a Knowledge-Based Society PUGIS 2003, Turin, Italy, 17-21.05.2003.

3. **Kciuk G., Roselli C., Houée-Levin Ch., Mirkowski J., Bobrowski K.**
   Chemical and radiation modification of dipeptides modelling enkephalin fragments.
   European Young Investigator Conference, Słubice, Poland, 07-11.05.2003.

4. **Korzeniowska-Sobczuk A., Mirkowski J., Hug G., Bobrowski K.**
   Radical cations, radicals, and final products derived from aromatic carboxylic acid containing thioeter groups. Pulse and steady-state study.
   European Young Investigator Conference, Słubice, Poland, 07-11.05.2003.

5. **Kulisa K., Polkowska-Motrenko H., Dybczyński R.**
   Oznaczanie zawartości SO_2 i NO_x w gazach spalinowych i analiza ekstraktów z popiołów pochodzących z elektrowni opalanych węglem (Determination of SO_2 and NO_x in flue gases and analysis of extracts of coal fly ashes from electro-power stations).
   Seminarium A.G.A. Analytical Warszawa, Kraków, Poland, 07.11.2003.

6. **Legocka I., Celuch M., Sadło J., Kostrzewa M.**
   Wstępne badania nad zachowaniem się poli(siloxanouretanów) pod wpływem sterylizujących dawek promieniowania jonizującego (Preliminary study on poly(siloxaneurethanes) under sterilization dose of ionizing radiation).
   XIII Konferencja Naukowa „Biomateriały w medycynie i weterynarii", Rytro, Poland, 14-19.10.2003.

7. **Łyczko K., Bilewicz A., Persson I.**
   Studies of bismuth trifluoromethanesulfonate solution in *N,N*-dimethylthioformamide.
   28th International Conference of Solution Chemistry, Debrecen, Hungary, 22-28.08.2003.

8. **Michalik J., Migdał W., Polkowska-Motrenko H., Stachowicz W., Starosta W.**
   Działalność Instytutu Chemii i Techniki Jądrowej na rzecz bezpieczeństwa żywności (Activity of the Institute of Nuclear Chemistry and Technology for food safety).
   Konferencja „Bezpieczeństwo żywności i żywienia jako problem zdrowia publicznego w Polsce w przededniu integracji z Unią Europejską", Warszawa, Poland, 29-31.10.2003.

9. **Migdał W.**
   Metoda utrwalania żywności za pomocą promieniowania jonizującego (Food preservation with the use of ionising radiation).
   Konferencja Kierowników Wojewódzkich Działów Higieny, Żywienia i Przedmiotów Użytku Głównego Inspektora Sanitarnego, Łańsk near Olsztyn, Poland, 24-26.09.2003.

10. **Migdał W., Stachowicz W.**
    Napromieniowanie żywności i jej wykrywanie – aktualna sytuacja w Polsce (Food irradiation and identification of irradiated foods – situation in Poland today).
    German-Polish EU Twinning Project: Ensuring Food Safety and Official Control of Foodstuffs, Warszawa, Poland, 18.07.2003.

11. Orska-Gawryś J., Surowiec I., Trojanowicz M.

Chromatografia cieczowa w badaniach zabytków (Liquid chromatography in heritage research).

Sesja Konserwatorska Muzeum Narodowego w Warszawie, Warszawa, Poland, 28.05.2003.

12. Pogocki D.

Alzheimer's beta-amyloid peptide as a source of free radicals: A computational study.

European Young Investigator Conference, Słubice, Poland, 07-11.05.2003.

13. Pogocki D., Serdiuk K.

Amyloidowy beta-peptyd jako źródło wolnych rodników (Amyloid β-peptide as a source of free radicals).

Konferencja Sprawozdawcza Interdyscyplinarnego Centrum Modelowania Matematycznego Uniwersytetu Warszawskiego, Serock, Poland, 26-28.11.2003.

14. Polkowska-Motrenko H.

Collection and preparation of candidate mushroom reference material; INT/1/054 Project Implementation.

Workshop on Preparation of In-house Reference Materials, Geel, Belgium, 15-19.09.2003.

15. Stachowicz W.

Application of EPR spectroscopy to study the origin and stability of free radicals and other paramagnetic entities evoked by ionising radiation in skeletal tissues.

40 Years of Radiation Sterilisation and Tissue Banking in Poland, Warszawa, Poland, 29.01.2003.

16. Stachowicz W.

Identyfikacja napromieniowania żywności (Detection of irradiated foods).

Konferencja Kierowników Wojewódzkich Działów Higieny, Żywienia i Przedmiotów Użytku Głównego Inspektora Sanitarnego, Łańsk near Olsztyn, Poland, 24-26.09.2003.

17. Włodzimirska B., Bilewicz A.

Influence on relativistic effects on hydrolysis of Ac^{3+}.

33 Journees des Actinides, Prague, Czech Republic, 27-29.04.2003.

SEMINARS

1. Bobrowski Krzysztof

Stabilization of sulfur radical cations in methionine-containing peptides: complementary conductometric and spectrophotometric pulse radiolysis studies

University of Calgary, Canada, 18.06.2003

2. Kałuska Iwona

Walidacja procesu sterylizacji radiacyjnej (Validation of radiation sterilization process)

Plant of Dressing Materials in Toruń, Poland, 24.01.2003

3. Kruszewski Marcin

DNA w promieniach, czyli jak komórki radzą sobie z popromiennymi uszkodzeniami (DNA in rays, or how cells cope with radiation damage)

Museum of Maria Skłodowska-Curie, Warszawa, Poland, 27.09.2003

4. Owczarczyk Andrzej

Application of tracers for transport investigations in unregulated rivers

International Atomic Energy Agency, Vienna, Austria, 20.05.2003

5. Polkowska-Motrenko Halina

Metody rozdzielcze rozwijane w Zakładzie Chemii Analitycznej Instytutu Chemii i Techniki Jądrowej (Separation methods developed in the Department of Analytical Chemistry of the Institute of Nuclear Chemistry and Technology)

Radioisotope Centre POLATOM, Świerk, Poland, 19.03.2003.

6. Sartowska Bożena

Phase transformations in the near surface layer of carbon steels modified with short intense nitrogen and argon plasma pulses

Institute of Physics of Materials, Academy of Science of the Czech Republic, Brno, Czech Republic, 07.10.2003

7. Stachowicz Wacław
Napromieniowanie żywności i metody umożliwiające wykrywanie napromieniowania w żywności (Food irradiation and method enabling detection of radiation treatment in foodstuffs)
Warszawa, Poland, 21.11.2003

8. Wójcik Andrzej
Biologiczne działanie promieniowania jonizującego (Biological effects of ionising radiation)
School of Cecylia Plater-Zyberkówna, Warszawa, Poland, 20.01.2003

9. Wójcik Andrzej
Historia zastosowania promieniowania jonizującego (History of application of ionising radiation)
Institute of Modern Civilization, Warszawa, Poland, 18.03.2003

10. Wójcik Andrzej
Działanie promieniowania na materię, dawki (Effects of radiation on matter, doses)
Institute of Modern Civilization, Warszawa, Poland, 25.03.2003

11. Wójcik Andrzej
Działanie promieniowania na komórkę (Effects of radiation on the cell)
Institute of Modern Civilization, Warszawa, Poland, 01.04.2003

12. Wójcik Andrzej
Działanie promieniowania na komórki (Effects of radiation on cells)
Institute of Experimental Physics, Warsaw University, Poland, 04.04.2003

13. Wójcik Andrzej
Działanie promieniowania na organizm (Effects of radiation on the organism)
Institute of Modern Civilization, Warszawa, Poland, 08.04.2003

14. Wójcik Andrzej
Ryzyko niskich dawek promieniowania (Risk of low doses of radiation)
Institute of Modern Civilization, Warszawa, Poland, 15.04.2003

15. Wójcik Andrzej
Izotopy promieniotwórcze w środowisku. Awaria w Czarnobylu (Radioactive isotopes in the environment. The Chernobyl accident)
Institute of Modern Civilization, Warszawa, Poland, 29.04.2003

16. Wójcik Andrzej
Promieniowanie UV i pola elektromagnetyczne (UV radiation and electromagnetic fields)
Institute of Modern Civilization, Warszawa, Poland, 06.05.2003

17. Wójcik Andrzej
Percepcja ryzyka (Risk perception)
Institute of Modern Civilization, Warszawa, Poland, 13.05.2003

18. Wójcik Andrzej
Działanie promieniowania na poziomie molekularnym, subkomórkowym i komórkowym (Effects of radiation at the molecular, subcellular and cellular levels)
Department of Nuclear Medicine and Magnetic Resonance, Warsaw Bródno Hospital, Poland, 27.10.2003

AWARDS IN 2003

1. First degree group award of Director of the Institute of Nuclear Chemistry and Technology for two experimental papers on the comet method in neutral pH (non-denaturing DNA) developed for the determination of DNA double strand breaks.
   Maria Wojewódzka, Iwona Buraczewska, Iwona Grądzka, Marcin Kruszewski
2. Second degree group award of Director of the Institute of Nuclear Chemistry and Technology for a series of papers on the synthesis and studies of properties of modern materials obtained with the sol-gel process.
   Andrzej Deptuła, Wiesława Łada, Tadeusz Olczak, Andrzej G. Chmielewski, Bożena Sartowska
3. Third degree individual award of Director of the Institute of Nuclear Chemistry and Technology for a series of three review papers concerning the actual problems of ensuring the quality in inorganic trace analysis, especially taking into account neutron activation analysis (NAA).
   Rajmund Dybczyński

INSTRUMENTAL LABORATORIES AND TECHNOLOGICAL PILOT PLANTS

I. DEPARTMENT OF NUCLEAR METHODS OF MATERIAL ENGINEERING

Laboratory of Materials Research

Activity profile: Studies of the structure and properties of materials and historical art objects.

- Scanning electron microscope

DSM 942, LEO-Zeiss (Germany)
Technical data: spatial resolution – 4 nm at 30 kV, and 25 nm at 1 kV; acceleration voltage – up to 30 kV; chamber capacity – 250x150 mm.
Application: SEM observation of various materials such as metals, polymers, ceramics and glasses. Determination of characteristic parameters such as molecule and grain size.

- Scanning electron microscope equipped with the attachment for fluorescent microanalysis

BS-340 and NL-2001, TESLA (Czech Republic)
Application: Observation of surface morphology and elemental analysis of various materials.

- Vacuum evaporator

JEE-4X, JEOL (Japan)
Application: Preparation of thin film coatings of metals or carbon.

- Gamma radiation spectrometer

HP-Ge, model GS 6020; Canberra-Packard (USA)
Technical data: detection efficiency for gamma radiation – 60.2%, polarization voltage – 4000 V, energy resolution (for Co-60) – 1.9 keV, analytical program "GENIE 2000".
Application: Neutron activation analysis, measurements of natural radiation of materials.

II. DEPARTMENT OF STRUCTURAL RESEARCH

1. Track-Etched Membranes Studies and Application Laboratory

Activity profile: Studies on structural defects in polymers created under influence of heavy ion beam irradiation. Manufacturing and determination of physical and structural parameters of TEM (Track-Etched Membranes) – modern filtration materials, obtained by chemical etching of latent heavy ions tracks in polymer films. Modification of TEM surface properties by physical methods. Research and developments on application of TEM in the field of sterilization, filtration and as microbiological barrier.

- Coulter Porometer II

Coulter Electronics Ltd (Great Britain)
Application: Pore size analysis in porous media.

- Vacuum chamber for plasma research

POLVAC Technika Próżniowa
Technical data: dimensions – 300x300 mm; high voltage and current connectors, diagnostic windows.
Application: Studies on plasma discharge influence on physicochemical surface properties of polymer films, particularly TEM.

2. Laboratory of Diffractional Structural Research

Activity profile: Studies on magnetic properties of new materials using neutron diffraction method. X-ray diffraction structural studies on metal-organic compounds originating as degradation products of substances naturally occurring in the environment. Röntgenostructural phase analysis of materials. Studies on interactions in a penetrant-polymer membrane system using small angle scattering of X-rays, synchrotron and neutron radiation. Studies of structural changes occurring in natural and synthetic polymers under influence of ionising radiation applying X-ray diffraction and differential scanning calorimetry.

- KM-4 X-ray diffractometer

KUMA DIFFRACTION (Poland)
Application: 4-cycle diffractometer for monocrystal studies.

- CRYOJET - Liquid Nitrogen Cooling System

Oxford Instruments

Application: Liquid nitrogen cooling system for KM-4 single crystal diffractometer.

- HZG4 X-ray diffractometer

Freiberger Präzisionsmechanik (Germany)

Application: Powder diffractometers for studies of polycrystalline, semicrystalline and amorphous materials.

- URD 6 X-ray diffractometer

Freiberger Präzisionsmechanik (Germany)

Application: Powder diffractometers for studies of polycrystalline, semicrystalline and amorphous materials.

3. Heavy Metal and Radioactive Isotopes Environment Pollution Studies Laboratory

Activity profile: Determination of elemental content of environmental and geological samples, industrial waste materials, historic glass objects and other materials by Energy Dispersive X-ray Fluorescence Spectrometry using a radioisotope excitation source as well as a low power X-ray tube and using 2 kW X-ray tube in total reflection geometry. Determination of radioactive isotope content in environmental samples and historic glass objects by gamma spectrometry.

- Gamma spectrometer in low-background laboratory

EGG ORTEC

Technical data: HPGe detector with passive shield; FWHM – 1.9 keV at 1333 keV, relative efficiency – 92%.

- Total reflection X-ray spectrometer

Pico TAX, Institute for Environmental Technologies (Berlin, Germany)

Technical data: Mo X-ray tube, 2000 W; Si(Li) detector with FHWM 180 eV for 5.9 keV line; analysed elements: from sulphur to uranium; detection limits – 10 ppb for optimal range of analysed elements, 100 ppb for the others.

Application: XRF analysis in total reflection geometry. Analysis of minor elements in water (tap, river, waste and rain water); analysis of soil, metals, raw materials, fly ash, pigments, biological samples.

- X-ray spectrometer

SLP-10180-S, ORTEC (USA)

Technical data: FWHM – 175 eV for 5.9 keV line, diameter of active part – 10 mm, thickness of active part of detector – 5.67 mm.

Application: X-ray fluorescence analysis.

4. Sol-Gel Laboratory of Modern Materials

Activity profile: The research and production of advanced ceramic materials in the shape of powders, monoliths, fibres and coatings by classic sol-gel methods with modifications – IChTJ Process or by CSGP (Complex Sol-Gel Method) are conducted. Materials obtained by this method are the following powders: alumina and its homogeneous mixtures with Cr_2O_3, TiO_3, Fe_2O_3, $MgO+Y_2O_3$, MoO_3, Fe, Mo, Ni and CaO, CeO_2, Y_2O_3 stabilized zirconia, β and β'' aluminas, ferrites, $SrZrO_3$, ceramic superconductors, type YBCO (phases 123, 124), BSCCO (phases 2212, 2223), $NdBa_2Cu_3O_x$, their nanocomposites, Li-Ni-Co-O spinels as cathodic materials for Li rechargeable batteries and fuel cells MCFC, $BaTiO_3$, $LiPO_4$, Li titanates: spherical for fusion technology, irregularly shaped as superconductors and cathodic materials, Pt/WO_3 catalyst. Many of the mentioned above systems, as well as sensors, type SnO_2, were prepared as coatings on metallic substrates. Bioceramic materials based on calcium phosphates (e.g. hydroxyapatite) were synthesized in the form of powders, monoliths and fibres.

- DTA and TGA thermal analyser

OD-102 Paulik-Paulik-Erdey, MOM (Hungary)

Technical data: balance fundamental sensitivity – 20-0.2 mg/100 scale divisions, weight range – 0-9.990 g, galvanometer sensitivity – $1x10^{-10}$ A/mm/m, maximum temperature – 1050°C.

Application: Thermogravimetric studies of materials up to 1050°C.

- DTA and TGA thermal analyser 1500

MOM (Hungary)

Technical data: temperature range – 20-1500°C; power requirements – 220 V, 50 Hz.

Application: Thermal analysis of solids in the temperature range 20-1500°C.

- Research general-purpose microscope

Carl Zeiss Jena (Germany)

Technical data: General purpose microscope, magnification from 25 to 2500 times, illumination of sample from top or bottom side.

- Metallographic microscope

EPITYP-2, Carl-Zeiss Jena (Germany)
Technical data: magnification from 40 to 1250 times.
Application: Metallographic microscope for studies in polarized light illumination and hardness measurements.

- Laboratory furnace

CSF 12/13, CARBOLITE (Great Britain)
Application: Temperature treatment of samples in controlled atmosphere up to 1500°C with automatic adjustment of final temperature, heating and cooling rate.

III. DEPARTMENT OF RADIOISOTOPE INSTRUMENTS AND METHODS

Laboratory of Industrial Radiometry

Activity profile: Research and development of non-destructive methods and measuring instruments utilizing physical phenomena connected with the interaction of radiation with matter: development of new methods and industrial instruments for measurement of physical quantities and analysis of chemical composition; development of measuring instruments for environmental protection purpose (dust monitors, radon meters); implementation of new methods of calibration and signal processing (multivariate models, artificial neural networks); designing, construction and manufacturing of measuring instruments and systems; testing of industrial and laboratory instruments.

- Multichannel analyser board with software for X and γ-ray spectrometry

Canberra

- Function generator

FG-513, American Reliace INC

IV. DEPARTMENT OF RADIOCHEMISTRY

1. Laboratory of Coordination and Radiopharmaceutical Chemistry

Activity profile: Preparation of novel complexes, potential radiopharmaceuticals, e.g. derivatives of tricarbonyltechnetium(I) (^{99m}Tc) with chelating ligands mono- and bifunctional. Studying of their hydrophilic-lipophilic properties, structure and their interactions with peptides. Also rhenium(VI) complexes with dendrimeric ligands are synthesised and studied. Novel platinum and palladium complexes with organic ligands, analogs of *cis*platin, are synthesised and studied as potential anti-tumor agents. Studies in the field of isotope chemistry of middle and heavy elements in order to find correlations between isotope separation factor and the structure of species which exchange isotopes in chemical systems, as well as to select the methods suitable for isotope enrichment.

2. Laboratory of Heavy Elements

Activity profile: Studies on chemical properties of the heaviest elements: nobelium, rutherfordium, dubnium, element 112. Studies on the influence of relativistic effects on the chemical properties (oxidation state, hydrolytic properties etc.). Synthesis of p-block metal complexes in uncommon oxidation states e.g. Bi^{+}, Po^{2+}. Elaboration of new methods for binding of ^{211}At to biomolecules. Studies on separation Lu^{3+} from Yb^{3+} in order to obtain non-carrier added ^{177}Lu.

- Two radiometric sets

ZM 701, ZZUJ POLON (Poland)
Application: Measurements of radioactivity of radiotracers and radioelements.

- Spectrometric set

ORTEC
Multichannel analyser, type 7150, semiconductor detector
Application: Measurements and identification of γ- and α-radioactive nuclides.

- Spectrometric set

TUKAN, IPJ (Świerk, Poland)
Multichannel analyser, type SILENA with a PC card type TUKAN
Application: Measurements and identification of γ-radioactive nuclides.

- Gamma radiation counter

ZR-11, ZZUJ POLON (Poland)
Application: Measurements of γ-radioactive samples, the volume of samples up to 5 ml.

- Counter of low activities

ZR-16, ZZUJ POLON (Poland)
Application: Measurements of low activities of α- and β-radioactive nuclides, also of low energies.

- Gas chromatograph

610, UNICAM (England)

Application: Analysis of the composition of mixtures of organic substances in the gas and liquid state.

- High Performance Liquid Chromatography system

Gradient HPLC pump L-7100, Merck (Germany) with γ-radiation detector, INCT (Poland)

Application: Analytical and preparative separations of radionuclides and/or various chemical forms of radionuclides.

- UV-VIS spectrophotometer

DU 68, Beckman (Austria)

Application: Recording of electronic spectra of metal complexes and organic compounds in solution. Analytical determination of the concentration of these compounds.

- FT-IR spectrophotometer

EQUINOX 55, Bruker (Germany)

Application: Measurements of the IR spectra of metal complexes and other species in the solid state and in solution.

V. DEPARTMENT OF NUCLEAR METHODS OF PROCESS ENGINEERING

1. Pilot Plant for Flue Gases Treatment

Activity profile: Pilot plant was installed for basic and industrial research on radiation processing application for flue gas treatment at the Electric-Power Station KAWĘCZYN.

- Two accelerator ELW-3A

Technical data: 50 kW power, 800 kV

- Analyser of gases

Model 17, Thermo Instrument (USA)

Application: Measurement of NO, NO_2, NO_x, NH_3 concentrations.

- Analyser 10AR (Shimadzu, Japan) with analysers NOA-305A for NO concentration determination and URA-107 for SO_2 determination
- Analysers CO/CO_2, O_2

2. Laboratory for Flue Gases Analysis

Activity profile: Experimental research connected with elaboration of technology for SO_2 and NO_x and other hazardous pollutants removal from flue gases.

- Ultrasonic generator of aerosols

TYTAN XLG

- Gas chromatograph

Perkin-Elmer (USA)

- Gas analyser LAND

Application: Determination of SO_2, NO_x, O_2, hydrocarbons, and CO_2 concentrations.

- Impactor MARK III

Andersen (USA)

Application: Measurement of aerosol particle diameter and particle diameter distribution.

3. Laboratory of Stable Isotope Ratio Mass Spectrometry

Activity profile: study of isotope ratios of stable isotopes in hydrogeological, environmental, medical and food samples.

- Mass spectrometer DELTA^{plus}

Finnigan MAT (Bremen, Germany)

Technical data: DELTA^{plus} can perform gas isotope ratio measurements of H/D, $^{13}C/^{12}C$, $^{15}N/^{14}N$, $^{18}O/^{16}O$, $^{34}S/^{32}S$.

Application: For measurements of hydrogen (H/D) and oxygen ($^{18}O/^{16}O$) in water samples with two automatic systems: H/Device and GasBench II. The system is fully computerized and controlled by the software ISODAT operating in multiscan mode (realtime). The H/Device is a preparation system for hydrogen from water and volatile organic compounds determination. Precision of hydrogen isotope ratio determination is about 0.5• for water. The GasBench II is a unit for on-line oxygen isotope ratio measurements in water samples by “continuous flow” techniques. With GasBench II, water samples (0.5 ml) can be routinely analyzed with a precision and accuracy of 0.05 . The total volume of water sample for oxygen and hydrogen determination is about 2 ml.

- Elemental Analyzer Flash 1112 NCS

Thermo Finnigan (Italy)

Application: For measurement of carbon, nitrogen and sulfur contents and their isotope composition in organic matter (foodstuff and environmental samples).

4. Radiotracers Laboratory

Activity profile: Radiotracer research in the field of: environmental protection, hydrology, underground water flow, sewage transport and dispersion in rivers and sea, dynamic characteristics of industrial installations and waste water treatment stations.

- Heavy lead chamber (10 cm Pb wall thickness) for up to 3.7×10^{10} Bq (1 Ci) radiotracer activity preparations in liquid or solid forms
- Field radiometers for radioactivity measurements
- Apparatus for liquid sampling
- Turner fluorimeters for dye tracer concentration measurements
- Automatic devices for liquid tracers injection
- Liquid-scintillation counter

Model 1414-003 „Guardian", Wallac-Oy (Finland)

Application: Extra-low level measurements of α and β radionuclide concentrations, especially for H-3, Ra-226, Rn-222 in environmental materials e.g. underground waters surface natural waters; in other liquid samples as waste waters biological materials, mine waters etc.

5. Membrane Laboratory

Activity profile: Research in the field of application of membranes for radioactive waste processing and separation of isotopes.

- Membrane distillation plant for concentration of solutions

Technical data: output ~0.05 m^3/h, equipped with spiral-wound PTFE module G-4.0-6-7 (SEP GmbH) with heat recovery in two heat-exchangers.

- Multi-stage MD unit (PROATOM) with 4 chambers equipped with flat sheet membranes for studying isotope separations
- US 150 laboratory stand (Alamo Water) for reverse osmosis tests

Technical data: working pressure – up to 15 bar, flow rate – 200 dm^3/h, equipped with two RO modules.

- Laboratory stand with 5 different RP spiral wound modules and ceramic replaceable tubular modules
- Laboratory set-up for small capillary and frame-and-plate microfiltration and ultrafiltration modules examination (capillary EuroSep, pore diameter 0.2 μm and frame-and-plate the INCT modules)
- The system for industrial waste water pretreatment

Technical data: pressure – up to 0.3 MPa; equipped with ceramic filters, bed Alamo Water filters with replaceable cartridge (ceramic carbon, polypropylene, porous or fibrous) and frame-and-plate microfiltration module.

- The set-up for chemically agressive solutions (pH 0-14), high-saline solutions (~50 g/l) in the whole pH range, and radioactive solutions treatment

Technical data: equipped with TONKAFLO high pressure pump, up to 7 MPa, chemically resistant Kiryat Weizmann module (cut-off 400 MW), and high-pressure RO module.

VI. DEPARTMENT OF RADIATION CHEMISTRY AND TECHNOLOGY

1. Pilot Installation for Radiation Processing of Polymers

Activity profile: The research is being performed in the field of polymer materials development particularly in relation with medical quality polypropylene suitable for radiation sterilization, thermomeltable glue and PE based composites for applications of thermoshrinkable products.

- Accelerator ILU-6

INP (Novosibirsk, Russia)

Technical data: beam power – 20 kW, electron energy – 0.7-2 MeV.

Application: Radiation processing.

- Extruder

PLV-151, BRABENDER-DISBURG (Germany)

Technical data: Plasti-Corder consists of: driving motor, temperature adjustment panel, thermostat, crusher, mixer, extruder with set of extrusion heads (for foils, rods, sleevs, tubes), cooling tank, pelleting machine, collecting device.

Application: Preparation of polymer samples.

- Equipment for mechanical testing of polymer samples

INSTRON 5565, Instron Co. (England)

Technical data: High performance load frame with computer control device, equipped with Digital Signal Processing and MERLIN testing software; max. load of frame is 5000 N with accuracy below 0.4% in full range; max. speed of testing 1000 mm/min in full range of load; total crosshead travel – 1135 mm; space between column – 420 mm; the environmental chamber 319-409 (internal dimensions 660x230x240 mm; temperature range from -70 to 250°C).

Application: The unit is designed for testing of polymer materials (extension testing, tension, flexure, peel strength, cyclic test and other with capability to test samples at low and high temperatures).

- Viscosimeter

CAP 2000+H, Brookfield (USA)

Technical data: Range of measurements – 0.8-1500 Pa*s, temperature range – 50-235°C, cone rotation speed – 5-1000 RPM, sample volume – 30 µl. Computer controlled via Brookfield CALPCALC® software.

Application: Viscosity measurements of liquids and polymer melts.

2. Radiation Sterilization Pilot Plant of Medical Devices and Tissue Grafts

Activity profile: Research and development studies concerning new materials for manufacturing single use medical devices (resistant to radiation up to sterilization doses). Elaboration of monitoring systems and dosimetric systems concerning radiation sterilization processing. Introducing specific procedures based on national and international recommendations of ISO 9000 and PN-EN 552 standards. Sterilization of medical utensils, approx. 70 million pieces per year.

- Electron beam accelerator

UELW-10-10, NPO TORIJ (Moscow, Russia)

Technical data: beam energy – 10 MeV, beam power – 10 kW, supply power – 130 kVA.

Application: Radiation sterilization of medical devices and tissue grafts.

- Spectrophotometer UV-VIS

Model U-1100, Hitachi

Technical data: wavelength range – 200-1100 nm; radiation source – deuterium discharge (D_2) lamp, and tungsten-iodine lamp.

- Spectrophotometer UV-VIS

Model SEMCO S/E, PZ EMCO (Warszawa, Poland)

Technical data: wavelength range – 340-1000 nm, radiation source – halogen lamp.

Application: Only for measurements of dosimetric foils.

- Bacteriological and culture oven with temperature and time control and digital reading

Incudigit 80L

Technical data: maximum temperature – 80°C, homogeneity – ±2%, stability – ±0.25% °C, thermometer error – ±2%, resolution – 0.1°C.

3. Laboratory of Radiation Microwave Cryotechnique

Activity profile: Radiation processes in solids of catalytic and biological importance: stabilization of cationic metal clusters in zeolites, radical reactions in polycrystalline polypeptides, magnetic properties of transition metals in unusual oxidation states; radical intermediates in heterogeneous catalysis.

- Electron spin resonance X-band spectrometer (ESR)

Bruker ESP-300, equipped with: frequency counter Hewlett-Packard 534 2A, continuous flow helium cryostat Oxford Instruments ESR 900, continuous flow nitrogen cryostat Bruker ER 4111VT, ENDOR-TRIPLE unit Bruker ESP-351.

Application: Studies of free radicals, paramagnetic cations, atoms and metal nanoclusters as well as stable paramagnetic centers.

- Spectrophotometer UV-VIS

LAMBDA-9, Perkin-Elmer

Technical data: wavelength range – 185-3200 nm, equipped with 60 nm integrating sphere.

4. Pulse Radiolysis Laboratory

Activity profile: Studies of charge and radical centres transfer processes in thioether model compounds of biological relevance in liquid phase by means of time-resolved techniques (pulse radiolysis and laser flash photolysis) and steady-state γ-radiolysis.

- Accelerator LAE 10 (nanosecond electron linear accelerator)

INCT (Warszawa, Poland)

Technical data: beam power – 0.2 kW, electron energy – 10 MeV, pulse duration – 7-10 ns and about 100 ns, repetition rate – 1, 12.5, 25 Hz and single pulse, pulse current – 0.5-1 A, year of installation 1999.

Application: Research in the field of pulse radiolysis.

- Gas chromatograph

GC-14B, Shimadzu (Japan)

Specifications: two detectors: thermal conductivity detectors (TCD) and flame ionization detector (FID). Column oven enables installation of stainless steel columns, glass columns and capillary columns. Range of temperature settings for column oven: room temperature to 399°C (in 1°C steps), rate of temperature rise varies from 0 to 40°C/min (in 0.1°C steps). Dual injection port unit with two lines for simultaneous installation of two columns.

Application: Multifunctional instrument for analysis of final products formed during radiolysis of sulphur and porphyrin compounds and for analysis of gaseous products of catalytic reactions in zeolites.

- Dionex DX500 chromatograph system

Dionex Corporation

Specifications: The ED40 electrochemical detector provides three major forms of electrochemical detection: conductivity, DC amperometry and integrated and pulsed amperometry. The AD20 absorbance detector is a dual-beam, variable wavelength photometer, full spectral capability is provided by two light sources: a deuterium lamp for UV detection (from 190 nm) and a tungsten lamp for VIS wavelength operation (up to 800 nm). The GP40 gradient pump with a delivery system designed to blend and pump mixtures of up to four different mobile phases at precisely controlled flow rates. The system can be adapted to a wide range of analytical needs by choice of the chromatography columns: AS11 (anion exchange), CS14 (cation exchange) and AS1 (ion exclusion).

Application: The state-of-the-art analytical system for ion chromatography (IC) and high-performance liquid chromatography (HPLC) applications. Analysis of final ionic and light-absorbed products formed during radiolysis of sulphur compounds. The system and data acquisition are controlled by a Pentium 100 PC computer.

- Digital storage oscilloscope

9354AL, LeCroy

Specifications: Bandwidth DC to 500 MHz; sample rate – 500 Ms/s up to 2 Gs/s (by combining 4 channels); acquisition memory – up to 8 Mpt with 2 Mpt per channel; time/div range – 1 ns/div to 1000 s/div; sensitivity – 2 mV/div to 5 V/div; fully variable, fully programmable *via* GPIB and RS-232C.

Application: Digital storage oscilloscope (DSO) with high speed and long memory controls pulse radiolysis system dedicated to the nanosecond electron linear accelerator (LAE 10). The multiple time scales can be generated by a computer from a single kinetic trace originating from DSO since the oscilloscope produces a sufficient number of time points (up to 8 M points record length).

- Digital storage oscilloscope

9304C, LeCroy

Specifications: Bandwidth DC to 200 MHz; sample rate – 100 Ms/s up to 2 Gs/s (by combining 4 channels); acquisition memory – up to 200 kpt per channel; time/div range – 1 ns/div to 1000 s/div; sensitivity – 2 mV/div to 5 V/div; fully variable.

Application: Digital osciloscope (DO) is used in pulse radiolysis system dedicated to the nanosecond electron linear accelerator (LAE 10).

- Nd:YAG laser

Surelite II-10, Continuum (USA)

Specifications: energy (mJ) at 1064 nm (650), 532 nm (300), 355 nm (160) and 266 nm (80); pulse width – 5-7 ns (at 1064 nm) and 4-6 ns (at 532, 355 and 266 nm); energy stability – 2.5-7%; can be operated either locally or remotely through the RS-232 or TTL interface.

Application: A source of excitation in the nanosecond laser flash photolysis system being currently under construction in the Department.

5. Research Accelerator Laboratory

Activity profile: Laboratory is equipped with accelerators providing electron beams which make capable to perform the irradiation of investigated objects within wide range of electron energy from 100 keV to 13 MeV and average beam power from 0.1 W do 20 kW, as well as with Co-60 gamma sources with activity 1.9×10^{10} to 1.3×10^{14} Bq and dose rate from 0.03 to 1.8 kGy/h.

- Linear electron accelerator

LAE 13/9, Institute of Electro-Physical Equipment (Russia)

Technical data: electron energy – 10-13 MeV; electron beam power – 9 kW.

Application: Radiation processing.

- Electron accelerator

AS-2000 (USA, the Netherlands)

Technical data: energy – 0.1-2 MeV, max. beam current – 100 μA.

Application: Irradiation of materials.

- Spectrometer

DLS-82E, SEMITRAP (Hungary)

Application: Research in radiation physics of semiconductors.

- Argon laser

ILA-120, Carl Zeiss (Jena, Germany)
Application: Measurements of optical properties.

- Spectrometer

DLS-81 (Hungary)
Application: Measurements of semiconductor properties.

- Argon laser

LGN-503 (Russia)
Application: Measurements of optical properties.

- Cobalt source I

"Spectrophotometric", developed in the INCT in 1962 (Warszawa, Poland)
Technical data: provided for the optical, periscopic access to the irradiation chamber surrounded with Co-60 rods. 6 rods – loaded initially to $3.7x10^{13}$ Bq, after many reloadings actual activity is $1.9x10^{10}$ Bq.
Application: Radiation research.

- Cobalt source II

Issledovatel (Russia)
Technical data: 32 sources with an actual activity of $1.3x10^{14}$ Bq.
Application: Radiation research.

- Cobalt source III

Irradiation chamber developed in the INCT (Warszawa, Poland)
Technical data: 8 rods with an initial activity of $2.66x10^{13}$ Bq; an actual activity is $1.9x10^{10}$ Bq. Variable geometry of the radiation field.
Application: Radiation research.

- Transiluminator UV

STS-20M, JENCONS (United Kingdom)
Technical information: six 15 W bulbs, emitted 312 nm wavelength, which corresponds to the fluorescence excitation maximum of ethidium bromide. Product description: For visualisation of ethidium bromide – stained nucleic acids fluorescence detection systems. Fluorescence intensity is enhanced, while photobleaching and photonicking of stained nucleic acids are reduced.

VII. DEPARTMENT OF ANALYTICAL CHEMISTRY

1. Laboratory of Spectral Atomic Analysis

Activity profile: atomic absorption and emission spectroscopy, studies on interference mechanisms, interpretation of analytical signals, service analysis.

- Atomic absorption spectrometer

SH-4000, Thermo Jarrell Ash (USA); equipped with a 188 Controlled Furnace Atomizer (CTF 188), Smith-Heftie background correction system and atomic vapor (AVA-440) accessory.
Application: For analyses of samples by flame and furnace AAS.

- Atomic absorption spectrometer

SP9-800, Pye Unicam (England); equipped with SP-9 Furnace Power Supply, PU-9095 data graphics system, PU-9095 video furnace programmer and SP-9 furnace autosampler.
Application: For analyses of samples by flame and furnace AAS.

2. Laboratory of Neutron Activation Analysis

Activity profile: The sole laboratory in Poland engaged for 40 years in theory and practice of neutron activation analysis in which the following methods are being developed: reactor neutron activation analysis (the unique analytical method of special importance in inorganic trace analysis), radiochemical separation methods, ion chromatography. The laboratory is also the main Polish producer of CRMs and the provider for Proficiency Testing exercises.

- Laminar box

HV mini 3, Holten (Denmark)
Technical data: air flow rate 300 m^3/h.
Application: Protection of analytical samples against contamination.

- Ion chromatograph

2000i/SP, Dionex (USA)
Technical data: calculating program AI-450, conductivity detector, UV/VIS detector.
Application: Analyses of water solutions, determination of SO_2, SO_3 and NO_x in flue gases and in air.

- Well HPGe detector

CGW-3223, Canberra, coupled with analog line (ORTEC) and multichannel gamma-ray analyzer TUKAN

Application: Instrumental and radiochemical activation analysis.

- Coaxial HPGe detector

POP-TOP, ORTEC (USA), coupled with analog line (ORTEC) and multichannel gamma-ray analyzer TUKAN

Application: Instrumental and radiochemical activation analysis.

- Well HPGe detector

CGW-5524, Canberra, coupled with multichannel gamma-ray analyzer (hardware and software) Canberra

- Analytical micro-balance

Sartorius MC5

Application: Mostly utilized for the preparation of mono- and multi-elemental standards – a proper solution is dropped onto a filter paper disc – as well as for weighing small mass samples, less than 10 mg, into the irradiation PE vials, for the purpose of neutron activation analysis.

- Liquid Scintillator Analyzer

TRI-CARB 2900TR, Packard BioScience Company

Application: β measurements.

- Planetary Ball Mill

PM 100, Retsch

Application: grinding and mixing: soft, medium hard to extremly hard, brittle or fibrous materials.

- Balance-drier

ADS50, AXIS (Poland)

Application: determination of mass and humidity of samples.

- Microwave digestion system

Uniclever II, PLAZMATRONIKA (Poland)

Application: microwave digestion of samples.

- Peristaltic pump

REGLO ANALOG MS-4/6-100, ISMATEC (Switzerland)

Application: regulation of flow of eluents during elution process.

3. Laboratory of Chromatography

Activity profile: Development of HPLC methods for determination of environmental pollutants, application of HPLC and ion-chromatography in monitoring of degradation of organic pollutants in waters and wastes using ionizing radiation, development of solid-phase extraction methods for preconcentration of organic environmental pollutants, development of chromatographic methods of identification of natural dyes used for ancient textiles.

- Apparatus for biological oxygen demand determination by respirometric method and dissolved oxygen measurement method

WTW-Wissenschaftlich-Technische Wersttätten (Germany)

Application: analyses of water and waste water samples.

- Apparatus for chemical oxygen demand determination by titrametric method

Behr Labor-Technik (Germany)

Application: analyses of water and waste water samples.

- Set-up for solid phase-extraction (vacuum chamber for 12 columns and vacuum pump)

Application: analyses of water and waste water samples.

- Shimadzu HPLC system consisted of: gradient pump LC-10AT, phase mixer FCV-10AL, diode--array detector SPD-M10A, column thermostat CTO-10AS

Application: analyses of natual dyes, radiopharmaceuticals, water and waste water samples.

VIII. DEPARTMENT OF RADIOBIOLOGY AND HEALTH PROTECTION

Laboratory of Cellular Microbiology

Activity profile: The laboratory serves for production of plasmid DNA, subsequently used for studies on DNA recombination repair, determination of topoisomerase I activity and for EPR studies.

- Equipment for electrophoretic analysis of DNA

CHEF III, BIO-RAD (Austria)

Application: Analysis of DNA fragmentation as a result of damage by various physical and chemical agents.

- Microplate reader

ELISA, ORGANON TEKNICA (Belgium)
Application: For measurement of optical density of solutions in microplates.

- Hybridisation oven

OS-91, BIOMETRA (Germany)
Technical data: work temperatures from 0 to 80°C; exchangeable test tubes for hybridisation.
Application: For polymerase chain reaction (PCR).

- Spectrofluorimeter

RF-5000, Shimadzu (Japan)
Application: For fluorimetric determinations.

- Transilluminator for electrophoretic gels

Biodoc, BIOMETRA (Great Britain)
Application: For analysis of electrophoretic gels.

- Laminar flow cabinet

1446, GV 1920
Application: For work under sterile conditions.

- Liquid scintillation counter

LS 6000LL, BECKMAN (USA)
Application: For determinations of radioactivity in solutions.

- Research microscope universal

NU, Carl Zeiss Jena (Germany)
Application: For examination of cytological preparations.
Comments: Universal microscope for transmission and reflected light/polarised light. Magnification from 25x to 2500x. Possibility to apply phase contrast.

- Incubator

T-303 GF, ASSAB (Sweden)
Technical data: 220 V, temperature range – 25-75°C.
Application: For cell cultures under 5% carbon dioxide.

- Incubator

NU 5500E/Nu Aire (USA)
Technical data: 220 V, temperature range from 18 to 55°C.
Application: for cell cultures under 0-20% carbon dioxide.

- Laminar flow cabinet

V-4, ASSAB (Sweden)
Application: For work under sterile conditions.

- Image analysis system

Komet 3.1, Kinetic Imaging (Great Britain)
Application: For comet (single cell gel electrophoresis) analysis.

- ISIS 3

Metasystem (Germany)
Application: Microscopic image analysis system for chromosomal aberrations (bright field and fluorescence microscopy).

IX. LABORATORY FOR DETECTION OF IRRADIATED FOODS

Activity profile: Detection of irradiated foods. Specially adapted analytical methods routinely used in the lab are based on electron paramagnetic resonance spectroscopy (EPR) and thermoluminescence measurements (TL). The research work is focused on the development of both methods as well as on validation and implementation of other detection methods as gas chromatographic determination of volatile hydrocarbons in fats, DNA comet assay (decomposition of single cells) and statistical germination study. The quality assurance system is adapted in the Laboratory in agreement with the PN-EN 150/IEC 17025:2001 standard and fully documented. Laboratory posses Certificate of Testing Laboratory Accreditation NR L 262/I/99 issued by the Polish Centre for Testing and Accreditation and Accreditation Certificate for Testing Laboratory issued by the Polish Centre for Accreditation valid from 25.10.2002 to 25.10.2006.

- Thermoluminescence reader

TL-DA-15 Automated, Risoe National Laboratory (Denmark)
Technical data: turntable for 24 samples, heating range – 50÷500°C, heating speed – 0.5÷10.0°C/s, optical stimulated luminescence (OSL) system.

Application: Detection of irradiated foods, research work on irradiated foods, thermoluminescence dosimetry.

- Fluorescence microscope

OPTIPHOT Model X-2, NIKON (Japan)

Technical data: halogen lamp 12 V-100 W LL; mercury lamp 100 W/102 DH; lenses (objectives) CF E Plan Achromat 4x, CF E Plan Achromat 40x; CF FLUOR 20x.

Application: Detection of irradiated foods by the DNA comet assay, research work on apoptosis in mammalian cells, biological dosimetry, analysis of DNA damage in mammalian cells.

- Compact EPR spectrometer

EPR 10-MINI, St. Petersburg Instruments Ltd. (Russia)

Technical data: sensitivity $3x10^{10}$, operating frequency (X band) – 9.0-9.6 GHz, max. microwave power – 80 mW, magnetic field range – 30-500 mT, frequency modulation – 100 kHz.

Application: Detection of irradiated foods, bone and alanine dosimetry, research work on irradiated foods and bone tissues.

X. EXPERIMENTAL PLANT FOR FOOD IRRADIATION

1. Microbiological Laboratory

Activity profile: optimization of food irradiation process by microbiological analysis.

- Sterilizer

ASUE, SMS (Warszawa, Poland)

Application: Autoclaving of laboratory glass, equipment, and microbiological cultures.

- Fluorescence microscope

BX, Olimpus (Germany)

Application: Quantitative and qualitative microbiological analysis.

2. Experimental Plant for Food Irradiation

Activity profile: Development of new radiation technologies for the preservation and hygienization of food products and feeds. Development and standarization of the control system for electron beam processing of food and feeds. Development of analytical methods for the detection of irradiated food. Organization of consumer tests with radiation treated food products.

- Accelerator ELEKTRONIKA (10 MeV, 10 kW)

UELW-10-10, NPO TORIJ (Moscow, Russia)

Application: Food irradiation.

INDEX OF THE AUTHORS